

**Studies Towards the Total Synthesis of
Anthracimycin**

Laksamee Jeanmard

Doctor of Philosophy

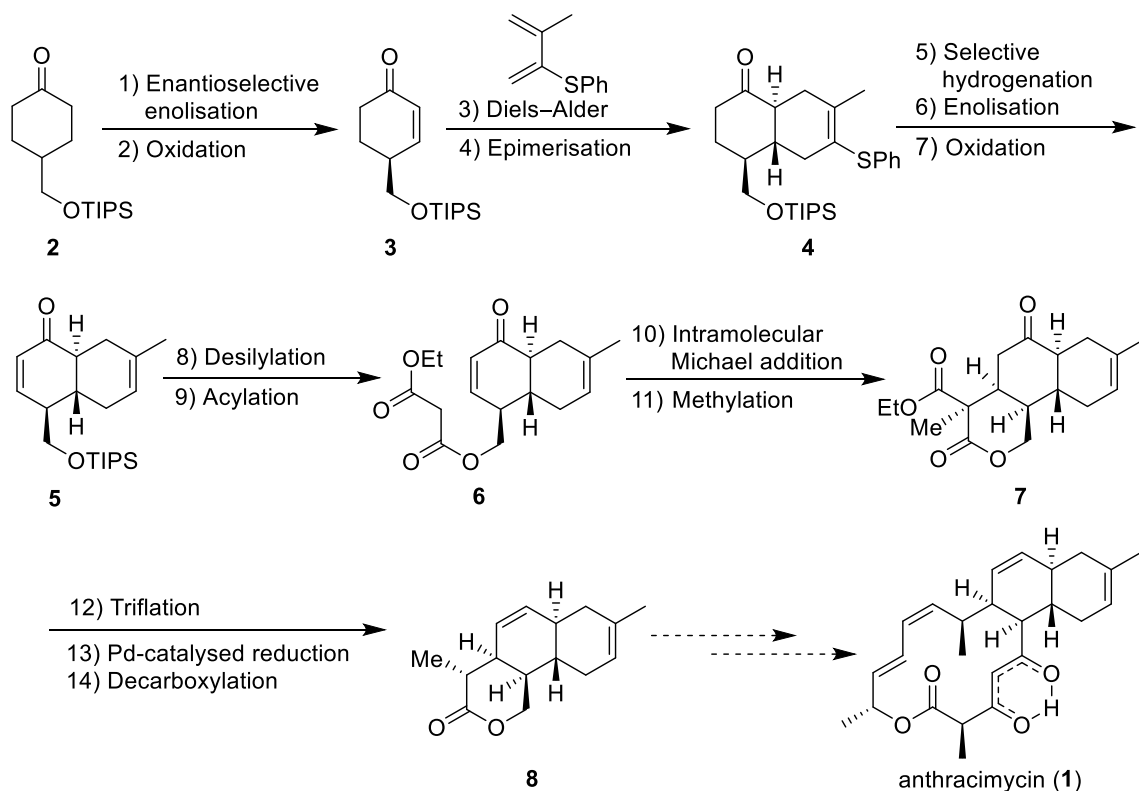
University of York

Chemistry

December 2022

Abstract

Anthracimycin (**1**) was first isolated from a culture of the marine microorganism of *Streptomyces* sp. CNH365 by the Fenical group in 2013. The isolated natural product displayed significant activities against methicillin-resistant *Staphylococcus aureus* (MRSA), vancomycin-resistant *Staphylococcus aureus* (VRSA) and pathogen *B. Anthracis*. In 2020, Brimble and co-workers reported the first total synthesis of **1** in which the key step involved a bioinspired intramolecular Diels–Alder (IMDA) reaction to furnish the decalin core as a partially separable mixture of three diastereomers with a ratio of 7:1:7 (*trans:trans:cis*). In our work towards the core structure of **1** in 14 steps, the key reactions include an enantioselective enolisation to form the key enantioenriched enone **3**, a stereo- and regioselective Diels–Alder cycloaddition, followed by epimerisation to afford the decalin core **4**. The synthesis of malonate **6** was achieved in five steps from *trans*-decalin **4**. The unprecedented intramolecular Michael addition of malonate **6** using the combination of $\text{La}(\text{O}-i\text{-Pr})_3$ and Hunig's base constructed tricyclic lactone **7** as a single diastereomer. Methylation of **7**, followed by triflation and Pd-catalysed reduction sequence, and decarboxylation generated the core structure of anthracimycin as illustrated in **Scheme 1**.



Scheme 1: The formation of the anthracimycin core

Contents

Abstract.....	2
Contents.....	3
Acknowledgements	13
Declaration.....	15
1. Introduction.....	16
1.1 Importance of natural products	16
1.2 Essential role of natural product synthesis	16
1.3 A need for new antibiotics	17
1.4 Mechanisms of action of antibiotics	18
1.5 Macrolide antibiotics.....	19
1.6 Anthracimycin.....	21
1.6.1 Biosynthesis of anthracimycin	22
1.6.2 Anthracimycin analogue	23
1.6.3 The first total synthesis of anthracimycin by the Brimble group	25
1.7 Justification for Clarke group work on the synthesis of anthracimycin.....	30
1.8 Decalin in natural products	30
1.9 Synthesis of natural products possessing a highly functionalised decalin.....	35
1.9.1 Diels–Alder cycloaddition approach	35
1.9.1.1 Intramolecular Diels–Alder cycloaddition.....	35
1.9.1.2 Intermolecular Diels–Alder cycloaddition.....	40
1.9.2 Nucleophilic and anionic cyclisation approaches	43
1.9.2.1 Robinson annelation	43
1.9.2.2 Allylation reaction	45
1.9.3 Cationic cyclisation approach	46
1.9.4 Radical cyclisation approach.....	48
1.10 Computational investigation of anthracimycin synthesis through an intramolecular Diels–Alder reaction and project outline	50
2. Results and Discussion	52
2.1 The retrosynthetic analysis of anthracimycin	52
2.2 Previous Clarke group work on the synthesis of the anthracimycin core	54

2.2.1 Previous Clarke group work on the Hosomi–Sakurai approach	56
2.2.2 Previous Clarke group work on the Mukaiyama–Michael approach	57
2.3 The synthesis of racemic cyclohexenone 3	58
2.4 The synthesis of enantioenriched cyclohexenone 3	66
2.4.1 Enantioselective Diels–Alder cycloaddition approach	66
2.4.2 Enantioselective enolisation approach.....	69
2.5 The synthesis of enone <i>trans</i> -decalin 5	72
2.6 Installation of a side chain to achieve the anthracimycin core.....	73
2.6.1 Hosomi–Sakurai 1,4-addition approach	73
2.6.2 Mukaiyama–Michael addition approach.....	78
2.6.3 Intramolecular Michael addition approach.....	88
2.7 The formation of the anthracimycin core	109
2.8 Alternative approaches to access the anthracimycin core	124
2.8.1 Palladium catalysed cyclisation	124
2.8.2 Radical cyclisation	129
3. Conclusion	135
4. Future Work	137
5. Experimental	139
5.1 General information	139
5.2 General procedure for IBX oxidation of TMS-enol ether	140
5.3 General procedure for Diels–Alder cycloaddition.....	140
5.4 General procedure for epimerisation	140
5.5 General procedure for selective hydrogenation	140
5.6 General procedure for TES-enol ether formation	141
5.7 General procedure for IBX oxidation of TES-enol ether.....	141
5.8 General procedure for TIPS deprotection	141
5.9 General procedure for hydrazone formation.....	142
5.10 General procedure for propionate formation.....	142
5.11 General procedure for malonate formation	142
5.12 Methods and characterisation of compounds	143
6. Abbreviations	189
7. References.....	193

List of Schemes

Scheme 1: The formation of the anthracimycin core	2
Scheme 2: The proposed biosynthetic pathway of anthracimycin by Alt and Wilkinson ...	23
Scheme 3: Brimble's synthesis of intramolecular Diels–Alder precursor 42	26
Scheme 4: Brimble's synthesis of <i>trans</i> -decalin scaffold 46	27
Scheme 5: The proposed transition states of intramolecular Diels–Alder reaction	28
Scheme 6: Brimble's synthesis of anthracimycin	29
Scheme 7: Structures of <i>trans</i> -decalin and <i>cis</i> -decalin.....	31
Scheme 8: Kalesse's synthesis of <i>trans</i> -decalin 76 , the core structure of chlorotonil A.....	36
Scheme 9: The directing effect of the bromine substituent on the IMDA precursor	37
Scheme 10: Lei's synthesis of the <i>epi</i> -core structure of alchivemycin A.....	37
Scheme 11: Miyaoka's synthesis of <i>trans</i> -decalin 91 , the core structure of kalihinol A.....	38
Scheme 12: Shenvi's synthesis of decalin 95 , the core structure of amphilectene	39
Scheme 13: Murai's synthesis of decalin 100 , the core structure of azadirachtin.....	39
Scheme 14: Lee's synthesis of Nicolaou's intermediate 105 , the core structure of platencin.....	40
Scheme 15: Krische's synthesis of <i>trans</i> -decalin 109 , the core structure of andrographolide.....	41
Scheme 16: Jung's synthesis of tricyclic ring 112 , the core structure of rhodexin A	42
Scheme 17: Cai's synthesis of <i>cis</i> -decalin 117 , the core structure of <i>cis</i> -crotonin.....	42
Scheme 18: Nicolaou's synthesis of <i>trans</i> -decalin 120 , the core structure of myceliothermophin E	43
Scheme 19: Bradshaw's synthesis of <i>cis</i> -decalin 127 , the core structure of anominine ...	44
Scheme 20: Maier's synthesis of the advanced precursor 131 for streptosetin A	45
Scheme 21: Anderson's synthesis of <i>cis</i> -decalin 139 , the core structure of popolohuanone E	46
Scheme 22: Baati's synthesis of <i>trans</i> -decalin 142 , the core structure of triptolide and plausible mechanism of 6- <i>endo</i> -trig cyclisation.....	47
Scheme 23: Yoshimitsu's synthesis of <i>cis</i> -decalin 150 , the core structure of platencin	48
Scheme 24: Carreira's synthesis of lactone 154 , the core structure of crotogoudin	49
Scheme 25: The retrosynthetic analysis of anthracimycin	53

Scheme 26: Previous Clarke group work on the formation of racemic enone 3 and sulfur-substituted diene 163	54
Scheme 27: Previous Clarke group work on the formation of enone <i>trans</i> -decalin 5	55
Scheme 28: Previous Clarke group work on the Hosomi–Sakurai 1,4 addition of enone 5 and (<i>E</i>)-crotyltrimethylsilane 171	56
Scheme 29: Previous Clarke group work on the Mukaiyama–Michael addition and transformation of tricyclic system	57
Scheme 30: The formation of racemic enone 3 developed by Dr Ian George	59
Scheme 31: The formation of racemic enone 3 developed by Dr Giacomo Lodovici	59
Scheme 32: The examples of Diels–Alder reaction of Rawal’s diene 181 with dienophiles 182 and 183	60
Scheme 33: The conversion of cycloadduct 184 to enone 188	60
Scheme 34: The attempted formation of racemic alcohol 193 via Diels–Alder cycloaddition between Rawal’s diene 181 and acrolein 191	61
Scheme 35: The attempted formation of cycloadduct 186–187 via Diels–Alder cycloaddition between Rawal’s diene 181 and methyl acrylate 183	62
Scheme 36: The formation of racemic cyclohexenone 3	63
Scheme 37: The IBX oxidation of silyl enol ethers	64
Scheme 38: Previous Clarke group work on the transformation of ketone 168 to enone 5	64
Scheme 39: The formation racemic enone 3 through the IBX oxidation of TMS-enol ether	65
Scheme 40: Nishida’s synthesis of cyclohexenone 205 via an asymmetric Diels–Alder cycloaddition	66
Scheme 41: The preparation of Danishefsky’s diene 202	67
Scheme 42: The preparation of dienophile 201	67
Scheme 43: The preparation of BINAMIDE ligand 203	68
Scheme 44: The attempted formation of cycloadduct 204 via an enantioselective Diels–Alder reaction catalysed by Yb(III)-BINAMIDE complex	68
Scheme 45: Desymmetrisation of cyclohexanone 211	69
Scheme 46: Smith’s synthesis of (<i>R</i>)-cyclohexenone 217 via an enantioselective enolisation	70
Scheme 47: The synthesis of (<i>S</i>)-cyclohexenone 3 via an enantioselective enolisation	71

Scheme 48: The synthesis of sulfur-substituted diene 163	72
Scheme 49: The synthesis of enone <i>trans</i> -decalin 5	73
Scheme 50: Previous Clarke group work on the Hosomi–Sakurai 1,4-addition of enone 5 and allyltrimethylsilane 219	74
Scheme 51: The proposed synthetic route for the anthracimycin core 8	75
Scheme 52: The racemic synthesis of enone <i>trans</i> -decalin 5	75
Scheme 53: The Hosomi–Sakurai 1,4-addition of enone <i>trans</i> -decalin 5	76
Scheme 54: Previous Clarke group work on the Mukaiyama–Michael 1,4-addition of enone 5 and (<i>E</i>)-ethyl-propanoate silyl ketene acetal 174	78
Scheme 55: Ireland’s synthesis of (<i>Z</i>)-ethyl-propanoate silyl ketene acetal 228	79
Scheme 56: The attempted preparation of (<i>Z</i>)-ethyl-propanoate silyl ketene acetal 228 .	79
Scheme 57: The proposed the Mukaiyama–Michael 1,4-addition of (<i>E</i>)-ethyl-propanoate silyl ketene acetal 174 to enone <i>cis</i> -decalin 229	80
Scheme 58: The synthesis of enone <i>cis</i> -decalin 229	81
Scheme 59: The synthesis of (<i>E</i>)-ethyl-propanoate silyl ketene acetal 174	82
Scheme 60: The Mukaiyama–Michael 1,4-addition of enone <i>cis</i> -decalin 229	83
Scheme 61: The synthesis of hydrazone derivatives 234 and 235	83
Scheme 62: The Mukaiyama–Michael addition of enone <i>cis</i> -decalin 229	86
Scheme 63: The formation of hydrazone 240	87
Scheme 64: Ley’s synthesis of cyanolactone 243	89
Scheme 65: Isobe’s synthesis of bicyclic lactone 247	89
Scheme 66: Mander’s synthesis of tricyclic lactone 250	90
Scheme 67: The proposed synthesis of anthracimycin core 251 via an intramolecular Michael addition	90
Scheme 68: The attempted intramolecular Michael addition of propionate <i>cis</i> -decalin 254	91
Scheme 69: The formation of enone propionate 252	92
Scheme 70: The proposed mechanism to construct the desired tricyclic lactone 251 and undesired conjugated enone 257	94
Scheme 71: The proposed formation of tricyclic lactone 259 via the intramolecular Michael addition of enone malonate 6	94
Scheme 72: The formation of enone malonate 6	95

Scheme 73: The proposed mechanism to form the undesired conjugated enone 257 by a portion of enolate	97
Scheme 74: The proposed synthesis of tricyclic lactone 259 via a keto-enol formation	99
Scheme 75: Acylation of diethyl malonate 260 and ethyl acetoacetate 261 reported by Rathke and Cowan	100
Scheme 76: Unsworth's synthesis of 16-membered ring 268	101
Scheme 77: The proposed reversible intramolecular Michael addition of malonate 6	102
Scheme 78: The formation of malonate model system 270	103
Scheme 79: The formation of tricyclic lactone 259 through an intramolecular Mukaiyama–Michael addition approach	105
Scheme 80: The proposed enolisation of tricyclic lactone 259 under kinetic and thermodynamic conditions	106
Scheme 81: The enantioselective Michael reaction using a catalyst prepared from lanthanide salt and <i>i</i> -Pr ₂ NEt reported by Shibasaki and co-workers	107
Scheme 82: The formation of tricyclic lactone 259 via an intramolecular Michael addition	109
Scheme 83: The proposed synthetic route to accomplish the anthracimycin core 8	110
Scheme 84: Methylation of tricyclic lactone 259	110
Scheme 85: Previous Clarke group work on the transformation of ketone to alkene 281	113
Scheme 86: The attempted formation of vinyl triflate 282	114
Scheme 87: Matsuo's method for the transformation of ketone 283 to alkene 285	115
Scheme 88: The transformation of ketone 7 to alkene 277	115
Scheme 89: Decarboxylation of lactone 277	116
Scheme 90: The formation of the anthracimycin core 8	124
Scheme 91: Examples of Pd-catalysed cyclisation.....	125
Scheme 92: The proposed synthetic route for the Pd-catalysed cyclisation of 294	125
Scheme 93: The formation of allylic alcohols 297 and 298	126
Scheme 94: The formation of π -allyl precursor 294	127
Scheme 95: The attempted Pd-catalysed cyclisation of malonate 294	127
Scheme 96: Examples of the radical cyclisation to construct a six-membered ring	130
Scheme 97: The proposed synthesis of tricyclic lactone 251 via a radical cyclisation	130
Scheme 98: The proposed model study to investigate the radical cyclisation	131

Scheme 99: The synthesis of bromine propionate 309	131
Scheme 100: The attempted synthesis of bicyclic lactone 310 via a radical cyclisation ...	131
Scheme 101: Stabilisation of initially formed radical by the propionyl group of 309	132
Scheme 102: Stabilisation of initially formed radical by the malonyl group of 315	132
Scheme 103: The synthesis of bromo malonate 315	133
Scheme 104: The attempted radical cyclisation of bromo malonate 315	133
Scheme 105: The proposed mechanism to form the reduction product 270	134
Scheme 106: The formation of the anthracimycin core 8	136
Scheme 107: The proposed kinetic and thermodynamic epimerisation conditions for 287	137
Scheme 108: The proposed synthetic route to intercept Brimble's intermediate 51	138
Scheme 109: The proposed synthetic route to achieve anthracimycin (1)	138

List of Figures

Figure 1: Five major modes of antibiotic mechanism modified from Walsh's figure	19
Figure 2: Structures of selected 12-, 14-, 15-, and 16-membered macrolide antibiotics	20
Figure 3: The chemical structure of anthracimycin (1).....	21
Figure 4: The structure of anthracimycin (1) and anthracimycin BII-2619 (34)	24
Figure 5: Structures of selected antimalarial natural products containing a decalin	32
Figure 6: Structures of selected anticancer natural products containing a decalin	33
Figure 7: Structures of selected antibiotic natural products containing a decalin	33
Figure 8: Structures of selected biologically active products containing a decalin.....	34
Figure 9: The computational study of a biomimetic intramolecular cycloaddition to form the decalin scaffold of anthracimycin, by the Clarke group	51
Figure 10: The single crystal X-ray diffraction of tricyclic lactone 178	58
Figure 11: HPLC trace of racemic cyclohexenone 3	63
Figure 12: HPLC trace of (<i>S</i>)-cyclohexenone 3	71
Figure 13: The single crystal X-ray diffraction of hydrazone 234	84
Figure 14: The single crystal X-ray diffraction of hydrazone 235	85
Figure 15: The ¹ H NMR spectrum of tricyclic lactone 259	97
Figure 16: The nOe analysis of H-3 of tricyclic lactone 259	98
Figure 17: The nOe analysis of H-14 of tricyclic lactone 259	98
Figure 18: The single crystal X-ray diffraction of tricyclic lactone 259	99
Figure 19: The ¹ H NMR spectrum of tricyclic lactone 7	111
Figure 20: The nOe analysis of H-3 in tricyclic lactone 7	112
Figure 21: The nOe analysis of H-4 in tricyclic lactone 7	112
Figure 22: The nOe analysis of H-18 in tricyclic lactone 7	113
Figure 23: The ¹ H NMR spectrum of tricyclic lactone 8	117
Figure 24: The nOe analysis of H-3 in tricyclic lactone 8	118
Figure 25: The nOe analysis of H-4 in tricyclic lactone 8	118
Figure 26: The nOe analysis of H-15 in tricyclic lactone 8	119
Figure 27: The 2D NOESY analysis of tricyclic lactone 8	119
Figure 28: The ¹ H NMR spectrum of tricyclic lactone 287	120
Figure 29: The nOe analysis of H-3 in tricyclic lactone 287	121
Figure 30: The nOe analysis of H-4 in tricyclic lactone 287	121

Figure 31: The nOe analysis of H-14 in tricyclic lactone 287	122
Figure 32: The nOe analysis of H-15 in tricyclic lactone 287	122
Figure 33: The 2D NOESY analysis of tricyclic lactone 287	123

List of Tables

Table 1: Evaluation of antibiotic resistance to use in medicine	17
Table 2: Different antibiotic class generations developed by derivatisation	18
Table 3: Biological activity of anthracimycin BII-2619 compared to anthracimycin	24
Table 4: Simpkins’s screening temperature for the desymmetrisation of ketone 211	70
Table 5: Screening conditions for the Hosomi–Sakurai 1,4-addition of enone 5	77
Table 6: Screening conditions for the IBX oxidation of TES-enol ether <i>cis</i> -decalin 231	82
Table 7: Screening conditions for the intramolecular Michael addition of propionate 252	93
Table 8: Screening conditions for the intramolecular Michael addition of malonate 6	96
Table 9: Screening conditions for the intramolecular Michael addition of malonate 6 using magnesium chloride and tertiary amine bases.....	101
Table 10: Screening conditions for the intramolecular Mukaiyama–Michael addition of malonate model system 270	103
Table 11: Screening conditions for the intramolecular Michael addition of malonate 270	108
Table 12: Screening conditions for the Pd-catalysed cyclisation of acetate 294	128

Acknowledgements

First and foremost, I would like to express my sincere gratitude to my supervisor, Prof. Paul A. Clarke, for providing me with an excellent opportunity to work on the challenging anthracimycin project and for his invaluable support, continuous encouragement, and professional guidance throughout four years of my PhD, especially during the COVID-19 pandemic. As a result, I have been able to overcome all the difficulties, and I have matured as a chemist and as a person.

I am very grateful to the Development and Promotion of Science and Technology Talents Project (DPST) for the financial support over the course of my PhD. I also would like to thank Dr William Unsworth, my IPM, for his advice and support during friendly TAP meetings. My sincere thanks go to Prof. Peter O'Brien in particular for his helpful proofreading of my thesis during a tough time. My thanks also go to Heather Fish for her NMR assistance, Karl Heaton for MS data and Adrian Whitwood for crystal structure analysis.

Due to the Clarke group, working in the lab was enjoyable and joyful. I would like to thank former and current Clarke group members for all their help and support. To Chris for teaching me how to deal with my baby - Kugelrohr, Schlenk line and many things when I started. To Athanasia for happy working songs and fun stories. To Lee for continuing to help the lab function smoothly even after he left the group. In addition, I felt like I was the youngest sister, especially since there were PAC ladies around (Khadra, Selin and Saikiran). To Khadra for being an always supportive and encouraging person. Her guidance, chocolates and lemon cakes motivated me a lot. To Selin, for being a lovely friend throughout my sunny and cloudy days. Exchanging experiences, discussing many different topics, and going outside with you were awesome. Special credit goes to Saikiran for being a wonderful friend, sharing all the good and bad and remote helping when I need it. Discussing interesting chemistry and drawing mechanisms on the sash of all fume hoods with you was so much fun and knowledgeable. The amazing Portugal trip would not be possible without you!

Four years in York are special and highly memorable. Big thanks go to P'Natta, who made my first step in York smooth and joyful. To Mon and Pandy for being such close friends and

fantastic housemates so far. Not only incredible trips, stunning photographs, fun stories, and laughs but also a lot of tears throughout my PhD journey were supported by both of you! I also would like to thank Jane, Fair and Ben for keeping in touch and sharing experiences.

Last but not least, I most gratefully acknowledge Benz - my boyfriend, Nilo - my sister, my parents and the rest of my family for their everlasting support, always being there for me, being proud of me and believing in me along the way to achieve my PhD.

Declaration

I hereby declare that the substance of this thesis has not been submitted, nor is currently being submitted, in candidature for any other degree.

I also declare that the work embodied in this thesis is the result of my own investigations and in the event the work of others has been used this has been fully acknowledged in the text as references.

1. Introduction

1.1 Importance of natural products

Metabolites are intermediates generated during the metabolic process within cells and thus are divided into two major types. The chemical compounds produced during the stage of growth, development and reproduction processes, such as proteins, lipids, nucleic acids and carbohydrates, which are essential to all living organisms, are known as "primary metabolites".^{1,2} Substances that are not required for the organism's viability but are crucial for environmental adaptation or serving as a proactive defence against predators called "secondary metabolites".^{1,3} Secondary metabolites are organic compounds produced by modifying primary metabolite biosynthesis.^{3,4} They are frequently discovered to be specific to an organism or an expression of a specie individuality and used as biologically active compounds, also known as natural products.^{2,3} As natural products have chemical diversity and unique pharmacological and biological activities, they have been utilised in both traditional and modern medicine for treating illness. Consequently, natural products play an important role in the development and discovery of new drugs.⁵

1.2 Essential role of natural product synthesis

As a consequence of their promising biological profiles, several natural products have been considered for drug candidates.² For instance, acetylsalicylic acid, commonly known as aspirin, is an anti-inflammatory agent originally isolated from the bark of the willow tree.⁶ Morphine, a typical painkiller, is derived from the plant *P. somniferum*. Eribulin, substantially part of the larger natural product halichondrin B, is a chemotherapeutic drug used in the treatment of patients suffering late-stage metastatic breast carcinoma.⁷ It is feasible to isolate natural compounds and evaluate their biological activities in a variety of circumstances. However, the quantities accessible from natural sources are so scarce that total synthesis of natural products from readily available bulk or fine chemicals is required to provide material on the milligram-to-gram scale for further biological evaluation.⁸ To determine whether natural products are useful for drug development, natural product synthesis is a vital first step.⁸ On the other hand, bioactive natural products are intricate in their stereochemistry and architecture, posing a challenge for organic synthetic chemists to successfully synthesise these molecules. Hence, developing innovative methods and

devising synthetic approaches to achieve satisfactory target molecules with exceptional quantity is highly desirable.⁹

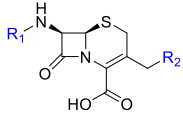
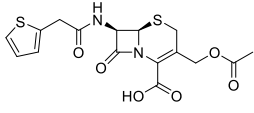
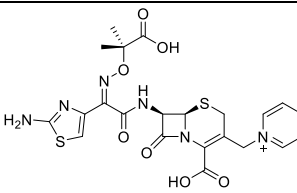
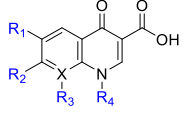
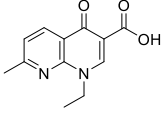
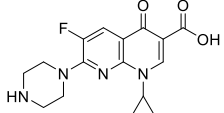
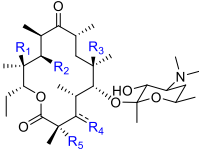
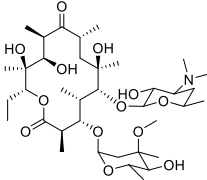
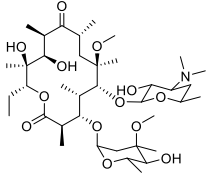
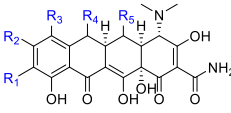
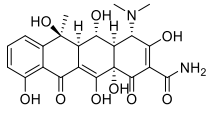
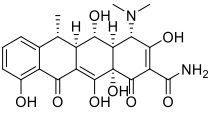
1.3 A need for new antibiotics

The rate of methicillin-resistant *Staphylococcus aureus* (MRSA), *Clostridium difficile* (C. Diff), *Enterobacteriaceae*, and other resistant infections have been steadily increasing over the past few decades, and this has had an impact on world health.¹⁰ Strongly antibiotic-resistant bacteria cannot be treated with current and front-line antibiotics due to the establishment of resistance. In order to combat MRSA, new antibiotics with innovative mechanisms of action must be discovered.^{11,12} The following table compares the year when antibiotics were first utilised to the year that clinical resistance was detected to understand how quickly bacteria developed resistance (**Table 1**).¹⁰ As a result of high infection and global mortality rates, developing the next generation of antibiotics to combat these resistances is urgently needed. Therefore, the chemical structures of antibiotics were modified to deliver new generations of antibiotics in an effort to overcome resistance as shown in **Table 2**.¹⁰

Table 1: Evaluation of antibiotic resistance to use in medicine

Antibiotics	Year deployed	Clinical resistance observed
Sulfonamides	1930	1940
Penicillin	1943	1946
Streptomycin	1943	1959
Chloramphenicol	1947	1959
Tetracycline	1948	1953
Erythromycin	1952	1988
Vancomycin	1956	1988
Methicillin	1960	1961
Ampicillin	1961	1973
Cephalosporins	1960	late 1960
Nalidixic acid	1962	1962
Fluoroquinolones	1980	1980
Linezolid	1999	1999
Daptomycin	2003	2003
Retapamulin	2007	2007
Fidaxomycin	2011	2011

Table 2: Different antibiotic class generations developed by derivatisation

Antibiotic Class	Generation 1	Generation 2	Generation 3
Cephalosporins			
Quinolones			
Macrolides			
Tetracyclines			

1.4 Mechanisms of action of antibiotics

Human bacterial infections have been continually treated with antibiotics, which resist infectious microorganisms in the body by obliterating their structure or capacity for reproduction. Different antibiotic classes suppress microorganisms in unique manners, categorised into five main pathways as depicted in **Figure 1**.¹⁰ Attacking the bacterial cell wall directly, which is a target of β -lactams and the vancomycin type glycopeptides, is the first way used to prevent bacterial reproduction. Daptomycin disrupts the integrity of bacterial membranes, which is a second target region.¹³ A third pathway is the blocking of folate biosynthesis by sulfonamides.¹³ The fourth mode of action is blocking DNA replication and RNA transcription which is found in fluoroquinolone. The last mode of action of antibiotics is the inhibition of protein biosynthesis through binding to the ribosomal subunit operated by macrolide classes.¹³

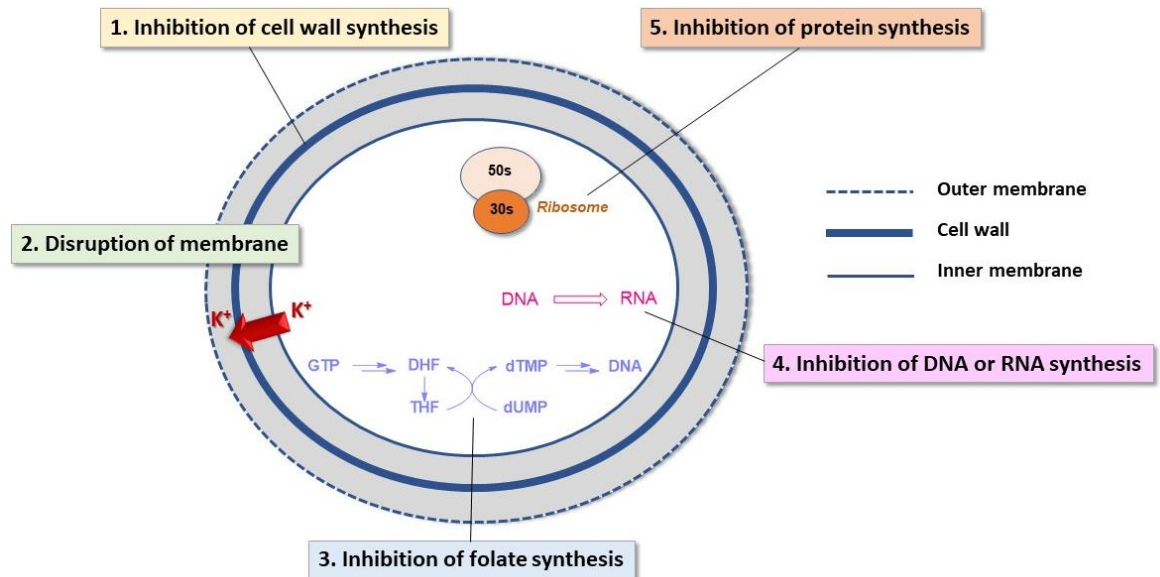


Figure 1: Five major modes of antibiotic mechanism modified from Walsh's figure¹⁰

1.5 Macrolide antibiotics

Macrolides are a large class of antibiotics that are employed to treat bacterial infections in humans. Most macrolide antibiotics function through the inhibition of protein synthesis by binding to the 50s bacterial ribosomes. The chemical structure of macrolides is composed of a macrocyclic lactone with different ring sizes, such as 12-, 14-, 15- and 16-membered rings.¹⁴ Some macrolide examples grouped by ring size are shown in **Figure 2**. The majority of macrolides are derived from a *Streptomyces* strain. Gram-positive bacteria, including *Staphylococcus*, *Streptococcus* and *Diplococcus* sp. are significantly resistant to the inhibitory effects of macrolide antibiotics, while Gram-negative bacteria (*Neisseria gonorrhoea*, *Haemophilus influenzae*, *Bordetella pertussis* and *Neisseria meningitis* sp.) have limited susceptibility. Additionally, they severely inhibit a number of *Mycoplasmas*. Typically, 14-membered macrolides, such as erythromycin (**12**), clarithromycin (**13**), and flurithromycin (**15**), were discovered to be more effective against *Streptococci* and *Bordetella pertussis* than 15- and 16-membered macrolides such as azithromycin (**17**), miocamycin (**20**) and rokitamycin (**21**).¹⁵

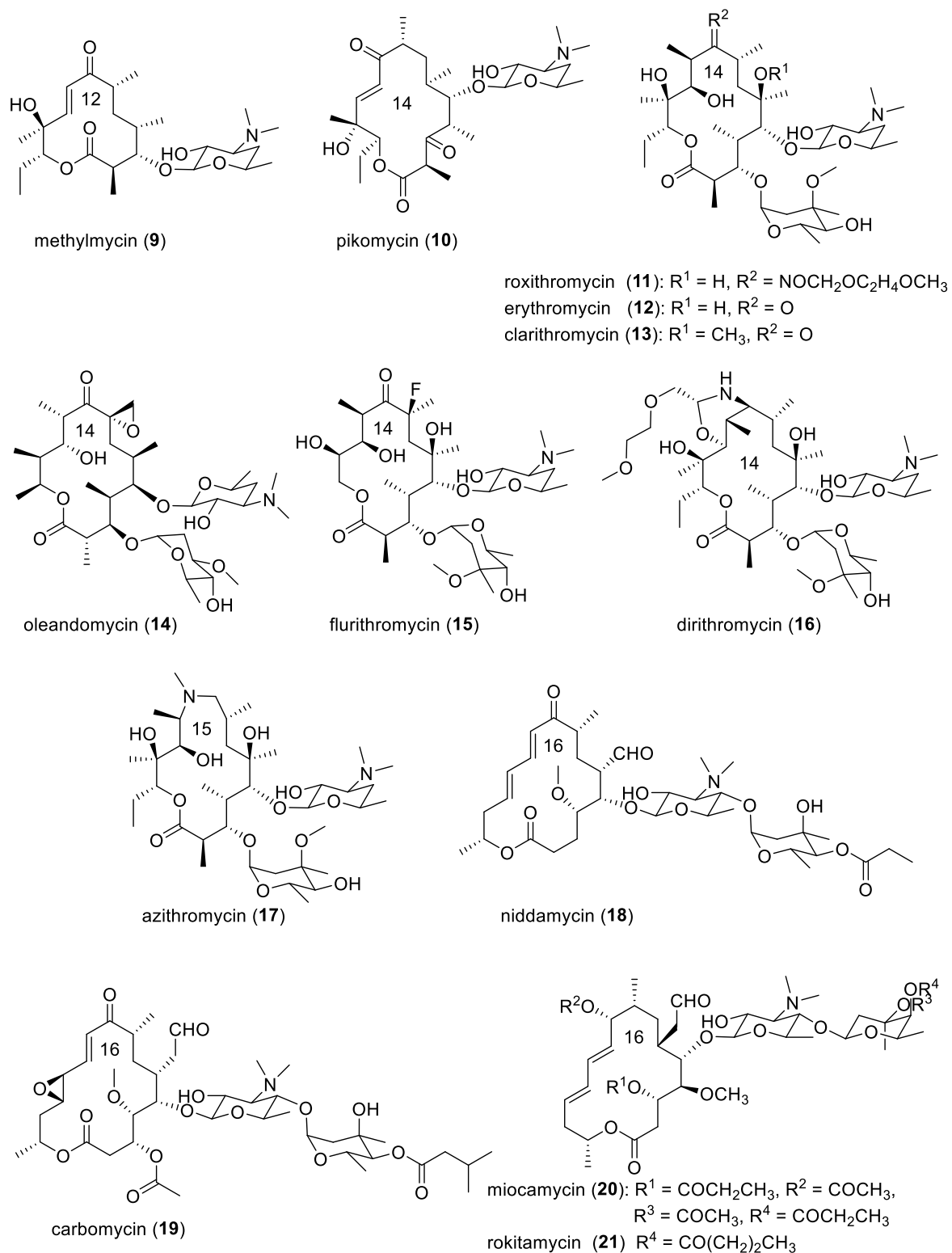


Figure 2: Structures of selected 12-, 14-, 15-, and 16-membered macrolide antibiotics

The macrolide family has led to significant contributions in activity against Gram-positive and Gram-negative bacteria; therefore, developing or exploring new generations of macrolides would be promising in responding to the severe increase in resistance.¹⁴

1.6 Anthracimycin

As both the prevalence of methicillin-resistant *Staphylococcus aureus* (MRSA) infections increases and antibiotics require a while to develop,^{16,17,18} there is an urgent need for research to discover new powerful antibiotics.¹⁹ Secondary metabolites derived from microorganisms possessing potent antimicrobial properties are important for potential drug discovery.²⁰ Marine macrolide derived from bacteria was found to exhibit MRSA activity, which has been proven to solve the issue of an increasing MRSA infection rate.^{21,22} Interestingly, the Fenical group discovered culture extracts from a marine microorganism of *Streptomyces* sp. CNH365 off the coast of Santa Barbara, California (USA) in 2013.²² These culture extracts were found to possess significant antibacterial activity ($\leq 0.06 \mu\text{g/mL}$) towards Gram-positive bacteria, including methicillin-resistant *Staphylococcus aureus* (MRSA) and vancomycin-resistant *Staphylococcus aureus* (VRSA) with a MIC value of $< 0.25 \text{ mg/mL}$.²² The selective fractionation of extracts having impressive antibacterial activity resulted in a pure white solid anthracimycin (**1**). Additionally, anthracimycin (**1**) demonstrates remarkable activities against pathogens *B. Anthracis* (MIC $0.031 \mu\text{g/mL}$) and *M. tuberculosis* (MIC $1\text{--}2 \mu\text{g/mL}$), as well as a minimal toxic effect to eukaryotic cells against human cancer cell lines with an $\text{IC}_{50} = 70 \mu\text{g/mL}$.^{22,23} Anthracimycin (**1**) with a molecular formula $\text{C}_{25}\text{H}_{32}\text{O}_4$ is a 14-membered macrolide, which features seven stereogenic centres on a tricyclic ring system containing a 14-membered macrocycle and a *trans*-decalin scaffold determined by NMR spectroscopy and X-ray crystallography.²² The 14-membered ring was defined by the existence of a lactone functional group and an enolised β -diketone moiety confirmed by the equidistant position of the proton between each oxygen atom on X-ray analysis. In addition, the vicinal coupling constant of 10.5 Hz for the *Z*-alkene and 15.2 Hz for the *E*-alkene provided further evidence that two double bonds were present in the 14-membered ring (**Figure 3**).

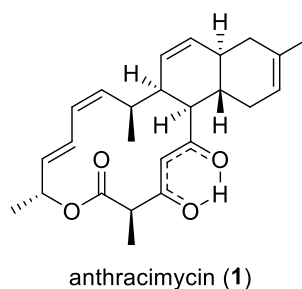
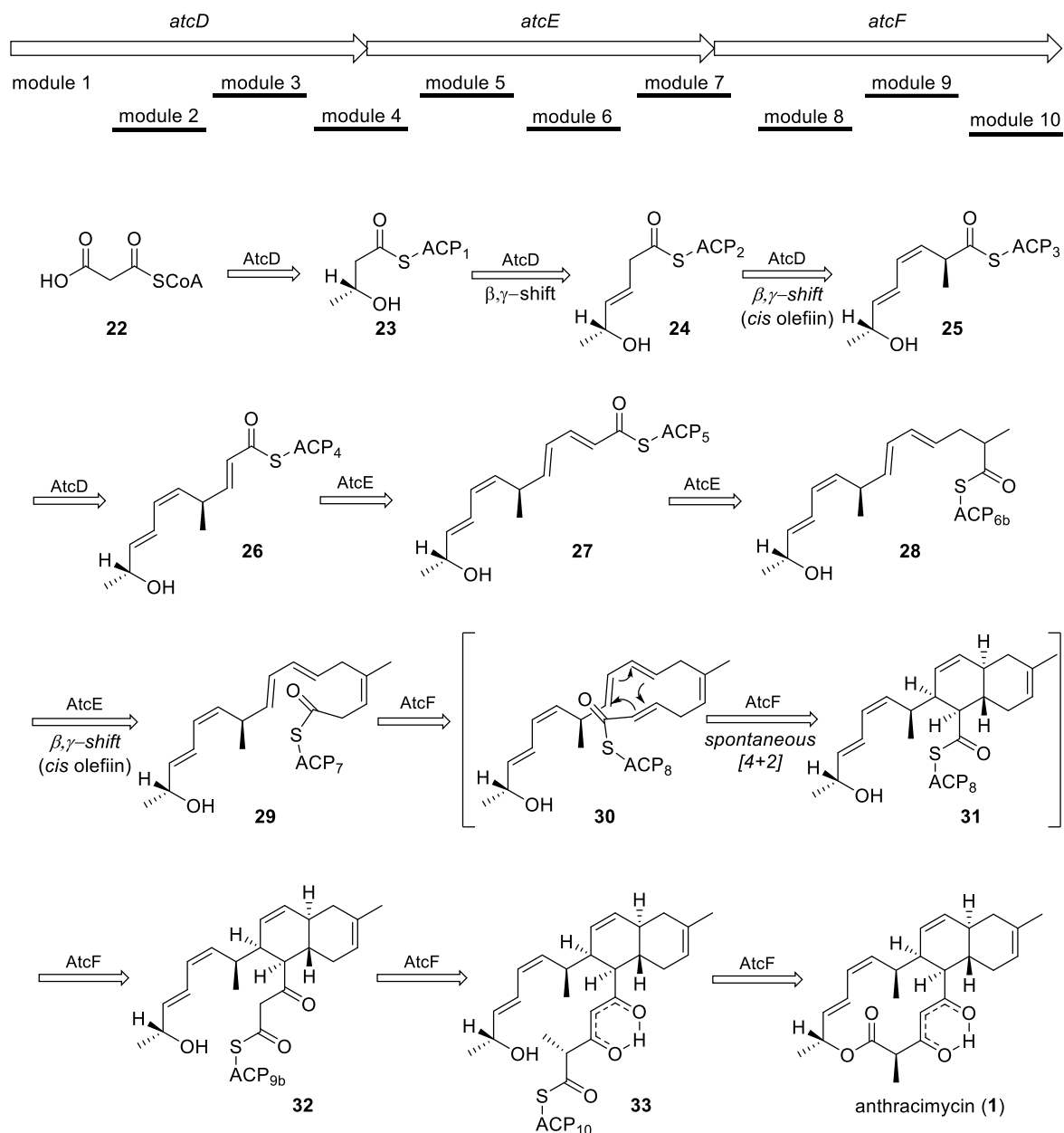


Figure 3: The chemical structure of anthracimycin (**1**)

1.6.1 Biosynthesis of anthracimycin

The biosynthesis of anthracimycin (**1**) was elucidated by Alt and Wilkinson in 2015.²⁴ They classified type I, iterative type II and acyl-carrier protein (ACP)-independent type III as three major classes of PKSs. It was suggested that a type I polyketide synthase (PKS) pathway is involved in the synthesis of polyketide **1**. A type I polyketide synthase (PKS) significantly contributes to the formation of intermediates by selecting and loading carboxylic acid precursors for the chain assembly. In addition, a group of type I PKSs is required as a catalyst for a decarboxylative Claisen-like condensation to generate metabolite intermediates in the chain elongation step. As a result, it was envisioned for the biosynthesis of **1** to begin with the formation of the acylated ACP₁ intermediate **23** from the malonyl-CoA precursor **22** via decarboxylation and reduction. The ACP₂ intermediate **24**, ACP₃ intermediate **25**, ACP₄ intermediate **26**, and ACP₅ intermediate **27** could subsequently be produced, each with a β,γ -double bond, by repeating the chain elongation. Additional methylation and chain elongation of **27** could generate ACP₆ intermediate **28**, which could then be further extended to form ACP₈ intermediate **30**. The key stage to construct the *trans*-decalin moiety in **31** would be hypothesised through the *endo*-selective intramolecular Diels–Alder cycloaddition of **30**. The last three-step sequence of chain elongation, macrocyclisation and chain release would yield the natural product **1** (**Scheme 2**).



Scheme 2: The proposed biosynthetic pathway of anthracimycin by Alt and Wilkinson²⁴

1.6.2 Anthracimycin analogue

In 2017, Sirota and co-workers discovered an anthracimycin derivative isolated from the actinobacterial microorganism *Nocardiosis kunsanensis*, an alternative anthracimycin-producing organism. According to **Figure 4**, this natural product was identified as anthracimycin BII-2619 (**34**) and was purified into a white powder with the same molecular formula as anthracimycin (**1**) determined by NMR spectroscopy analysis. The absolute configurations were confirmed to be identical to the configurations of **1** with the exception that the methyl group is present at the 8-position rather than the 2-position.²⁵

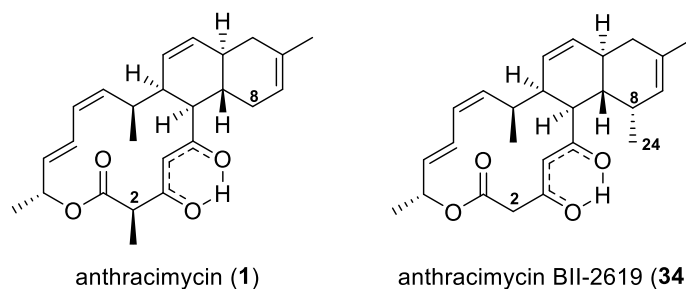


Figure 4: The structure of anthracimycin (**1**) and anthracimycin BII-2619 (**34**)

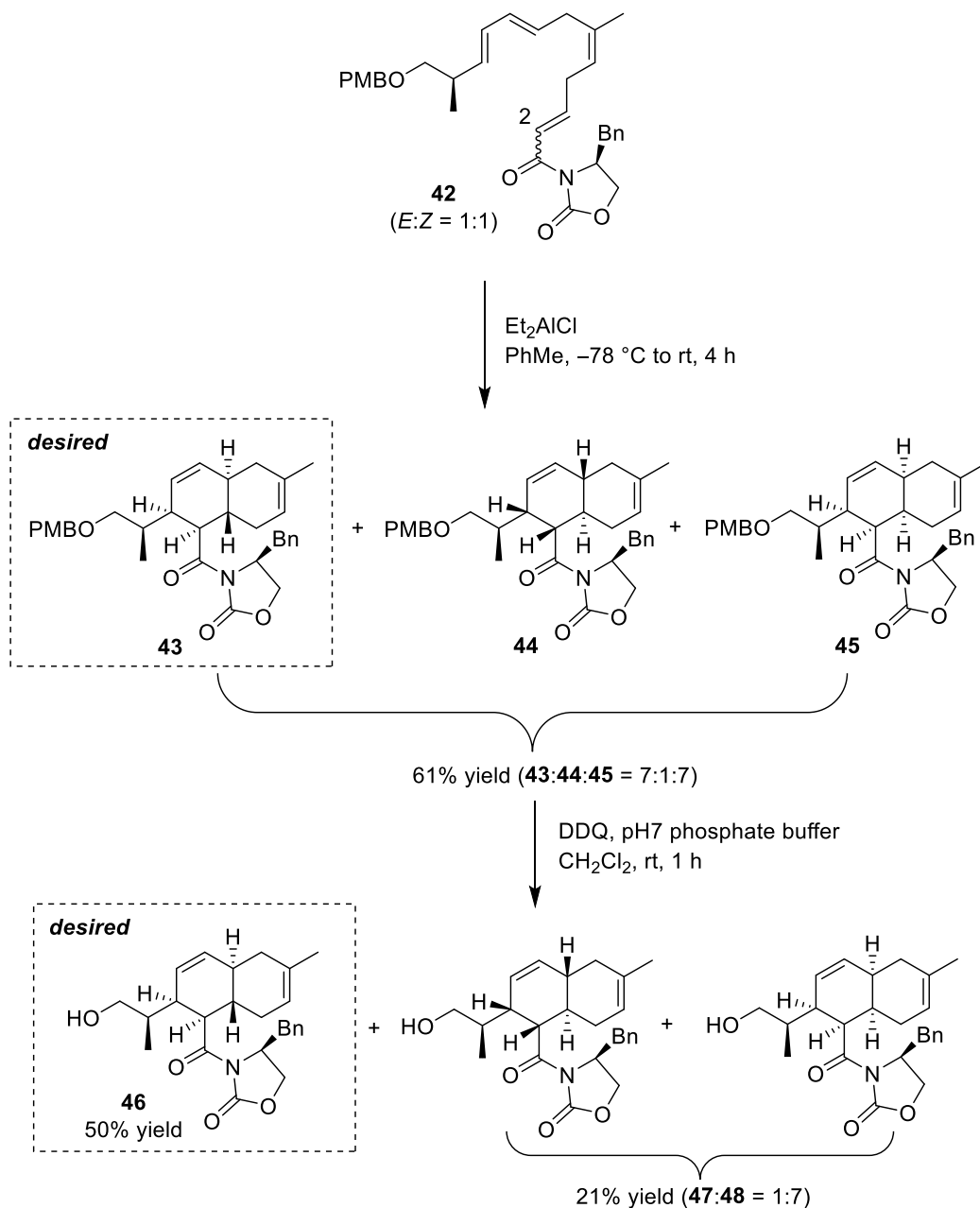
Although anthracimycin analogue **34** was efficient against Gram-positive bacteria, the activity towards Gram-negative bacteria was significantly absent. However, compound **34** exhibited a similar level of activity against Hela cells as **1**. The structural difference between **34** and **1** seems to have no effect on the cytotoxicity, but it decreased the potent biological activity of **34** against Gram-positive bacteria, which was 50–100 fold less active than that of **1** (Table 3).²³

Table 3: Biological activity of anthracimycin BII-2619 compared to anthracimycin

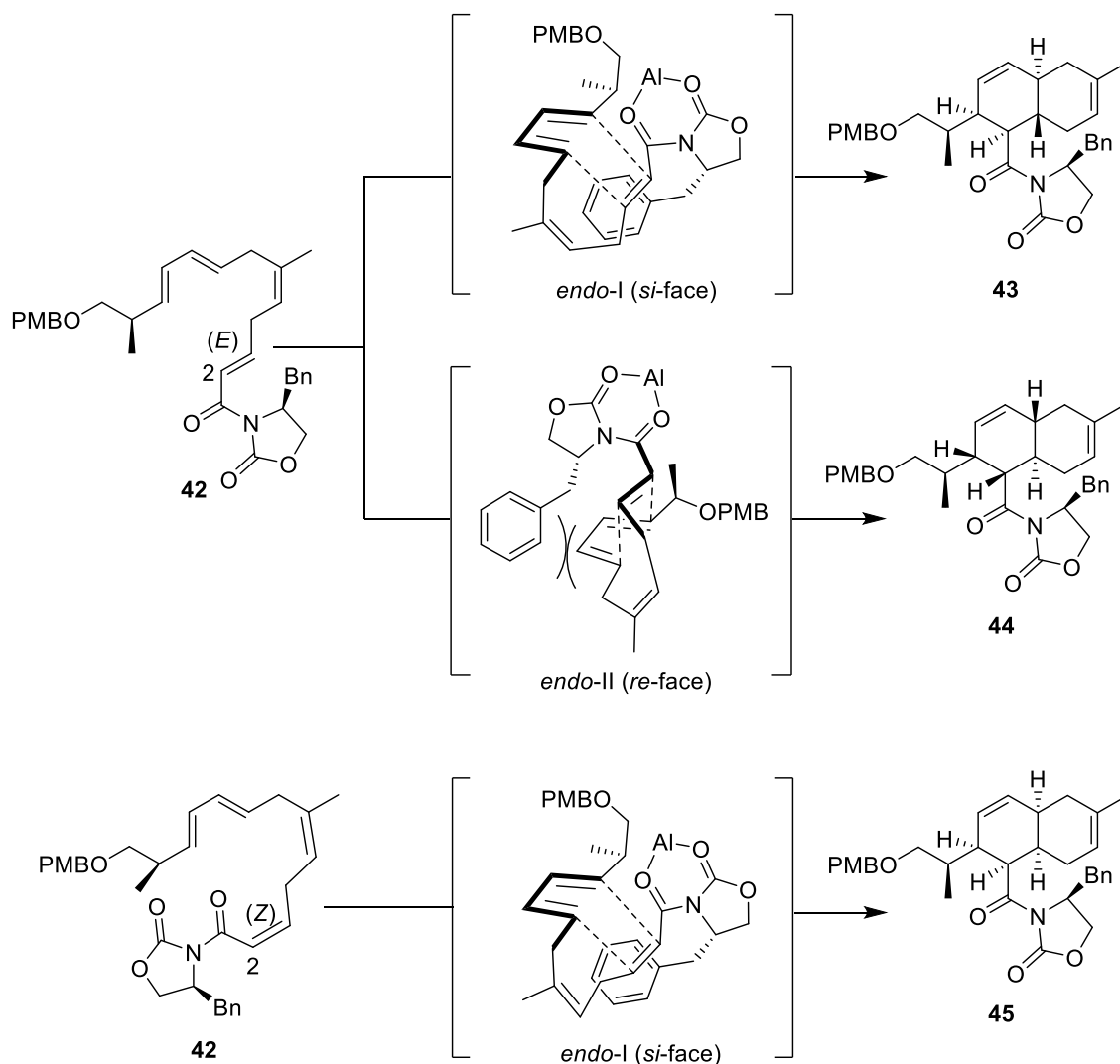
Target Organism or Cell Line	Activity ($\mu\text{g}/\text{mL}$)	
	anthracimycin (1)	BII-2619 (34)
Gram Positive Bacteria		
MRSA (ATCC 33591)	0.06	0.125
MRSA (ATCC 25923)	0.06	1
<i>Bacillus subtilis</i> (ATCC 6633)	0.5	64
<i>Enterococcus faecalis</i> (ATCC 29212)	0.125	8
Gram Negative Bacteria		
<i>Escherichia coli</i> (ATCC 25922)	>128	>128
<i>Pseudomonas aeruginosa</i> (ATCC 27853)	>128	>128
Mammalian Cells		
A549 Human lung carcinoma cells (ATCC CCL-185)	~32	35

1.6.3 The first total synthesis of anthracimycin by the Brimble group

Seven years after the isolation of anthracimycin (**1**), Brimble and co-workers reported the first total synthesis of **1** in the longest linear sequence of 20 steps as shown in **Scheme 3–6**.²⁶ They utilised a chiral auxiliary in the key *endo*-selective IMDA reaction inspired by the biomimetic pathway to access the *trans*-decalin core structure. The formation of IMDA precursor **42** began with a monosilylation of the commercially available 1,3-propanediol (**35**), followed by Swern oxidation to provide aldehyde **36** in 85% yield over two steps. Conversion of aldehyde **36** to α,β -unsaturated aldehyde **38** initially involved Stork–Zhao olefination to generate *in situ* iodo-ylide species, which was coupled with aldehyde **36** to afford *Z*-vinyl iodide **37** in 51% yield. Subsequent Kumada coupling of **37** with allylmagnesium chloride, followed by cross-metathesis with crotonaldehyde using the second-generation Grubbs catalyst furnished the conjugated aldehyde **38** in 63% yield over two steps. Elaboration of (*Z*)-diene commenced with Julia–Kocienski olefination of aldehyde **38** and sulfone **39** using Barbier-type protocol to generate the triene intermediate with a high *E*-selectivity (9:1 ratio). The resultant triene was then converted to the key IMDA substrate **42** in three steps via desilylation and oxidation with Dess–Martin periodinane (DMP) to give aldehyde, which was subjected to a gram-scale Wittig reaction with Evans' oxazolidinone phosphorane **41** to yield IMDA precursor **42** as an inseparable mixture of *E:Z* products (1:1) in 62% yield over two steps as illustrated in **Scheme 3**.²⁷



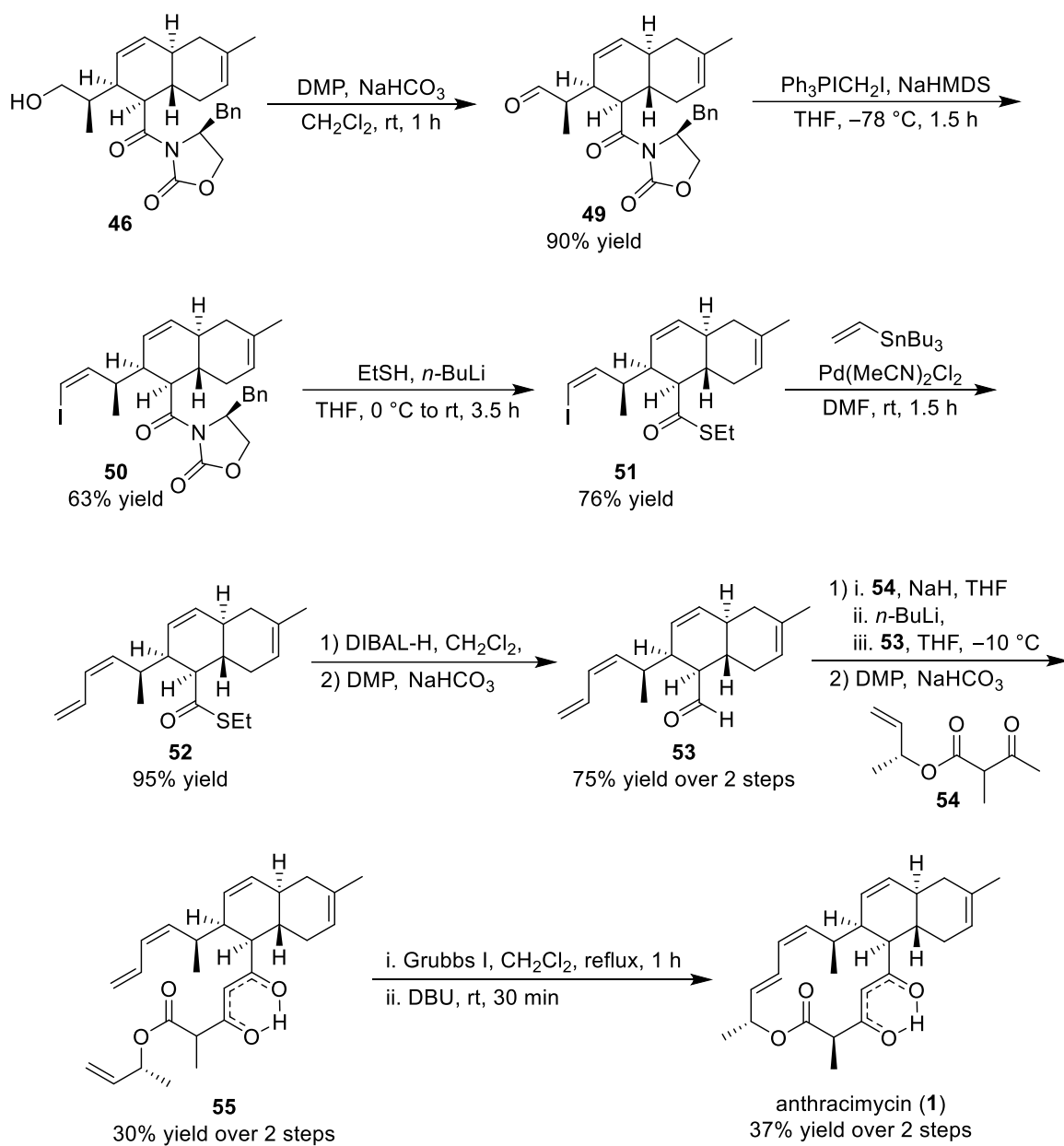
Scheme 4: Brimble's synthesis of *trans*-decalin scaffold **46**²⁶



Scheme 5: The proposed transition states of intramolecular Diels–Alder reaction²⁶

To complete the synthesis, alcohol **46** was converted to diene **52** in five steps. Initially, DMP oxidation of alcohol **46** smoothly delivered aldehyde **49**, which was subjected to Stork–Zhao olefination with iodomethylphosphonium salt to afford the requisite Z-vinyl iodide **50** in 63% yield. Owing to the attempted direct cleavage of a chiral auxiliary of **50** to an ester or aldehyde, thioester **51** was formed as an optional intermediate in 76% yield by coupling with ethanethiol. To install the diene portion, Stille coupling of **51** with tributyl(vinyl)tin provided the desired diene **52** in 95% yield. The thioester moiety of **52** was transformed to aldehyde **53** via DIBAL-H reduction, followed by oxidation with DMP. Next, condensation between aldehyde **53** and dianion of **54** delivered a mixture of diastereomer aldol products, which was oxidised with DMP to give a 1:1 mixture of RCM precursor **55** (C-2 epimers) in 30% yield over two steps. For the end-game, one-pot ring-closing metathesis of a mixture **55** using Grubbs I catalyst in refluxing dichloromethane generated a 1:1 mixture of

anthracimycin (**1**) and its epimer at C-2. The resultant was directly epimerised in the presence of DBU to furnish the natural product **1** in 37% yield as a single diastereomer as demonstrated in **Scheme 6**.²⁶



Scheme 6: Brimble's synthesis of anthracimycin²⁶

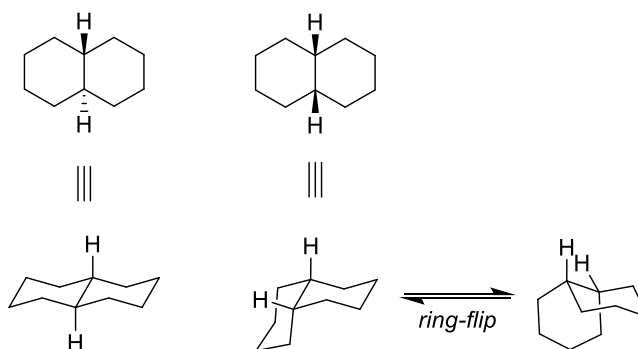
1.7 Justification for Clarke group work on the synthesis of anthracimycin

Although the first total synthesis of anthracimycin was published, we still work on this project in the Clarke group because we have been focusing on synthesising the anthracimycin core over the years. In particular, we aim to enhance the yield and stereoselectivity of the crucial step via different strategies to achieve the *trans*-decalin scaffold. Furthermore, the promising biological activities of anthracimycin inspire us to gain sufficient material from the total synthesis to further evaluate the unknown mode of its action. Finally, regarding Brimble's synthesis, they utilised an Evans chiral auxiliary to control the selectivity of the bioinspired intramolecular Diels–Alder cycloaddition of triene **42** to construct the *trans*-decalin framework. However, the desired *trans*-decalin **43** was obtained along with two diastereomers **44** and **45** in 61% yield with a 7:1:7 ratio (see **Scheme 4**).²⁶ In the Clarke group approach, we plan to improve on the overall stereoselectivity.

1.8 Decalin in natural products

As part of our ongoing programme devoted to synthesising the anthracimycin core, we have been working on alternative methods and different approaches for the efficient stereoselective formation of the decalin moiety. Recently, the discovery of novel strategies for synthesising decalin frameworks remains a priority in organic synthesis due to the importance of this skeleton as part of biologically relevant natural products.

Decalin (decahydronaphthalene) is two connected six-membered rings like those of cyclohexane, saturated hydrocarbon (bicyclo[4.4.0]decane). However, there are two possible decalins, *cis*- and *trans*- as illustrated in **Scheme 7**. Axial and equatorial bonds can join the two chair structures with the ring junction hydrogens on the same side known as *cis*-decalin. Each ring in *cis*-decalin can undergo a ring-flip forming two different chair-chair conformations of equal energy. In contrast, *trans*-decalin can be constructed by equatorial bonds from two rings with the opposite side of a hydrogen pair on the ring junction. *Trans*-decalin is incapable of ring flipping because it is locked in position. In terms of stability, *trans*-decalin is more energetically stable because of less steric interactions.



Scheme 7: Structures of *trans*-decalin and *cis*-decalin

The decalin structural motif is present in a wide range of secondary metabolites produced by microorganisms, mainly fungi and actinomycetes.²⁸ The decalin ring system is typically linked to highly multi-functionalised or architecturally intricate functional groups, displaying structural and functional diversity. Consequently, this class of natural products consisting of a decalin scaffold possesses remarkable and diverse biological properties. Herein, the structures and biological activities of selected natural products containing a decalin motif will be reviewed.

The selected examples of natural products having a decalin scaffold are grouped by different biological activities. The first group having a potent antimalarial activity is shown in **Figure 5**. Chlorotonil A (**56**), having a carbon skeleton similar to anthracimycin (**1**), was isolated from the myxobacteria *Sorangium cellulosum*.²⁹ It was originally found to exhibit promising antimalarial activity *in vitro* and *in vivo* against *Plasmodium falciparum* strains with a 50% inhibitory concentration between 4 and 32 nM.³⁰ The second antimalarial natural product kalihinol A (**57**) was initially derived from the marine sponge *Acanthella* sp.³¹ Diterpenoid **57** bearing isocyano and chlorine moieties, shows remarkable cytotoxicity against *Plasmodium falciparum* with an EC₅₀ value of 1.2 nM.³² In addition, compound **57** was discovered to display *in vitro* activity against *Bacillus subtilis*, *Staphylococcus aureus*, and *Candida albicans*.³¹ Another marine isocyano diterpene demonstrating antimalarial activity is amphilectene (**58**), which is highly active towards chloroquine-resistant (W2) *P. falciparum* (IC₅₀ = 31 nM).³³

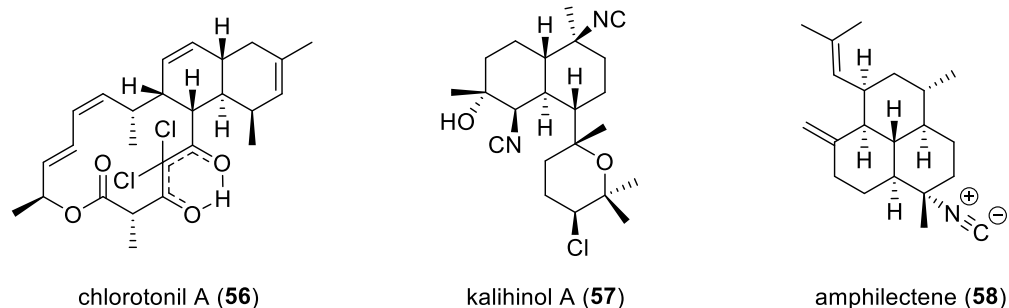


Figure 5: Structures of selected antimalarial natural products containing a decalin

The second group of natural products containing a decalin system displays remarkable anticancer activities as depicted in **Figure 6**. Popolohuanone E (**59**) was isolated from the sponge *Dysidea*, exhibiting a selective cytotoxicity against A549 non-small cell lung cancer cells ($IC_{50} = 2.5 \mu\text{g/mL}$) and P388 murine leukemia cells ($IC_{50} = 20 \mu\text{g/mL}$), and being a potent inhibitor of Topoisomerase II.³⁴ Streptosetin A (**60**) was discovered from yeast and identified during the screening of the extract libraries of marine-derived actinomycetes. Compound **60** displays inhibition of the human class III histone deacetylases (HDACs SIRT 1 and 2), which is attractive as other inhibitors demonstrate apoptotic and autophagic cell death in breast cancer cell lines.³⁵ The labdane diterpene andrographolide **61** was derived from the Indian medicinal plant *Andrographis paniculata* of the family *Acanthaceae* known as the “King of Bitters”.³⁶ Andrographolide (**61**) demonstrates a potent anticancer activity against human colorectal carcinoma Lovo cells by inhibiting cell cycle progression and also shows an active cytotoxic activity against KB (human epidermoid leukaemia) and P388 (lymphocytic leukaemia) cells.³⁷ Myceliothermophin E (**62**) containing a tetramic acid moiety was originally isolated from the methanolic extract of *Myceliophthora thermophila* by Wu and co-workers in 2007. Compound (**62**) demonstrates significant inhibitory effects against several human cancer cell lines, namely A549 lung carcinoma ($IC_{50} = 0.26 \mu\text{g/mL}$), Hep3B hepatocellular carcinoma ($IC_{50} = 0.41 \mu\text{g/mL}$), MCF-7 breast adenocarcinoma ($IC_{50} = 0.25 \mu\text{g/mL}$) and HepG2 hepatoblastoma ($IC_{50} = 0.28 \mu\text{g/mL}$).³⁸ Crotogoudin (**63**) derived from *Croton goudotii*, Madagascan plants, shows marked cytotoxic activities for human tumor cell lines such as human oral epidermoid carcinoma (KB, $IC_{50} = 1.5 \pm 0.03 \mu\text{M}$), human colon adenocarcinoma (HT29, $IC_{50} = 1.9 \pm 0.25 \mu\text{M}$), human lung adenocarcinoma (A549, $IC_{50} = 0.54 \pm 0.02 \mu\text{M}$) and human promyelocytic leukemia (HL60, $IC_{50} = 0.49 \pm 0.01 \mu\text{M}$) cell lines.³⁹

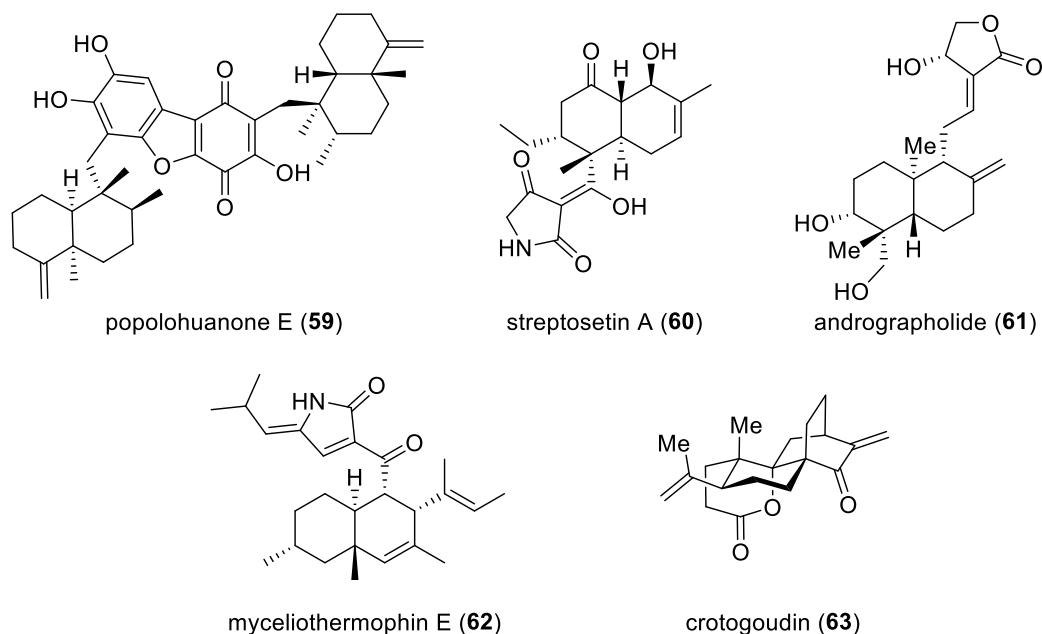


Figure 6: Structures of selected anticancer natural products containing a decalin

Next, antibiotics are represented in the third group as illustrated in **Figure 7**. A novel 17-membered polycyclic polyketide alchivemycin A (**64**) was discovered from the culture extract of a plant-derived actinomycete *Streptomyces* sp.⁴⁰ Alchivemycin A (**64**) displays a potent antimicrobial activity against Gram-positive *Micrococcus luteus* with a MIC value of 50 nM and a strong inhibitory effect against tumor cell invasion with an IC₅₀ value of 0.34 μ M with no indication of toxicity.⁴¹ Platencin (**65**) was isolated from *S. platensis* MA 7339, in a soil sample collected in Mallorca, Spain. Compound **65** shows potent antibiotic activity against Gram-positive bacteria by being an inhibitor of two proteins required for bacterial fatty acid biosynthesis, β -ketoacyl-acyl carrier protein (ACP) synthase II (FabF) and III (FabH).⁴² Moreover, compound **65** exhibits activities against MRSA-resistant bacteria (1 μ g/mL) and vancomycin-resistant *Enterococcus faecium* (<0.06 μ g/mL), and against *S. aureus* infection in a mouse model without showing cytotoxicity effects.⁴³

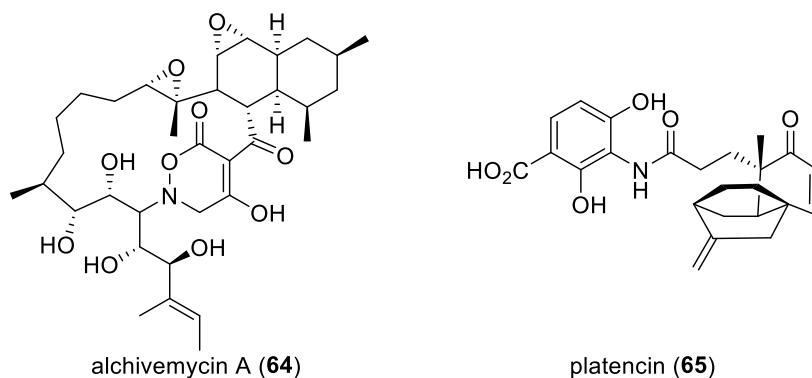


Figure 7: Structures of selected antibiotic natural products containing a decalin

The last group of natural compounds with a decalin moiety is found to have several interesting biological features in addition to antimalarial, anticancer, and antibacterial activities as shown in **Figure 8**. Rhodexin A (**66**) is one of a series of cardiac glycosides isolated from the leaves and roots of the Japanese evergreen *Rhodea japonica*.⁴⁴ Compound **66** not only exhibits a cardiotoxic activity but also has an active effect on human leukemia K562 cells ($IC_{50} = 19$ nM) and a potent antiproliferative activity to inhibit the synthesis of hypoxia inducible factor 1 (HIF-1R).⁴⁵ Triptolide (**67**), a Chinese traditional Chinese herbal medicine known as “Thunder God Vine” was derived from the extracts of *Tripterygium wilfordii* Hook F. The diterpenoid triepoxide **67** displays various promising antiproliferative, anti-fertility, anti-osteoporosis, immunosuppressive and anti-inflammatory activities.⁴⁶ Natural insecticide azadirachtin (**68**) is a C-seco limonoid, first isolated as an insect antifeedant from the Indian neem tree *Azadirachta indica*.⁴⁷ Compound **68** shows impressive antifeedant and growth disrupting effects against a wide range of insect species (> 200) without significant toxicity towards higher organisms.⁴⁸ Crotonin (**69**) is a 19-nor-clerodane, obtained from the *Croton* genus (bark and leaves of trees).⁴⁹ The crotonin family demonstrates various pharmacological activities, including antitumorogenic, anti-ulcerogenic, anti-hypoglycemic, and vasorelaxant activity.⁵⁰ Indole terpenoid anominine (**70**) was initially isolated from *Aspergillus* spp. by Gloer and co-workers. A family of naturally occurring indole diterpenoids shows interesting antiinsectant, antiviral, and anticancer activities.⁵¹

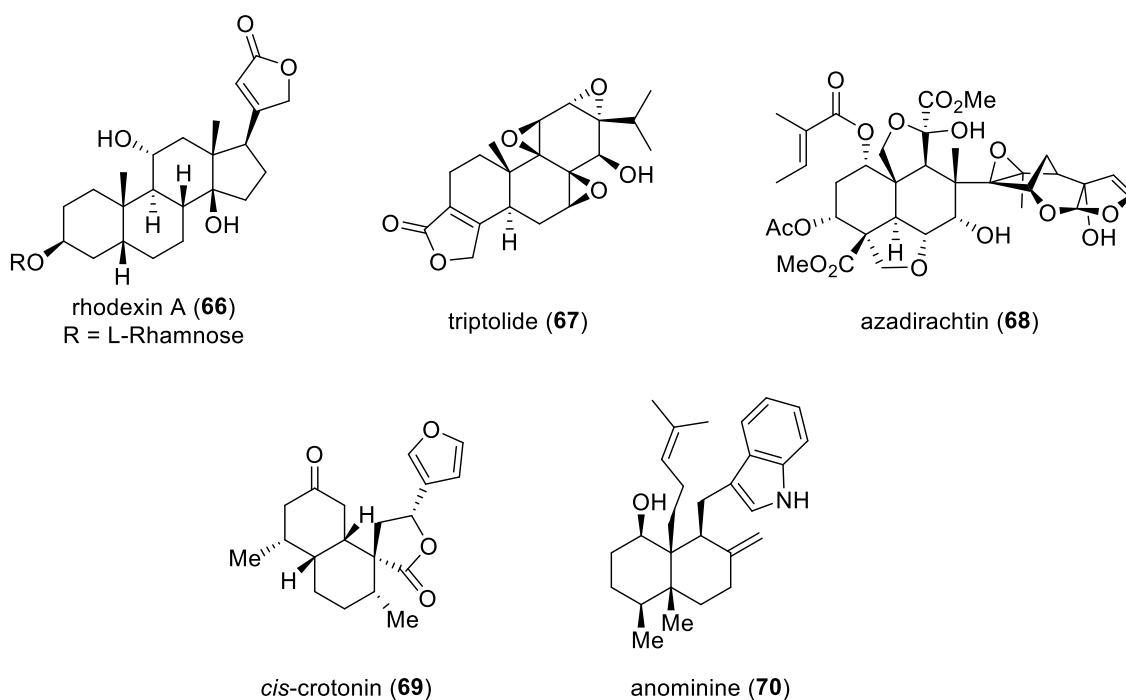


Figure 8: Structures of selected biologically active products containing a decalin

1.9 Synthesis of natural products possessing a highly functionalised decalin

Many synthetic organic research groups are becoming more interested in the synthetic programmes of enantioenriched decalin structural motifs found in natural products as a result of their diverse and outstanding biological profiles and complicated molecular architectures.²⁸ Although numerous synthetic methods have been developed for synthesising the decalin ring system, new strategies are still highly desirable due to the structural diversity of the requisite natural products.⁵² In this section, the literature precedent for the syntheses of decalin motifs mainly involving intra- and intermolecular Diels–Alder cycloadditions, intramolecular aldol reaction, intramolecular Sakurai addition, nucleophilic and anionic cyclisation, and cation- or radical-induced polyene cyclisation will be reviewed.

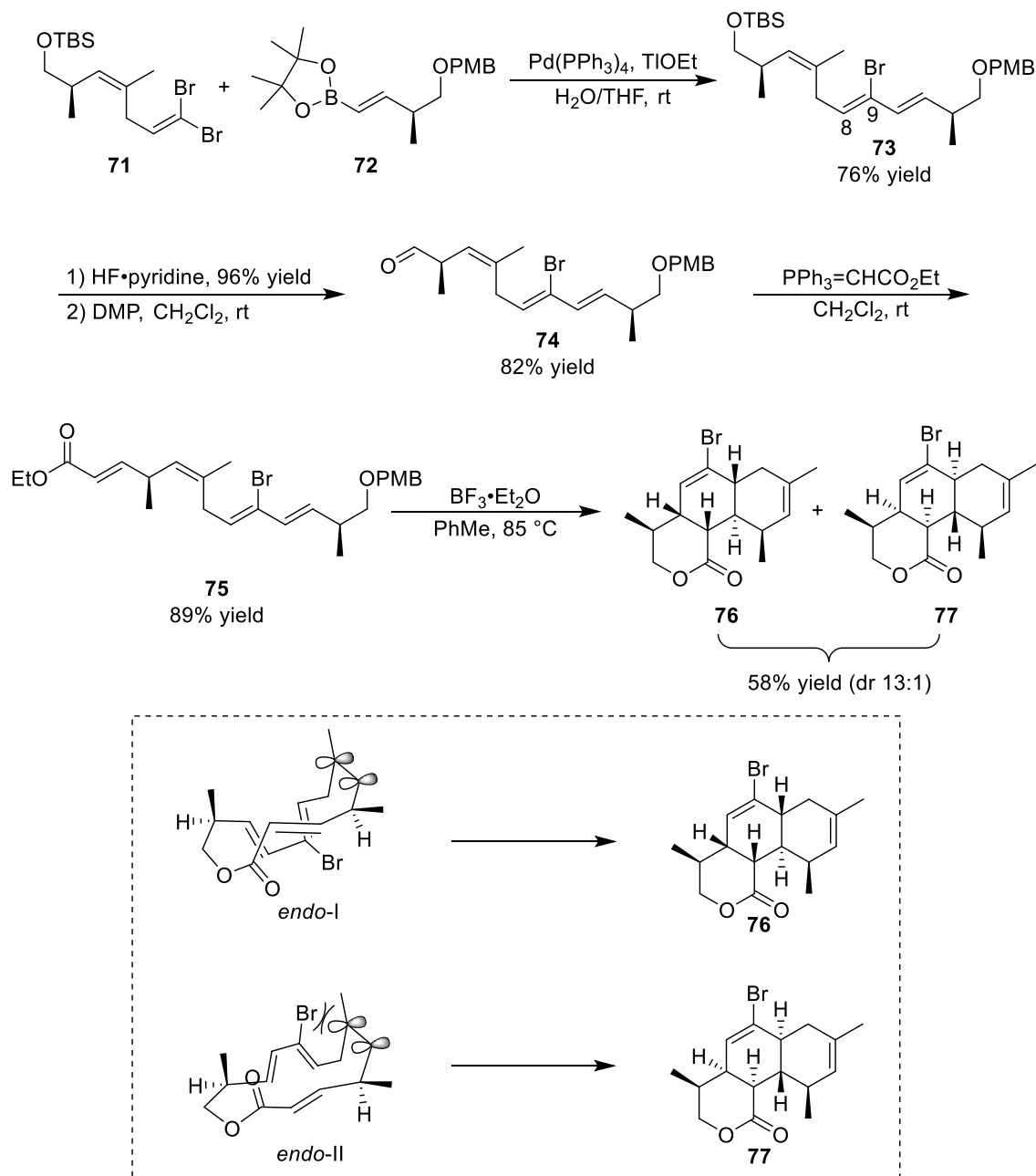
1.9.1 Diels–Alder cycloaddition approach

The Diels–Alder cycloaddition, the reaction between a conjugated diene and a substituted alkene (dienophile), is divided into intra- and intermolecular reactions to form unsaturated six-membered rings with reasonable control over the regio- and stereoselectivity. Hence, it has served as a powerful and widely applied method for the synthesis of decalin frameworks.

1.9.1.1 Intramolecular Diels–Alder cycloaddition

The intramolecular Diels–Alder (IMDA) reaction has been widely employed to construct decalin scaffolds, inspired by their biosynthesis. Selected examples for synthesising decalin ring systems via an intramolecular Diels–Alder cycloaddition will be illustrated. In 2008, Rahn and Kalesse reported the first total synthesis of chlorotonil A (**56**), containing a *trans*-decalin ring system as the core structure and having a carbon skeleton similar to anthracimycin (**1**) as shown in **Scheme 8**.⁵³ The IMDA precursor **75** was prepared in four steps from dibromoolefin **71**. The Suzuki cross-coupling between olefin **71** and boronic ester **72** in the presence of Pd(PPh₃)₄ catalyst constructed the (*E*)-double bond at C8–C9 to provide intermediate **73** in 76% yield. The conversion of silyl ether **73** to unsaturated ester **75** was carried out through desilylation with HF in pyridine, oxidation with Dess–Martin periodinane (DMP), followed by Wittig reaction to provide IMDA precursor **75** in high yield.

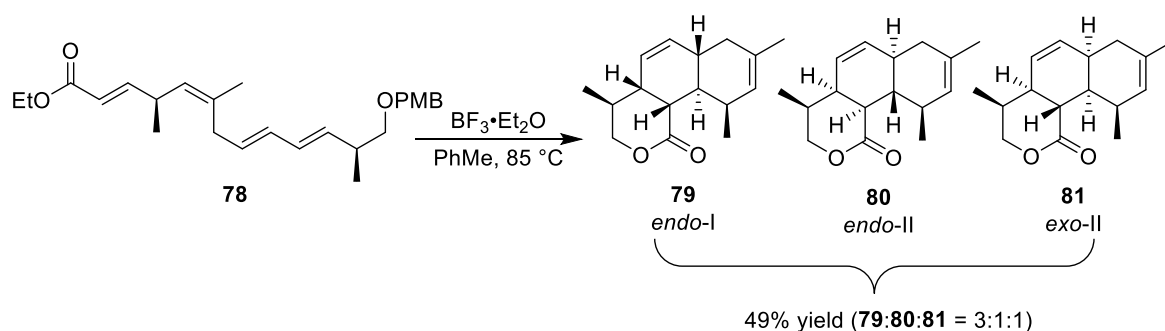
The key transannular IMDA reaction of **75** was carried out with $\text{BF}_3 \cdot \text{Et}_2\text{O}$ in toluene at 85°C for 3 hours, leading to simultaneous removal of the PMB group, transesterification, and Diels–Alder reaction. Due to the directing effect of the bromine substituent, *trans*-decalin **76** was obtained via a favoured *endo*-I transition state with a diastereomeric ratio of 13:1.⁵³



Scheme 8: Kalesse's synthesis of *trans*-decalin **76**, the core structure of chlorotonil A⁵³

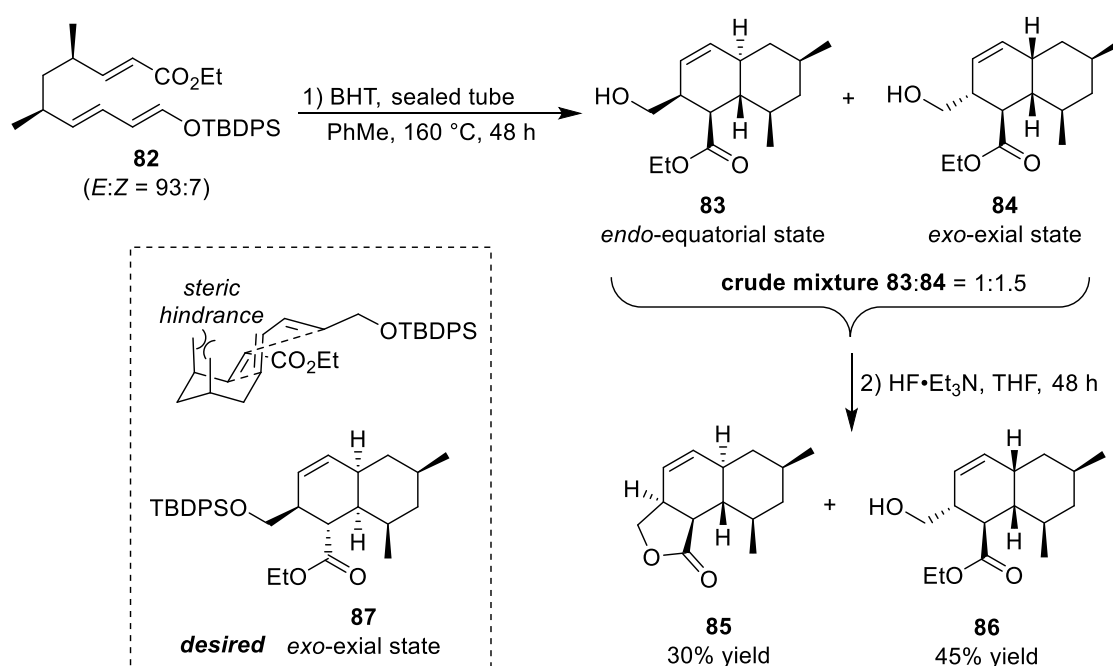
However, the stereoselectivity of the key intramolecular Diels–Alder cycloaddition was decreased when exploiting triene precursor **78** without the directing group effect of the bromine substituent under the same reaction conditions. A mixture of three cycloadducts

was obtained in 49% yield with a 3:1:1 ratio of the desired *endo*-I product **79** along with *endo*-II product **80** and *exo*-product **81**, respectively (**Scheme 9**).⁵³



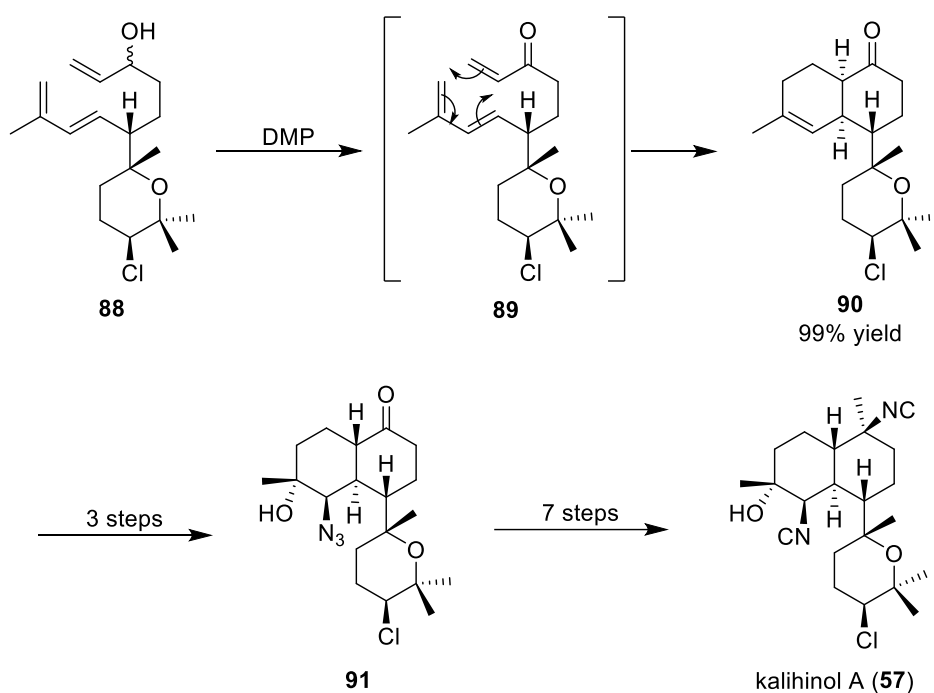
Scheme 9: The directing effect of the bromine substituent on the IMDA precursor⁵³

The second example utilising an intramolecular Diels–Alder cycloaddition to construct the *epi*-core structure of alchivemycin A (**64**) was illustrated by Lei and co-workers in 2016 (**Scheme 10**). Triene **82** was used as an IMDA precursor. The crucial IMDA cycloaddition of **82** was performed in toluene under thermal conditions to provide an inseparable mixture of **83** and **84**. The resultant mixture could be separated by column chromatography upon silyl deprotection with triethylamine trihydrofluoride to give lactone *trans*-decalin **85** as an *endo*-adduct and alcohol *cis*-decalin **86** as an *exo*-adduct in 30% and 45% yields, respectively. However, the desired *cis*-decalin **87** could not be obtained, due to a severe 1,3-diaxial methyl interaction of a high energy *exo*-axial transition state.⁴¹



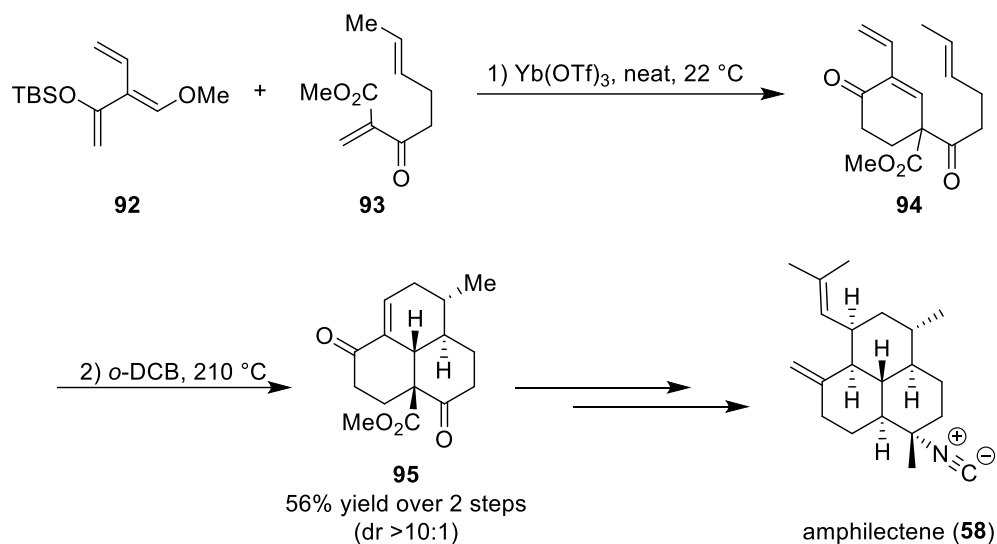
Scheme 10: Lei's synthesis of the *epi*-core structure of alchivemycin A⁴¹

The following example is presented on the selective intramolecular Diels–Alder reaction to form a *cis*-decalin, which is the functionalised core structure of kalihinol A (**57**) as shown in **Scheme 11**. Miyaoka and co-workers demonstrated the formation of *cis*-decalin **90** through the oxidation of allylic alcohol **88** with Dess–Martin periodinane to generate the unsaturated ketone intermediate **89**. The spontaneous cyclisation of **89** via an *endo*-selective intramolecular Diels–Alder cycloaddition furnished *cis*-decalin **90** as a single product in excellent yield. *Cis*-decalin **90** was then epimerised to *trans*-decalin **91**, which was functionalised to kalihinol A (**57**) in seven steps.⁵⁴



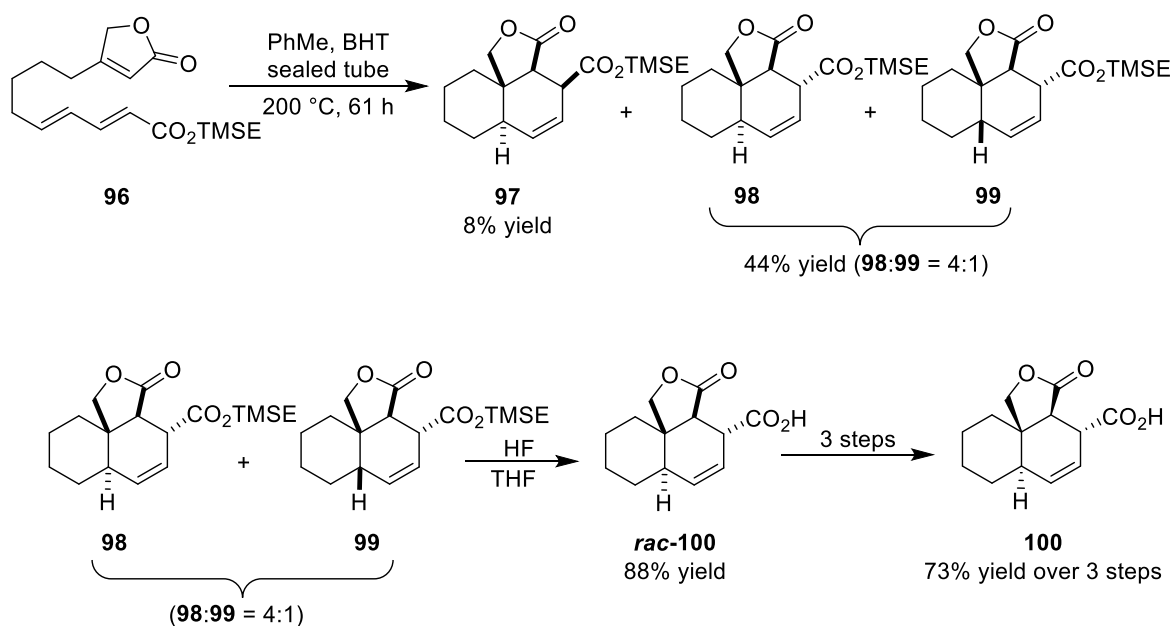
Scheme 11: Miyaoka's synthesis of *trans*-decalin **91**, the core structure of kalihinol A⁵⁴

Another example of synthesising the amphilectene skeleton containing a *cis*-decalin scaffold was described by Shenvi and Pronin (**Scheme 12**). The intermolecular cycloaddition reaction of Danishefsky dendralene **92** with methyl ester **93** in the presence of 5 mol% Yb(OTf)₃ at ambient temperature produced the intermediate cross-conjugated enone **94**. Upon heating of **94** in *o*-dichlorobenzene in a microwave reactor, a second Diels–Alder cycloaddition furnished tricycle **95** in 56% yield over two steps with a diastereomeric ratio of >10:1. Tricyclic ring system **95** bearing a *cis*-decalin scaffold was then used as a core structure for the synthesis of amphilectene (**58**).⁵⁵



Scheme 12: Shenvi's synthesis of decalin **95**, the core structure of amphilectene⁵⁵

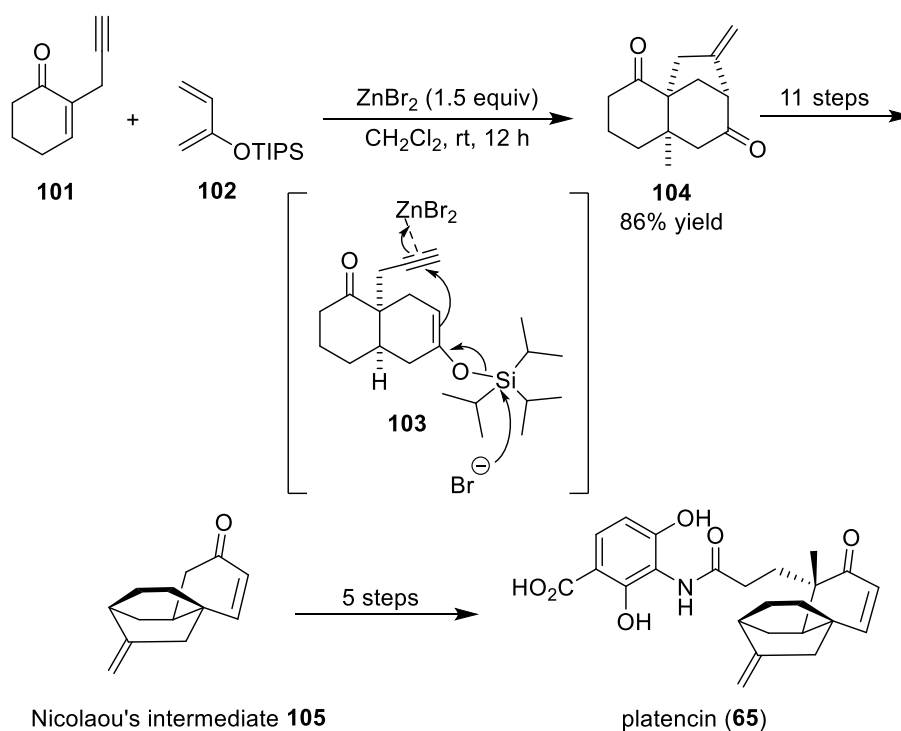
The last example of exploiting an IMDA reaction to form a decalin motif is illustrated by the formation of the core structure of azadirachtin (**Scheme 13**). Murai and co-workers investigated the IMDA cycloaddition of triene **96** in toluene at 200 °C in a sealed tube to provide three diastereomers: *trans*-decalin **97** in 8% yield and an inseparable mixture of *trans*-decalin **98** and *cis*-decalin **99** in 44% yield with a 4:1 ratio. The mixture of **98** and **99** was then treated with hydrogen fluoride to give racemic carboxylic acid *trans*-decalin **100**, which was subjected to resolution furnishing enantioenriched azadirachtin building block **100** in 73% yield over three steps.⁵⁶



Scheme 13: Murai's synthesis of decalin **100**, the core structure of azadirachtin⁵⁶

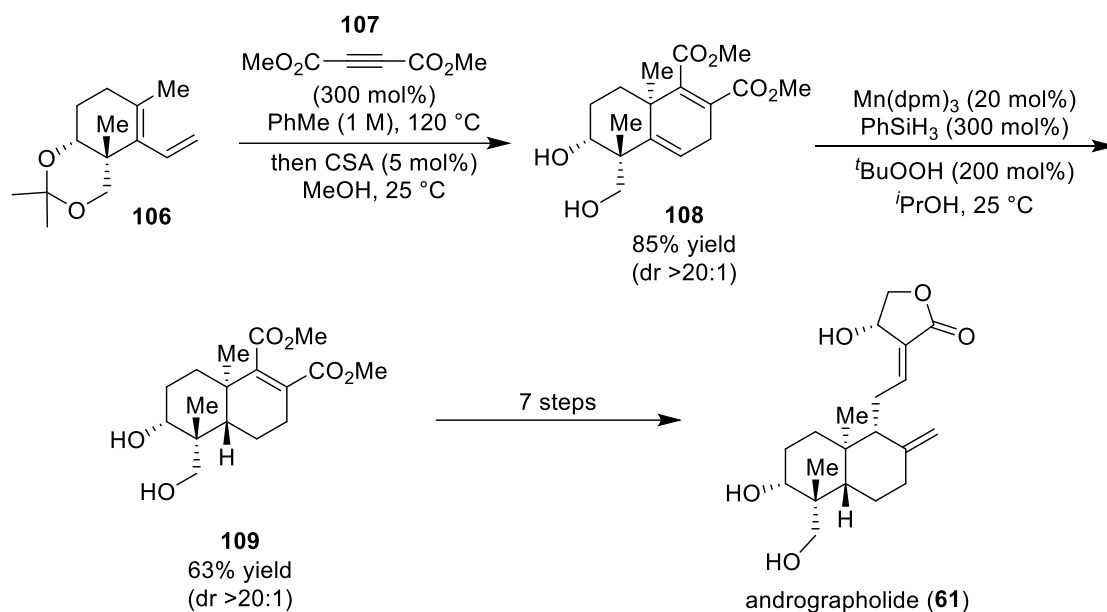
1.9.1.2 Intermolecular Diels–Alder cycloaddition

Intermolecular Diels–Alder cycloaddition can also be used to accomplish the synthesis of six-membered rings. A couple of examples are reviewed in this part. Lee and co-workers reported the use of ZnBr_2 to catalyse a Diels–Alder/carbocyclisation cascade cyclisation reaction to form Nicolaou's intermediate **105**, the core structure of platencin (**65**), as depicted in **Scheme 14**. The tricyclic ring **104** was prepared via the Diels–Alder reaction of enone **101** with silyl diene **102**. The use of mild-dual mode ZnBr_2 in this crucial step generated the σ -complex with enone **101** for inducing [4+2] cycloaddition to form the cycloadduct **103**. Subsequently, the π -complex formation of **103** was induced by the Lewis acid leading to a spontaneous carbocyclisation without causing hydrolysis of the silyl enol ether to yield tricyclic ring **104** in good yield. Finally, the intermediate **104** was functionalised to Nicolaou's intermediate **105**, the building block to achieve platencin (**65**).^{43,57}



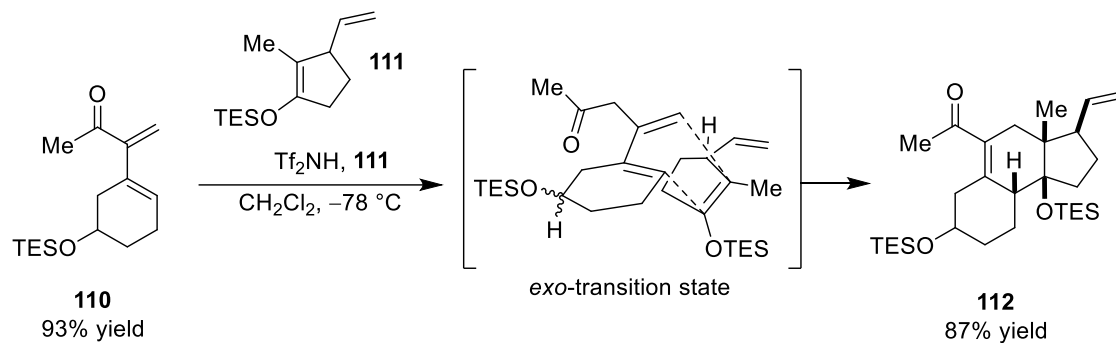
Scheme 14: Lee's synthesis of Nicolaou's intermediate **105**, the core structure of platencin^{43,57}

Krische and co-workers also utilised this method to synthesise the core structure of andrographolide A (**61**) as shown in **Scheme 15**. Diels–Alder cycloaddition of diene **106** with methyl acetylene dicarboxylate (DMAD) **107** in refluxing toluene, followed by *in situ* hydrolysis of the acetonide moiety with camphorsulfonic acid gave cycloadduct **108** in 85% yield with high stereoselectivity. Reduction of **108** via hydrogen atom transfer (HAT) was performed in the presence of catalytic $\text{Mn}(\text{dpm})_3$ to deliver *trans*-decalin **109**, which was then functionalised to give the natural product **61** in seven steps.³⁶



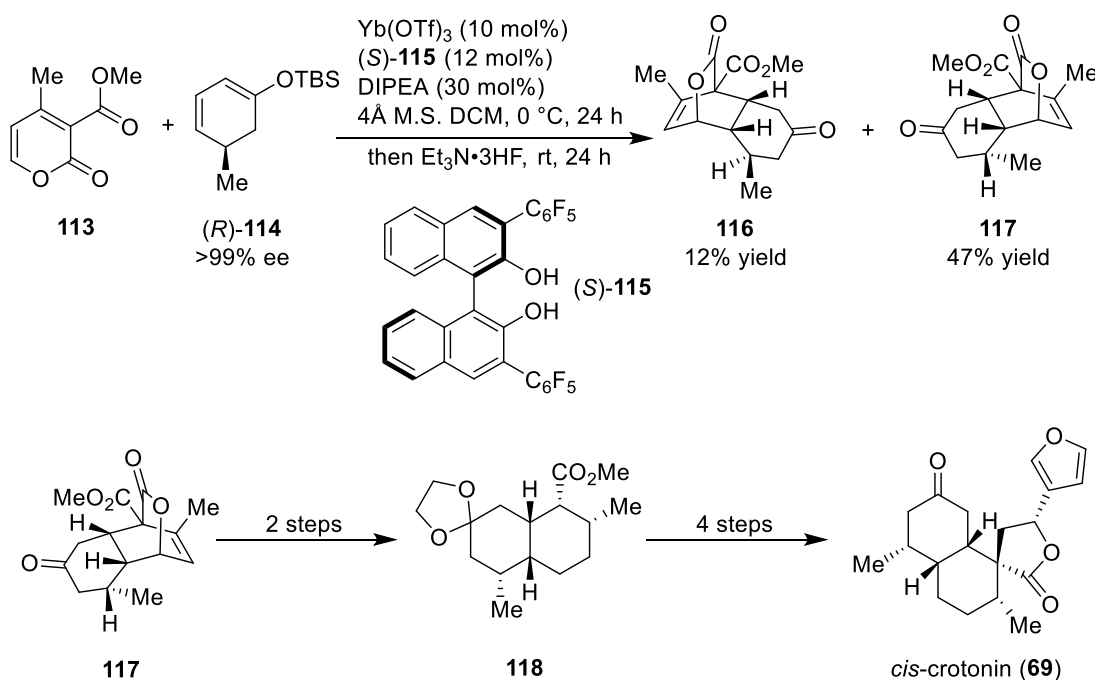
Scheme 15: Krische's synthesis of *trans*-decalin **109**, the core structure of andrographolide³⁶

Another type of intermolecular Diels–Alder cycloaddition is an inverse-electron-demand Diels–Alder reaction. This approach is widely applied for natural product syntheses. The Jung group exploited this method to construct tricyclic system **112**, which was prepared from diene **110** and vinyl silyl enol ether **111** under the conditions of triflimide (10 mol%) as a Lewis acid in dichloromethane at $-78\text{ }^\circ\text{C}$. After 5 minutes, the desired tricyclic ring **112** was formed through a selective *exo*-transition state in good yield as a 2:1 mixture of two diastereomers at the secondary silyl ether group (**Scheme 16**).⁴⁵



Scheme 16: Jung's synthesis of tricyclic ring **112**, the core structure of rhodexin A⁴⁵

Another example of using inverse-electron-demand Diels–Alder reaction to form a decalin ring was demonstrated by Cai *et al.* (**Scheme 17**). The core structure of *cis*-crotonin **117** was obtained via the stereodivergent Diels–Alder reaction of pyrone **113** and enantiopure dienophile **114** in the presence of 10 mol% $\text{Yb}(\text{OTf})_3$ and 12 mol% chiral ligand (*S*)-**115** to afford two diastereomers **116** and **117** in 12% and 47% yields, respectively upon *in situ* desilylation. The major *cis*-decalin **117** was carried forward to accomplish the synthesis of natural product **69**.⁵²



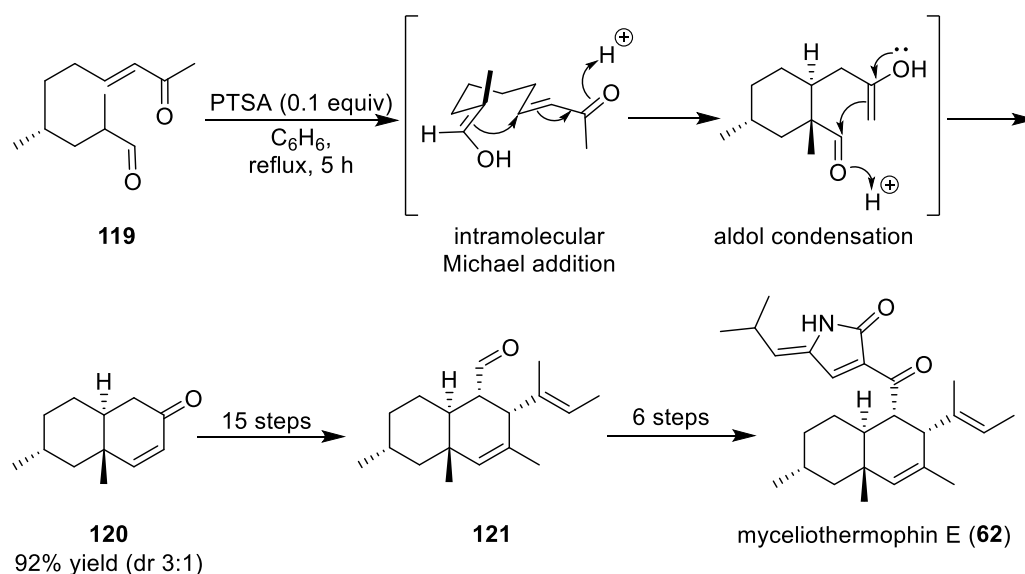
Scheme 17: Cai's synthesis of *cis*-decalin **117**, the core structure of *cis*-crotonin⁵²

1.9.2 Nucleophilic and anionic cyclisation approaches

The nucleophilic and anionic cyclisation is a type of condensation reaction providing a powerful method for constructing six-membered rings. A few examples accomplished via different cyclisations are given in this part.

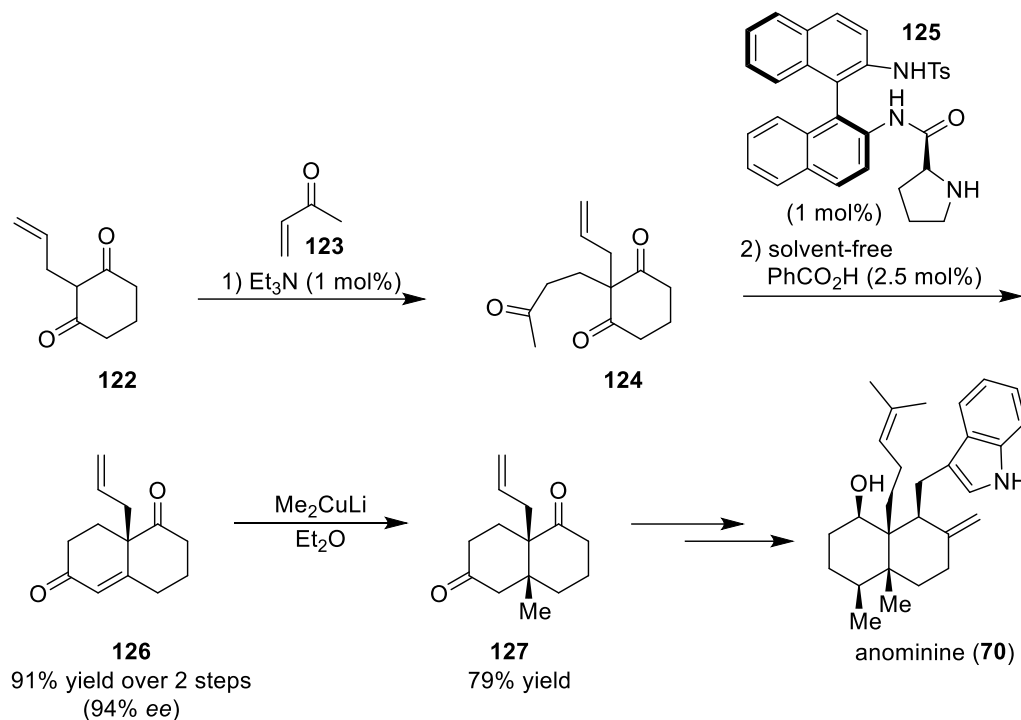
1.9.2.1 Robinson annelation

Nicolaou and co-workers reported the synthesis of *trans*-decalin scaffold **120** as a core structure of myceliothermophin E (**62**) via a cascade reaction (**Scheme 18**). Acid-catalysed cyclisation of ketoaldehyde **119** initially proceeded through an intramolecular Michael addition, followed by an aldol condensation to furnish *trans*-decalin **120** in excellent yield with a 3:1 diastereomeric ratio.⁵⁸



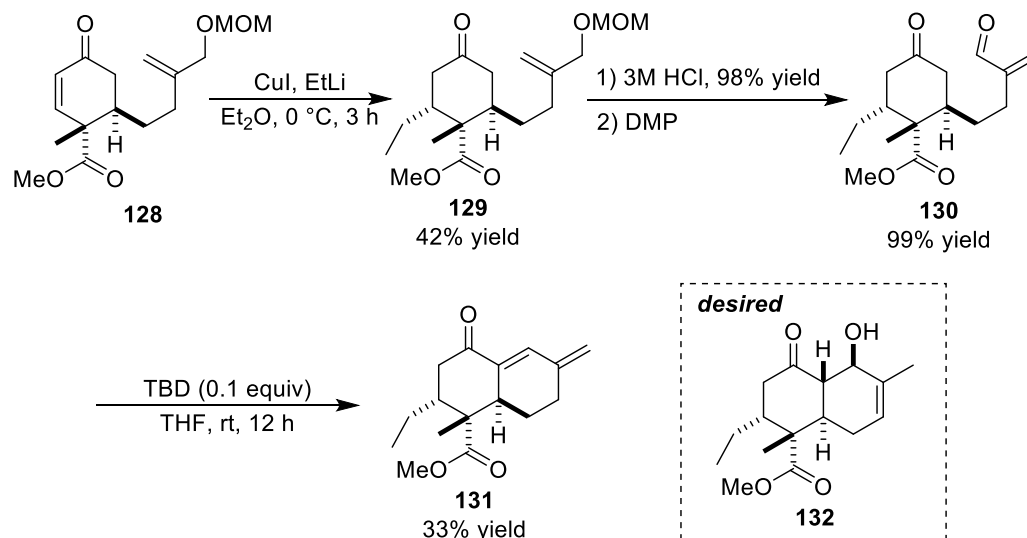
Scheme 18: Nicolaou's synthesis of *trans*-decalin **120**, the core structure of myceliothermophin E⁵⁸

In addition, the core structure of anominine (**70**) was also completed through an asymmetric Robinson annelation (**Scheme 19**). A sequence of Michael addition of diketone **122** with methyl vinyl ketone **123** to give triketone intermediate **124**, followed by *N*-Ts- (S_a) -binam-L-Pro-catalysed aldol condensation under solvent-free conditions afforded highly enantioenriched decalin **126** in excellent yield. Conjugate addition to **126** furnished the requisite *cis*-decalin **127**, an essential building block for anominine (**70**).^{59,60}



Scheme 19: Bradshaw's synthesis of *cis*-decalin **127**, the core structure of anominine^{59,60}

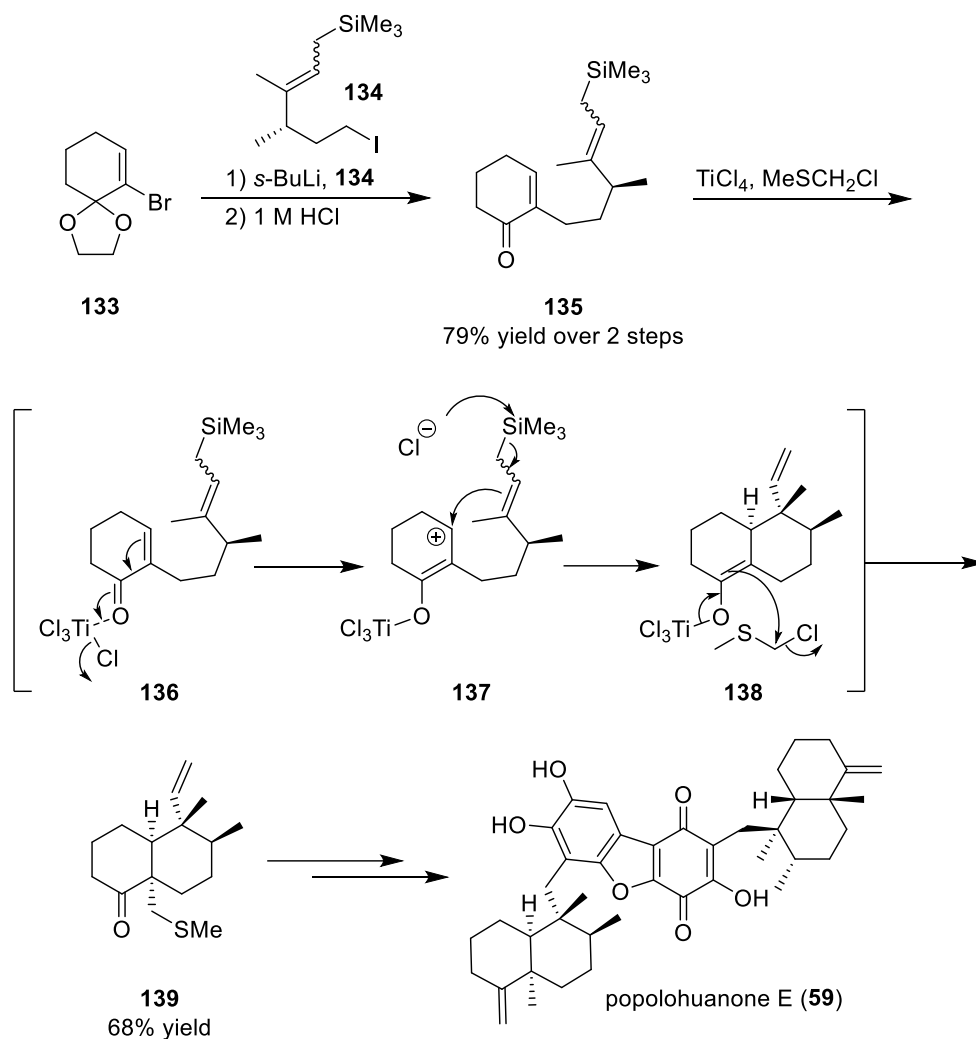
The last example of preparing a decalin moiety by intramolecular aldol reaction is demonstrated in **Scheme 20**. Maier and Hess reported the undesired precursor **131** during the attempted synthesis of streptosestin A (**60**). The preparation of aldol precursor **130** began with the introduction of a sidechain by organocuprate addition to enone **128**, followed by removal of the MOM group under acidic conditions, to deliver allylic alcohol in excellent yield. The resultant alcohol was then oxidised with Dess–Martin periodinane to furnish ketoenal **130** in quantitative yield. To generate the aldol adduct **132**, ketoenal **130** was then treated with the guanidine base 1,5,7-triazabicyclo[4.4.0]dec-5-en (TBD) in THF. However, the reaction could not be stopped at the aldol product **132**, but instead provided the condensation product **131** in 33% isolated yield. The facile dehydration is proposed to take place as the axial OH group from the aldol reaction is antiperiplanar to the bridgehead hydrogen.⁶¹



Scheme 20: Maier's synthesis of the advanced precursor **131** for streptosetin A⁶¹

1.9.2.2 Allylation reaction

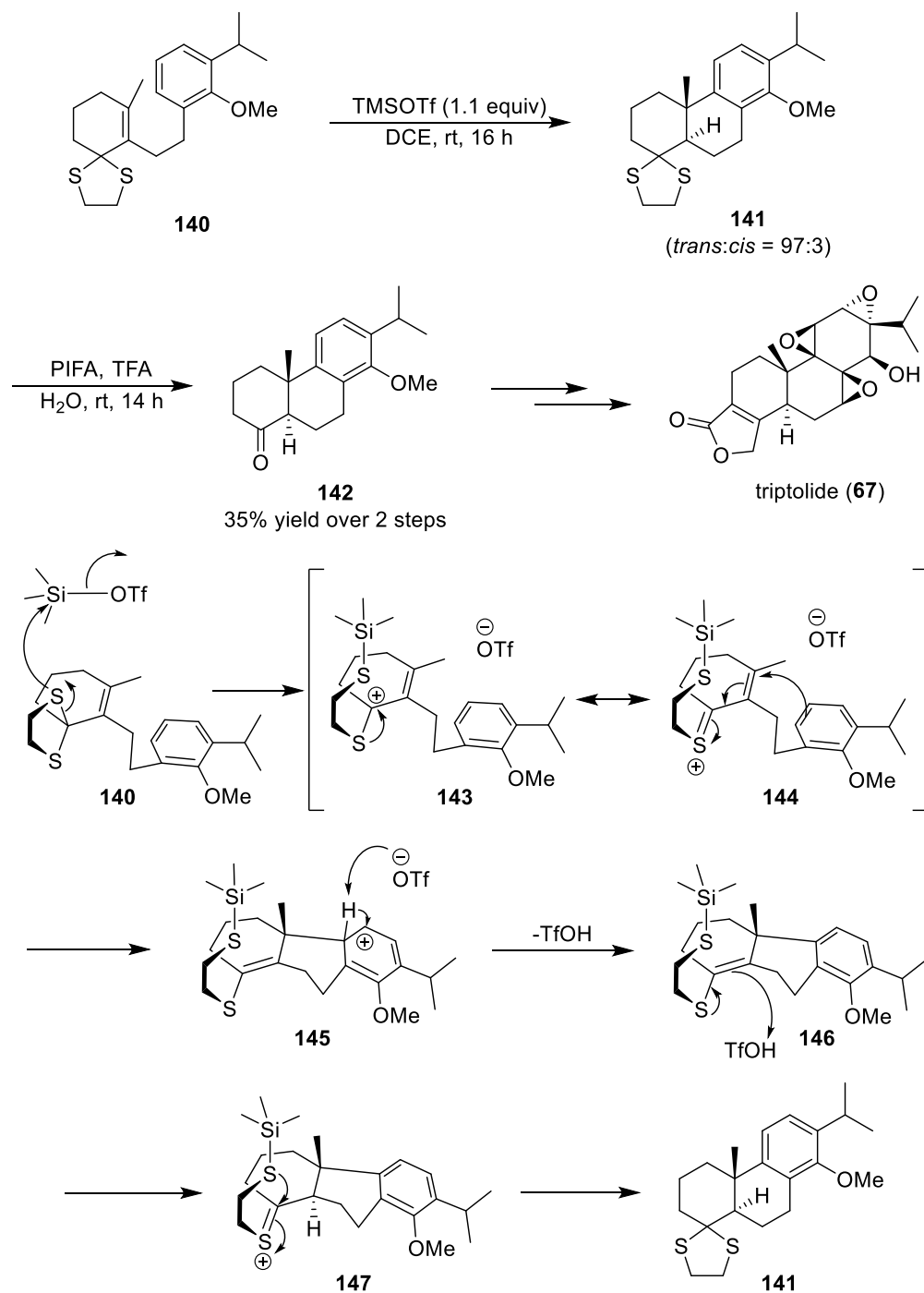
An intramolecular allylation reaction, a nucleophilic cyclisation reaction, has been used to generate six-membered rings for natural product synthesis. Using intramolecular Hosomi-Sakurai addition to furnish the precursor for popolohuanone E (**59**) is illustrated in **Scheme 21**. The allylation precursor **135** was derived from the coupling of vinyl bromide **133** and iodide **134**, followed by hydrolysis of the ketal motif. Subsequently, treatment of allyl silane **135** with titanium tetrachloride in the presence of MeSCH₂Cl provided the desired *cis*-decalin **139** in 68% yield as a single diastereomer.⁶²



Scheme 21: Anderson's synthesis of *cis*-decalin **139**, the core structure of popolohuanone E

1.9.3 Cationic cyclisation approach

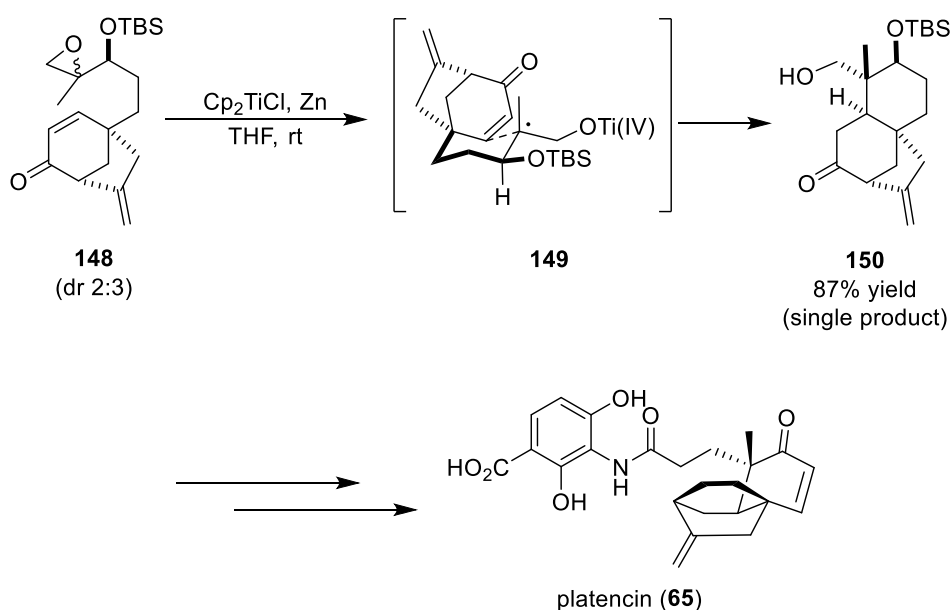
A powerful alternative approach for the formation of functionalised decalin **142** with an impressive *trans*-stereoselection is illustrated in **Scheme 22**. Baati *et al.* exploited 6-*endo*-trig cyclisation to construct the core structure of triptolide (**67**). One-pot Lewis acid-induced diastereoselective 6-*endo*-trig cyclisation of 1,3-dithiolane **140**, followed by *in situ* thioketal cleavage furnished ketone *trans*-decalin **142** in 35% yield over two steps with excellent diastereomeric ratio (97:3). The mechanism for 6-*endo*-trig cyclisation of 1,3-dithiolane **140** is suggested to occur through thioketal-opening and reinstallation. In addition, the stereochemical outcome of **142** could be explained by a steric hindrance of the methyl group on the β -face of **146**. Thus, the proton is delivered from the opposite side supporting the *trans*-addition.⁶³



Scheme 22: Baati's synthesis of *trans*-decalin **142**, the core structure of triptolide and plausible mechanism of 6-endo-trig cyclisation⁶³

1.9.4 Radical cyclisation approach

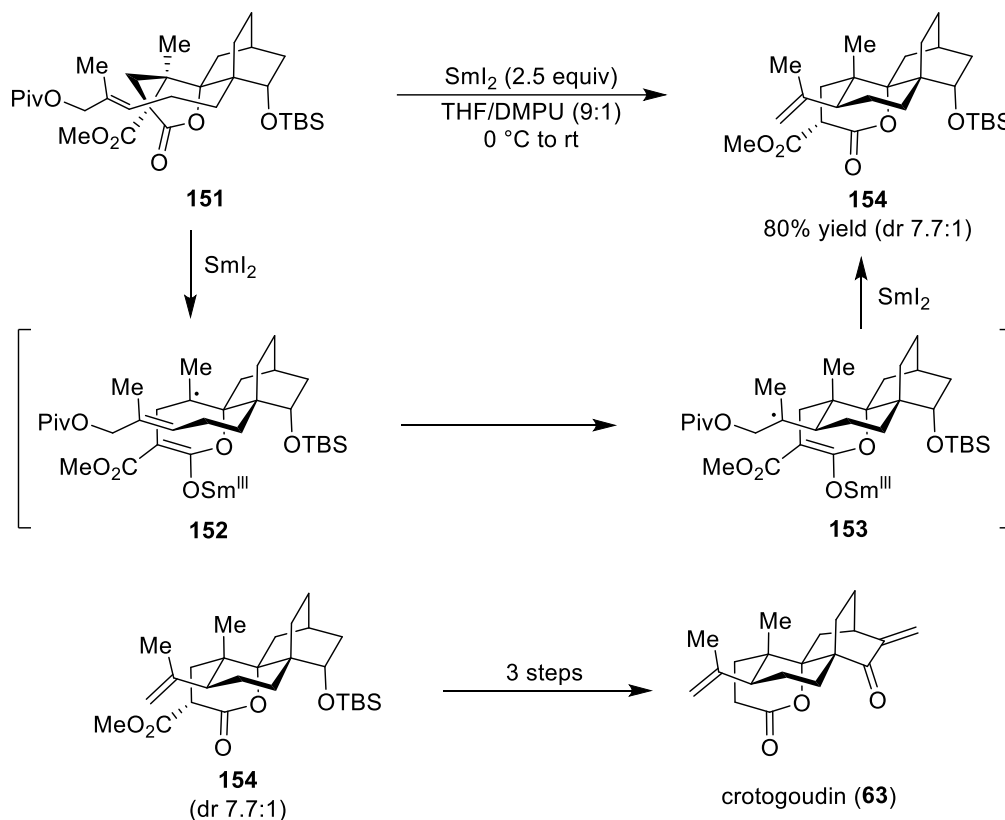
The radical-mediated polyene cyclisation has recently emerged as a powerful approach for the stereoselective construction of complex frameworks exhibiting functionalised decalin units. The antibiotic platencin (**65**) is attractive owing to its promising biological properties. We first reviewed Lee's synthesis of platencin core structure **105** through Diels–Alder cycloaddition as shown in **Scheme 14**. However, a different efficient synthetic pathway is also attractive to discuss. Yoshimitsu *et al.* demonstrated the total synthesis of **65** via highly stereoselective radical addition to construct a *cis*-decalin ring (**Scheme 23**). The radical was generated by titanium(III)-mediated cyclisation. Epoxide **148** underwent homolytic cleavage to generate tertiary radical intermediate **149**, which was then cyclised to form *cis*-decalin **150** as a single diastereomer in good yield. Interestingly, the stereoselectivity of the formation of cyclised product **150** could be explained through rapid epimerisation of the radical carbon centre. The sterically bulky silyl group was preferentially positioned in the equatorial position under thermodynamic conditions, allowing intermediate **149** to undergo stereoselective cyclisation.⁴²



Scheme 23: Yoshimitsu's synthesis of *cis*-decalin **150**, the core structure of platencin⁴²

In 2013, Carreira and co-workers reported the total synthesis of crotogoudin (**63**) via a novel radical cyclopropane-opening/annulation/elimination cascade promoted by SmI_2 as a key feature (**Scheme 24**). Treatment of **151** with SmI_2 led to reductive cyclopropane-

opening to generate radical **152**, which subsequently underwent cyclisation onto the olefin to afford the intermediate **153**. Finally, SmI_2 provided the second single electron to generate an anion, which spontaneously underwent β -elimination to afford lactone **154** in 80% yield with high diastereoselectivity (dr 7.7:1). Crotogoudin (**63**) was achieved from the tricyclic lactone **154** in three steps.⁶⁴



Scheme 24: Carreira's synthesis of lactone **154**, the core structure of crotogoudin⁶⁴

All of the summarised synthetic protocols above indicate several interests in synthesising bioactive natural products bearing functionalised decalin scaffolds. Hence, the innovative and reliable new methodologies based on inter- and intramolecular Diels–Alder cycloadditions, condensation, allylation, and radical reaction are promising tools to achieve the efficient and highly stereoselective synthesis of decalin ring frameworks.

1.10 Computational investigation of anthracimycin synthesis through an intramolecular Diels–Alder reaction and project outline

The published total synthesis of anthracimycin (**1**) by Brimble and a similar carbon skeleton chlorotonil A (**56**) by Kalesse utilised intramolecular Diels–Alder reactions to access the *trans*-decalin core^{26,53} which were inspired by their biosynthesis.^{20,24} Since the first total synthesis of **1** is preceded, a new highly stereoselective synthetic pathway is desirable. Therefore, computational studies were conducted to decide whether to follow a similar approach or whether a new synthetic direction would be more appropriate. As highlighted in the biosynthetic pathway of anthracimycin, the polyketide formation is involved in the enzyme to construct the *trans*-decalin scaffold.²⁴ This IMDA reaction could generate four possible decalin cycloadducts; however, only one isomer was isolated from the natural resources.

Dr Ian George, a former postdoctoral researcher in the Clarke group, investigated the four possibilities of anthracimycin core structure through a computational study to better understand the formation of the molecule *via* a biomimetic synthesis (**Figure 9**).⁶⁶ Notably, computational calculations showed that the generation of two intermediates **157** and **158** had a significantly lower activation barrier (ΔE_a) than the others. Compound **157**, having the required stereochemistry for anthracimycin (**1**), exhibited the activation energy (ΔE_a) value of 58 kJ mol⁻¹ and the energy difference $\Delta H = -259.9$ kJ mol⁻¹ being both the kinetic and thermodynamic products. In addition, the *exo*-Diels–Alder product **158**, generated from the diene approaching the opposite face of the dienophile, also showed a low energy barrier ($\Delta E_a = 65$ kJ mol⁻¹). On the other hand, diene approaching the same face of nucleophile delivered *exo*-Diels–Alder compound **155** and *endo*-Diels–Alder compound **156** with high activation energy (ΔE_a) values of 335.36 kJ mol⁻¹ and 268.55 kJ mol⁻¹, respectively, indicating that it would be unlikely for **155** and **156** to form via this approach. However, as the ΔE_a values of **157** and **158** are similar, it would be possible to generate a mixture of both **157** and **158** instead of the selective anthracimycin core **157**. As a result, biomimetic synthesis may not be an appropriate strategy for preferentially obtaining the natural product **1**.⁶⁶

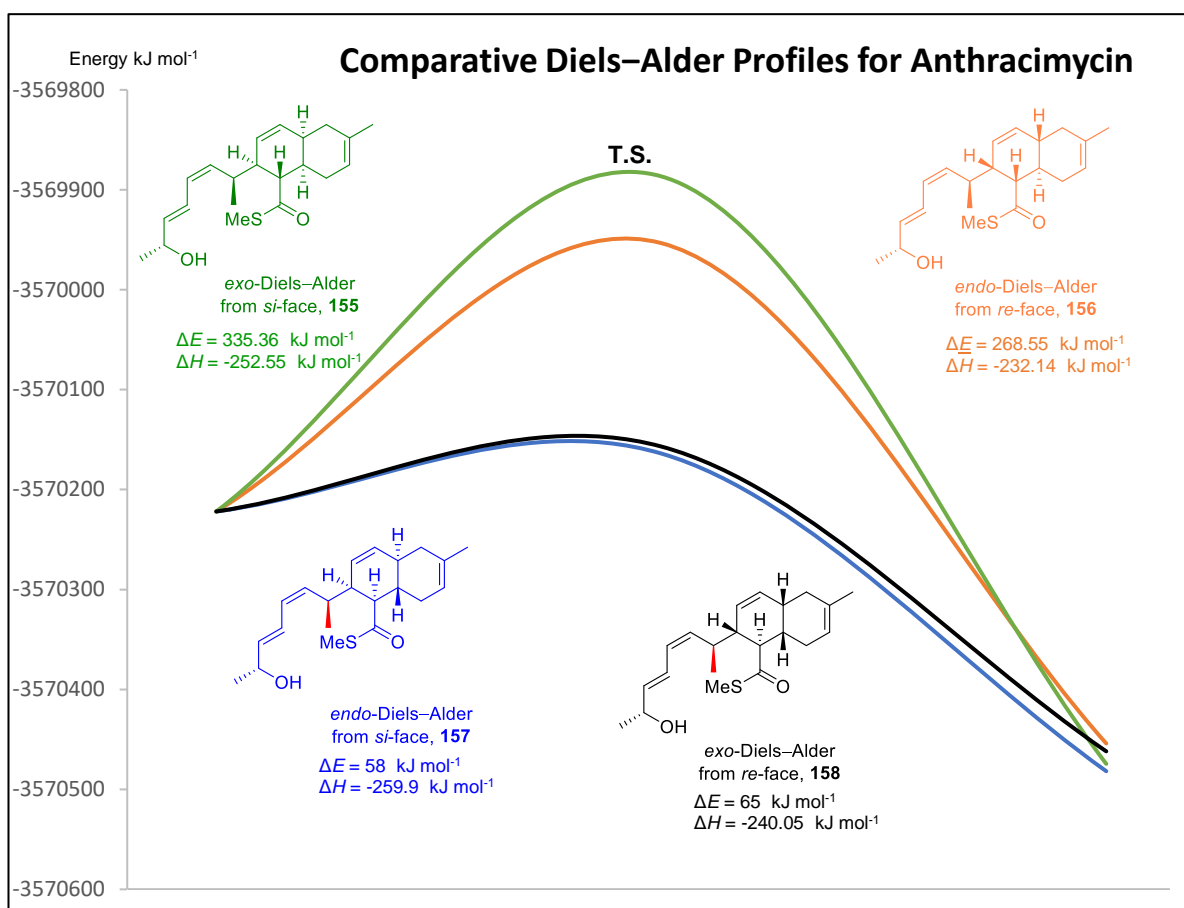


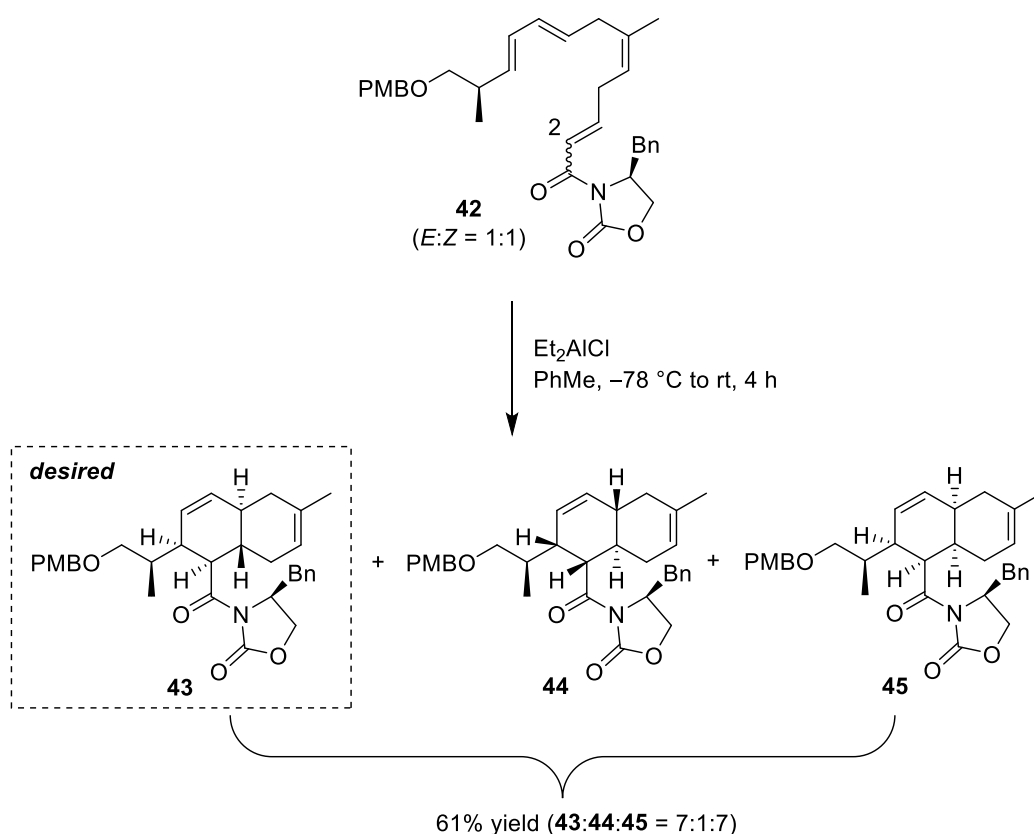
Figure 9: The computational study of a biomimetic intramolecular cycloaddition to form the decalin scaffold of anthracimycin, by the Clarke group⁶⁶

The computational results studied by the Clarke group suggested that they could not selectively construct the *trans*-decalin core of anthracimycin via an intramolecular Diels–Alder cycloaddition. Additionally, exploiting this strategy as the key feature of the first total synthesis of anthracimycin by the Brimble group demonstrated that three diastereomers with a partially separable mixture were obtained (see **Scheme 4**). Consequently, a common intermolecular Diels–Alder cycloaddition strategy to install the decalin unit with angular substituents in a stereoselective manner will be initially explored and discussed in detail in the next chapter. This was the primary aim of the work described in this thesis.

2. Results and Discussion

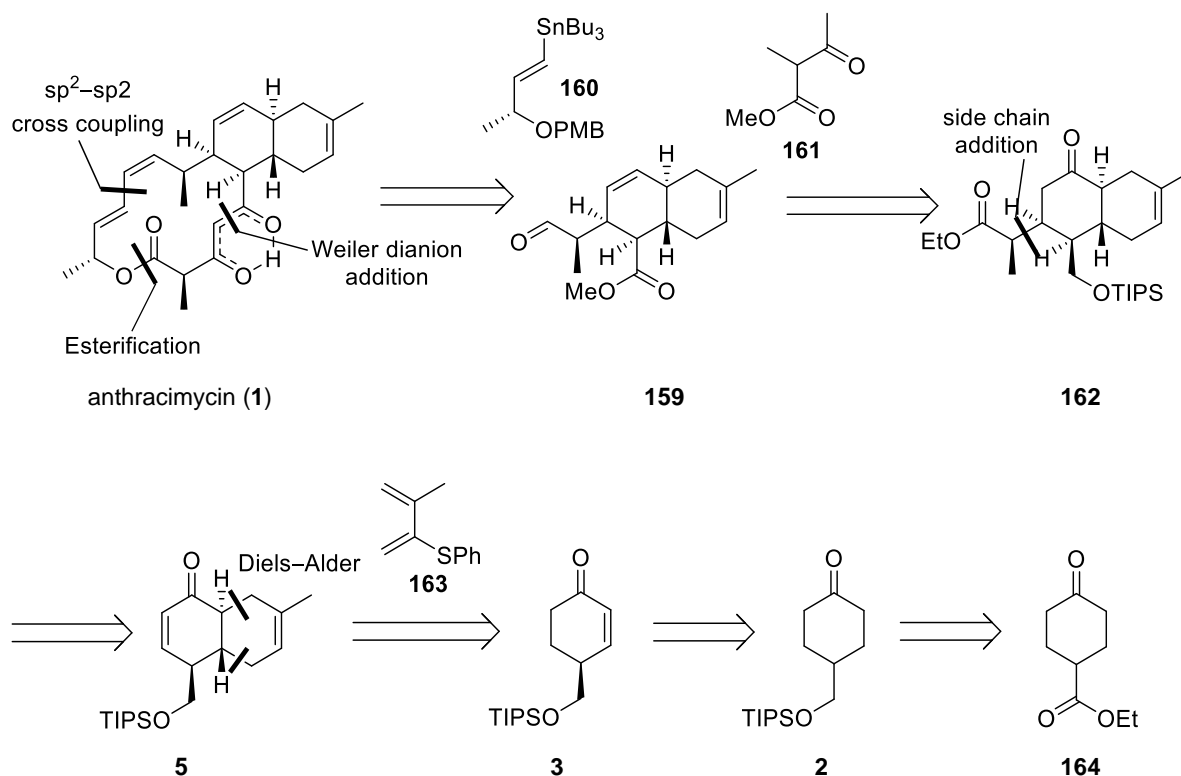
2.1 The retrosynthetic analysis of anthracimycin

Over the last few years, several natural product syntheses have been exploiting a biomimetic approach. Focusing on those with a *trans*-decalin framework, these include Kalesse's synthesis of chlorotonil A (**56**)⁶⁵ and Brimble's synthesis of anthracimycin (**1**).^{26,27} Both syntheses have succeeded via a biomimetic and highly stereocontrolled intramolecular Diels–Alder (IMDA) cycloaddition to form a *trans*-decalin scaffold. The first asymmetric total synthesis of anthracimycin (**1**) mentioned in the previous chapter, was achieved through a gram-scale IMDA reaction of an inseparable mixture of triene **42** (*E:Z* = 1:1). Interestingly, Evans chiral auxiliary controlled the stereoselectivity of this crucial stage to provide a partially separable mixture of three diastereomers with a decalin motif **43**, **44**, and **45** (7:1:7) in 61% yield as depicted in **Scheme 4**.²⁶



Scheme 4: Brimble's synthesis of *trans*-decalin scaffold **43**²⁶

Regarding Brimble's synthesis, we aimed to improve the selectivity and yield of the key step to form a *trans*-decalin moiety. Before carrying out synthetic experiments, we decided to simulate the possible approach to access the anthracimycin core using computational studies which were carried out by Dr Ian George, a former postdoctoral researcher in the Clarke group. The results demonstrated a possible mixture of intramolecular Diels–Alder cycloadducts. Therefore, an alternative strategy was explored for synthesising **1**. Previous Clarke group work on the synthesis of the anthracimycin core was carried out by Dr Giacomo Lodovici.⁶⁶ The retrosynthetic analysis identified the disconnection of **1** into three key fragments: anthracimycin core **159**, tributylvinyltin **160**, and β -ketoester **161** through sp^2 - sp^2 cross-coupling, Weiler dianion addition, and esterification. Anthracimycin core **159** would be obtained from ester **162**, while installing a side chain on the decalin system would be another challenge in our task. We envisaged that enone *trans*-decalin **5** would then be set through the Diels–Alder cycloaddition of enantioenriched cyclohexenone **3** and electron-rich sulfur-substituted diene **163**. At the same time, enone **3** would be accessible from the commercially available ethyl-4-oxocyclohexane-carboxylate **164** (Scheme 25).

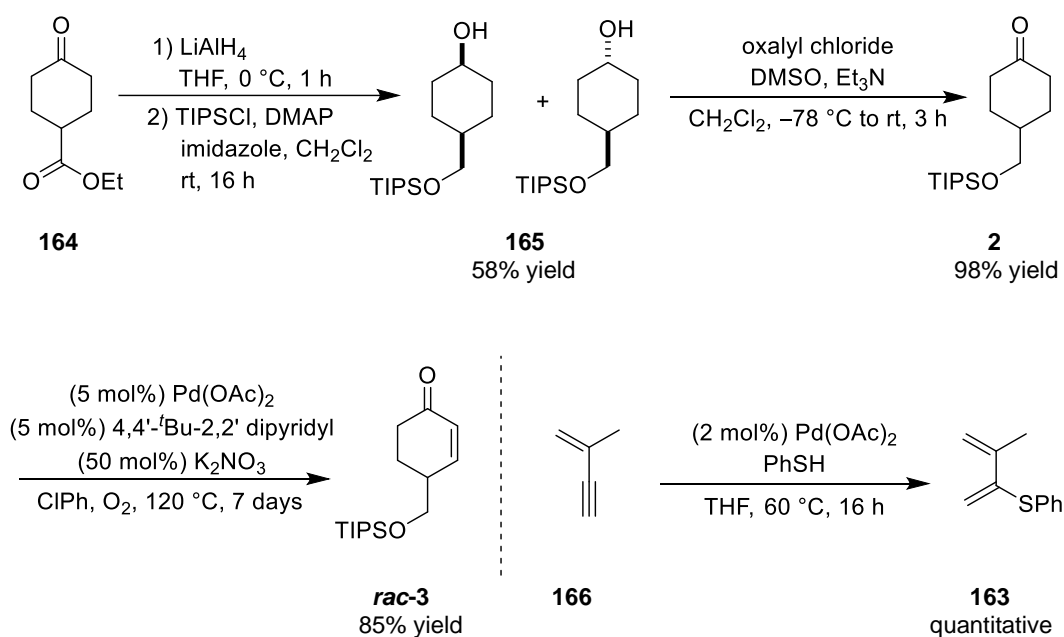


Scheme 25: The retrosynthetic analysis of anthracimycin

2.2 Previous Clarke group work on the synthesis of the anthracimycin core

The Clarke group began synthetic studies with a racemic pathway to prove the possibility of the proposed synthetic route and to save the precious enantioenriched material. Before accessing the synthesis of a decalin system, the group focused on preparing Diels–Alder cycloaddition precursors **3** and **163**.

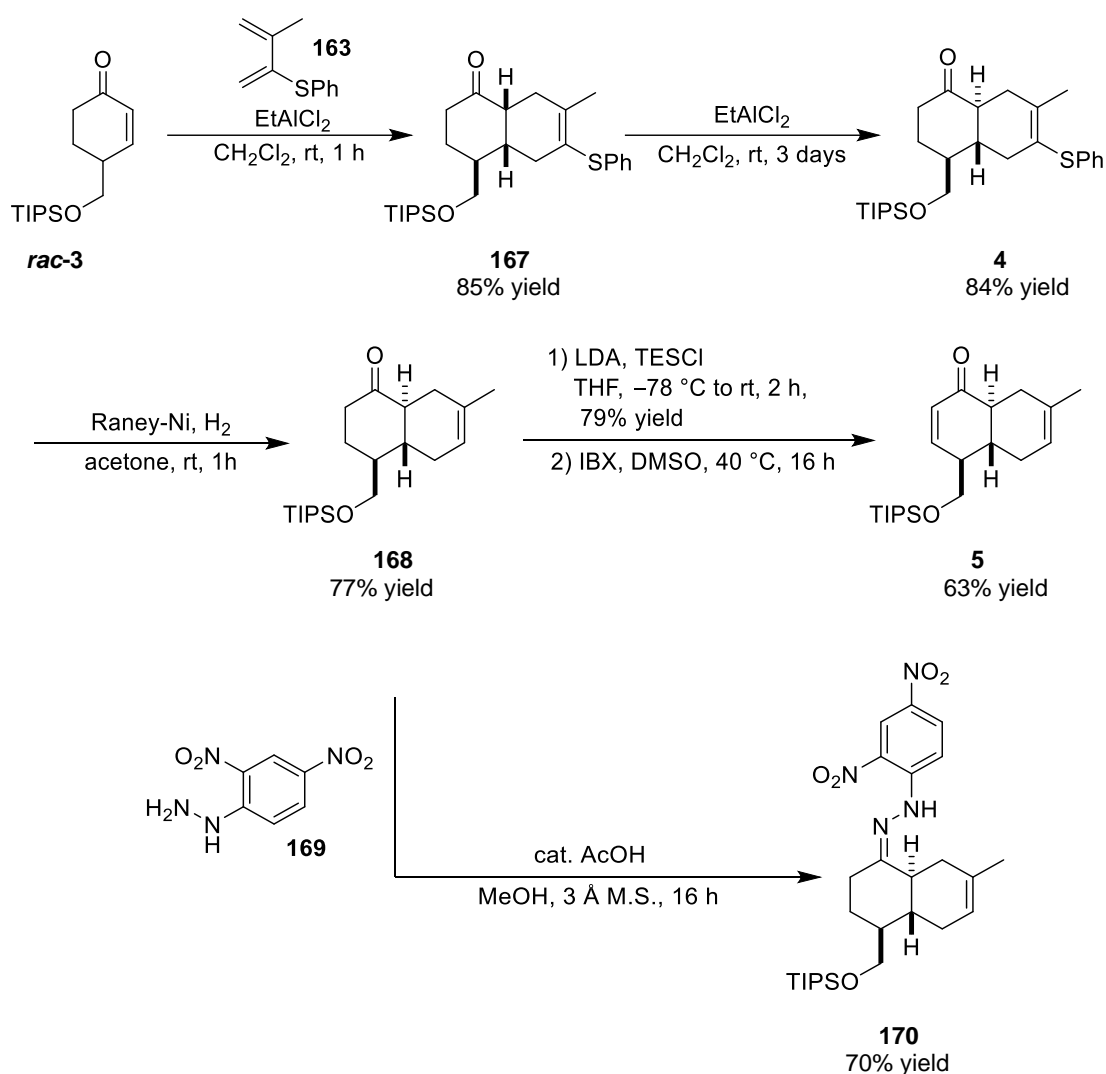
Racemic enone **3** was prepared from known cyclohexanone **2** in a single step via Pd-catalysed oxidation, while cyclohexanone **2** was initially generated through the LiAlH₄ reduction of commercially available ethyl-4-oxocyclohexane carboxylate **164**, followed by selective silylation and oxidation under Swern conditions. Sulfur-substituted diene **163** was synthesised in one step from 2-methyl-1-buten-3-yne **166** in the presence of 2 mol% Pd(OAc)₂ and thiophenol (Scheme 26).⁶⁶



Scheme 26: Previous Clarke group work on the formation of racemic enone **3** and sulfur-substituted diene **163**⁶⁶

With both racemic enone **3** and sulfur-substituted diene **163** in hand, the challenging task of accessing the decalin scaffold was investigated in the presence of ethylaluminum dichloride (EtAlCl₂) via Diels–Alder cycloaddition to provide *cis*-decalin **167** as a single *cis*-diastereomer in 85% yield. The stereochemistry of *cis*-decalin **167** was confirmed by the nOe ¹H-NMR analysis. Due to the decomposition rate of sulfur-substituted diene **163** being

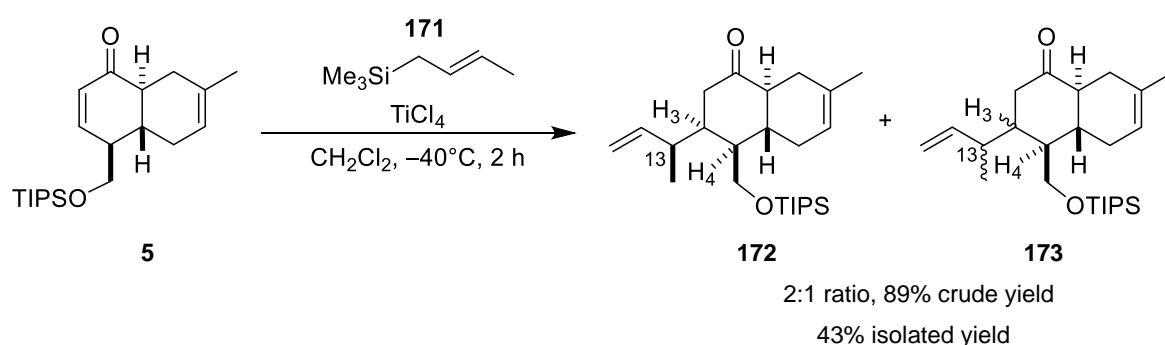
faster than that of cycloadduct formation, a significant excess of diene **163** (10 equivalents) was required. As a *trans*-decalin system was necessary for the natural product, *cis*-decalin **167** was then epimerised under the same conditions of EtAlCl₂ at room temperature for three days to afford *trans*-decalin **4** in 84% yield. The thiophenyl group was removed through selective Raney-Nickel hydrogenation to generate the desired *trans*-decalin **168** in 77% yield. The stereochemistry of *trans*-decalin **168** was determined by X-ray diffraction of hydrazone derivative **170**. Ketone *trans*-decalin **168** was then functionalised to enone *trans*-decalin **5** in 63% yield via enolisation and IBX oxidation (Scheme 27).⁶⁶



Scheme 27: Previous Clarke group work on the formation of enone *trans*-decalin **5**⁶⁶

2.2.1 Previous Clarke group work on the Hosomi–Sakurai approach

Having successfully synthesised enone *trans*-decalin **5**, the group moved forward to address the anthracimycin core **159** by installing a side chain on enone *trans*-decalin **5** via the Hosomi–Sakurai strategy. To generate a 1,4-addition product, enone **5** was treated with (*E*)-crotyltrimethylsilane **171** in the presence of TiCl₄ at –40 °C which gave an inseparable mixture of two diastereomers **172** and **173** in 43% isolated yield. Since the side chain along with the methyl group was installed, two new stereogenic centres at the 3-position and the 13-position were set up. To progress the total synthesis, stereochemistry determination of the newly installed stereogenic centres was needed. After an extended effort, the major diastereomer **172** was isolated in a small quantity, which was adequate for the stereochemistry determination. Gratifyingly, the relationship between H-3 and H-4 was confirmed to be a *syn*-relationship, and the stereochemistry of the methyl group at C-13 was also proved to be as required for the natural product (**Scheme 28**).⁶⁶

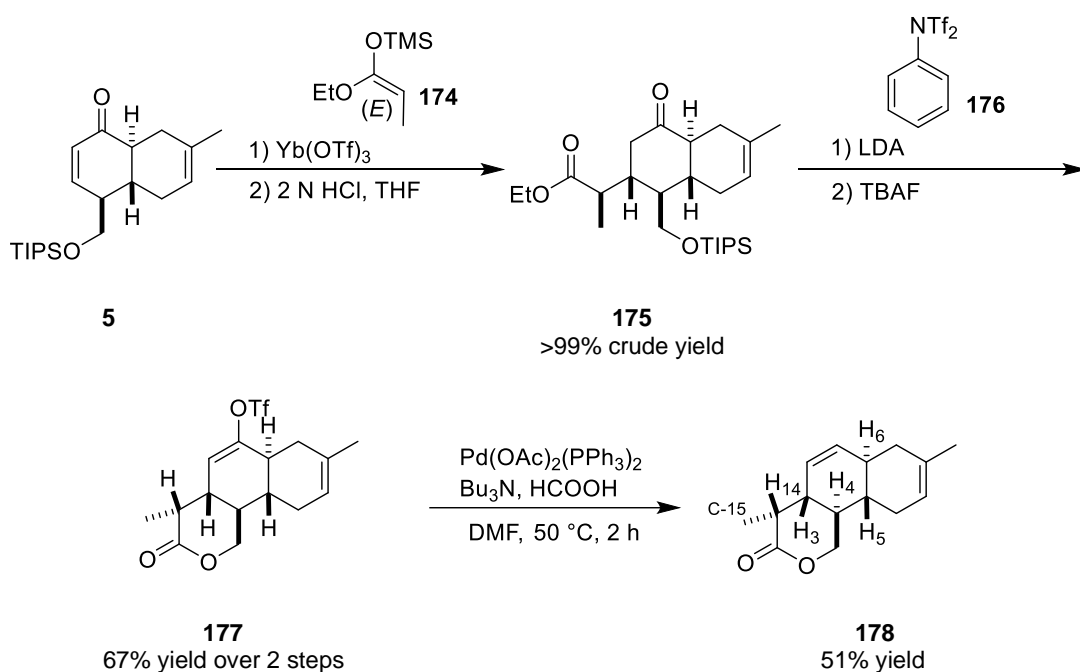


Scheme 28: Previous Clarke group work on the Hosomi–Sakurai 1,4 addition of enone **5** and (*E*)-crotyltrimethylsilane **171**⁶⁶

Due to the separation difficulty of both diastereomers **172** and **173**, the Hosomi–Sakurai approach could not be used to progress the synthesis of the anthracimycin core. Consequently, a new strategy to introduce a side chain was then explored.

2.2.2 Previous Clarke group work on the Mukaiyama–Michael approach

As the group could not obtain sufficient material **172** for the synthesis of the anthracimycin core, the known Mukaiyama–Michael 1,4-addition was explored to build the side chain. The attempted synthesis of the anthracimycin core **159** was carried out through the Mukaiyama–Michael 1,4-addition of (*E*)-ethyl-propanoate silyl ketene acetal **174** to enone *trans*-decalin **5**. To achieve a 1,4-addition product, the reaction was performed in the presence of Yb(OTf)₃. Subsequently, hydrolysis under 2 N HCl conditions gave ester **175** in quantitative yield. The stereochemistry determination of **175** through single crystal X-ray diffraction required the conversion of **175** to tricyclic lactone **178**. The ketone portion of **175** was functionalised to the olefin as required for the natural product via formation of vinyl triflate and desilylation with TBAF. The corresponding vinyl triflate **177** was obtained in 67% yield over two steps. Vinyl triflate **177** was finally reduced in the presence of catalytic palladium to deliver tricyclic lactone **178** in 51% yield as illustrated in **Scheme 29**.⁶⁶



Scheme 29: Previous Clarke group work on the Mukaiyama–Michael addition and transformation of tricyclic system⁶⁶

The single crystal X-ray diffraction of the tricyclic lactone **178** showed an *anti*-relationship between H-3 and H-4 instead of the required *syn*-relationship. These results indicated that the attack of (*E*)-ethyl-propanoate silyl ketene acetal **174** favoured the bottom face of enone **5** due to the sterically bulky triisopropylsilylmethoxy chain. However, the methyl

group at C-15 had the required stereochemistry for the core of the natural product as shown in **Figure 10**.⁶⁶

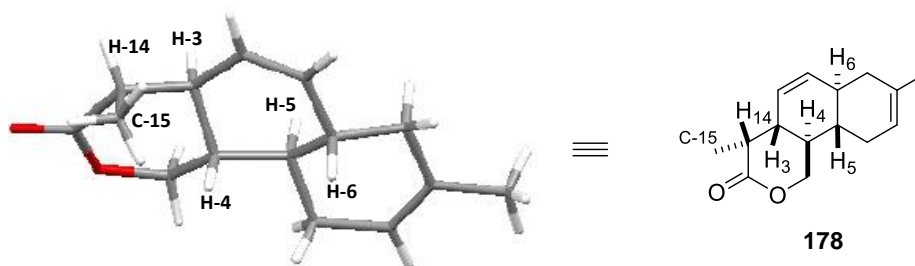


Figure 10: The single crystal X-ray diffraction of tricyclic lactone **178**⁶⁶

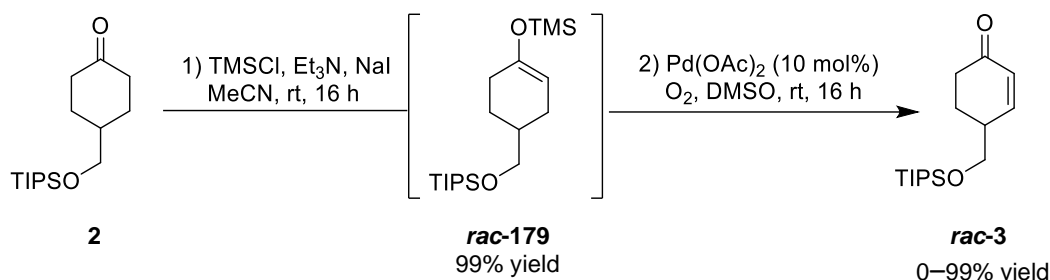
In conclusion, the Clarke group attempted to synthesise the anthracimycin core using two strategies. The Mukaiyama–Michael 1,4-addition of enone *trans*-decalin **5** with (*E*)-ethylpropanoate silyl ketene acetal **174** afforded the *epi*-anthracimycin core **178**, which would be suitable for the synthesis of its analogues. Even though the Hosomi–Sakurai approach furnished the desired 1,4-addition product **172** with the required stereochemistry, the inseparable mixture of two diastereomers hindered progress towards the total synthesis. However, the previous findings by the Clarke group inspired us to extend our studies on introducing a side chain to the decalin scaffold.

2.3 The synthesis of racemic cyclohexenone **3**

Inspired by previous work in the Clarke group, we aimed to build on Lodovici's findings and progress the total synthesis with an asymmetric synthetic route. Our initial efforts pointed to accessing key enantiomerically pure cyclohexenone **3** for the Diels–Alder reaction. However, to trial the proposed synthesis and conserve the precious enantioenriched cyclohexenone **3**, racemic enone **3** was required.

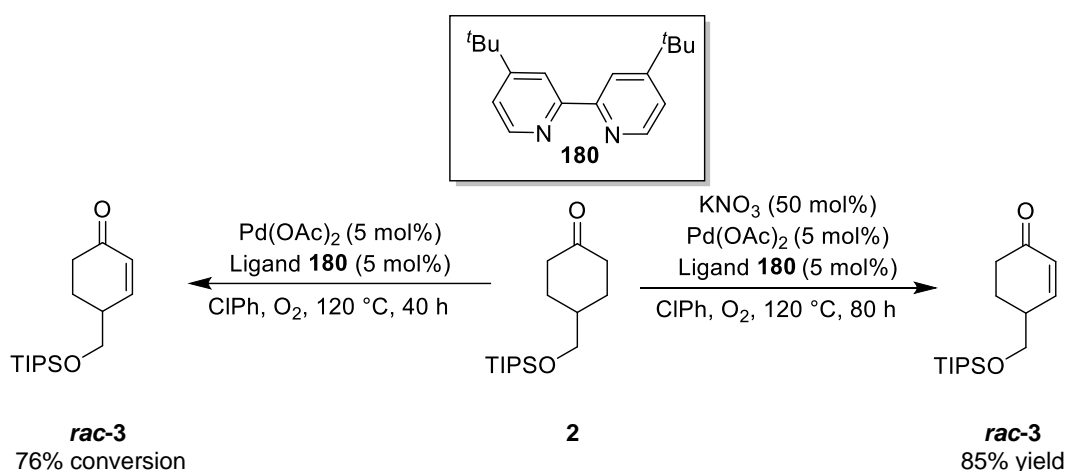
The Clarke group has reported the synthesis of racemic cyclohexenone **3** by two different methods, which were developed by Dr Ian George and Dr Giacomo Lodovici.⁶⁶ The racemic enone **3** was derived from the known cyclohexanone **2** in two steps. Ketone **2** was initially converted to racemic silyl enol ether **179** through an enolisation, which was subjected to Ito–Saegusa oxidation to give racemic enone **3**. It should be noted that *rac*-enone **3** was

obtained in unreliable conversion due to the instability of *rac*-silyl enol ether intermediate **179** (Scheme 30).⁶⁶



Scheme 30: The formation of racemic enone **3** developed by Dr Ian George⁶⁶

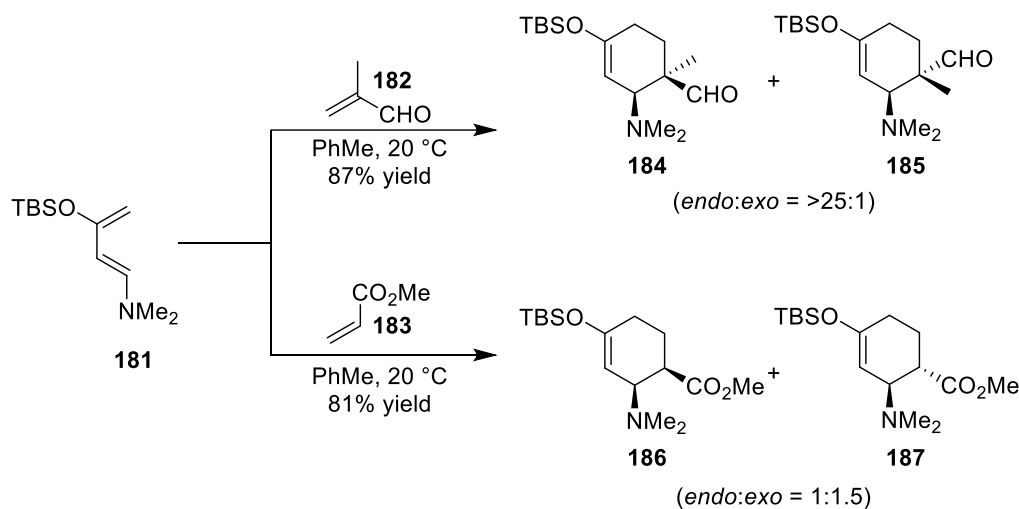
To develop the oxidation conditions, palladium-catalysed oxidation inspired by Tsuji's work was then investigated.⁶⁷ The addition of 5 mol% bipyridine ligand **180** to the oxidation of ketone **2** in the presence of Pd(OAc)₂ in chlorobenzene heating at 120 °C provided the desired racemic enone **3** in 76% conversion after stirring under an O₂ atmosphere for 40 hours. Gratifyingly, the yield of this step was improved to 85% on a ten-gram scale by the addition of 50 mol% co-catalyst KNO₃ (Scheme 31).⁶⁶



Scheme 31: The formation of racemic enone **3** developed by Dr Giacomo Lodovici⁶⁶

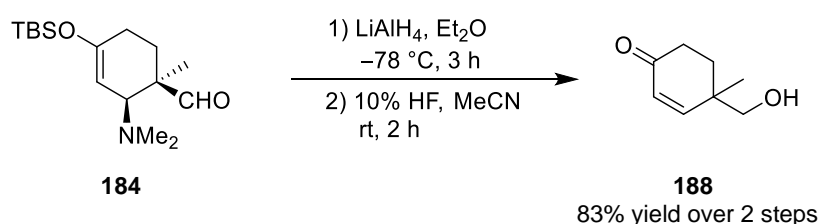
Even though the synthesis of racemic enone **3** was achieved through palladium-catalysed oxidation with high yield, the developed conditions required high temperature, re-freshing of the O₂ atmosphere and prolonged reaction time.⁶⁶ To tackle problems from a different angle, either new conditions or a novel strategy to deliver racemic enone **3** was desirable. Therefore, we considered a common method to form substituted cyclohexene derivatives involving the use of Diels–Alder cycloaddition. Kozmin and Rawal reported the studies of

1-amino-3-siloxy-1,3-butadienes **181** described in Diels–Alder reactions.⁶⁸ Some examples of cycloadduct formation from Rawal’s diene **181** and different dienophiles **182** and **183** are outlined in **Scheme 32**.



Scheme 32: The examples of Diels–Alder reaction of Rawal’s diene **181** with dienophiles **182** and **183**⁶⁸

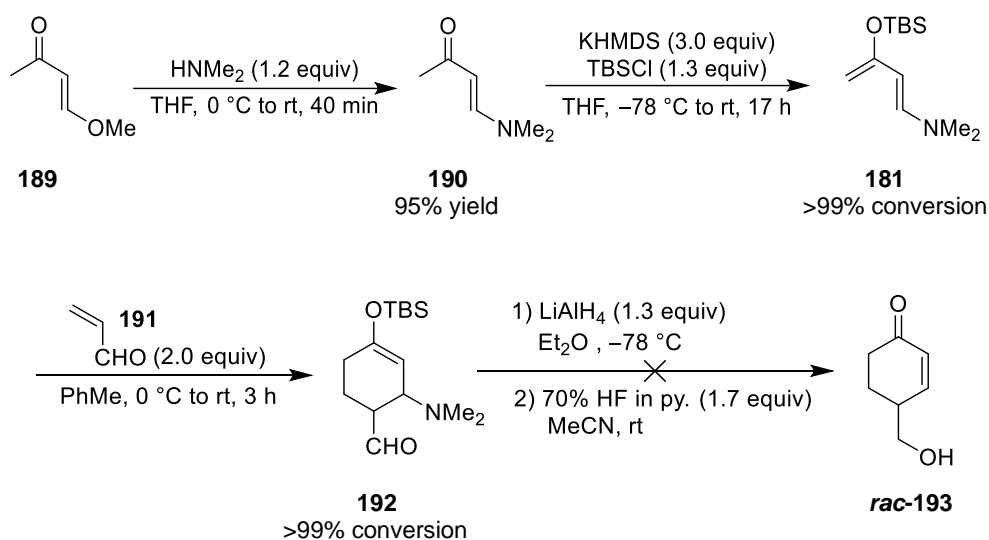
Rawal’s diene **181** was found to be relatively stable to handle and further purified by vacuum distillation.⁶⁸ The cycloadducts **184** and **186** were delivered in good yield with different diastereoselectivity under mild conditions. Interestingly, the β -amino enol silyl ether portion of the cycloadduct **184** smoothly converted to the corresponding enone **188** in good yield through reduction with LiAlH_4 and hydrolysis (**Scheme 33**).⁶⁸



Scheme 33: The conversion of cycloadduct **184** to enone **188**⁶⁸

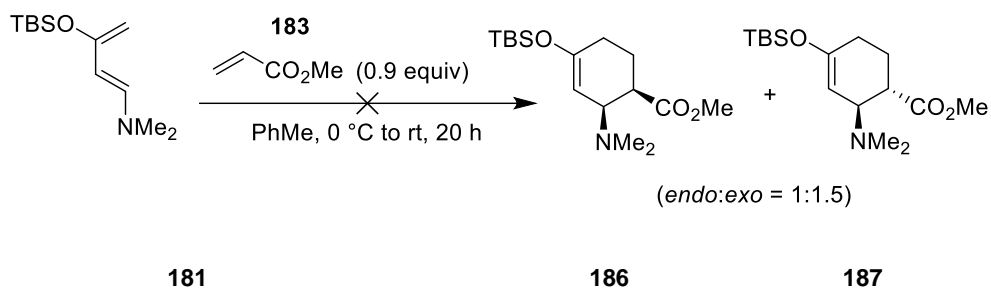
Based on Rawal’s work, we envisioned that racemic enone **3** would be prepared in the same fashion starting from Rawal’s diene **181** via a Diels–Alder reaction. Rawal’s diene **181** was derived in two steps from the commercially available *trans*-4-methoxy-3-buten-2-one **189**. First, an addition-elimination reaction of vinylogous ester **189** gave vinylogous amide **190**, which was subjected to enolisation to afford Rawal’s diene **181** in >99% conversion.⁶⁸ The

crude material was directly used for the next step without purification. With diene **181** in hand, acrolein **191** was chosen as a dienophile which was identified to be more reactive than methacrolein **182**. Therefore, setting the reaction at a low temperature was required for an initial study. The formation of cycloadduct **192** proceeded through the Diels–Alder reaction of Rawal’s diene **181** and acrolein **191** (2.0 equivalents) in toluene at 0 °C and the reaction mixture was allowed to reach room temperature. The consumption of diene **181** was completed and the cycloadduct **192** was obtained in >99% conversion after 3 hours confirmed by ¹H-NMR. Due to the instability of the silyl enol ether moiety on silica, the crude material was directly used for the reduction using LiAlH₄, followed by hydrolysis (70% HF in pyridine). Disappointingly, none of the desired racemic alcohol **193** could be observed, as illustrated in **Scheme 34**.



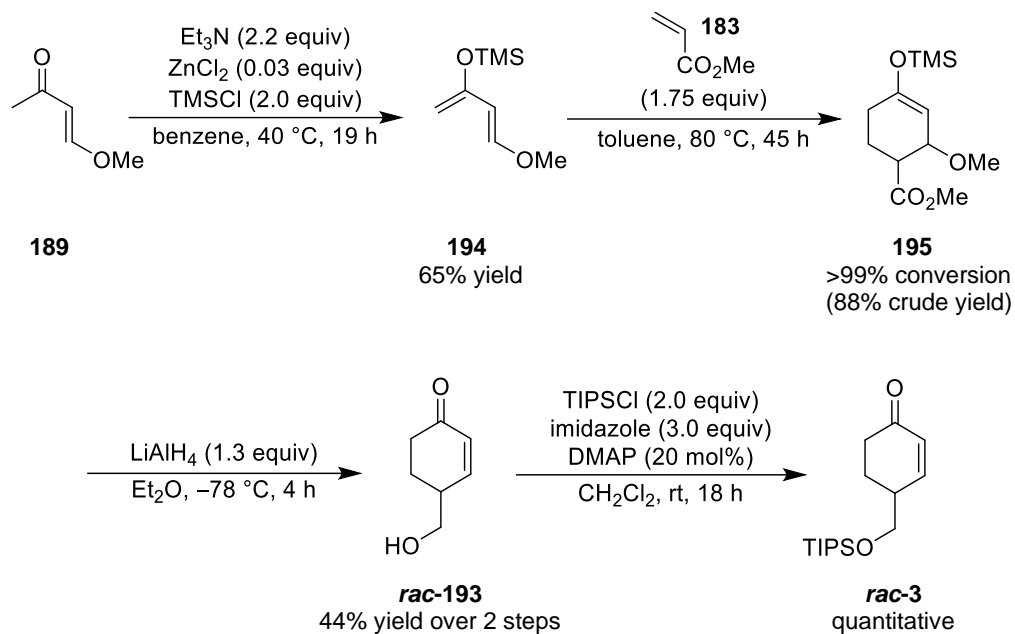
Scheme 34: The attempted formation of racemic alcohol **193** via Diels–Alder cycloaddition between Rawal’s diene **181** and acrolein **191**

Carrying Rawal’s diene **181** through cycloaddition with acrolein **191**, followed by reduction and removal of the silyl group without purification over three steps failed to provide racemic alcohol **193**. Due to the unprecedented cycloaddition of Rawal’s diene **181** with acrolein **191** and volatility of **191**, it was challenging to handle acrolein **191** for the Diels–Alder reaction. Hence, more stable methyl acrylate **183** was used as a dienophile instead. Nevertheless, neither cycloadduct **186** nor **187** could be observed by using 0.9 equivalents of methyl acrylate **183** as a dienophile in toluene at 0 °C to room temperature after 20 hours (**Scheme 35**).⁶⁸



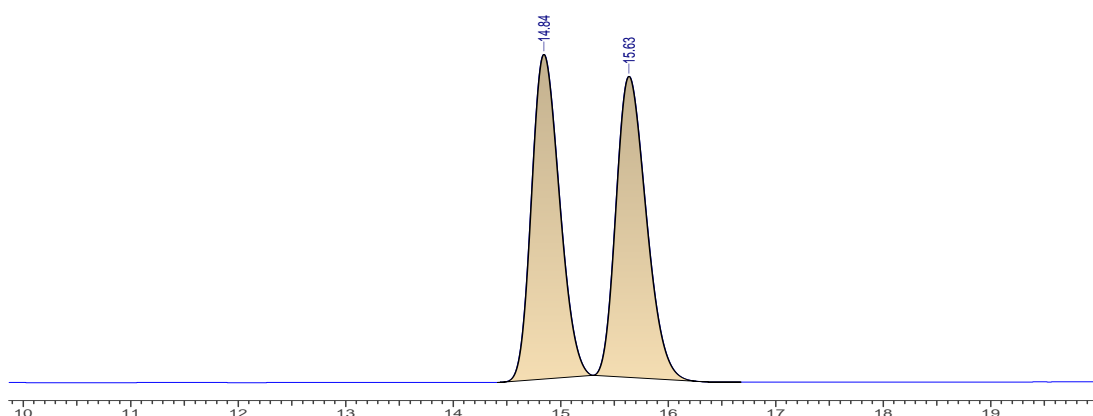
Scheme 35: The attempted formation of cycloadduct **186–187** via Diels–Alder cycloaddition between Rawal’s diene **181** and methyl acrylate **183**

The use of crude Rawal’s diene **181** without purification probably impeded a smooth Diels–Alder reaction leading to failure in both cases. While the instability and difficulty of purification of **181** were disappointing, the known Danishefsky’s diene **194** could provide access racemic cyclohexenone **3**.⁶⁹ Danishefsky’s diene **194** was prepared in a single step from *trans*-4-methoxy-3-buten-2-one **189** and TMSCl in the presence of Et₃N and ZnCl₂.⁷⁰ The formation of cycloadduct **195** was investigated through the Diels–Alder reaction of diene **194** with 1.75 equivalents of methyl acrylate **183** in toluene heating at 80 °C.⁷¹ After 45 hours, the desired cyclohexene **195** was obtained in >99% conversion with 88% crude yield. Due to the instability of a silyl enol ether moiety, the crude cycloadduct **195** was directly carried out for the next step without purification. Reduction of crude **195** with LiAlH₄ in Et₂O at –78 °C pleasingly afforded the desired racemic alcohol **193** in 44% yield over two steps. To achieve the requisite racemic enone **3**, silylation of primary alcohol **193** was performed under the conditions of TIPSCl (2.0 equivalents), imidazole (3.0 equivalents), and catalytic DMAP (20 mol%) in CH₂Cl₂ at room temperature.⁷² After purification by flash column chromatography, racemic cyclohexenone **3** was isolated in quantitative yield (**Scheme 36**).



Scheme 36: The formation of racemic cyclohexenone **3**

With racemic cyclohexenone **3** in hand, we identified HPLC conditions which could be used for the separation of *rac*-enone **3**, which would be utilised to analyse the enantiomeric excess of enantioenriched cyclohexenone **3** from the asymmetric synthesis. The best separation of the two enantiomers of the racemic compound was achieved by HPLC analysis using CHIRALCEL[®] IC column eluting with 1% *i*-PrOH/hexane (flow rate = 1.0 mL/min, temp = 40 °C, λ = 216 nm) to give two peaks of equal areas (**Figure 11**).

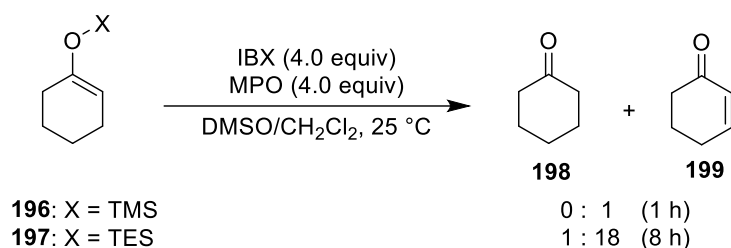


No.	tR	Peak Area (Y units*ms)	Area (%)	Width
1	14.84	9815495.000	49.969	0.482
2	15.63	9827507.000	50.031	0.516

Figure 11: HPLC trace of racemic cyclohexenone **3**

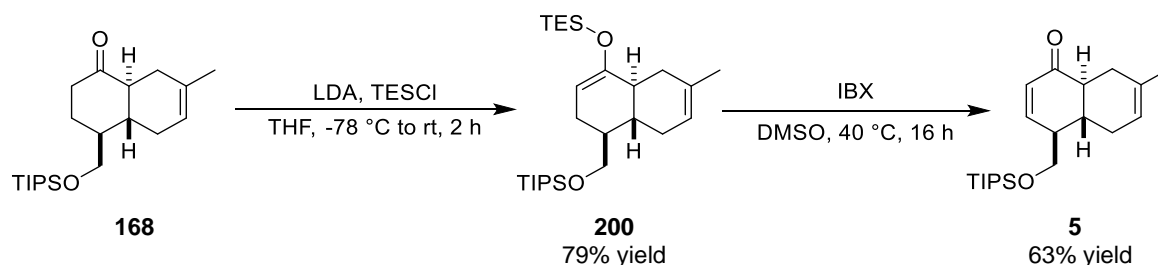
Due to the length of time required to access racemic cyclohexenone **3** via Diels–Alder cycloaddition of Danishefsky’s diene **194** with methyl acrylate **183**, a milder and more efficient method was proposed for delivering *rac*-enone **3** quicker with a better yield.

Nicolaou *et al.* reported the oxidation of silyl enol ethers promoted by the combination of IBX and MPO.⁷³ The oxidation of either silyl enol ether **196** or **197** was investigated under the same conditions. The less bulky trimethyl silyl group (TMS) of **196** was oxidised smoothly at room temperature to generate cyclohexenone **199** in >99% conversion, while the oxidation of TES-enol ether **197** took 8 hours at the same temperature to give the desired enone **199** and ketone **198** as a side product by hydrolysis with a ratio of 18:1 as illustrated in **Scheme 37**.



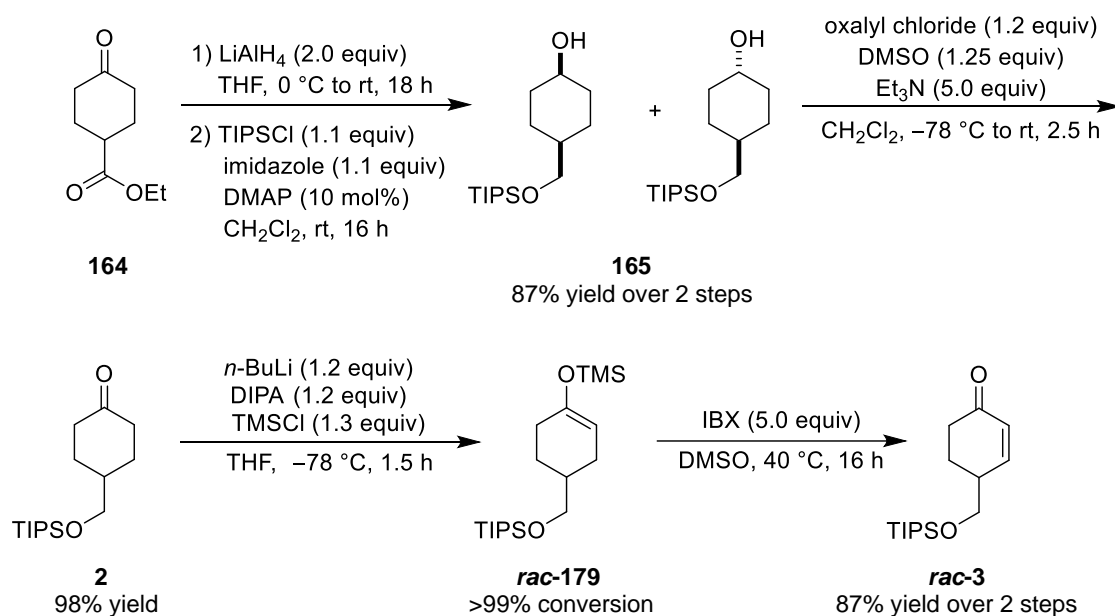
Scheme 37: The IBX oxidation of silyl enol ethers⁷³

A similar method from previous work in the Clarke group illustrates the transformation of ketone **168** to enone *trans*-decalin **5** via IBX oxidation of TES-enol ether. The oxidation of TES-enol ether **200** using 2.5 equivalents of IBX in DMSO at 40 °C provided enone *trans*-decalin **5** in 63% yield (**Scheme 38**).⁶⁶



Scheme 38: Previous Clarke group work on the transformation of ketone **168** to enone **5**⁶⁶

Considering both cases (**Scheme 37–38**), we planned to form racemic TMS-enol ether **179** as a key intermediate for the IBX oxidation (**Scheme 39**). The cyclohexanone **2** was derived from commercially available ethyl-4-oxocyclohexane carboxylate **164** in excellent yield within three steps, following our previous procedure.⁶⁶ Enolisation of cyclohexanone **2** in the presence of LDA and TMSCl smoothly provided *rac*-enol ether **179** in >99% conversion. Due to the instability of silyl enol ether on silica, we proceeded to the next step without purification. The crude *rac*-enol ether **179** was directly subjected to IBX oxidation in DMSO at 40 °C. Again, instability of the silyl enol ether was of concern and excess IBX (5.0 equivalents) was therefore used to overcome the decomposition of *rac*-enol ether **179**. The oxidation of *rac*-**179** was completed in 16 hours to deliver the requisite racemic cyclohexenone **3** in 87% yield over two steps as shown in **Scheme 39**.



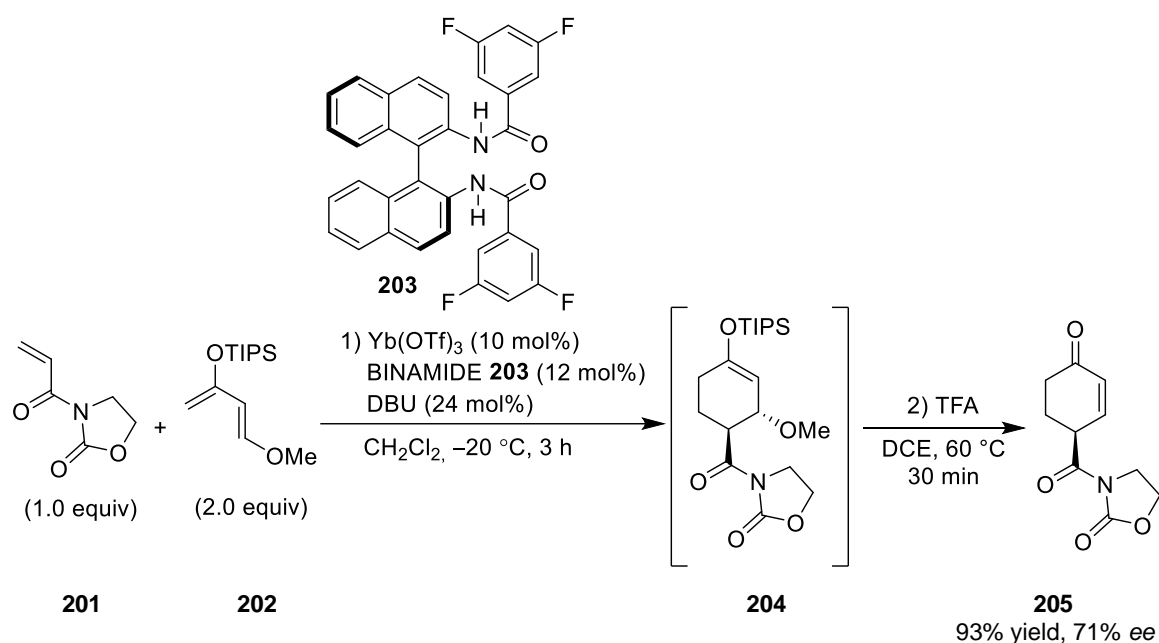
Scheme 39: The formation racemic enone **3** through the IBX oxidation of TMS-enol ether

Gratifyingly, we have successfully synthesised racemic cyclohexenone **3** via two strategies, including an established Diels–Alder cycloaddition of Danishefsky’s diene **194** and methyl acrylate **183** and an efficient sequence of enolisation and IBX oxidation from the commercially available starting material **164** under mild conditions in high yield. Hence, our attention turned to an asymmetric synthetic pathway to progress the total synthesis. The enantioenriched cyclohexenone **3** would be a key precursor for the next goal.

2.4 The synthesis of enantioenriched cyclohexenone 3

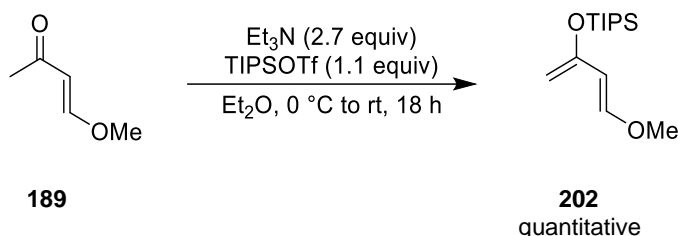
2.4.1 Enantioselective Diels–Alder cycloaddition approach

Since we have completed the synthesis of racemic enone **3** by the Diels–Alder cycloaddition of Danishefsky's diene **194** with methyl acrylate **183**, this inspired us to produce enantiomerically pure enone **3** in the same fashion. A highly enantioselective Diels–Alder reaction to form enantioenriched cyclohexenone **205** was demonstrated by Nishida and co-workers.⁷⁴ Using the known Danishefsky's diene **202** and electron-deficient alkene **201**, a Diels–Alder reaction catalysed by Yb(III)-BINAMIDE complex furnished cycloaddition adduct **204**. Treatment of **204** with trifluoroacetic acid generated the desired cyclohexenone **205** in excellent yield with a modest enantiomeric excess of 71% ee as shown in **Scheme 40**.



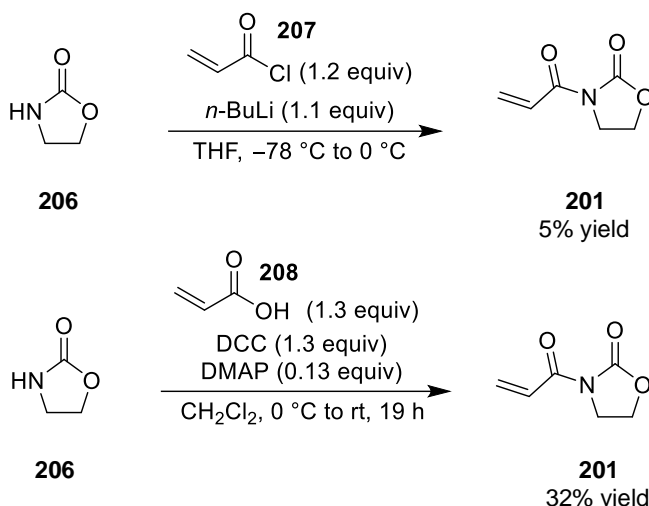
Scheme 40: Nishida's synthesis of cyclohexenone **205** via an asymmetric Diels–Alder cycloaddition⁷⁴

Mimicking Nishida's protocol,⁷⁴ we first prepared Danishefsky's diene **202** from *trans*-4-methoxy-3-buten-2-one **189** in the presence of Et₃N (2.7 equivalents) and TIPSOTf (1.1 equivalents). The desired crude product **202** was obtained in quantitative yield, which was used directly for the next step without purification due to the instability of the silyl enol ether portion on silica (**Scheme 41**).⁷⁵



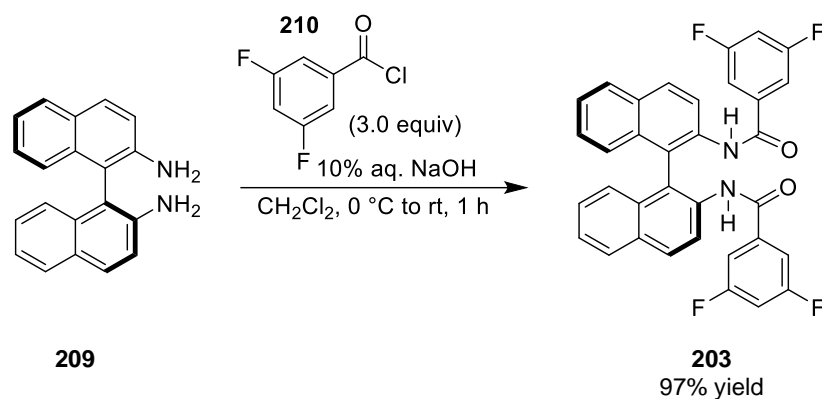
Scheme 41: The preparation of Danishefsky's diene **202**

With the diene **202** in hand, we next focused on the preparation of dienophile **201**. The coupling of 2-oxazolidinone **206** with 1.2 equivalents of acryloyl chloride **207** was performed in the presence of *n*-BuLi (1.1 equivalents) in THF at -78 °C to 0 °C to afford dienophile **201** in a very poor yield (5% yield).⁷⁶ To improve the yield, we switched to DCC coupling.⁷⁷ The 2-oxazolidinone **206** was coupled with 1.3 equivalents of acrylic acid **208** under the conditions of *N,N'*-dicyclohexylcarbodiimide (DCC) to furnish the desired dienophile **201** in 32% yield (**Scheme 42**).



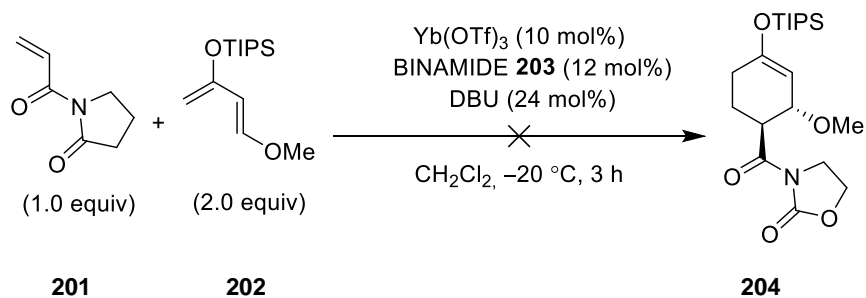
Scheme 42: The preparation of dienophile **201**

Even though the yields of dienophile **201** from both coupling conditions were surprisingly low, we had enough material to move forward and test the Diels–Alder chemistry. The chiral ligand **203** was also required for the enantioselective Diels–Alder reaction. The BINAMIDE ligand **203** was synthesised from (*S*)-1,1'-binaphthyl-2,2'-diamine **209** in excellent yield (97% yield) via an amide coupling using 3.0 equivalents of 3,5-difluorobenzoylchloride **210** and 10% aqueous solution of NaOH (**Scheme 43**).⁷⁴



Scheme 43: The preparation of BINAMIDE ligand **203**

Having all the required precursors, the asymmetric Diels–Alder cycloaddition of dienophile **201** with 2.0 equivalents of Danishefsky’s diene **202** catalysed by chiral Yb(III)-BINAMIDE complex was commenced in CH₂Cl₂ at –20 °C.⁷⁴ Unfortunately, the formation of cycloadduct **204** could not be observed after 3 hours. Unreacted diene **202** and dienophile **201** were recovered. It was unclear whether using Danishefsky’s diene **202** without purification or insufficient drying of Yb(OTf)₃ and BINAMIDE ligand **203** caused the reaction to fail. After extended efforts, the cycloaddition adduct **204** could not be obtained via an enantioselective Diels–Alder reaction (**Scheme 44**).

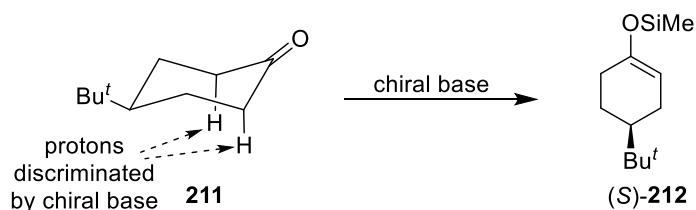


Scheme 44: The attempted formation of cycloadduct **204** via an enantioselective Diels–Alder reaction catalysed by Yb(III)-BINAMIDE complex

Owing to the unsuccessful synthesis of cycloadduct **204** via an enantioselective Diels–Alder reaction catalysed by Yb(III)-BINAMIDE complex, a new approach to obtain enantiomerically enriched enone **3** was then sought.

2.4.2 Enantioselective enolisation approach

There have been various developments in the use of chiral lithium amide bases, and many research groups have exploited them in asymmetric synthesis over the past few years.⁷⁸ The chiral lithium amide bases have been used successfully in asymmetric desymmetrisation of conformationally locked prochiral cyclic ketones, which the Simpkins group initially reported in 1986.^{78,79} The chiral base differentiates between a pair of enantiotopic protons in a substrate, symmetrically substituted or cyclic prochiral ketone, possessing a plane of symmetry to generate an enantioenriched product.^{78,80} This can be described in a stereoelectronic preference for deprotonation of the axial protons, and an appropriate chiral base should be able to differentiate between the two protons to preferentially produce one enantiomer of silyl enol ether **212** as illustrated in **Scheme 45**.⁷⁸



Scheme 45: Desymmetrisation of cyclohexanone **211**⁷⁸

In order to obtain high enantioselectivity in chiral base-mediated-ketone deprotonations, trapping the lithium enolates as silyl enol ethers by Corey's internal quench method⁸¹ is recommended. As outlined in **Table 4**, Simpkins investigated the enantioselectivity of (*S*)-silyl enol ether **212** via deprotonation of cyclohexanone **211** by using chiral bases (*R,R*)-**213**, followed by silylation with TMSCl under Corey's internal quench protocol at different temperatures. This suggested that lower temperature gave a better enantiomeric excess of (*S*)-**212**.⁸⁰

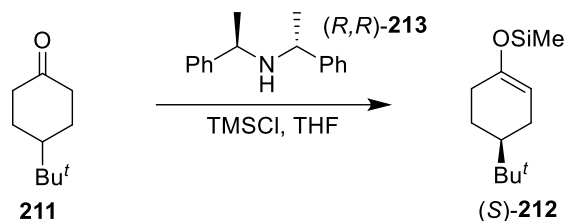
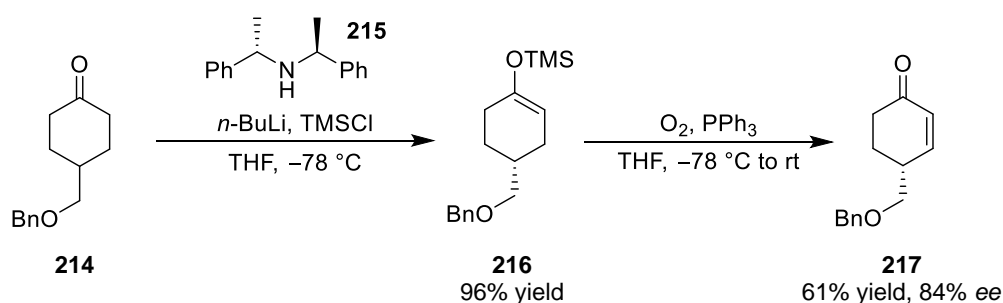


Table 4: Simpkins's screening temperature for the desymmetrisation of ketone **211**⁸⁰

Temp/ °C	Yield (%)	ee (%)
-78	73	69
-90	66	88

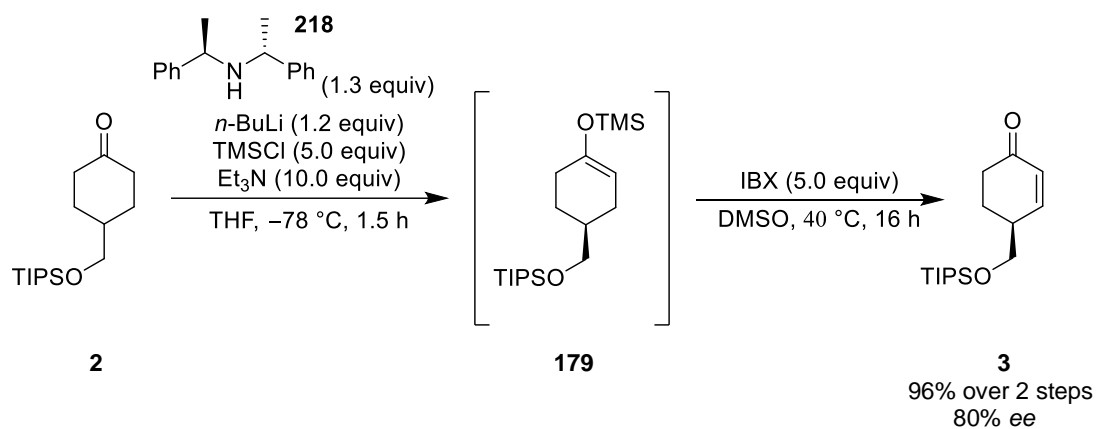
Based on Simpkins's findings, a number of research groups have utilised asymmetric deprotonation in total synthesis. For example, in 1995, the Smith group reported the synthesis of (*R*)-enone **217**, the precursor for synthesising penitrem D, from the simple 4-substituted cyclohexanone **214** through a two-step asymmetric induction tactic.⁸² Asymmetric deprotonation of achiral cyclohexanone **214** using the lithium amide of chiral base (*S,S*)-**215**, followed by internal quench conditions with TMSCl gave functionalised silyl enol ether **216** in excellent yield (96% yield). The TMS-enol ether **216** was then oxidised to the corresponding (*R*)-enone **217** in 61% yield with 84% enantiomeric excess (**Scheme 46**).



Scheme 46: Smith's synthesis of (*R*)-cyclohexenone **217** via an enantioselective enolisation⁸²

Due to the high level of enantioselectivity of cyclohexenone **217** by the Smith group,⁸² we envisioned forming enantioenriched cyclohexenone **3** through an enantioselective enolisation. The chiral lithium amide base (*R,R*)-**218** was used under kinetic conditions at -78 °C producing the lithium enolates, which was trapped with excess TMSCl (5.0 equivalents) to give the enantioenriched silyl enol ether **179** in >99% conversion. Mirroring

our method on the synthesis of racemic cyclohexenone **3**, subsequent oxidation of crude TMS-enol ether **179** with 5.0 equivalents of IBX provided the requisite enantioenriched cyclohexenone **3** (80% ee) in excellent yield over two steps (**Scheme 47**).



Scheme 47: The synthesis of (*S*)-cyclohexenone **3** via an enantioselective enolisation

The enantiomeric excess of (*S*)-cyclohexenone **3** was determined by HPLC analysis under the same conditions as the racemic compound using CHIRALCEL® IC column eluting with 1% *i*-PrOH/hexane (flow rate = 1.0 mL/min, temp = 40 °C, λ = 216 nm) as shown in **Figure 12**.

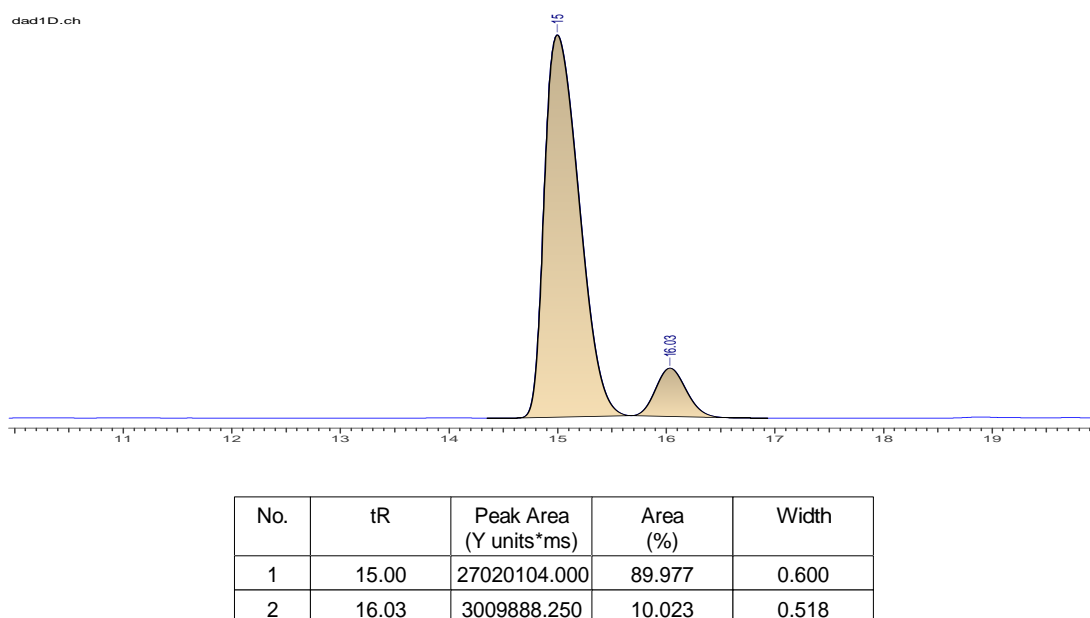
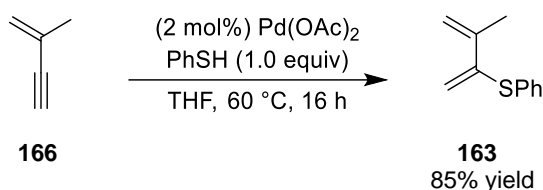


Figure 12: HPLC trace of (*S*)-cyclohexenone **3**

To this end, we have successfully synthesised the enantiomerically enriched cyclohexenone **3** on a gram-scale with modest enantioselectivity (80% *ee*) and excellent yield through an efficient sequence of chiral lithium amide base-mediated enantioselective enolisation and IBX oxidation. The next goal to construct the decalin system via an asymmetric Diels–Alder cycloaddition will be described in the next section.

2.5 The synthesis of enone *trans*-decalin **5**

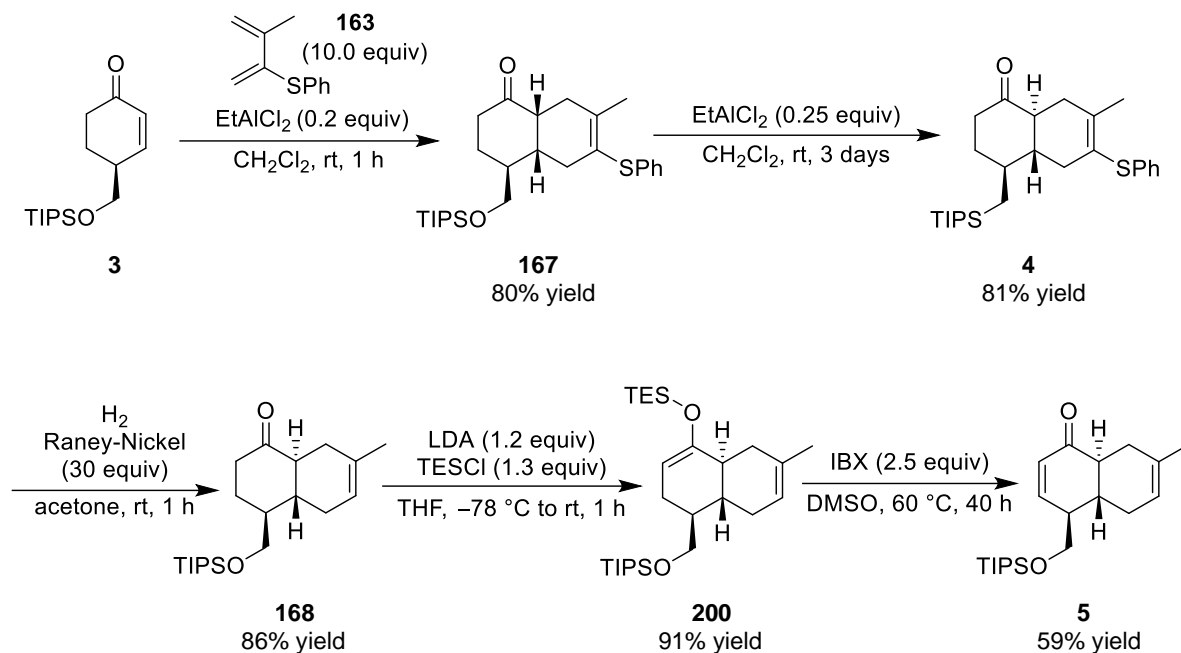
With the important building block **3** in hand, this would be the crucial stage to construct the decalin scaffold and set up the required stereogenic centres. The racemic route for preparing the decalin moiety via Diels–Alder cycloaddition discovered by the Clarke group would pave the way for our asymmetric approach to access the enantioenriched anthracimycin core.⁶⁶ With the readily available cyclohexenone **3** in hand, we prepared the key sulfur-substituted diene **163** from 2-methyl-1-buten-3-yne **166** and thiophenol in the presence of a catalytic amount of Pd(OAc)₂, in THF at 60 °C. The sulfur-substituted diene **163** was generated in 85% yield (**Scheme 48**).⁸³



Scheme 48: The synthesis of sulfur-substituted diene **163**

As our point of departure, the enantioenriched enone **3** was subjected to stereo- and regioselective Diels–Alder cycloaddition with electron-rich diene **163** in the presence of a catalytic amount of EtAlCl₂ (0.2 equivalents) to afford *cis*-decalin **167** in 80% yield as a single diastereomer.^{84,85} For this stage, the silyl chain of enone **3** blocked the addition of the diene **163** from the top face, while the thiophenyl group on diene **163** promoted the regioselectivity. As the *trans*-decalin is present in the natural product, *cis*-decalin **167** was epimerised to *trans*-decalin **4** in 81% yield under the same conditions for three days. The stereochemistry of *cis*- and *trans*-decalin was confirmed by the NMR method compared to Lodovici's finding in symmetric synthesis.⁶⁶ Removal of the thiophenyl group via a selective reduction required a large excess of Raney-Nickel (30 equivalents) to furnish *trans*-decalin

168 in 86% yield.^{84,85} Enone *trans*-decalin **5** was obtained from ketone **168** in two steps by enolisation to produce TES-enol ether **200**, which was subjected to IBX oxidation to give the corresponding enone *trans*-decalin **5** in 59% yield (**Scheme 49**).⁶⁶



Scheme 49: The synthesis of enone *trans*-decalin **5**

In summary, we have completed the asymmetric synthesis of enone *trans*-decalin **5** in five steps from enantioenriched building block **3** via a stereo- and regioselective Diels–Alder reaction. To establish the core structure of anthracimycin, a stereocontrolled installation of a side chain to the decalin scaffold would be the next challenging goal.

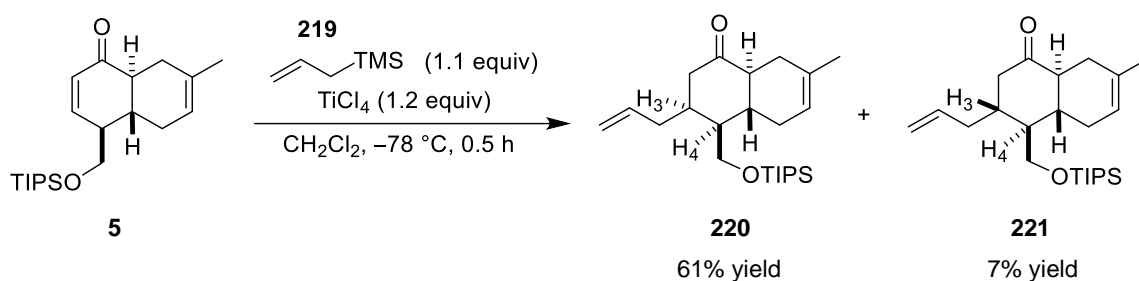
2.6 Installation of a side chain to achieve the anthracimycin core

2.6.1 Hosomi–Sakurai 1,4-addition approach

Hosomi–Sakurai addition is a type of conjugate addition reaction to form a carbon-carbon bond involving a Lewis acid-promoted allylation of allylsilane and several electrophiles.^{86,87} Based on the study of Hosomi–Sakurai 1,4-addition in the Clarke group, the TiCl_4 -promoted allylation of enone **5** with (*E*)-crotyltrimethylsilane **171** provided an inseparable mixture of two diastereomers.⁶⁶ Regarding separation difficulty, this approach could not be used

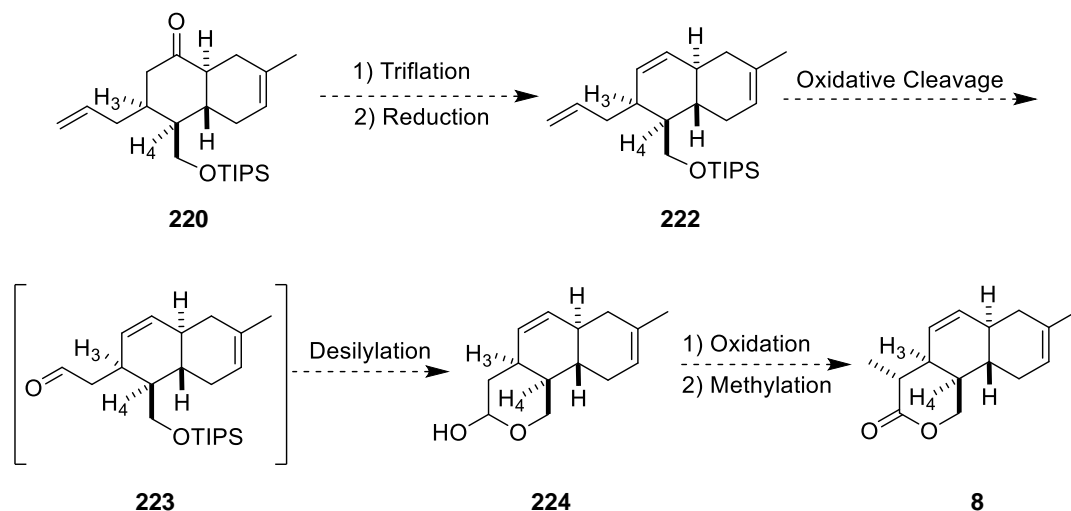
towards the total synthesis even though this method delivered the major product with the desired stereochemistry (see **Scheme 28**).

Since this approach successfully set up the required stereochemistry for the anthracimycin core, the Clarke group further investigated the allylation of enone **5** with allyltrimethylsilane **219**. Two diastereomers **220** and **221** were obtained in 61% and 7% yields, respectively. Pleasingly, the stereochemistry of major product **220** was confirmed to be a *syn*-relationship between H-3 and H-4, while an *anti*-relationship between those protons was found in the minor diastereomer **221** determined by XRD of their hydrazone derivatives (**Scheme 50**).⁶⁶



Scheme 50: Previous Clarke group work on the Hosomi–Sakurai 1,4-addition of enone **5** and allyltrimethylsilane **219**⁶⁶

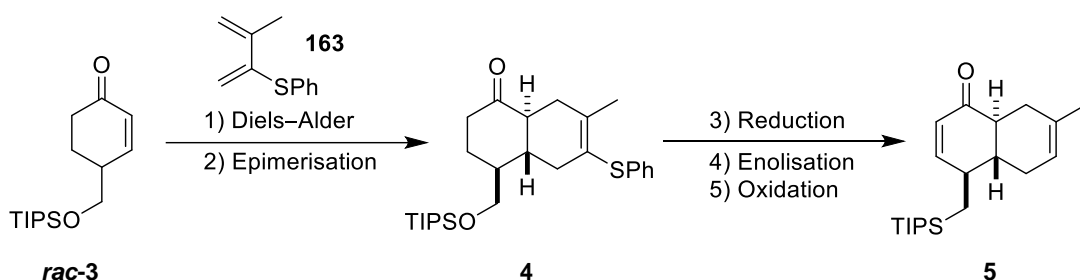
Therefore, since the Hosomi–Sakurai addition of enone *trans*-decalin **5** established the correct stereochemical configuration present in the natural product, we proposed utilising this synthetic route to access the anthracimycin core. The ketone functionality of **220** would be converted to olefin **222** in two steps via triflate formation, followed by Pd-catalysed reduction. Then, the terminal olefin of **222** would be cleaved and oxidised to form the aldehyde intermediate **223**. Removal of the TIPS group in **223** would lead to lactol **224** via spontaneous cyclisation of the primary alcohol in the presence of an aldehyde. The resultant lactol **224** would then be oxidised to a lactone moiety, and the methyl group would be installed by methylation to produce the anthracimycin core **8** (**Scheme 51**).



Scheme 51: The proposed synthetic route for the anthracimycin core **8**

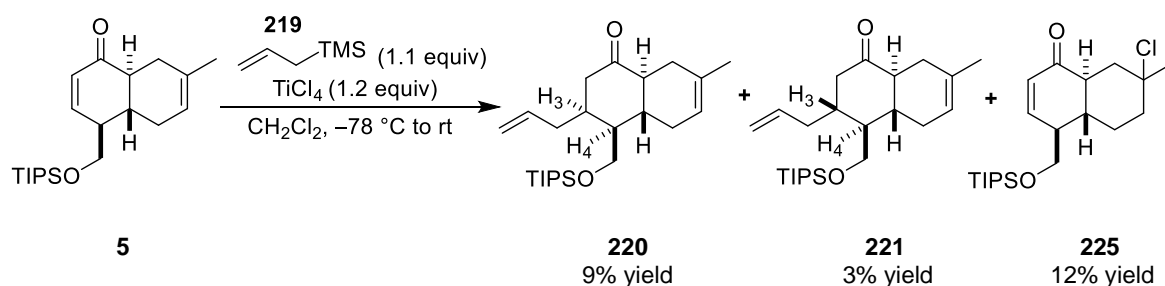
To explore the proposed synthetic pathway in **Scheme 51**, sufficient material to pursue the construction of lactone **8** was needed. To test the viability of the proposed synthesis and save the precious enantioenriched enone *trans*-decalin **5**, racemic material would be used. The racemic precursor **5** would be derived in five steps from racemic cyclohexenone **3** mirroring our previous asymmetric synthesis of **5**.

With racemic enone **3** and diene **163** in hand, the Diels–Alder cycloaddition delivered *cis*-decalin **167** as a single isomer, which was epimerised to *trans*-decalin **4** under the same conditions. Raney–Nickel reduction, enolisation, followed by oxidation gave the desired enone *trans*-decalin **5** as shown in **Scheme 52**.



Schem 52: The racemic synthesis of enone *trans*-decalin **5**

To pursue material for the construction of anthracimycin core, the promising key precursor **220** would be obtained from the Hosomi–Sakurai 1,4-addition. With the optimised conditions in hand,⁶⁶ the TiCl₄ (1.2 equivalents)-promoted allylation of enone *trans*-decalin **5** with allyltrimethylsilane **219** was commenced in CH₂Cl₂ at –78 °C. We realised that there was unreacted starting material in the reaction, as suggested by TLC analysis. However, increasing the temperature to room temperature to complete the consumption of starting material led to considerable decomposition. After purification of the crude residue by flash column chromatography, three diastereomers **220**, **221**, and **225** were obtained in 9%, 3%, and 12% yields, respectively. The desired product **220** was obtained with a very poor yield. However, the unexpected enone **225**, which contained an unreacted enone **5**, was identified as the major product (**Scheme 53**).



Scheme 53: The Hosomi–Sakurai 1,4-addition of enone *trans*-decalin **5**

Due to the formation of **225** via chlorination of enone **5** in the presence of a stoichiometric amount of TiCl₄, these results warranted the investigation of alternative Lewis acids to promote the allylation reaction (**Table 5**). To minimise the chlorination product **225**, the use of different Lewis acids was studied. Using 10 mol% of trifluoromethanesulfonimide (HNTf₂), the reaction was conducted at –78 °C and rapidly warmed to room temperature and this resulted in decomposition (entry 2).⁸⁸ Maintaining the temperature at –78 °C for 3 hours returned unreacted starting material (entry 3). Further increments in temperature to –40 °C led to the recovery of unreacted enone **5** (entry 4).

Owing to the failure of using HNTf₂, new Lewis acid was sought. Lee *et al.* demonstrated that an additive of TMSCl in the presence of catalytic InCl₃ efficiently promoted inter- and intramolecular Sakurai reactions.^{89,90} We followed their method to improve the conversion and yield. Allylation of enone **5** with allyltrimethylsilane **219** was commenced with a catalytic amount of InCl₃ (20 mol%) and TMSCl (1.0 equivalent) as an activator at room

temperature for 1 hour resulting in decomposition (entry 5). To gain the desired product **220**, the reaction was repeated, carefully monitored, and quenched within 30 minutes. Finally, the corresponding allylation product **220** was obtained in 23% yield together with its diastereomer **221** in 2% yield as outlined in entry 6.

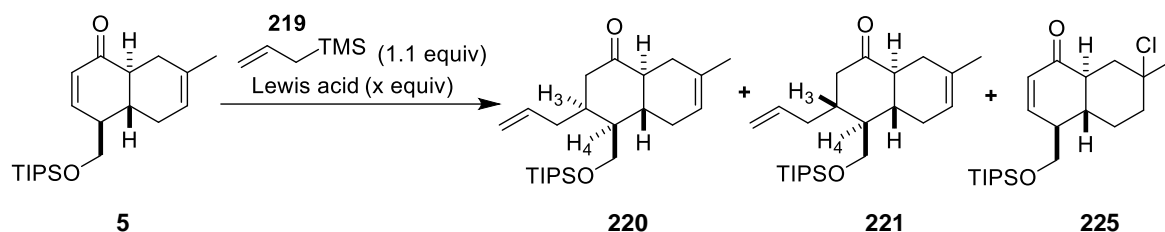


Table 5: Screening conditions for the Hosomi–Sakurai 1,4-addition of enone **5**

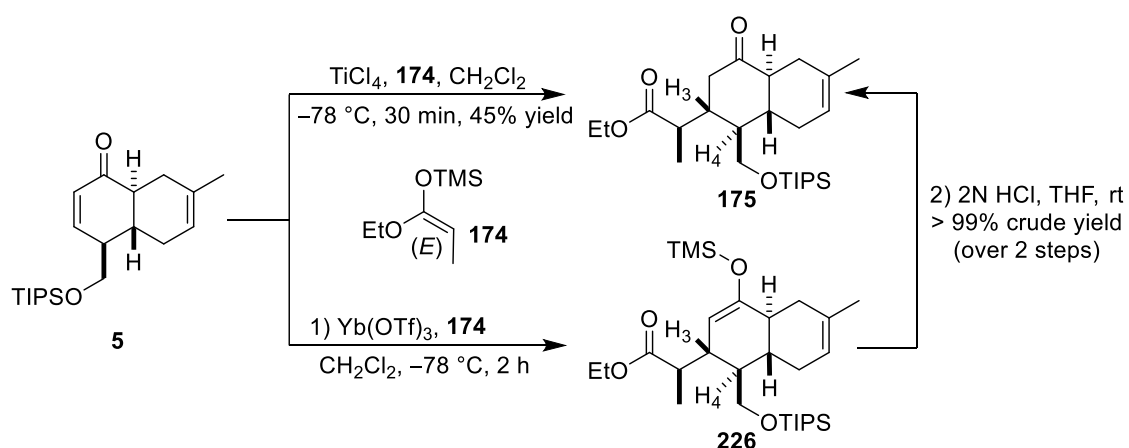
Entry	Lewis acid	Conditions	Conversion	Result ^b
				220 : 221 : 225
1	TiCl ₄ (1.2 equiv)	-78 °C to rt, 2 h	>99%	9% : 3% : 12%
2	HNTf ₂ (10 mol%)	-78 °C to rt, 1 h	Decomp.	–
3	HNTf ₂ (10 mol%)	-78 °C, 3 h	n.r.	–
4	HNTf ₂ (10 mol%)	-78 °C to -40 °C, 4 h	n.r.	–
5	InCl ₃ (20 mol%) ^a	rt, 1 h	Decomp.	–
6	InCl ₃ (20 mol%) ^a	rt, 30 min	>99%	23% : 2% : –

^a TMSCl (1.0 equiv) was used as additive. ^b Result was described in % isolated yield

Under the optimised reaction conditions, the Hosomi–Sakurai 1,4-addition of allyltrimethylsilane **219** to enone *trans*-decalin **5** promoted by different Lewis acids produced the desired product **220** in a surprisingly low yield due to the decomposition and instability of the product during the purification process. For this reason, this approach proved unsuitable for pursuing sufficient material towards the total synthesis.

2.6.2 Mukaiyama–Michael addition approach

Mukaiyama–Michael addition was one of the strategies investigated by the Clarke group to install a side chain on a *trans*-decalin scaffold.^{66,91,92,93} The conditions developed using different Lewis acids were utilised to access the epimer of anthracimycin core. The Mukaiyama–Michael 1,4-addition of **5** with (*E*)-ethyl-propanoate silyl ketene acetal **174** in the presence of TiCl₄ provided the 1,4-addition adduct **175** directly in 45% yield. Meanwhile, use of Yb(OTf)₃ gave the silyl enol ether intermediate **226**, which required hydrolysis under acid conditions to furnish **175** in excellent crude yield over two steps. However, both screened conditions delivered ester **175** as a single diastereomer with the undesired *anti*-relationship between H-3 and H-4 identified to be the epimer of anthracimycin core as shown in **Scheme 54**.⁶⁶

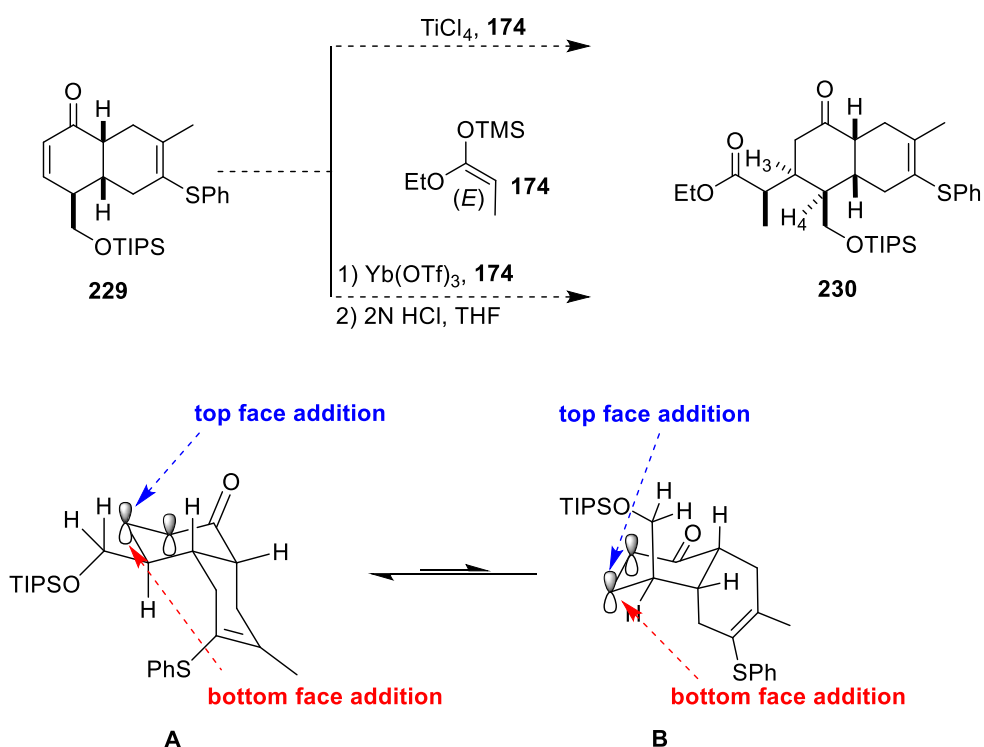


Scheme 54: Previous Clarke group work on the Mukaiyama–Michael 1,4-addition of enone **5** and (*E*)-ethyl-propanoate silyl ketene acetal **174**⁶⁶

Since the Mukaiyama–Michael addition of enone *trans*-decalin **5** with (*E*)-ethyl-propanoate silyl ketene acetal **174** set up the undesired stereochemistry of **175**, insight into the key parameters to control the stereoselectivity was needed. Considering the facial selectivity, this could be controlled by either nucleophile geometry or electrophile conformation. Therefore, we planned to study the geometry of the nucleophile by using (*Z*)-ethyl-propanoate silyl ketene acetal **228** instead of (*E*)-isomer **174**. The selective formation of (*Z*)-silyl ketene acetal **228** from the commercially available ethyl propionate **227** was illustrated by Ireland and co-workers in 1991.⁹⁴ The combined use of THF with 45% of the dipolar aprotic solvent *N,N'*-Dimethylpropyleneurea (DMPU) favoured a stable (*E*)-enolate leading

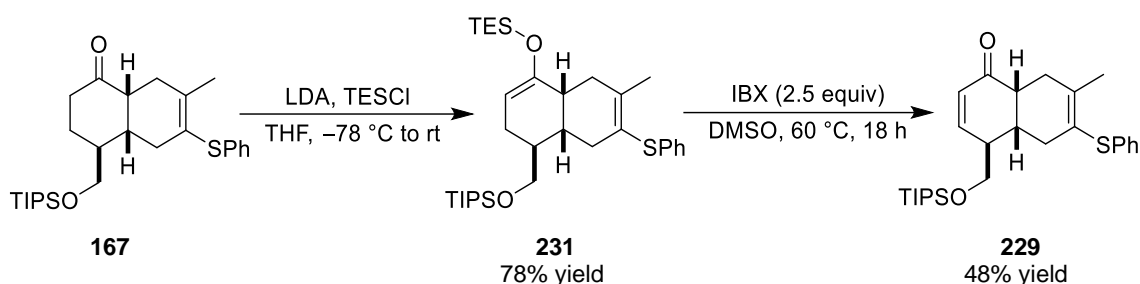
applied. Disappointingly, conversion to either the desired (*Z*)-isomer **228** or (*E*)-isomer **174** could not be observed. Due to the unsuccessful preparation of (*Z*)-ethyl-propanoate silyl ketene acetal **228**, the study on the effect of nucleophile geometry for Mukaiyama–Michael addition could not be attempted. Hence, the effect of electrophile conformation on the stereochemistry of Mukaiyama–Michael addition would be investigated.

Based on a previous study in the Clarke group, the addition of (*E*)-ethyl-propanoate silyl ketene acetal **174** to the bottom face of enone *trans*-decalin **5** produced **175** with the *anti*-relationship between H-3 and H-4 (see **Scheme 54**).⁶⁶ Since the direction of the nucleophile controlled the stereoselectivity in the product, the addition of **174** from the bottom face of the *cis*-decalin would be sterically disfavored by a steric hindrance of the concave (tent-like) shape of *cis*-decalin ring **229**. As expected, an attack of **174** as a nucleophile on the top face of enone *cis*-decalin **229** could provide the anthracimycin core **230** with the required stereochemistry between H-3 and H-4 (**Scheme 57**).



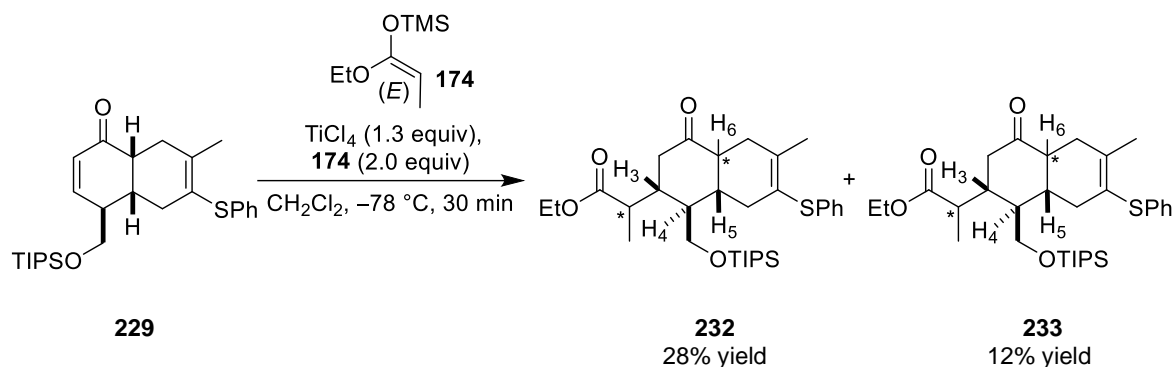
Scheme 57: The proposed the Mukaiyama–Michael 1,4-addition of (*E*)-ethyl-propanoate silyl ketene acetal **174** to enone *cis*-decalin **229**

In equilibrium, *cis*-decalin has two possible conformations, as depicted by A and B, owing to its flexibility and ring-flipping. However, we considered the conformation of *cis*-decalin **229** and proposed that A was more stable than B because the axial sterically bulky CH₂OTIPS group would experience 1,3-diaxial interactions (**Scheme 57**). Hence, it would favour A and support our hypothesis on the top face preference of nucleophile attack. Based on the proposed synthesis above, enone *cis*-decalin **229** would be required for this study. The precursor **229** was prepared via the same key Diels–Alder cycloaddition of racemic enone **3** and diene **163**. With *cis*-decalin **167** in hand, we functionalised ketone **167** to silyl enol ether **231** in 78% yield in the presence of LDA and TESCl (**Scheme 58**).



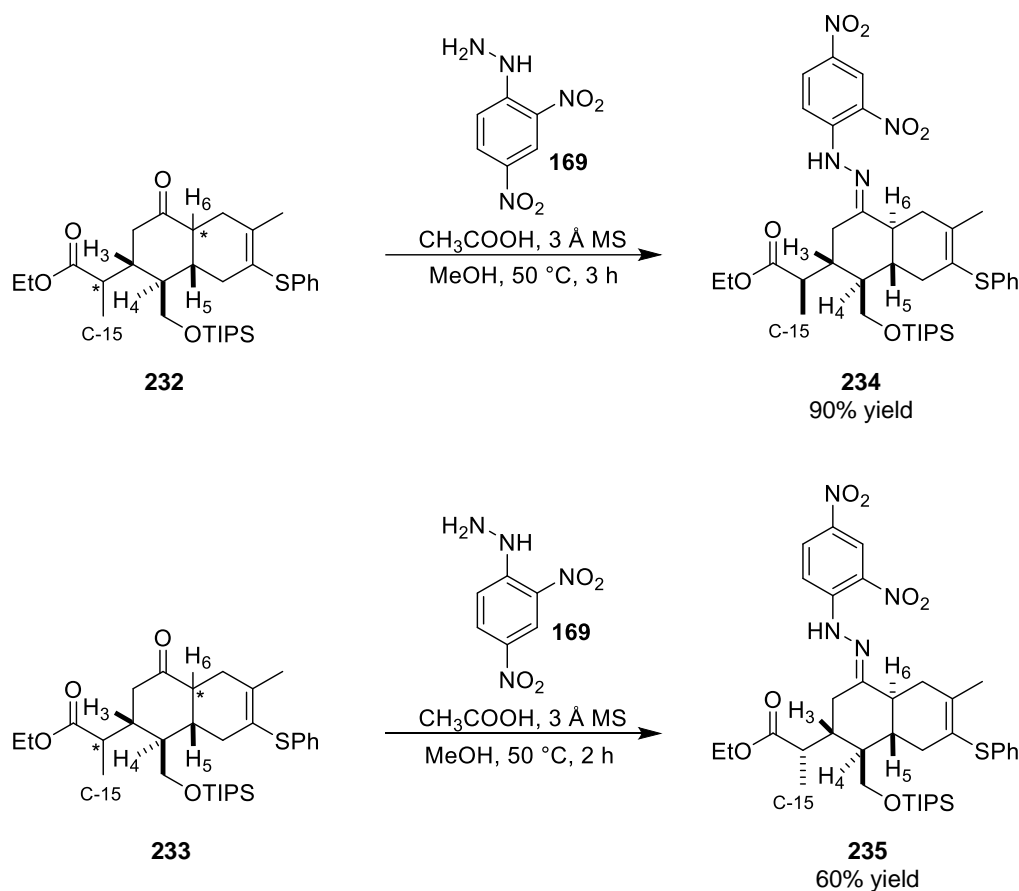
Scheme 58: The synthesis of enone *cis*-decalin **229**

To form the enone *cis*-decalin **229**, optimisation of the conditions for IBX oxidation was required. The IBX oxidation of TES-enol ether was reported by the previous work in the Clarke group, where it was noted that the stoichiometry of IBX significantly affected the formation of enone.⁶⁶ Following Lodovici's conditions, we initially carried out the silyl enol ether **231** under the conditions of IBX (2.5 equivalents) in DMSO at 40 °C. However, none of enone **229** was observed after 19 hours. The unreacted TES-enol ether **231** was fully recovered as shown in entry 1 (**Table 6**). To enhance the conversion, the temperature was increased from 40 °C to 60 °C. The formation of enone *cis*-decalin **229** was observed in >99% conversion after 18 hours. The desired enone *cis*-decalin **229** was isolated in 48% yield along with ketone *cis*-decalin **167** and ketone *trans*-decalin **4** in 2% and 7% yields, respectively (entry 2). It was assumed that ketones **167** and **4** were produced from the hydrolysis of TES-enol ether **231** by some water in DMSO at the higher temperature. Interestingly, the tautomerisation of enol intermediate to the keto-form favoured *trans*-decalin **4** due to the stability of the conformation. To improve the yield of **229**, the amount of IBX was then increased from 2.5 to 5.0 equivalents while keeping the other parameters unchanged. Although silyl enol ether **231** was entirely consumed after 22 hours, the



Scheme 60: The Mukaiyama–Michael 1,4-addition of enone *cis*-decalin **229**

In order to progress the synthesis of the anthracimycin core, it was important to understand the stereochemical outcome of this reaction. Hence, the stereochemistry of the two diastereomers **232** and **233** was determined by X-ray crystallography. We formed the crystals by conversion of **232** and **233** to their respective hydrazones. Consequently, ketones **234** and **235** were separately treated with 2,4-dinitrophenyl hydrazine **169** and glacial acetic acid in MeOH at 50 °C to afford hydrazones **234** and **235** in 90% and 60% yields, respectively (**Scheme 61**).



Scheme 61: The synthesis of hydrazone derivatives **234** and **235**

The X-ray crystallography results revealed that the hydrazone **234** consisted of the desired *syn*-relationship between the methyl group at the 15-position and the CH₂OTIPS group. In contrast, the undesired stereochemistry of the methyl group at the same position was confirmed in hydrazone **235**. However, the *anti*-relationship between H-3 and H-4 was obtained in both hydrazone derivatives **234** and **235** instead of a *syn*-relationship. In addition, the crystal structures of **234** and **235** showed the *anti*-relationship between the decalin junction, which were confirmed to be *trans*-decalins (**Figure 13–14**). It was observed that the *cis*-decalin was epimerised unintentionally to the *trans*-decalin during Mukaiyama–Michael 1,4-addition and hydrazone formation, but it was still unclear which step caused the epimerisation. The accidental epimerisation did not affect our synthesis since we proposed to eventually epimerise the *cis*-decalin to the *trans*-decalin in the late stage.

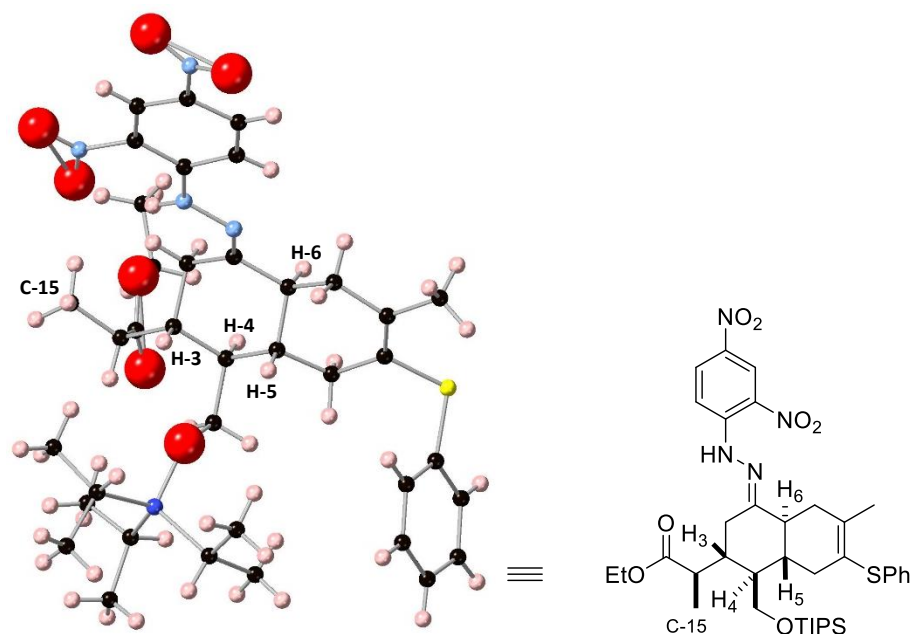


Figure 13: The single crystal X-ray diffraction of hydrazone **234**

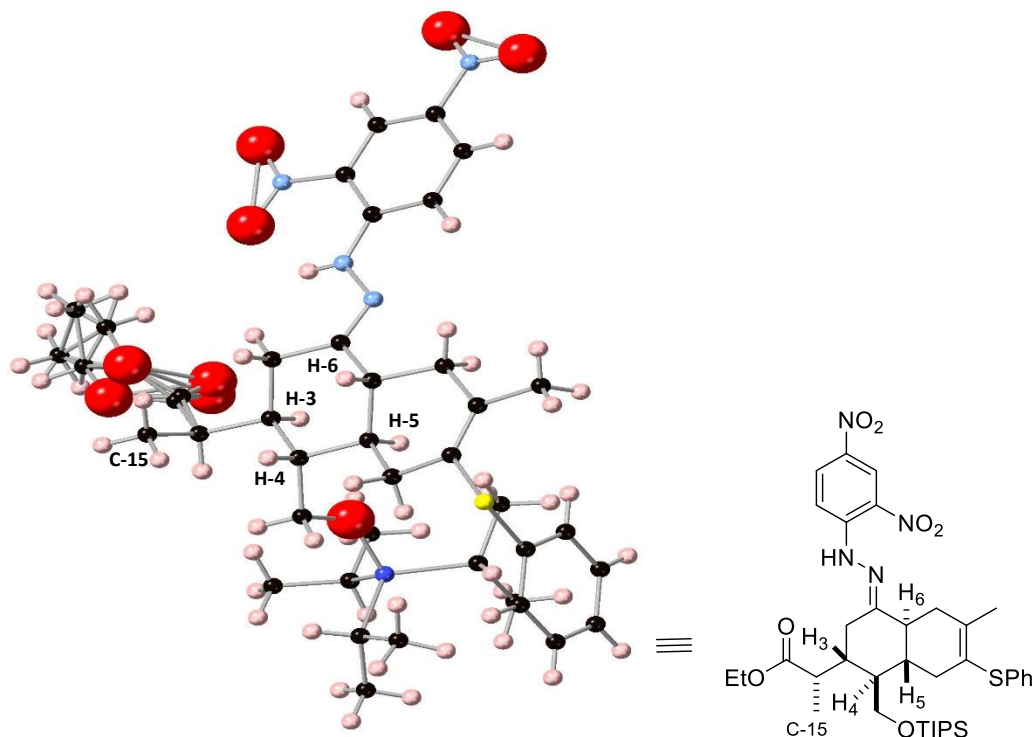
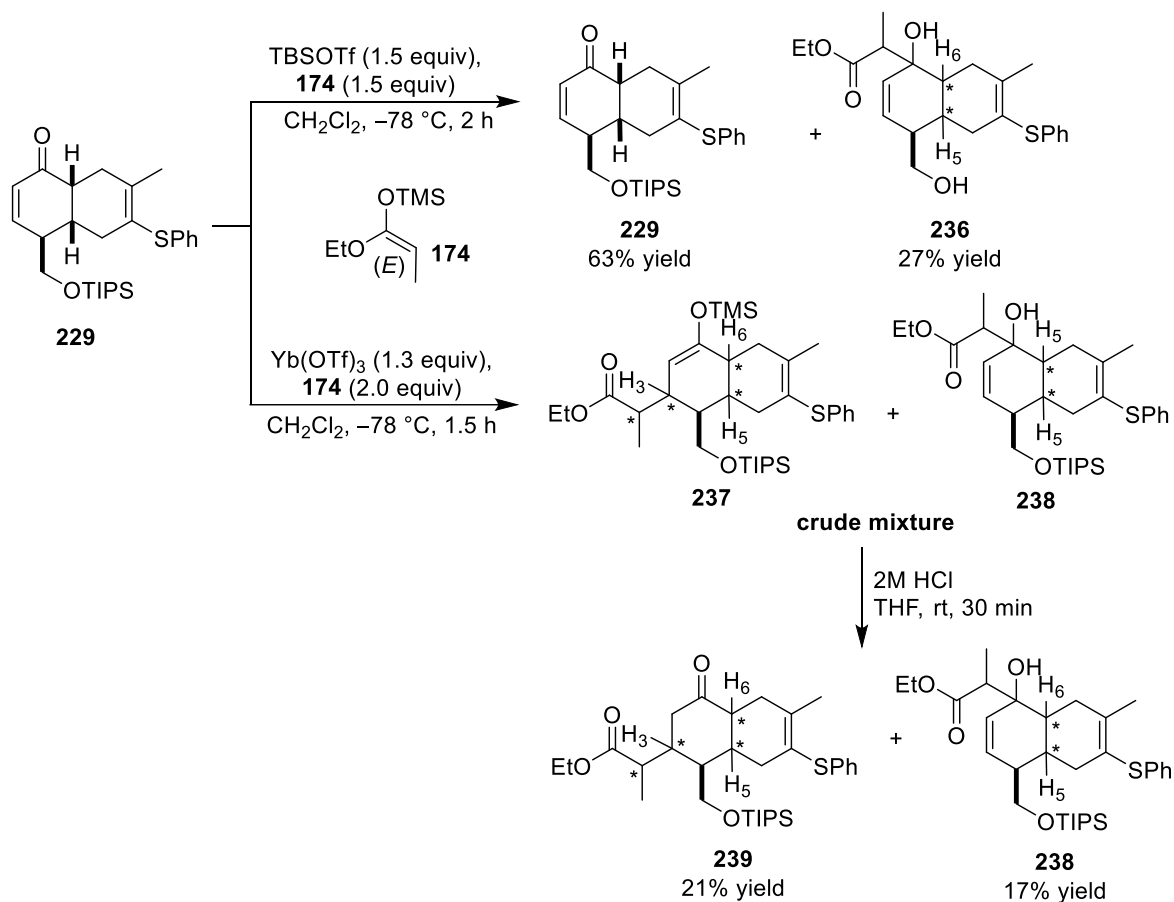


Figure 14: The single crystal X-ray diffraction of hydrazone **235**

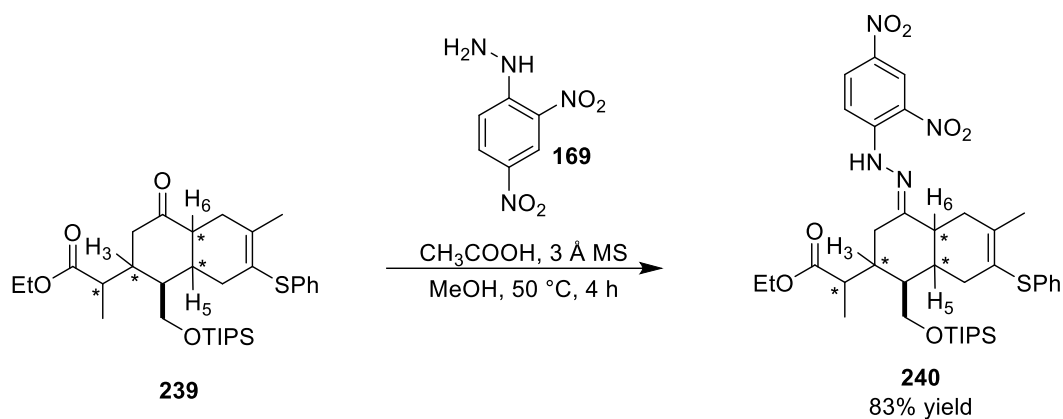
The use of stoichiometric TiCl_4 promoted the Mukaiyama–Michael 1,4-addition of enone *cis*-decalin **229**, yielding the epimer of anthracimycin core (**Scheme 60**). Therefore, an alternative Lewis acid that could catalyse the Mukaiyama–Michael 1,4-addition to access the core structure of anthracimycin had to be used. On careful consideration of Lewis acids, strong Lewis acids could lead to facile epimerisation. In order to prevent an eventual epimerisation of the decalin system, the conditions of either TBSOTf^{96} or $\text{Yb}(\text{OTf})_3^{66}$ were chosen to trial. Attempted TBSOTf -promoted Mukaiyama–Michael 1,4-addition of **174** to enone *cis*-decalin **229** afforded mainly aldol product **236** in 27% yield, whereas the starting material **229** was returned in 63% yield (**Scheme 62**).⁹⁶ To circumvent 1,2 addition, the conditions of $\text{Yb}(\text{OTf})_3$ employed in the earlier study by the Clarke group were then screened.⁶⁶ Switching the Lewis acid to $\text{Yb}(\text{OTf})_3$ under the same conditions for 1.5 hours gave access to a mixture of TMS-enol ether **237** and alcohol **238** with a 1:1 ratio. Acid treatment of the crude mixture generated the 1,4-addition adduct **239** and alcohol **238** in 21% and 17% yields, respectively. Although the reactions were commenced under kinetic conditions, the undesired aldol products **236** and **238** were obtained from both conditions. In addition, it was assumed that triflate species under the conditions of TBSOTf readily

removed the silyl group in the presence of the aldol intermediate to produce diol **236** as a single product (**Scheme 62**).



Scheme 62: The Mukaiyama–Michael addition of enone *cis*-decalin **229**

It should be noted that the Mukaiyama–Michael 1,4-addition of **174** to enone *cis*-decalin **229** under the conditions of TBSOTf afforded mainly 1,2-addition adduct **236**. However, performing the reaction in the presence of Yb(OTf)₃, subsequent hydrolysis generated the 1,4-addition adduct **239** and aldol product **238** in a 1:1 ratio. The 1,4-addition adduct **239** was further modified to hydrazone derivative **240** in good yield (**Scheme 63**). The NMR data of **240** was completely different to **234** and **235** as depicted in **Figure 15**. Therefore, we needed the crystal structure of **240** to determine the stereochemistry.



Scheme 63: The formation of hydrazone 240

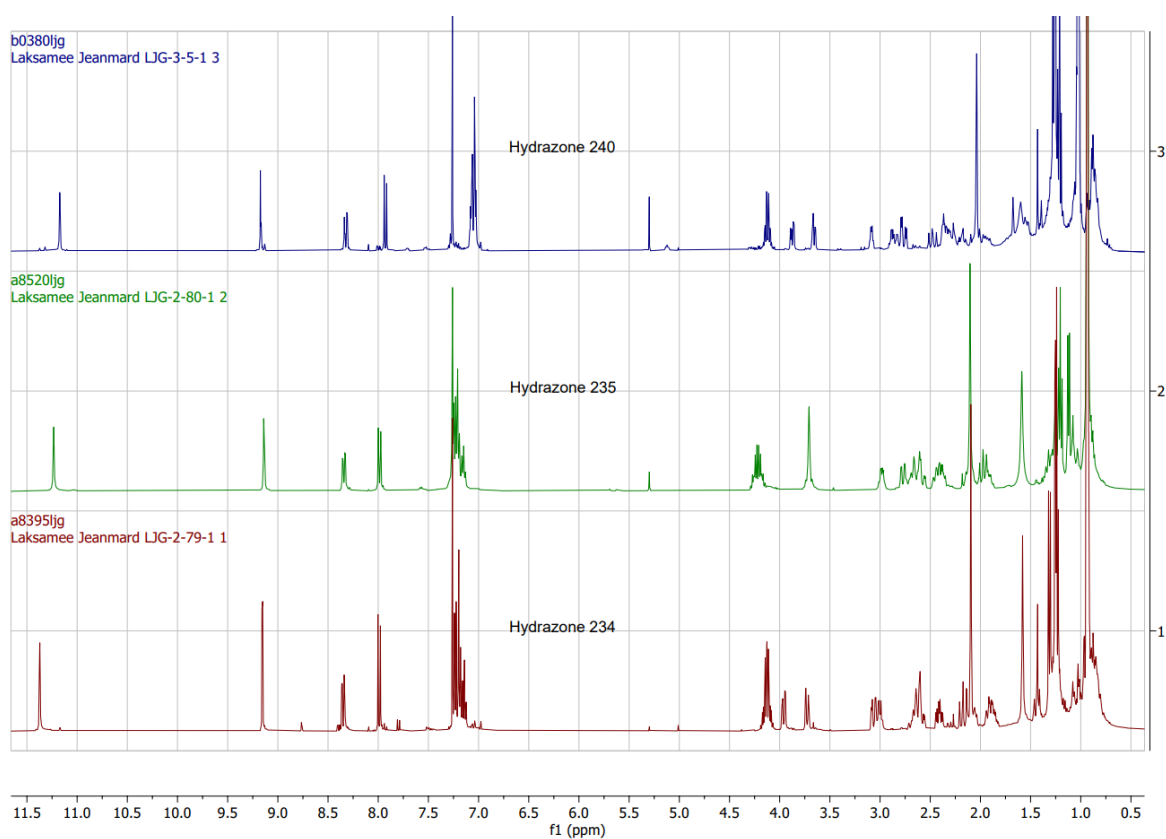


Figure 15: The ^1H NMR spectrum of hydrazone 240 compared to hydrazones 234 and 235

Unfortunately, we were unable to grow crystals after extended efforts, so the stereochemistry of **240** was still unknown. Due to a 1:1 ratio of 1,4 addition adduct **239** and aldol product **238** obtained from the conditions of $\text{Yb}(\text{OTf})_3$, the stereochemistry outcome of **239** was not crucial to pursue the synthesis of anthracimycin core.

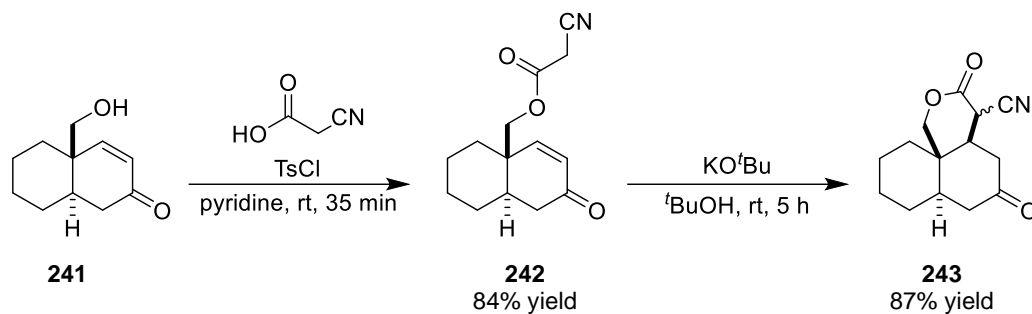
To summarise, the installation of a side chain via the Mukaiyama–Michael 1,4-addition was investigated on the *cis*-decalin scaffold. In addition, various Lewis acids were screened to study the effect on stereoselectivity highlighted in our synthesis. Under optimised conditions, TiCl₄-promoted the Mukaiyama–Michael 1,4-addition of the *cis*-decalin produced the *epi*-anthracimycin core with the undesired *anti*-relationship between H-3 and H-4, indicating that the conformation of *cis*-decalin did not hinder the addition of nucleophile from the bottom face. This approach would be suitable for synthesising anthracimycin analogues. However, a suitable strategy for the anthracimycin core was still required.

2.6.3 Intramolecular Michael addition approach

Since we aimed to build a side chain on the decalin system and set up the new stereogenic centre, intermolecular 1,4-additions had been investigated so far. Attempted either Sakurai addition or Mukaiyama–Michael 1,4-addition could not progress our synthesis. Consequently, substrate control would be a promising tool to afford the anthracimycin core with the desired stereochemistry.

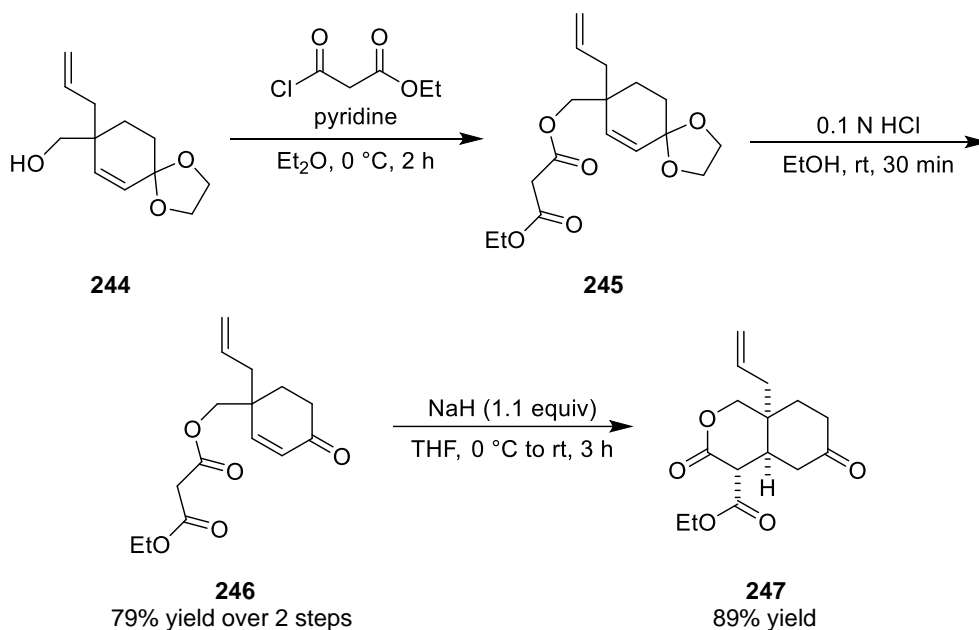
An intramolecular addition is widely used for ring formation. This approach would be a convenient way to access the requisite stereochemistry. Hence, we speculated that a side chain could be introduced by ring formation, where stereochemistry could be controlled by an enantioenriched starting material. The efficient intramolecular Michael addition is utilised to construct 6-membered lactones or bicyclic rings with high stereoselectivity, essential for synthesising natural products.

In 1996, Ley and co-workers synthesised the azadirachtin framework using an intramolecular Michael addition to construct cyclic lactone intermediate **243**.⁹⁷ The Michael precursor **242** was prepared in good yield from alcohol enone **241** and cyanoacetic acid in the presence of *p*-toluenesulfonyl chloride in pyridine through esterification. Cyanoacetate **242** was subsequently treated with potassium *tert*-butoxide via an intramolecular Michael addition furnishing cyclic nitrile intermediate **243** as a 1:1 inseparable mixture of cyano epimers in 87% yield as illustrated in **Scheme 64**.



Scheme 64: Ley's synthesis of cyanolactone **243**⁹⁷

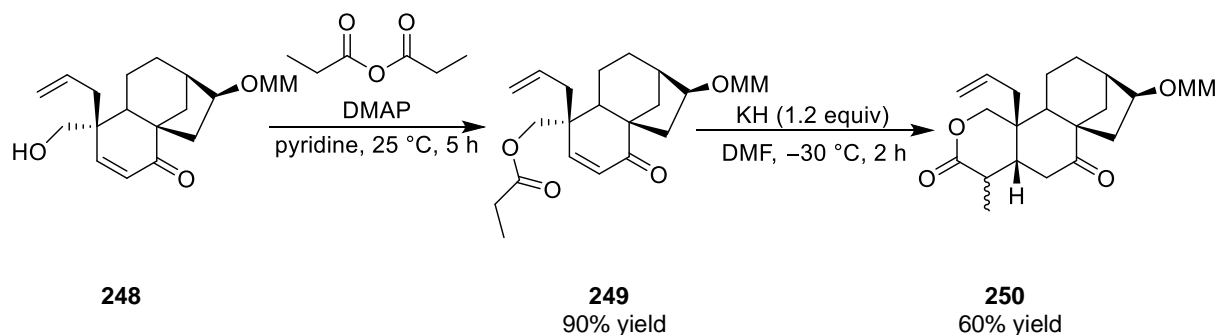
The second example of using an intramolecular Michael addition to form bicyclic ring **247**, a key intermediate for the total synthesis of antitumor sesquiterpene vernolepin, was reported by the Isobe group.⁹⁸ The bicyclic lactone **247** was accomplished in a three-step sequence from ketal alcohol **244**. The alcohol **244** was esterified by ethyl malonyl chloride and pyridine, in Et₂O at 0 °C to give ketal malonate **245**, which was directly hydrolysed with 0.1 N HCl affording the intramolecular Michael precursor **246** in 79% over two steps. Intramolecular Michael addition to enone malonate **246** with sodium hydride (1.1 equivalents) in THF at 0 °C delivered a single lactone **247** in 89% yield (**Scheme 65**).



Scheme 65: Isobe's synthesis of bicyclic lactone **247**⁹⁸

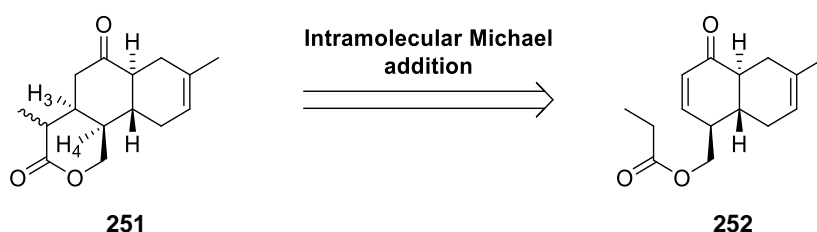
In addition, the synthesis of 15-desoxyeffusin derivatives was achieved by utilising an intramolecular Michael addition to afford the key tricyclic lactone **250** illustrated in

Mander's synthesis (**Scheme 66**).⁹⁹ The coupling of alcohol **248** with propionic anhydride under catalytic DMAP in pyridine generated the intramolecular Michael precursor **249** in 90% yield. Subsequently, treatment of **249** with 1.2 equivalents of potassium hydride led to an intramolecular Michael addition to produce the corresponding tricyclic lactone **250** in a moderate yield.



Scheme 66: Mander's synthesis of tricyclic lactone **250**⁹⁹

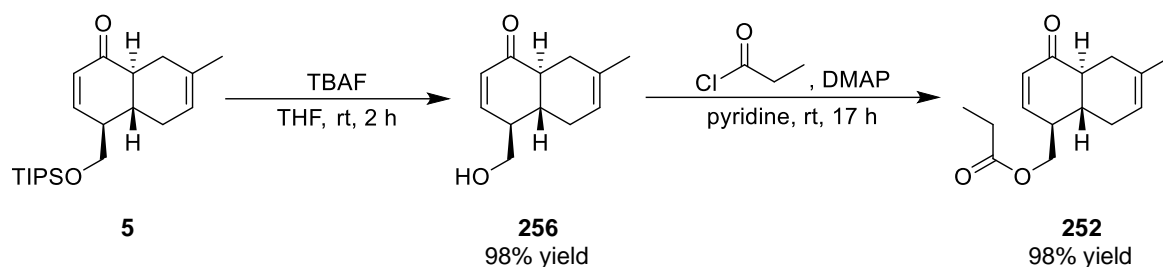
As the examples above embodied some desirable features, we anticipated that introducing a side chain on the decalin moiety to access the anthracimycin core via intramolecular conjugate addition could be possible. In refining our synthetic direction, we planned to employ the successful cyclisation of propionate under basic conditions inspired by Mander's synthesis⁹⁹ to install the methyl group and set the requisite stereochemistry. Accordingly, we hypothesised that the lactone ring **251** could be constructed from propionate **252**. The desired stereochemistry of H-3 and H-4 could be controlled by the cyclisation on the same side of the propionyl chain via the top face addition of formed enolates (**Scheme 67**).



Scheme 67: The proposed synthesis of anthracimycin core **251** via an intramolecular Michael addition

through an intramolecular Michael addition required a reasonable reaction scale and an enantioenriched precursor to address the requisite tricyclic lactone directly. Having absolute stereochemistry in the single crystal would be an advantage in clear results analysed by X-ray crystallography.

To progress the asymmetric synthetic route, enantioenriched enone propionate **252** was prepared from enone *trans*-decalin **5**. The silyl group of **5** was removed smoothly by TBAF in THF to give alcohol **256** in excellent yield. Treatment of **256** with propionyl chloride in the presence of pyridine and catalytic DMAP provided the corresponding propionate **252** in 98% yield as illustrated in **Scheme 69**.



Scheme 69: The formation of enone propionate **252**

With propionate **252** in hand, we investigated the formation of tricyclic lactone **251** via an intramolecular Michael addition as shown in **Table 7**. Following Mander's protocol, the formation of tricyclic lactone **251** was initially investigated under the presence of potassium hydride (1.2 equivalents) in DMF at $-30\text{ }^{\circ}\text{C}$ for 3.5 hours. However, no desired product **251** was observed from these conditions, while the conjugated enone **257** was generated in 15% conversion and obtained in 14% isolated yield after purification by flash column chromatography. Propionate **252** was recovered in 85% yield (entry 1). In an attempt to circumvent this elimination of the propionyl group, we explored more sterically bulky bases to favour the deprotonation of a less hindered proton (H-14) on the propionate motif. The formation of **251** could not be observed under the use of KHMDS at $-78\text{ }^{\circ}\text{C}$ within 1 hour. Increasing the temperature from $-78\text{ }^{\circ}\text{C}$ to room temperature immediately provided the mainly conjugated enone **257** in 71% conversion, whereas the unreacted propionate **252** was returned (entry 2). To minimise the formation of **257**, another sterically bulky base was then investigated. The intramolecular Michael addition of **252** was commenced in the presence of LDA at $-78\text{ }^{\circ}\text{C}$. Once again, the conversion to tricyclic lactone **251** could not be

observed. The reaction mixture was, therefore, slowly warmed to room temperature. However, the conjugated enone **257** was obtained in 22% conversion after being stirred for a further 6 hours (entry 3).

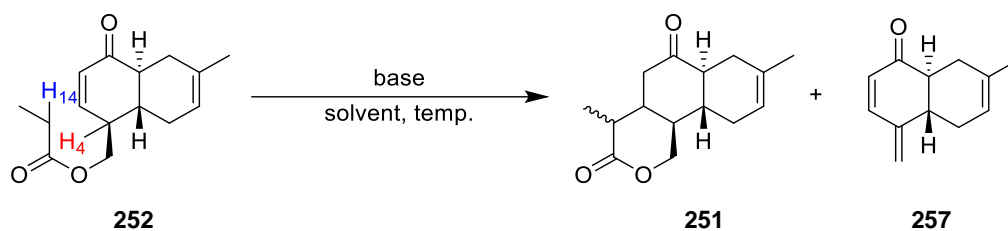
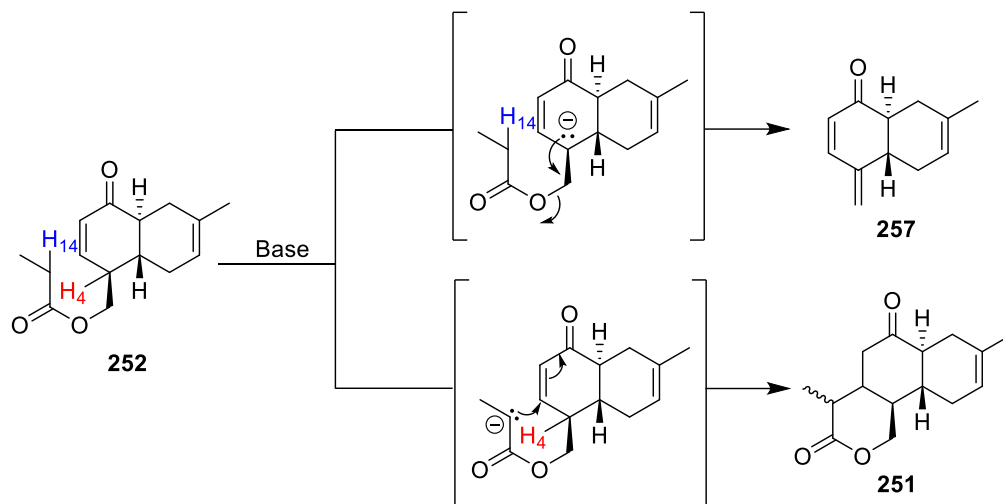


Table 7: Screening conditions for the intramolecular Michael addition of propionate **252**

Entry	Conditions	Temperature	Result (% conversion)	
			251	257
1	KH (1.2 equiv), DMF	-30 °C, 3.5 h	-	15% ^a
2	KHMDS (1.1 equiv), THF	-78 °C to rt, 1 h	-	71%
3	LDA (1.1 equiv), THF	-78 °C to rt, 7 h	-	22%

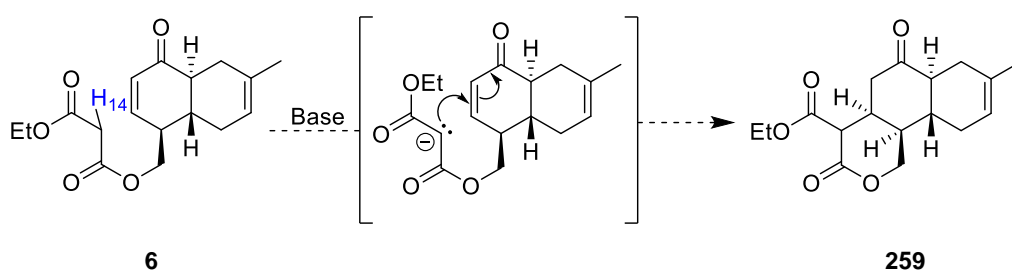
^a Unreacted propionate **252** was recovered in 85% yield

As the results above show, the conjugated enone **257** was obtained mainly among the bases tested in a range of 15–71% conversion, while the formation of the desired tricyclic lactone **251** could not be observed. Therefore, it was unclear how different the acidity of H-4 and H-14 would be. However, we confirmed from the experimental results that the deprotonation under basic conditions favoured the H-4 leading to the conjugated enone **257** as a single product. The formation of tricyclic lactone **251** and enone **257** was proposed in two mechanism pathways as depicted in **Scheme 70**.



Scheme 70: The proposed mechanism to construct the desired tricyclic lactone **251** and undesired conjugated enone **257**

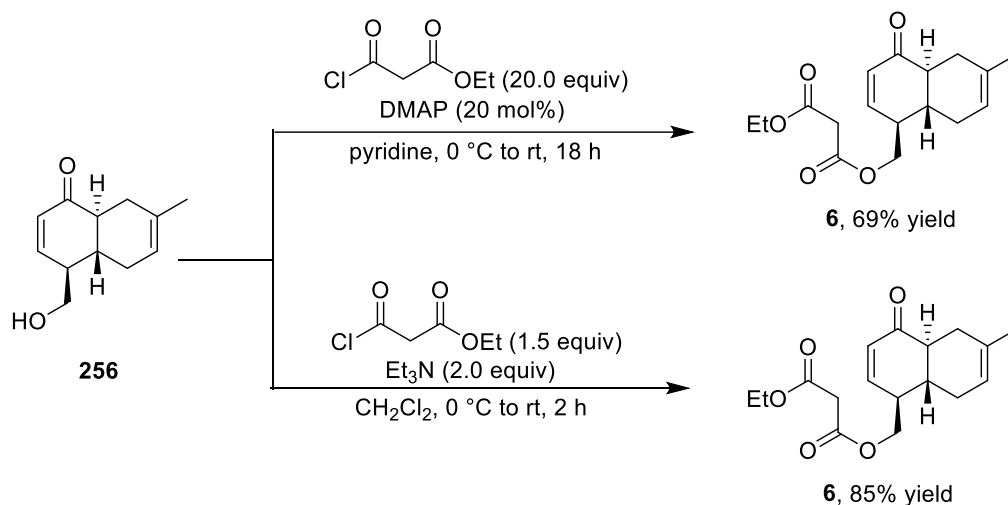
Owing to the failure of all cases, an alternative approach was devised to help to overcome the removal of the propionyl group. To drive the cyclisation and minimise the elimination product **257**, we envisioned enhancing the acidity of H-14 by having another electron-withdrawing group on the intramolecular Michael precursor. Consequently, the key enone propionate **252** would be modified to enone malonate **6**. The resonance effect of the diester group would stabilise an enolate under basic conditions and force an intramolecular Michael addition to construct the desired tricyclic lactone **259** as proposed in **Scheme 71**.



Scheme 71: The proposed formation of tricyclic lactone **259** via the intramolecular Michael addition of enone malonate **6**

Thus, the intramolecular Michael precursor **6** was prepared in the same fashion as enone propionate **252**. Alcohol **256** was treated with ethyl malonyl chloride (20.0 equivalents) in pyridine and catalytic DMAP to deliver the corresponding malonate **6** in 69% yield. To improve the yield, changing the base to triethylamine (2.0 equivalents) and using less ethyl

malonyl chloride (1.5 equivalents) in CH₂Cl₂ worked much better in the work-up step and smoothly furnished the desired malonate **6** in 85% yield (**Scheme 72**).



Scheme 72: The formation of enone malonate **6**

Having successfully synthesised malonate **6**, our next task would be the formation of tricyclic lactone **259** via an intramolecular Michael addition. Based on Isobe's synthesis, the use of 1.1 equivalents of sodium hydride through the intramolecular Michael addition of enone malonate **246** efficiently produced the corresponding bicyclic lactone **247** in high yield (see **Scheme 65**).⁹⁸

As expected, in the presence of the malonyl group in **6**, it would be facile to deprotonate H-14; therefore, mild conditions for the key step would be required. Inspired by Isobe's method, the intramolecular Michael addition of malonate **6** was initially investigated using sodium hydride in DMF at 0 °C for 1 hour and then warmed to room temperature for a further 4 hours.⁹⁸ To our delight, the corresponding tricyclic lactone **259** was observed in 71% conversion and obtained as a single diastereomer in 30% isolated yield. In contrast, the conversion to conjugated enone **257** was observed in trace amounts as illustrated in entry 1 (**Table 8**). To improve the conversion and yield of **259**, an alternative amide base was explored. Treatment of malonate **6** with KHMDS in THF was commenced at -78 °C to 0 °C for 8 hours. The formation of the desired tricyclic lactone **259** and the conjugated enone **257** was then observed with a crude ratio of 1:2.6 (entry 2). As the conjugated enone **257** was mainly obtained under the conditions of KHMDS, changing the base to tertiary

amine bases was further studied. Disappointingly, the conjugated enone **257** was produced in >99% conversion under the conditions of DBU (entry 3). On the other hand, the unreacted malonate **6** was only observed and entirely recovered in the presence of Et₃N in THF at 0 °C for 2 hours even though increasing the temperature from 0 °C to room temperature, and to 40 °C for a further 20 hours was then applied (entry 4).

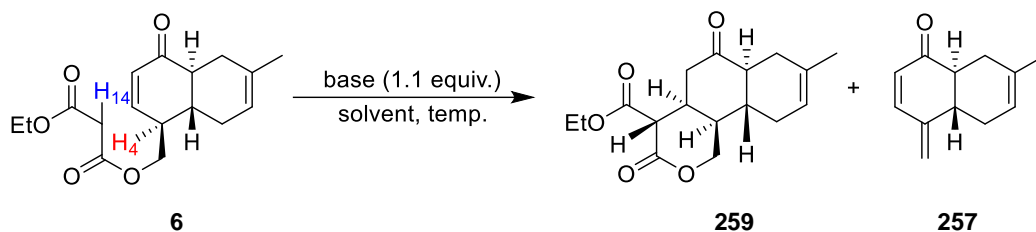
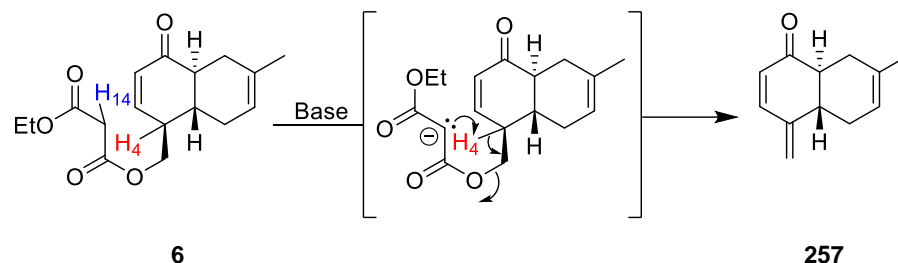


Table 8: Screening conditions for the intramolecular Michael addition of malonate **6**

Entry	Conditions	Temperature	Crude Ratio ^a	Isolated
			259 : 257 : 6	Yield 259
1	NaH, DMF	0 °C to rt, 5 h	16.6 : 1 : 5.6	30%
2	KHMDS, THF	-78 °C to 0 °C, 8 h	1 : 2.6 : 0	–
3	DBU, THF	0 °C to rt, 23 h	only 257	–
4	Et ₃ N, THF	0 °C to rt to 40 °C, 23 h	n.r.	–

^a Crude ratio was determined by integration of peak in ¹H NMR

At this stage, we have achieved the synthesis of tricyclic lactone **259** from enone malonate **6** via an intramolecular Michael addition. Among the bases tested, sodium hydride gave the best conversion to tricyclic lactone **259** even with a moderate isolated yield. Changing the base to KHMDS and DBU led to the formation of the conjugated enone **257** as a major product. Based on these results, we hypothesised that the malonate proton (H-14) could be deprotonated under those basic conditions producing a portion of enolate. In addition, some of the formed enolate could deprotonate H-4 to generate the conjugated enone **257** by eliminating the malonyl group. It was concluded that the generated enolate, under basic conditions, could play a dual role as a Michael donor and a base (**Scheme 73**).



Scheme 73: The proposed mechanism to form the undesired conjugated enone **257** by a portion of enolate

With tricyclic lactone **259** in hand, the stereochemistry determination of **259** was required to progress the total synthesis. The relationship between H-3 and H-4 was determined by the nOe ^1H NMR analysis. The results revealed a through-space correlation between H-3 and H-4 (nOe = 2.36%) as illustrated in **Figure 16**. In addition, no through-space interaction was observed between H-4 and H-14 (**Figure 17**). According to the nOe data, the structure of **259** was deduced to be tricyclic lactone **259** with the desired *syn*-relationship between H-3 and H-4 as required for the natural product core. Moreover, the relationship between H-3 and H-14 was confirmed to be the *anti*-relationship by the vicinal coupling constant of 11.4 Hz (J_{axial}) as shown in **Figure 15**. Once again, the absolute configuration of five stereogenic centres in tricyclic lactone **259** was proved by single crystal X-ray diffraction (**Figure 18**).

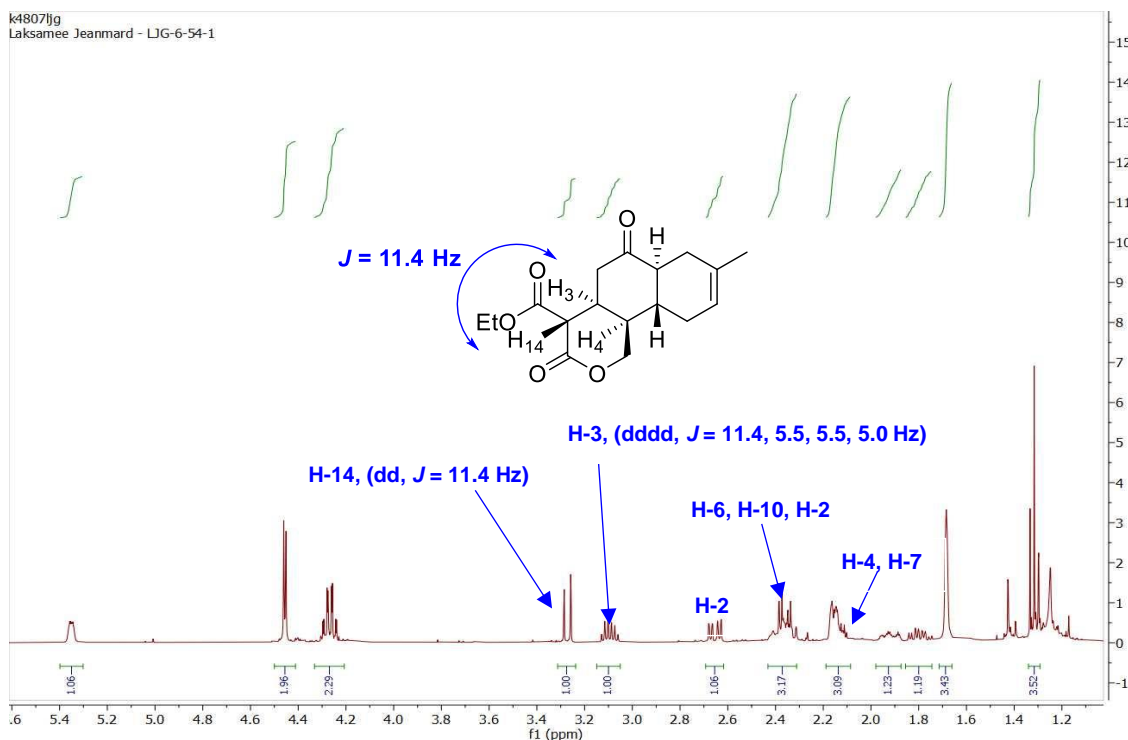


Figure 15: The ^1H NMR spectrum of tricyclic lactone **259**

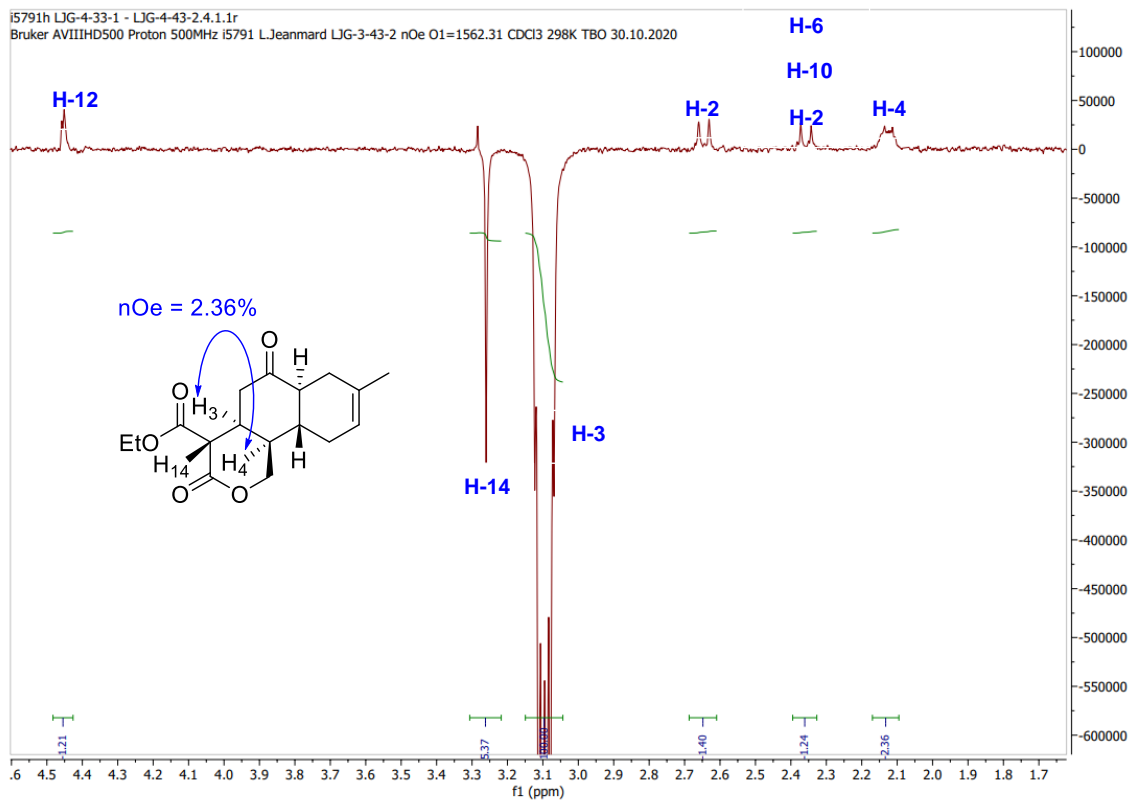


Figure 16: The *nOe* analysis of H-3 of tricyclic lactone **259**

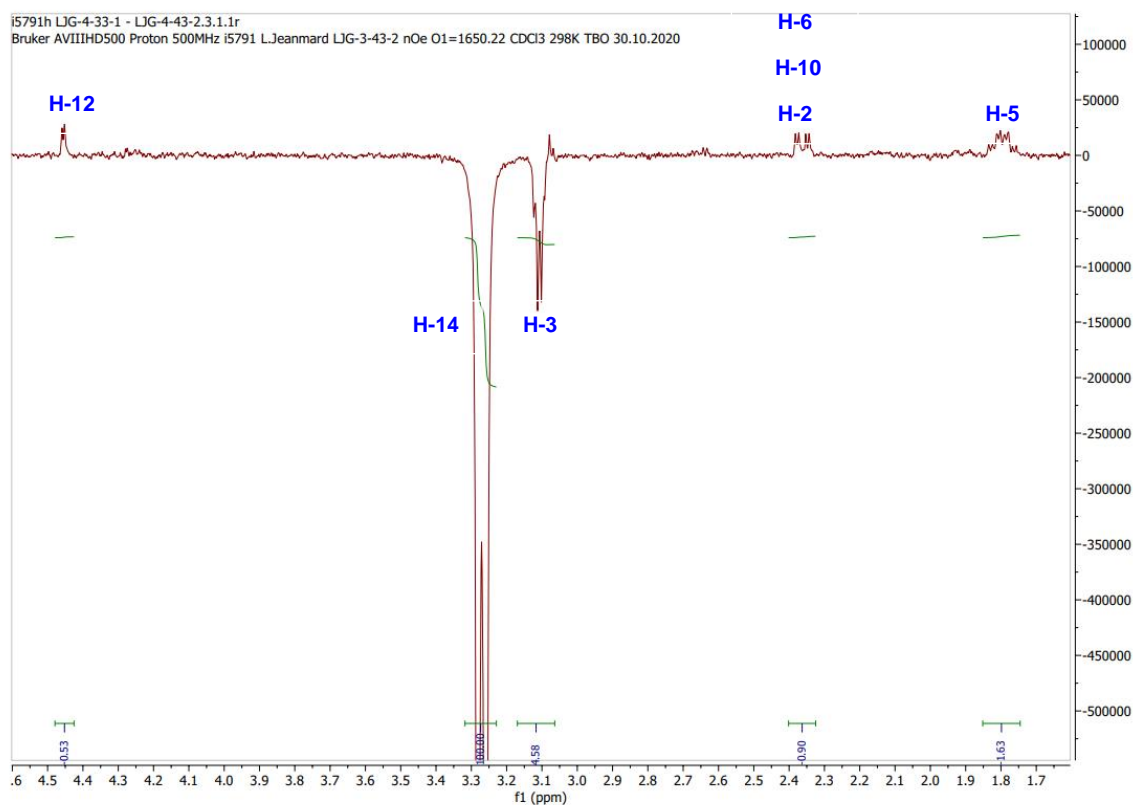


Figure 17: The *nOe* analysis of H-14 of tricyclic lactone **259**

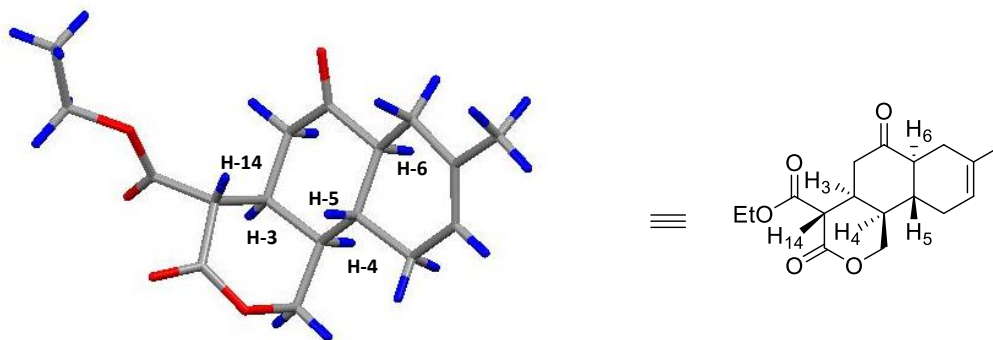
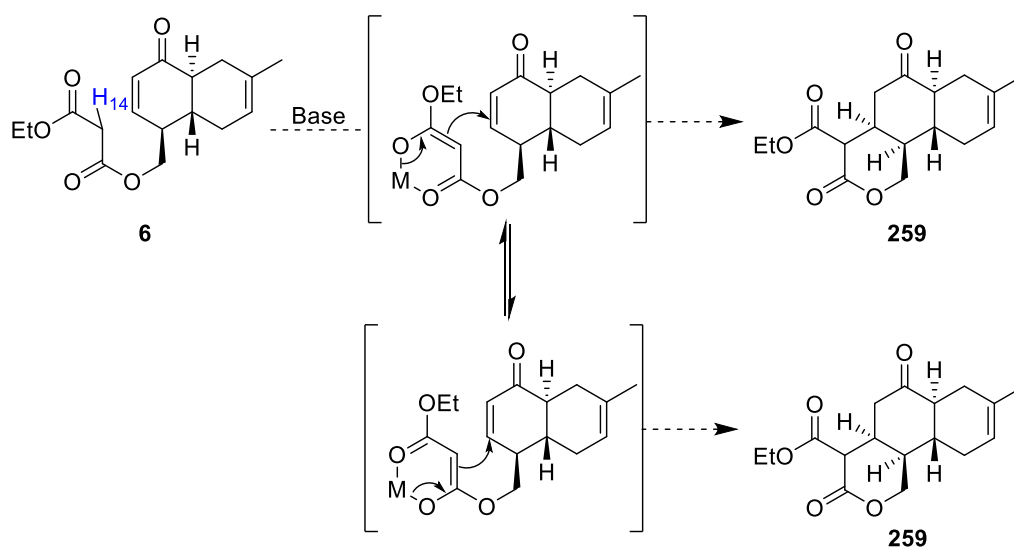


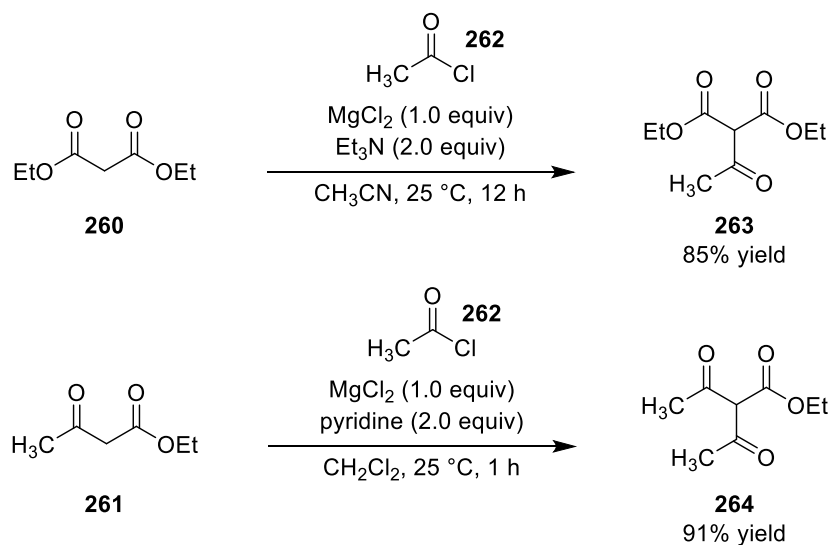
Figure 18: The single crystal X-ray diffraction of tricyclic lactone **259**

Gratifyingly, the intramolecular Michael addition approach accomplished the formation of tricyclic lactone **259** with the requisite stereochemistry. However, the conversion and yield of **259** under our optimised basic conditions were unsatisfactory. As a result, the conjugated enone **257** was obtained as a major product instead of tricyclic lactone **259**, leading to an inherent problem under basic conditions. Therefore, the hypothesis on an initiated portion of enolate could play a dual role under basic conditions described in **Scheme 73**. To gain insight into our hypothesis, we considered that a soft enolate would be a solution to stop a free-generated enolate from being a base in the reaction. To this end, the reversible keto-enol formation stabilised by metal complexation was envisaged to achieve our goal as proposed in **Scheme 74**.



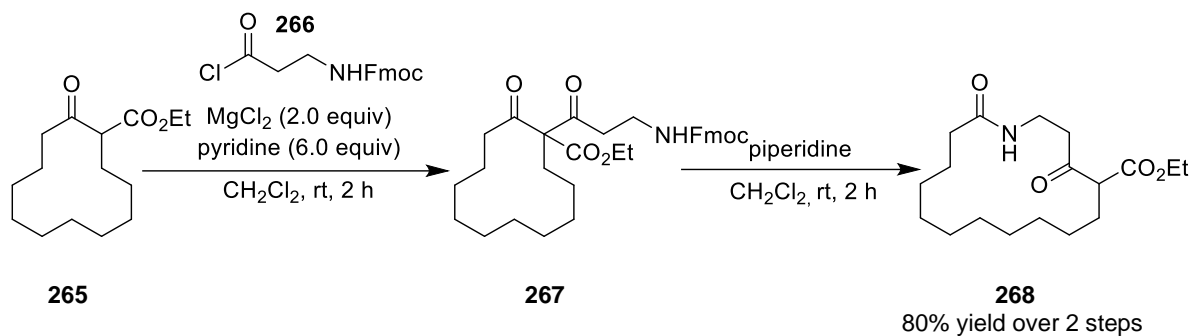
Scheme 74: The proposed synthesis of tricyclic lactone **259** via a keto-enol formation

To access our proposed direction, alternative procedures to generate a keto-enol portion from the malonate moiety of **6** were sought. Rathke and Cowan reviewed the single-step acylation of diethyl malonate **260** and ethyl acetoacetate **261** using magnesium chloride to enhance acidity to the point where mild tertiary amine bases could be used.¹⁰⁰ Acetylation of diethyl malonate **260** and ethyl acetoacetate **261** in the presence of magnesium chloride (1.0 equivalent) and either Et₃N or pyridine (2.0 equivalents) yielded a portion of enolate, which was directly acylated by acid chloride **262** to provide the desired products **263** and **264** in excellent yields (**Scheme 75**).



Scheme 75: Acylation of diethyl malonate **260** and ethyl acetoacetate **261** reported by Rathke and Cowan¹⁰⁰

Another procedure of C-acylation employing magnesium chloride to enhance the acidity of cyclic β -keto ester **265** was reported in the synthesis of macrocycles via acylation/ring expansion sequence by Unsworth and co-workers in 2015.¹⁰¹ The acylation reaction of 12-membered ring cyclic β -keto ester **265** with acid chloride **266** was performed under the conditions of magnesium chloride (2.0 equivalents) and excess pyridine (6.0 equivalents), in CH₂Cl₂ at room temperature to generate the tricarbonyl intermediate **267** successfully as illustrated in **Scheme 76**.



Scheme 76: Unsworth's synthesis of 16-membered ring **268**¹⁰¹

In the search for an efficient keto-enol formation protocol,^{100,101} exploiting a combination of magnesium chloride and tertiary amine base in acylation reactions displays the generation of a portion of keto-enol stabilised by magnesium ion. Herein, the concept of using metal complexation to enhance the acidity of the malonate would be utilised to form a Michael donor and avoid the formation of a free-generated enolate. Thus, we followed Unsworth's procedure and investigated the intramolecular Michael addition of malonate **6** under two different conditions (**Table 9**).

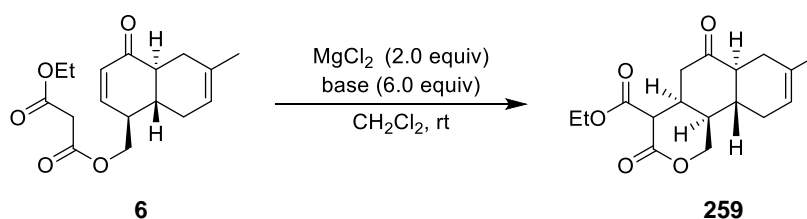
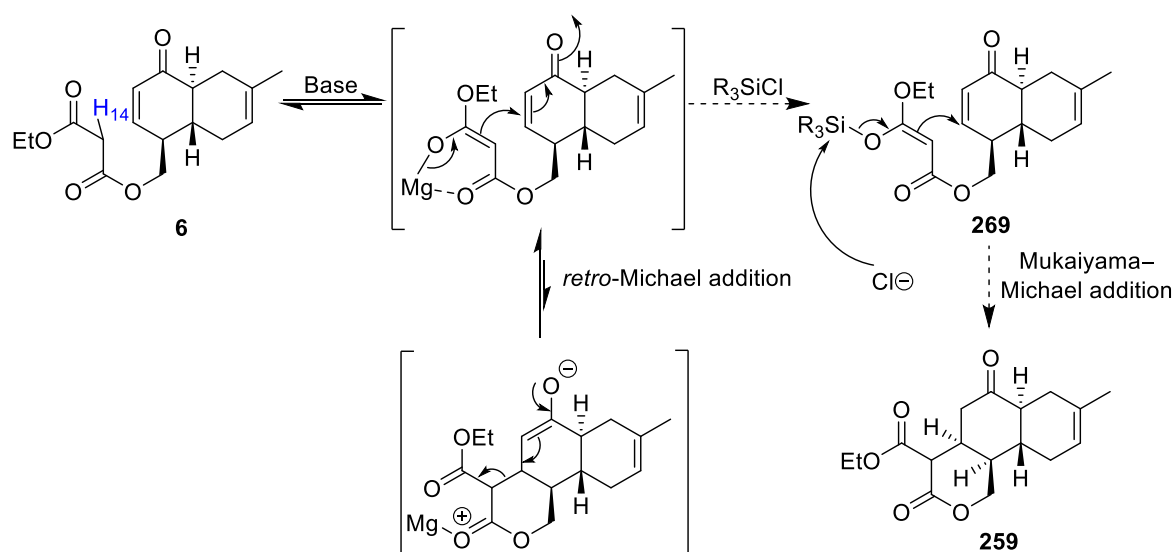


Table 9: Screening conditions for the intramolecular Michael addition of malonate **6** using magnesium chloride and tertiary amine bases

Entry	Base	Time (hours)	% Conversion
1	pyridine	22	n.r.
2	Et ₃ N	6	n.r.

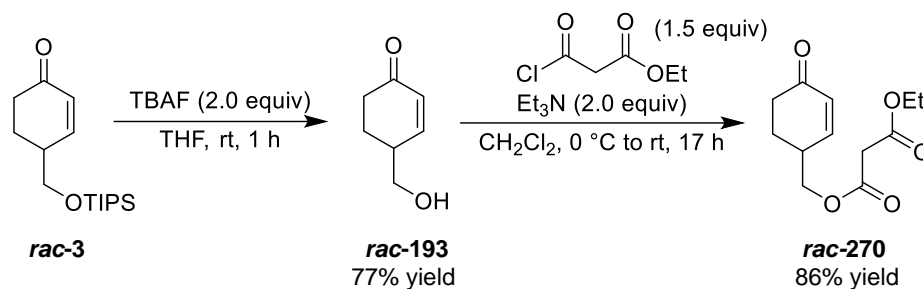
In initial experiments, we set up the intramolecular Michael reaction of malonate **6** in the presence of magnesium chloride (2.0 equivalents) and a large portion of pyridine (6.0 equivalents) in CH₂Cl₂ at room temperature.¹⁰¹ However, the desired tricyclic lactone **259** could not be observed after 22 hours, and the unreacted malonate **6** was entirely recovered (entry 1). Switching the base to triethylamine (6.0 equivalents) under the same conditions

for 6 hours returned the unreacted malonate **6** in quantitative yield (entry 2).¹⁰⁰ It should be noted that tricyclic lactone **259** could not be produced under both conditions. Based on the data obtained, we propose that the intramolecular Michael addition of malonate **6** would be involved in an enolate equilibration, which may favour the *retro*-Michael addition. The magnesium enolate would be trapped with a silyl group to prevent *retro*-Michael fragmentation. Inspired by our previous study on the Mukaiyama–Michael addition, we envisioned that the silyl ketene acetal **269** would ultimately drive the cyclisation to accomplish the corresponding lactone **259** as shown in **Scheme 77**.



Scheme 77: The proposed reversible intramolecular Michael addition of malonate **6**

Toward a deeper understanding of the mechanism and to explore our hypothesis, we planned to overcome the *retro*-intramolecular Michael addition by trapping the enolate with a silyl group leading to silyl ketene acetal **269**. A malonate model system would be utilised for this study to save the enantioenriched starting material. As we know that the intramolecular Michael addition of the malonate produces the lactone with the desired stereochemistry, a racemic model study would be reasonable to use. Therefore, we prepared the malonate model system **270** from the in-hand racemic enone **3** in two steps. Desilylation of *rac*-enone **3** with TBAF furnished *rac*-alcohol **193** in 77% yield. The resultant alcohol underwent acylation (ethyl malonyl chloride, Et_3N , in CH_2Cl_2 at 0 °C to room temperature) to deliver the model system **270** in 86% yield as shown in **Scheme 78**.



Scheme 78: The formation of malonate model system **270**

Having successfully synthesised malonate **270**, an intramolecular Mukaiyama–Michael addition of **270** was then explored through the formation of silyl ketene acetal **271** as illustrated in **Table 10**.

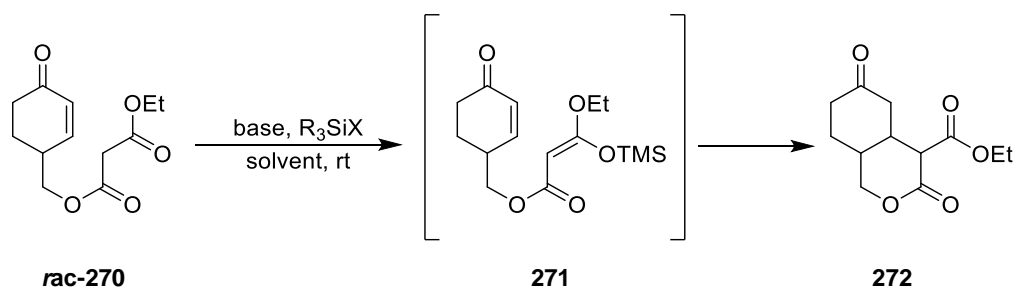


Table 10: Screening conditions for the intramolecular Mukaiyama–Michael addition of malonate model system **270**

Entry	Conditions	Time (hours)	% Conversion
1	Et ₃ N (2.0 equiv), TMSOTf (1.5 equiv), CH ₂ Cl ₂ , rt to 40 °C	18	Decomposition
2	Et ₃ N (2.0 equiv), TMSCl (1.5 equiv), CH ₂ Cl ₂ , rt to 40 °C	18	n.r.
3	Et ₃ N (6.0 equiv), MgCl ₂ (2.0 equiv), TMSCl (3.0 equiv), DCE, rt	1.5	90% ^a (71% isolated yield)
4	Et ₃ N (6.0 equiv), MgCl ₂ (2.0 equiv), TMSCl (3.0 equiv), DCE, rt	6.5	66% ^b
5	Et ₃ N (6.0 equiv), MgCl ₂ (2.0 equiv), DCE, rt	1.5	n.r.

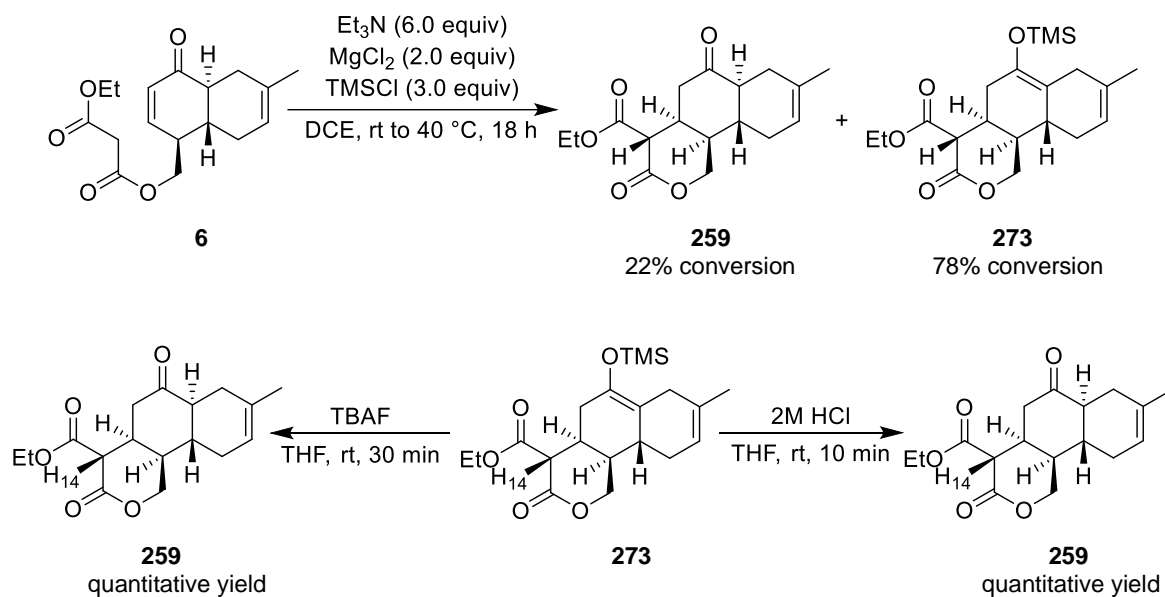
^a TMSCl was added after stirring the pre-mixture for 0.5 hours

^b TMSCl was added after stirring the pre-mixture for 1.5 hours

The conversion of malonate **270** to silyl ketene acetal intermediate **271** was initially investigated under the mild conditions of Et₃N (2.0 equivalents) and TMSOTf (1.5 equivalents) at room temperature and warmed up to 40 °C for 18 hours.^{102,103} Disappointingly, the reaction caused extensive decomposition with TMSOTf at 40 °C (entry 1). In contrast, bicyclic lactone **272** could not be observed in the presence of TMSCl under the same conditions. Instead, malonate **270** was recovered in quantitative yield (entry 2). As either silyl ketene acetal **271** or lactone **272** could not be observed under the conditions above, driving the cyclisation to furnish lactone **272** was considered. We envisioned that using a Lewis acid and increasing the temperature would enhance the acidity of malonate protons and force cyclisation, respectively. Inspired by Unsworth's method,¹⁰¹ investigation of the intramolecular Michael addition was then pursued under the conditions of MgCl₂ (2.0 equivalents) and excess Et₃N (6.0 equivalents) in DCE due to requiring a higher temperature. The pre-mixing of malonate **270** with a combination of MgCl₂ and Et₃N in DCE at room temperature for 30 minutes was carried out before adding TMSCl (3.0 equivalents). Gratifyingly, bicyclic lactone **272** was observed in 90% conversion after stirring for a further 1 hour and obtained in 71% isolated yield after purification by flash column chromatography (entry 3). To improve the conversion to lactone **272**, malonate **270** and a combination of MgCl₂ and Et₃N were pre-mixed at room temperature for 1.5 hours before TMSCl was added. The requisite lactone **272** was then observed in 66% conversion after stirring at room temperature for a further 5 hours (entry 4). However, extending the reaction time did not improve the conversion to the cyclised product **272**. In order to confirm the proposed mechanism, the reaction was conducted under the presence of MgCl₂ and Et₃N, in DCE at room temperature for 1.5 hours without the addition of TMSCl. It should be noted that none of the desired lactone **272** could be observed, whereas the malonate **270** was recovered in quantitative yield (entry 5). These results indicated that magnesium chloride played an important role in enhancing the acidity of malonate **270** and promoting the intramolecular Michael addition. It was concluded that the formation of lactone **272** was achieved through an *in situ* enolisation and intramolecular Mukaiyama–Michael addition sequence.

Due to the success of the model study, this method would next be exploited in the real decalin system. With the optimised conditions in hand, the key reaction of malonate *trans*-decalin **6** was initially performed at room temperature leading to a small conversion to

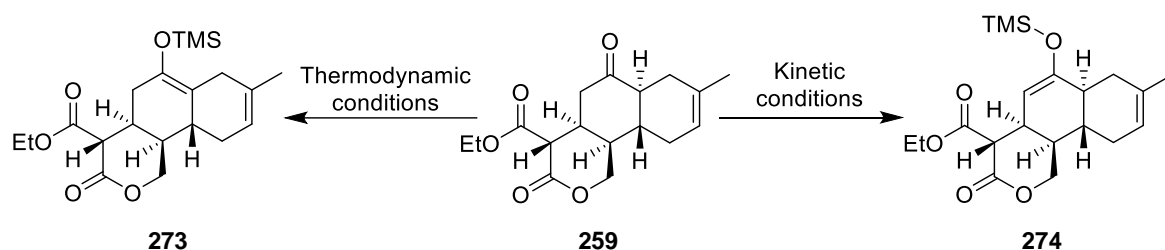
tricyclic lactone **259** after 2.5 hours. To complete the consumption of malonate **6**, the temperature was increased to 40 °C for a further 15 hours producing tricyclic lactone **259** in 22% conversion, while the silyl enol ether **273** was observed in 78% conversion. However, the resultant silyl enol ether **273** was subjected to hydrolysis with 2M HCl to deliver the desired tricyclic lactone **259** in quantitative yield. Moreover, the removal of the silyl group in **273** with TBAF also provided the corresponding tricyclic lactone **259** in excellent yield as illustrated in **Scheme 79**.



Scheme 79: The formation of tricyclic lactone **259** through an intramolecular Mukaiyama–Michael addition approach

Based on the model study, the intramolecular Mukaiyama–Michael addition of malonate model system **270** required a combination of excess Et_3N (6.0 equivalents) and MgCl_2 (2.0 equivalents), and the addition of TMSCl (3.0 equivalents) to smoothly furnish the desired bicyclic lactone **272** in high conversion and good isolated yield. However, applying the same conditions for the malonate **6** required a higher temperature and additional portions of reagents to complete the reaction. Moreover, the use of excess TMSCl to overcome the cyclisation led to the formation of silyl enol ether **273**. It should be noted that the silyl enol ether **273** was generated in the more stable tri-substituted alkene under the thermodynamic conditions, which uninstalled our *trans*-decalin moiety as proposed in **Scheme 80**. On the other hand, the required hydrolysis of silyl enol ether **273** returned lactone **259** with the *trans*-decalin motif along with the epimerisation at the 14-position.

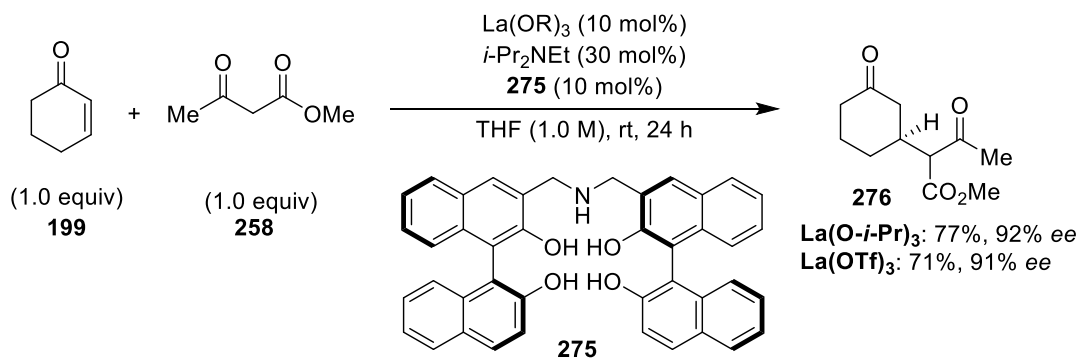
To prevent the epimerisation of installed stereogenic centres, alternative methods to deliver tricyclic lactone **259** directly would be explored.



Scheme 80: The proposed enolisation of tricyclic lactone **259** under kinetic and thermodynamic conditions

In light of our recent studies, we explained this remarkable acidity enhancement of malonate moiety by magnesium chloride for an intramolecular Michael addition. As metal complexation proved successful, an alternative efficient metal complex to construct tricyclic lactone **259** was studied.

In 2005, Shibasaki and co-workers successfully used a combination of lanthanide salt and *i*-Pr₂NEt (Hunig's base), and NR-linked-BINOL ligand for the enantio- and diastereoselective Michael addition of α -substituted β -keto esters to cyclic enones.¹⁰⁴ The key concept is utilising an alternative catalyst to promote a keto-enol formation required for a Michael donor. The enantioselective Michael reaction of cyclohexenone **199** and methyl acetoacetate **258** using a combination of 10 mol% of La(*O-i*-Pr)₃, 30 mol% of *i*-Pr₂NEt, and 10 mol% of BINOL ligand **275** provided Michael adduct **276** in 77% yield with 92% *ee*. Owing to the commercial availability and high tolerance to air and moisture of La(OTf)₃, the Michael addition of methyl acetoacetate **258** to cyclohexenone **199** in the presence of La(OTf)₃ was also investigated. In this case, the Michael adduct **276** was produced in a low lower yield, while identical enantioselectivity was obtained (**Scheme 81**).



Scheme 81: The enantioselective Michael reaction using a catalyst prepared from lanthanide salt and $i\text{-Pr}_2\text{NEt}$ reported by Shibasaki and co-workers¹⁰⁴

Inspired by Shibasaki's procedure, the combination of lanthanide salt and Hunig's base would be applied to our system in order to produce a Michael donor.¹⁰⁴ However, the chiral ligand would not be imperative for our case. To screen the reaction and save our precious enantioenriched precursor, the model system **270** would be used. The optimised conditions for the intramolecular Michael addition of malonate model system **270** were screened in **Table 11**. Indeed, we began employing readily available and moisture-tolerable La(OTf)_3 as a catalyst. Following Shibasaki's method, the intramolecular Michael addition of malonate **270** was performed in the presence of La(OTf)_3 (10 mol%) and $i\text{-Pr}_2\text{NEt}$ (30 mol%) in THF at room temperature. After 25 hours, bicyclic lactone **272** was observed in only 5% conversion (entry 1). Changing the solvent to DME did not improve the conversion to lactone **272** (entry 2). Based on the original method from the Shibasaki group, various BINOL ligands were used to form the metal complex catalyst for an asymmetric Michael addition.¹⁰⁴ Therefore, the addition of racemic BINOL (10 mol%) was trialed. However, very poor conversion to lactone **272** was observed (entry 3). To improve the conversion to lactone **272**, an increase in temperature to 40 °C furnished bicyclic lactone **272** in 13% conversion (entry 4). Using a stoichiometric amount of La(OTf)_3 (1.0 equivalent) and Hunig's base (1.0 equivalent) and keeping other parameters unchanged, malonate **270** was completely consumed after 25 hours. The conversion to bicyclic lactone **272** and alcohol **193** was obtained with a ratio of 1:3 (entry 5). To minimise the amount of alcohol **193**, changing the Lewis acid to $\text{La(O-}i\text{-Pr)}_3$ was then investigated. The formation of lactone **272** was further improved up to 34% conversion after 7 hours without the competitive formation of alcohol **193** (entry 6). The reactivity was then enhanced by using 2.0 equivalents of Hunig's base.

Gratifyingly, bicyclic lactone **272** was observed in 95% conversion after 6 hours and obtained in 78% isolated yield (entry 7).

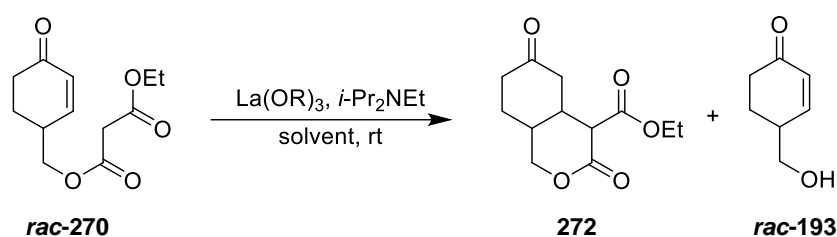


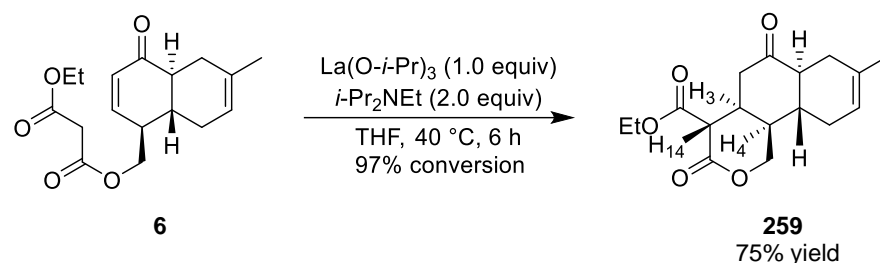
Table 11: Screening conditions for the intramolecular Michael addition of malonate **270**

Entry	La(OR) ₃	<i>i</i> -Pr ₂ NEt	Solvent	Temp.	Time	Result	
						Conv	Ratio
						272 : 193	
1	La(OTf) ₃ (10 mol%)	30 mol%	THF	rt	25 h	5% ^a	1 : 0
2	La(OTf) ₃ (10 mol%)	30 mol%	DME	rt	25 h	4% ^a	1 : 0
3	La(OTf) ₃ (10mol%), <i>rac</i> -BINOL (10 mol%)	30 mol%	THF	rt	25 h	3% ^a	3 : 0
4	La(OTf) ₃ (10 mol%)	30 mol%	THF	40 °C	25 h	13% ^a	1 : 0
5	La(OTf) ₃ (1.0 equiv)	1.0 equiv	THF	40 °C	25 h	>99%	1 : 3
6	La(<i>O</i> - <i>i</i> Pr) ₃ (1.0 equiv)	1.0 equiv	THF	40 °C	7 h	34% ^a	1 : 0
7	La(<i>O</i> - <i>i</i> Pr) ₃ (1.0 equiv)	2.0 equiv	THF	40 °C	6 h	95% ^b	1 : 0

^a Unreacted malonate **270** was recovered

^b Bicyclic lactone **272** was isolated in 78% yield

Since we have successfully synthesised bicyclic lactone **272** from malonate model system **270** using a combination of La(*O*-*i*Pr)₃ and *i*-Pr₂NEt through an intramolecular Michael addition, the developed conditions were utilised for synthesising tricyclic lactone **259**. Malonate *trans*-decalin **6** was then treated with a combination of La(*O*-*i*Pr)₃ (1.0 equivalent) and *i*-Pr₂NEt (2.0 equivalents) in THF at 40 °C. To our delight, the corresponding tricyclic lactone **259** was observed in 97% conversion after 6 hours and isolated in 75% yield after purification by column chromatography as shown in **Scheme 82**.

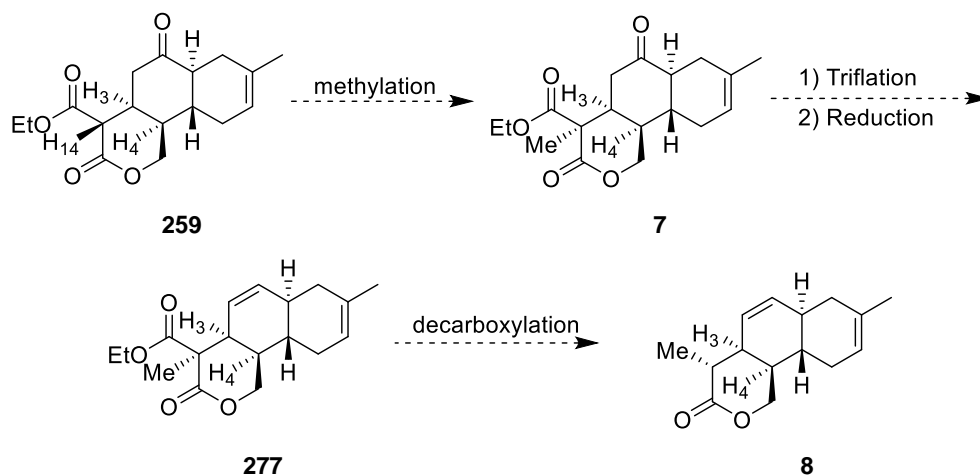


Scheme 82: The formation of tricyclic lactone **259** via an intramolecular Michael addition

To summarise, we have installed a side chain on the *trans*-decalin scaffold via an intramolecular Michael addition of enone malonate **6** to construct the corresponding tricyclic lactone **259** with the desired stereochemistry as required for anthracimycin (**1**). The intramolecular Michael addition of enone malonate **6** was investigated under various conditions. For instance, a formed enolate portion under basic conditions was proposed to deprotonate the H-4 furnishing the undesired conjugated enone **257** as a major product through an E₁cB pathway (see **Scheme 73**). To solve this problem, alternative methods were used to generate a keto-enol form as a Michael donor. Interestingly, we found the usefulness of metal complexes MgCl₂, La(OTf)₃, and La(O-*i*-Pr)₃ to enhance the acidity of malonate protons to the point where tertiary amine bases could be used. With the key tricyclic lactone **259** in hand, the construction of the anthracimycin core to progress the total synthesis of **1** will be discussed in the next section.

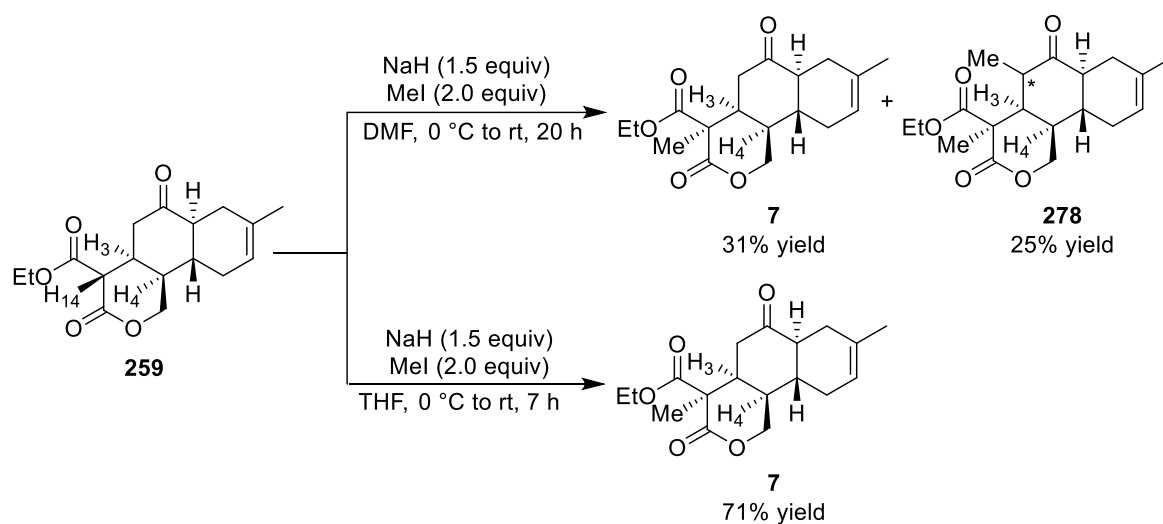
2.7 The formation of the anthracimycin core

Having successfully synthesised the tricyclic lactone **259**, the transformation of **259** to anthracimycin core **8** would be required to complete the total synthesis. Hence, we proposed a synthetic route to accomplish the anthracimycin core **8** in five steps. First, a methyl group as necessary for the natural product would be installed by methylation of tricyclic lactone **259** to furnish lactone **7**. The ketone functionality of **7** would then be transformed into an alkene moiety in **277** via a vinyl triflation/reduction sequence.¹⁰⁵ To obtain the anthracimycin core **8**, the ester group of **277** would be finally removed under decarboxylation conditions (**Scheme 83**).



Scheme 83: The proposed synthetic route to accomplish the anthracimycin core **8**

The installation of a methyl group on the tricyclic lactone **259** was initially investigated using sodium hydride (1.5 equivalents) and methyl iodide (2.0 equivalents) in DMF at 0 °C to room temperature. The desired product **7** was obtained in only 31% isolated yield after 20 hours, while the undesired product **278** was obtained in 25% yield by double methylation. To reduce the reactivity of the base, changing the solvent to THF was explored and this prevented the competitive double methylation process. As a result, the requisite tricyclic system **7** was produced in >99% conversion and isolated in 71% yield after purification by column chromatography as shown in **Scheme 84**.



Scheme 84: Methylation of tricyclic lactone **259**

With the key intermediate **7** in hand, we determined the stereochemistry of tricyclic lactone **7** by ^1H NMR nOe analysis. The relationship of the methyl group at the 18-position and H-3 and the relationship of the methyl group at the 18-position and H-4 were the key information. ^1H NMR nOe analysis revealed a through-space correlation between H-3 and H-4 (nOe = 2.82%) and a correlation between H-3 and the methyl group (nOe = 2.62%) as illustrated in **Figure 20**. However, the proton at the 4-position overlapped with protons at the 5- and 6-positions. When we irradiated H-4, both H-5 and H-6 were also irradiated. Hence, a small correlation between H-4 and H-3 was observed (nOe = 0.83%), and a correlation between H-4 and protons of the methyl group at the 18-position was determined at 0.26% (**Figure 21**). In addition, protons from the methyl group at the 18-position were irradiated, providing through-space correlations with H-3 and H-4 at 1.73% and 0.09%, respectively (**Figure 22**).

Regarding the nOe analysis, the stereochemistry of tricyclic lactone **7** was confirmed to be the *syn*-relationship between the methyl group at the 18-position and H-3 and between the methyl group at the 18-position and H-4.

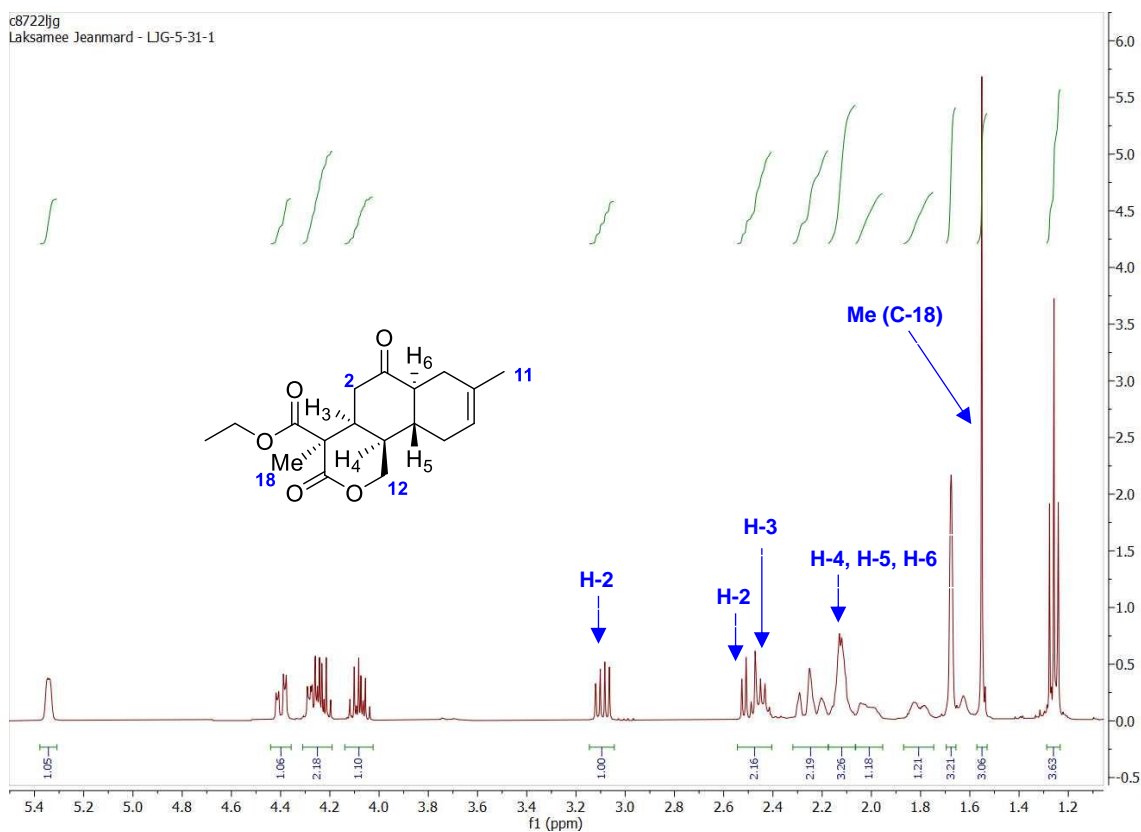


Figure 19: The ^1H NMR spectrum of tricyclic lactone **7**

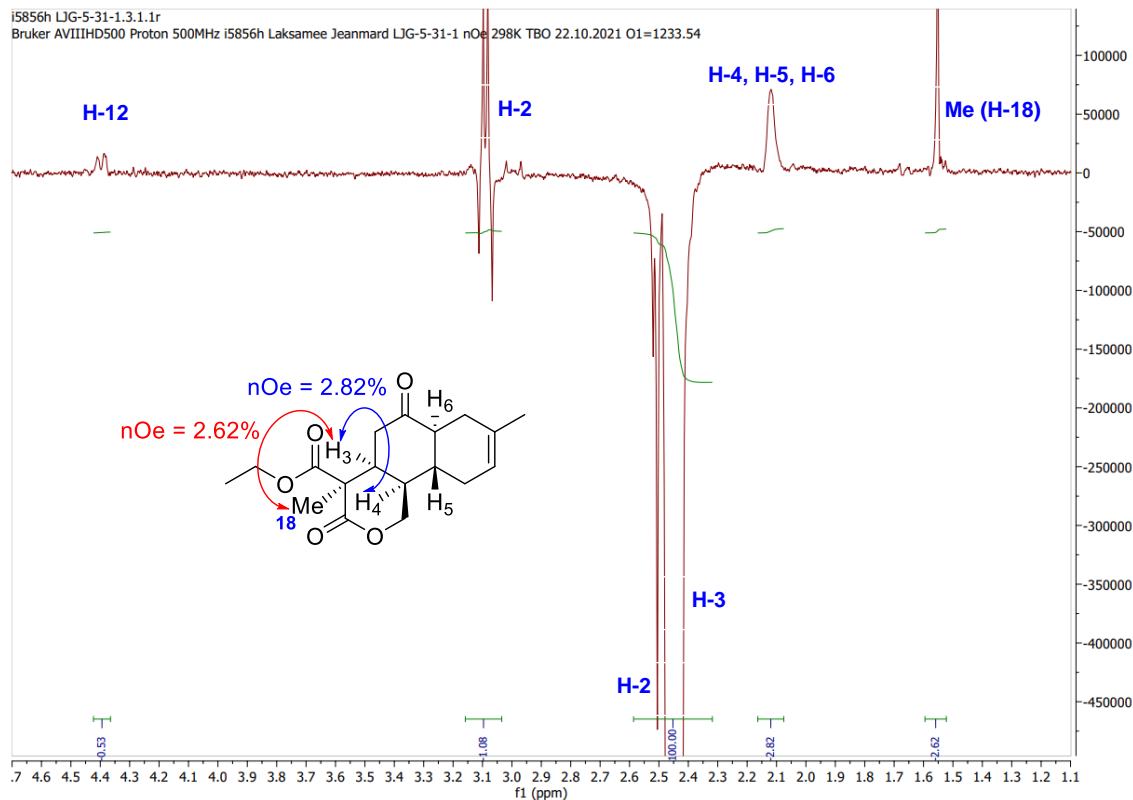


Figure 20: The nOe analysis of H-3 in tricyclic lactone **7**

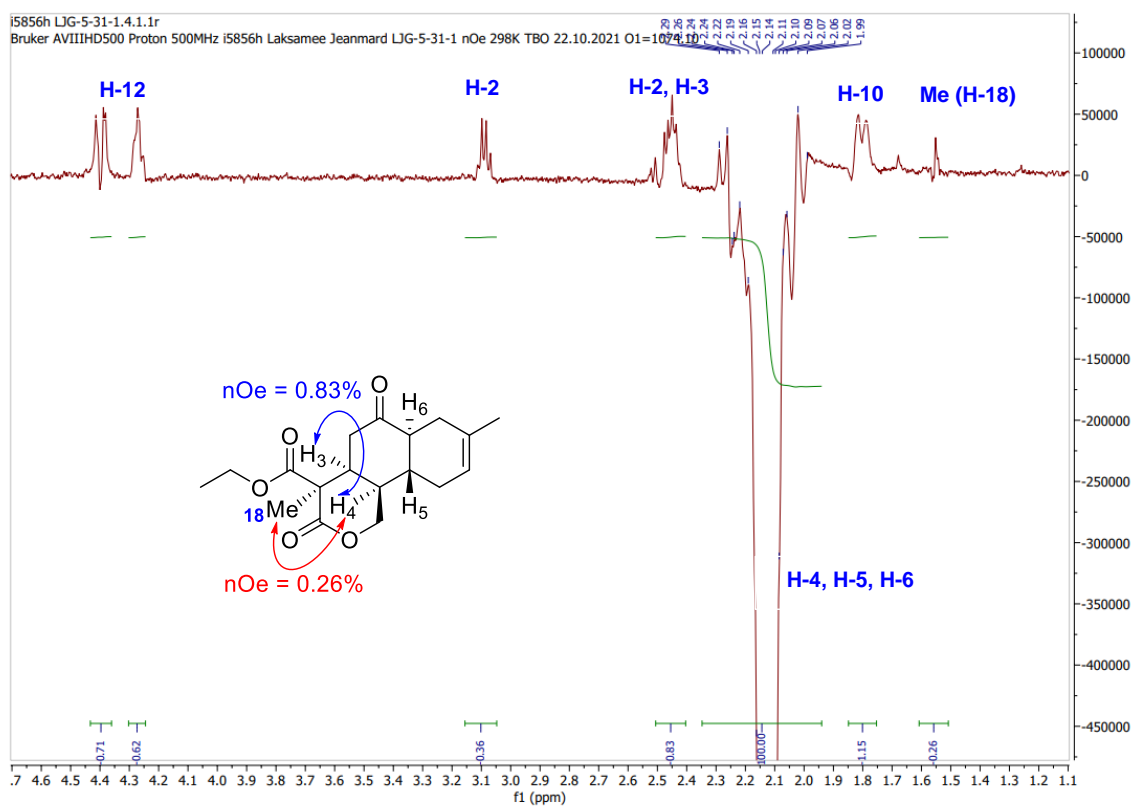


Figure 21: The nOe analysis of H-4 in tricyclic lactone **7**

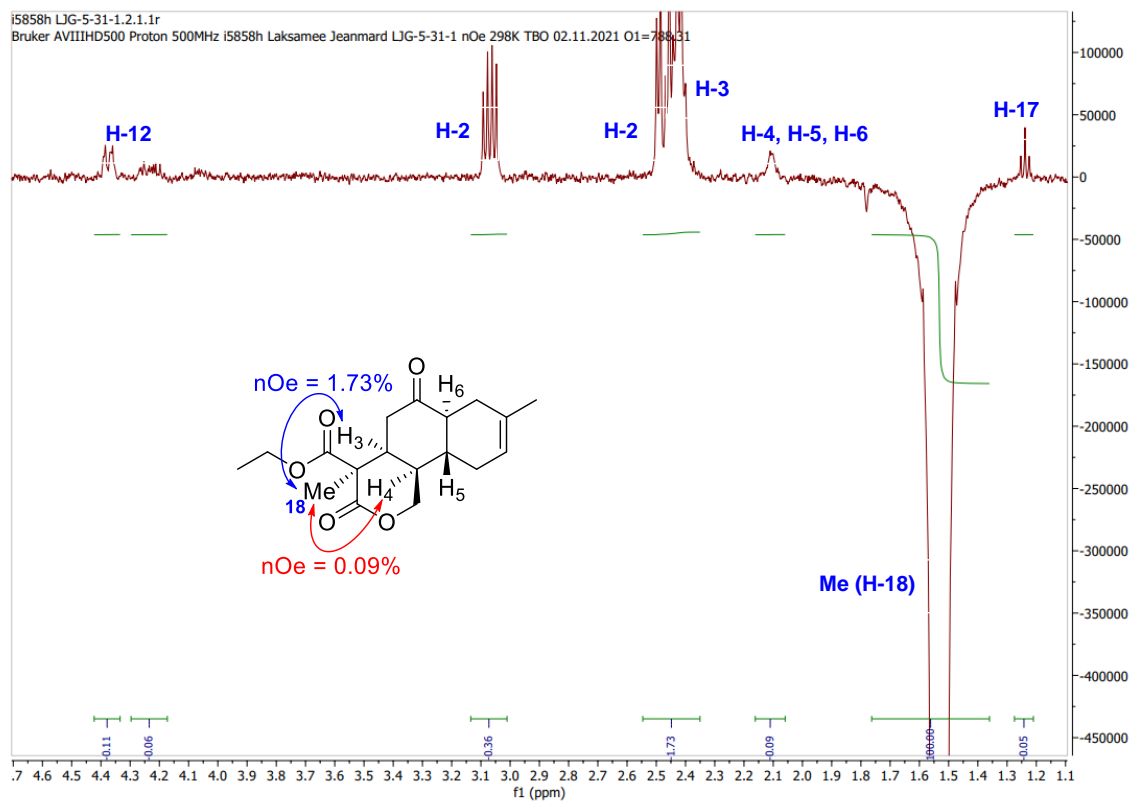
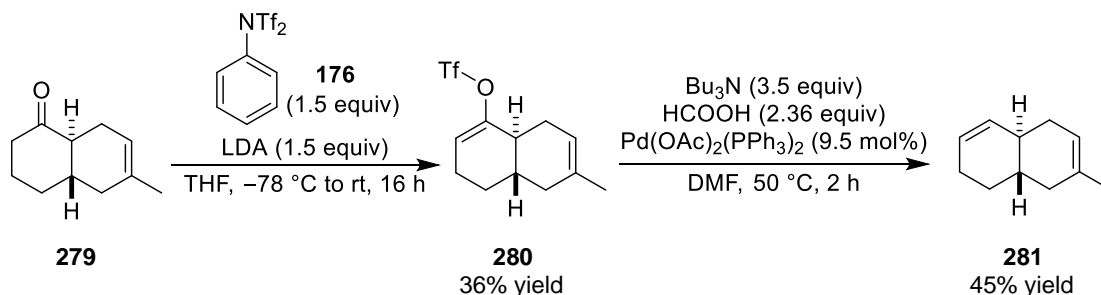


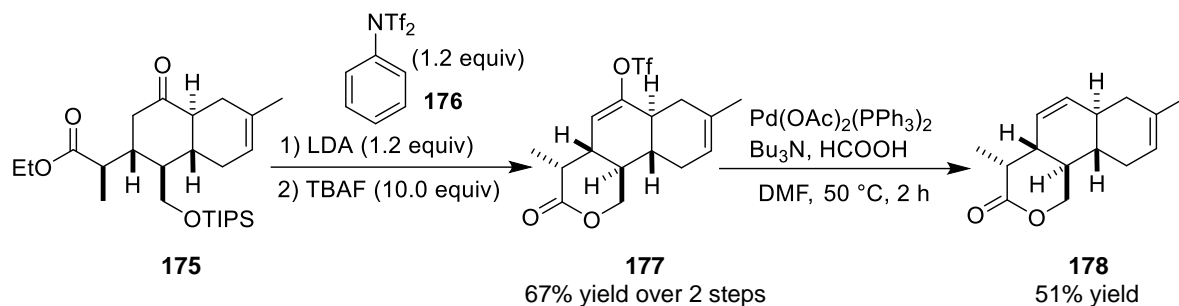
Figure 22: The *nOe* analysis of H-18 in tricyclic lactone **7**

After completing lactone **7**, our next goal would be to synthesise the anthracimycin core **8**. The transformation of the ketone functionality in lactone **7** to the alkene moiety would require the formation of vinyl triflate, followed by reduction to furnish alkene **277**. Regarding previous work in the Clarke group, the conversion of a ketone group to an alkene moiety was achieved in the model system **279**.⁶⁶ Treatment of ketone *trans*-decalin **279** with LDA and *N*-phenyl-bis-trifluoromethanesulfonimide **176** provided vinyl triflate **280** in 36% yield. Palladium reduction of **280** in the presence of Pd(OAc)₂(PPh₃)₂, Bu₃N, and formic acid furnished the desired alkene **281** in 45% yield (**Scheme 85**).



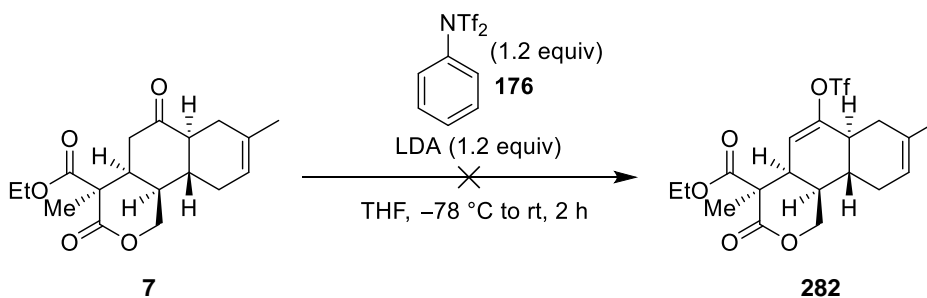
Scheme 85: Previous Clarke group work on the transformation of ketone to alkene **281**⁶⁶

The Clarke group has completed the conversion of Mukaiyama Michael adduct **175** to tricyclic lactone **178**.⁶⁶ The ketone moiety of **175** was functionalised to an alkene via formation of a vinyl triflate, followed by desilylation with TBAF to provide tricyclic lactone **177** in 67% yield over two steps. Vinyl triflate **177** was then reduced by Pd-catalysed reduction to deliver tricyclic lactone **178** in 51% yield as shown in **Scheme 29**.



Scheme 29: Previous Clarke group work on the transformation of ketone to alkene **178**⁶⁶

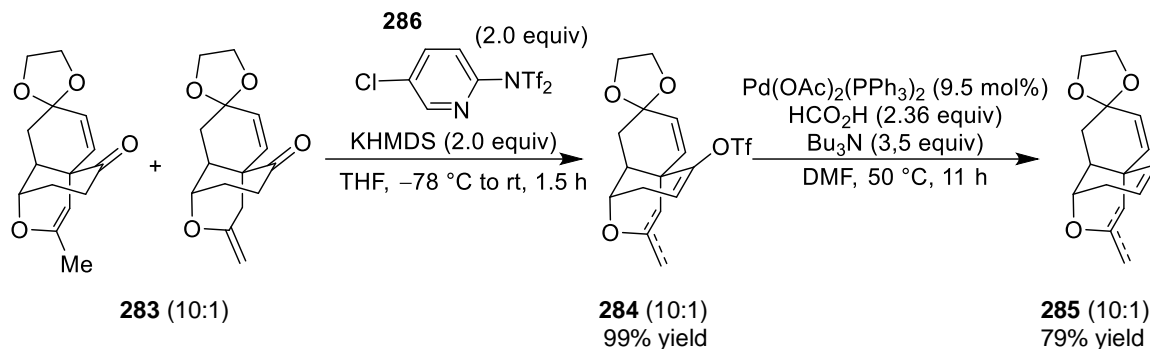
Following Lodovici's method, the functionalisation of ketones to vinyl triflates using *N*-phenyl-bis-trifluoromethanesulfonimide **176** was utilised for our tricyclic system **7**. The conversion of ketone **7** to vinyl triflate **282** was conducted in the presence of LDA and *N*-phenyl-bis-trifluoromethanesulfonimide **176** at -78°C and warmed to room temperature. Unfortunately, none of the desired vinyl triflate **282** was observed as the reaction resulted in decomposition as shown in **Scheme 86**.



Scheme 86: The attempted formation of vinyl triflate **282**

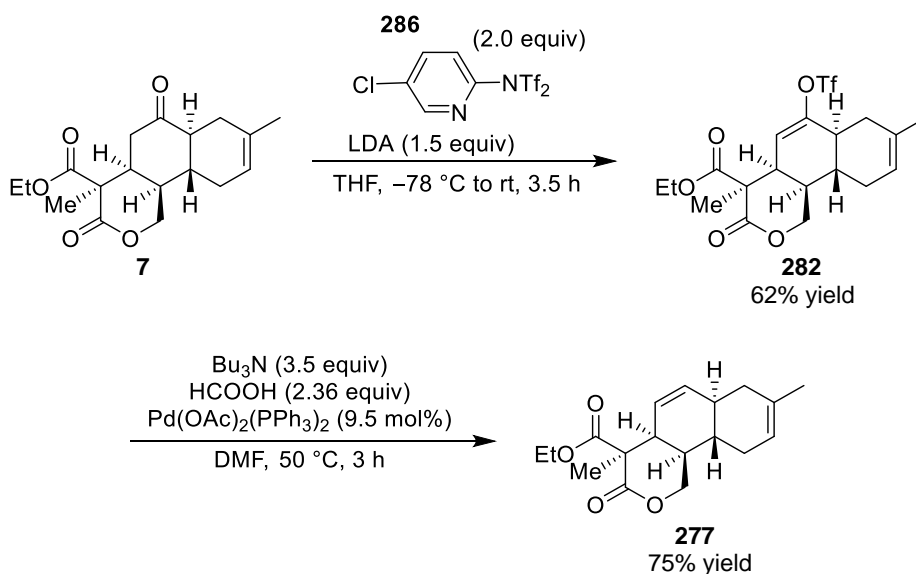
Probably due to a small-scale reaction and challenging reaction conditions, the vinyl triflate **282** could not be obtained. To develop the conditions for a complex molecule, a more reactive pyridine-derived triflating reagent was sought. In 2008, Matsuo and co-workers reported the transformation of ketone **283** to alkene **285** through a reduction of vinyl

triflate **284**, which was produced under the conditions of KHMDS and *N*-(5-chloro-2-pyridyl)triflimide (Comins' reagent) **286**.¹⁰⁶ As a result, the vinyl triflate **284** was generated in excellent yield. Subsequent reduction of triflate **284** using a palladium catalyst, formic acid, and tributylamine furnished the desired alkene **285** in 79% yield (**Scheme 87**).



Scheme 87: Matsuo's method for the transformation of ketone **283** to alkene **285**¹⁰⁶

Due to an excellent yield of vinyl triflate **284** obtained using Matsuo's protocol, the more reactive Comins' reagent **286** would be applied to our substrate **7**. The conversion of ketone **7** to alkene **277** was performed under the conditions of LDA (1.5 equivalents) and Comins' reagent **286** (2.0 equivalents), delivering the vinyl triflate **282** in a reasonable yield. Reduction of triflate **282** in the presence of a palladium catalyst, formic acid, and tributylamine afforded the corresponding alkene **277** in 75% yield as shown in **Scheme 88**.

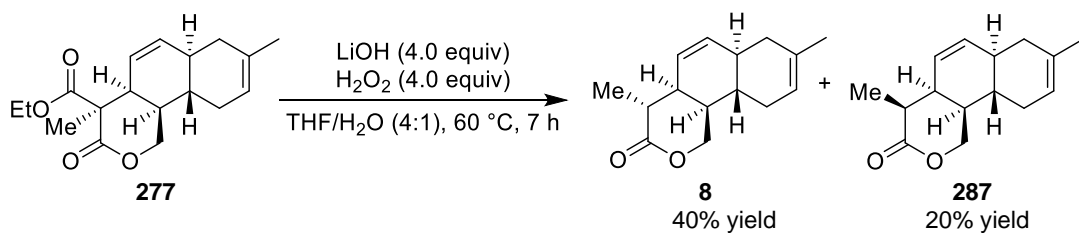


Scheme 88: The transformation of ketone **7** to alkene **277**

Switching the triflating agent to Comins' reagent **286** improved the conversion and yield of triflate **282**. Having the alkene **277** in hand, the next step towards the synthesis of the anthracimycin core **8** would be the removal of the ester group. Therefore, we envisioned conversion to lactone **8** through a decarboxylation.

Conditions for decarboxylation are similar to hydrolysis conditions, in which most hydroxide species are generally used as nucleophiles. In our case, hydrolysis of the ester group in the presence of a structurally complex molecule of **277** consisting of a lactone ring and five stereogenic centres would be considered challenging. All installed stereogenic centres are necessary for the core of the natural product, but the strength of hydroxide species is unknown. Hence, we planned to cleave the ester group under mild conditions in order to prevent the unexpected epimerisation of precious installed stereogenic centres. The conditions of LiOH and H₂O₂ would then be utilised as the less reactive *in situ* LiOOH-formed species seemed ideal for our proposes.

Cleavage of the ester group in **277** was carried out in the presence of LiOH and H₂O₂ in THF/H₂O at 60 °C. The LiOOH species was generated *in situ*, which hydrolysed the ester group and then the carboxylic acid intermediate underwent decarboxylation to provide two diastereomers **8** and **287** in 40% and 20% yields respectively, as demonstrated in **Scheme 89**.



Scheme 89: Decarboxylation of lactone **277**

Reaching the crucial stage, the stereochemistry of the methyl group in diastereomers **8** and **287** was important information to progress the synthesis towards the anthracimycin core. The key protons of the major diastereomer **8** were assigned by ¹H NMR analysis (**Figure 23**). Analysis of nOe data from ¹H NMR experiments of **8** revealed through space correlations between H-3 and H-4 (nOe = 1.49%), and between H-3 and H-15 of the methyl group (nOe

= 0.36%) as depicted in **Figure 24**. These correlations corresponded to the results when either H-4 or H-15 were irradiated (**Figure 25–26**). The nOe ^1H NMR analysis results were in accordance with the 2D NOESY data as shown in **Figure 27**. Analysing the results in hand, it was confirmed that there was a *syn*-relationship between H-3 and protons from the methyl group at the 15-position, which was desirable for the natural product.

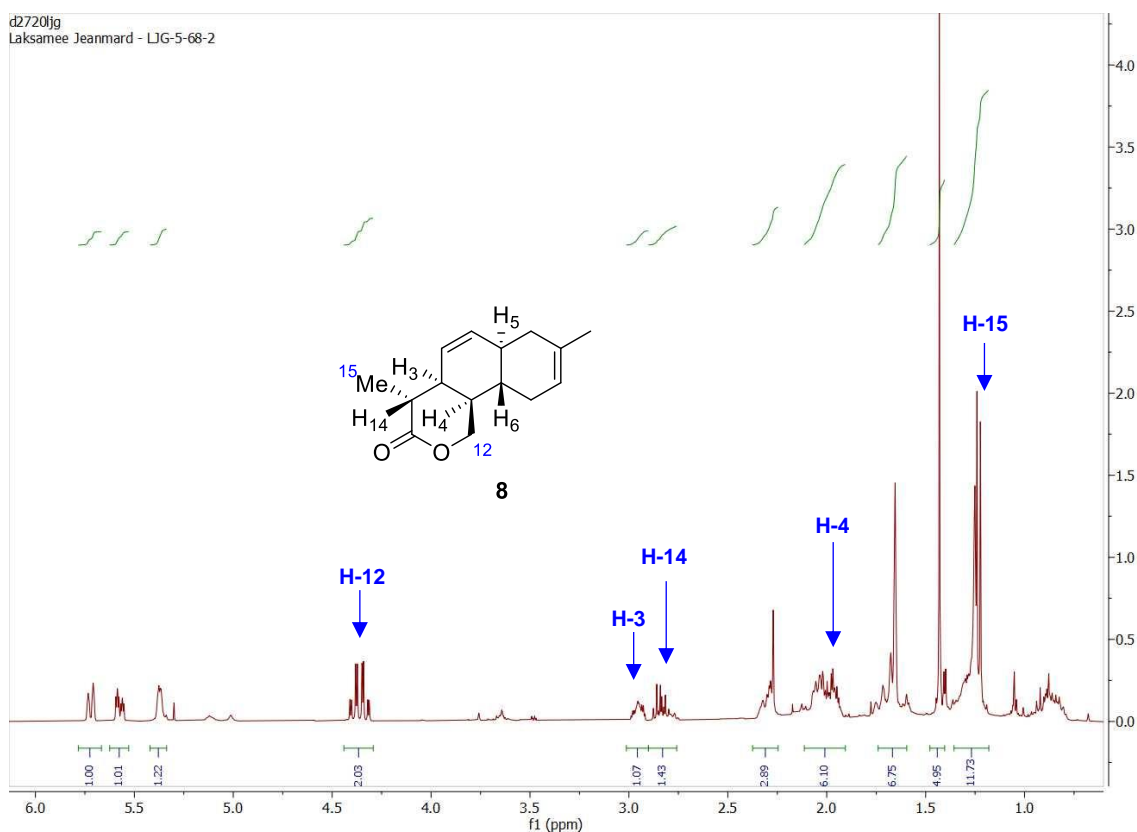


Figure 23: The ^1H NMR spectrum of tricyclic lactone **8**

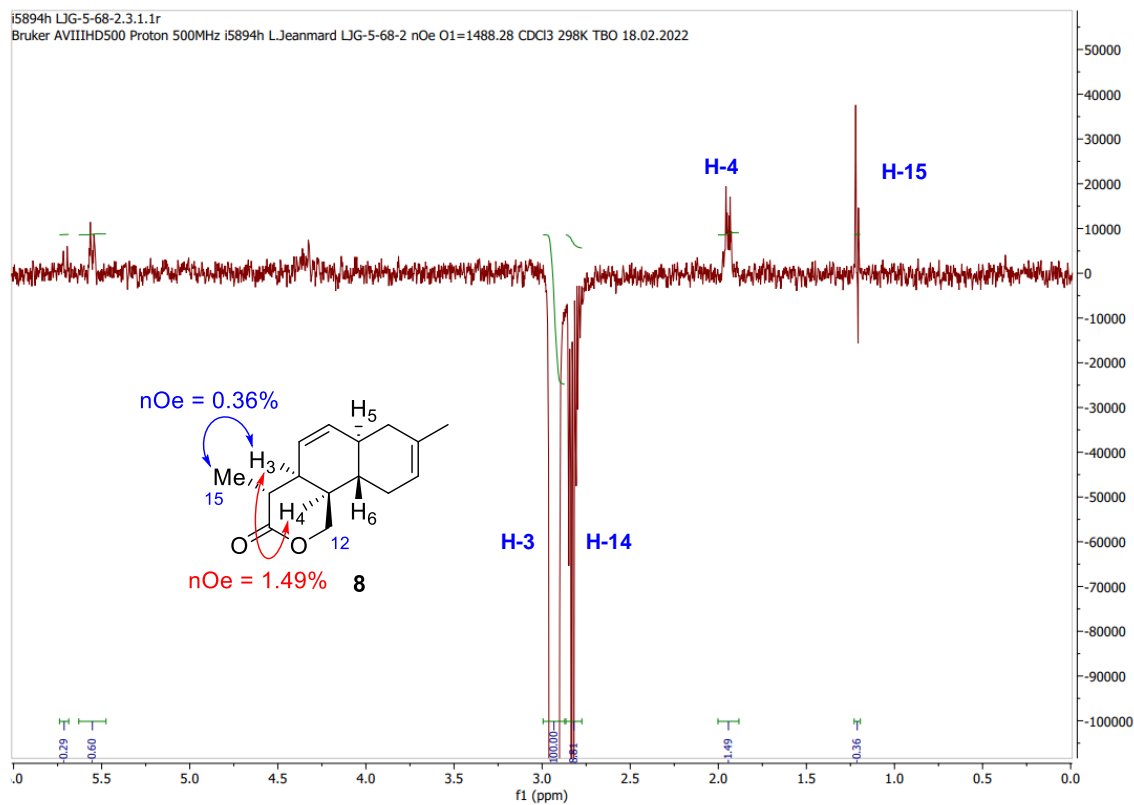


Figure 24: The nOe analysis of H-3 in tricyclic lactone **8**

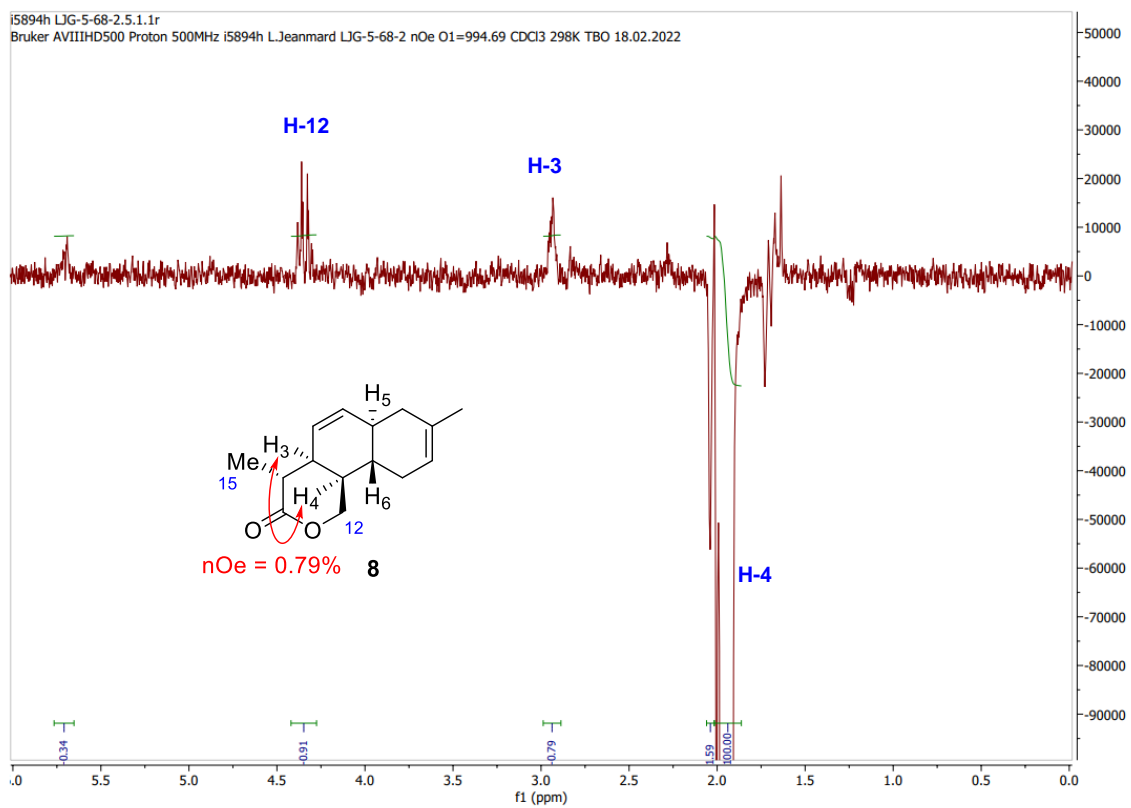


Figure 25: The nOe analysis of H-4 in tricyclic lactone **8**

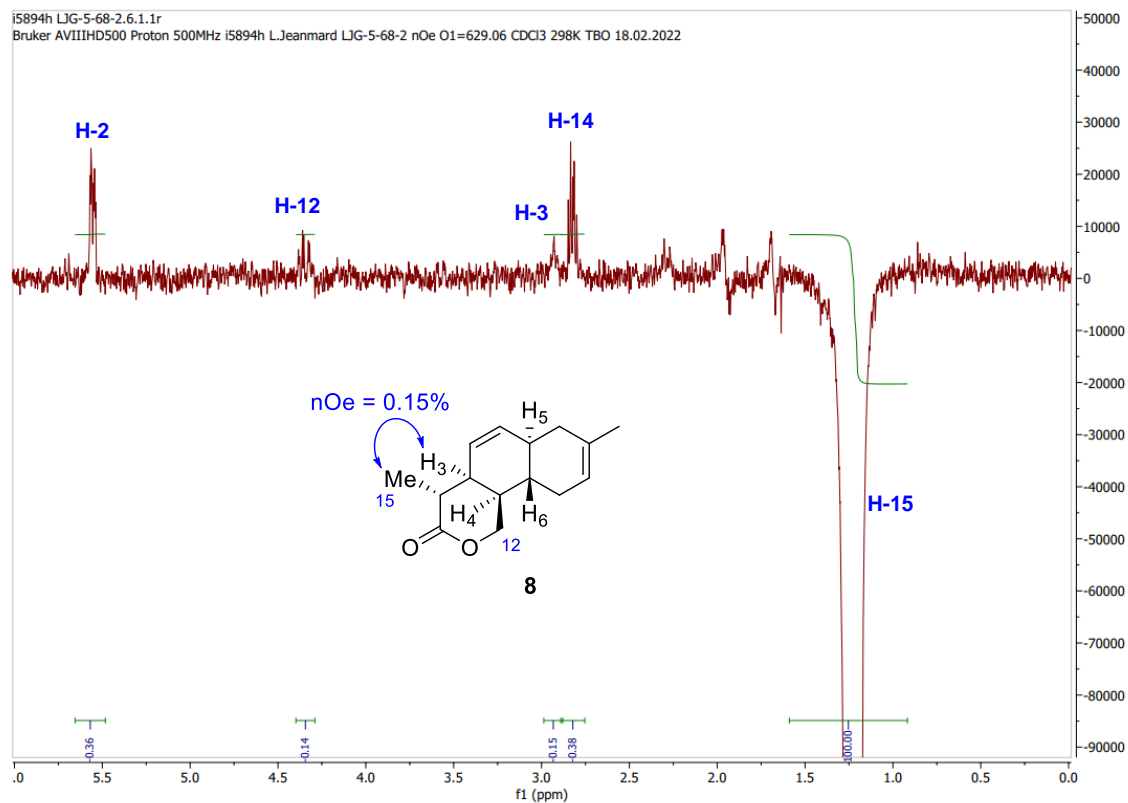


Figure 26: The nOe analysis of H-15 in tricyclic lactone **8**

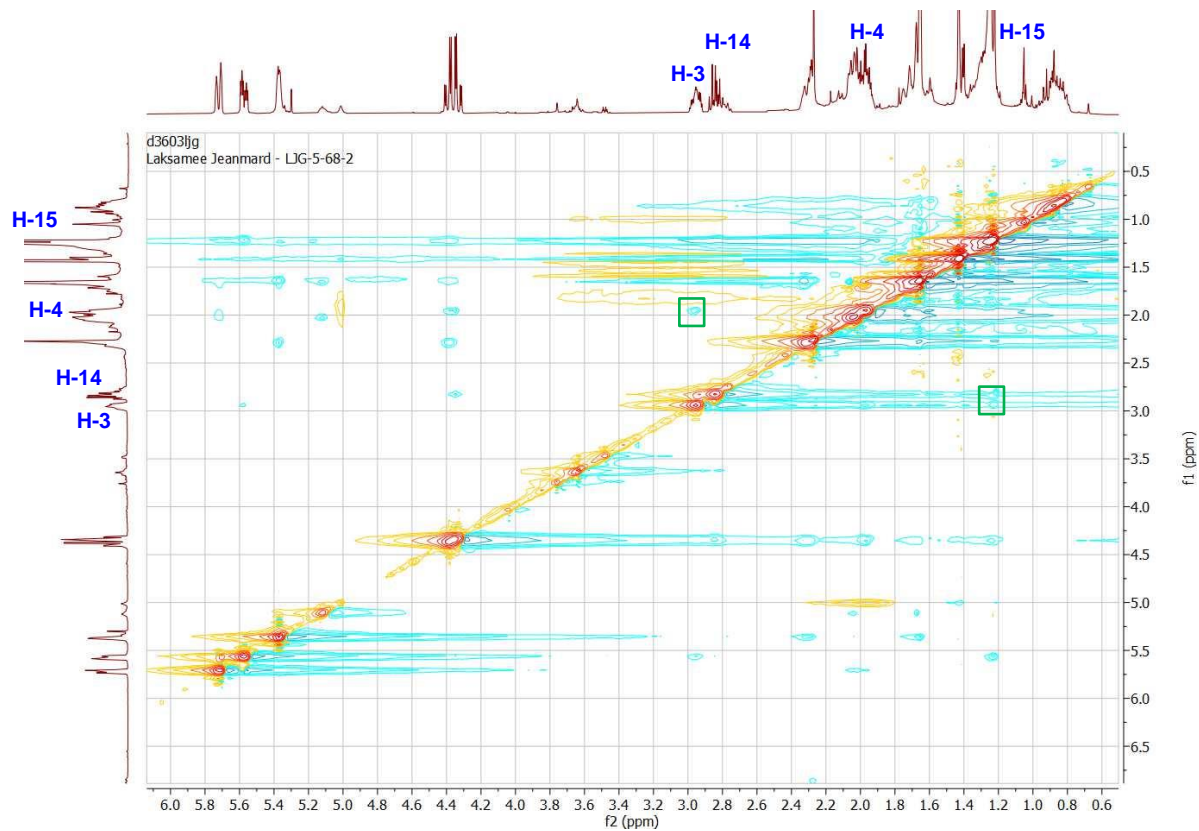


Figure 27: The 2D NOESY analysis of tricyclic lactone **8**

In addition, the stereochemistry of the minor product **287** was determined under the same analysis. The required protons of **287** were identified by ^1H NMR spectroscopy (**Figure 28**). The nOe ^1H NMR analysis of **287** showed a strong through space correlation between H-3 and H-14 (nOe = 3.08%), and a correlation between H-3 and H-15 of the methyl group (nOe = 1.09%) as depicted in **Figure 29**. However, 2D NOESY analysis results were unclear due to a small amount of sample (**Figure 33**). With as much as the nOe results in hand, it was confirmed to be an *anti*-relationship between H-3 and protons from the methyl group at the 15-position. Therefore, sufficient material of both diastereomers **8** and **287** would be required to confirm the stereochemistry by X-ray crystallography.

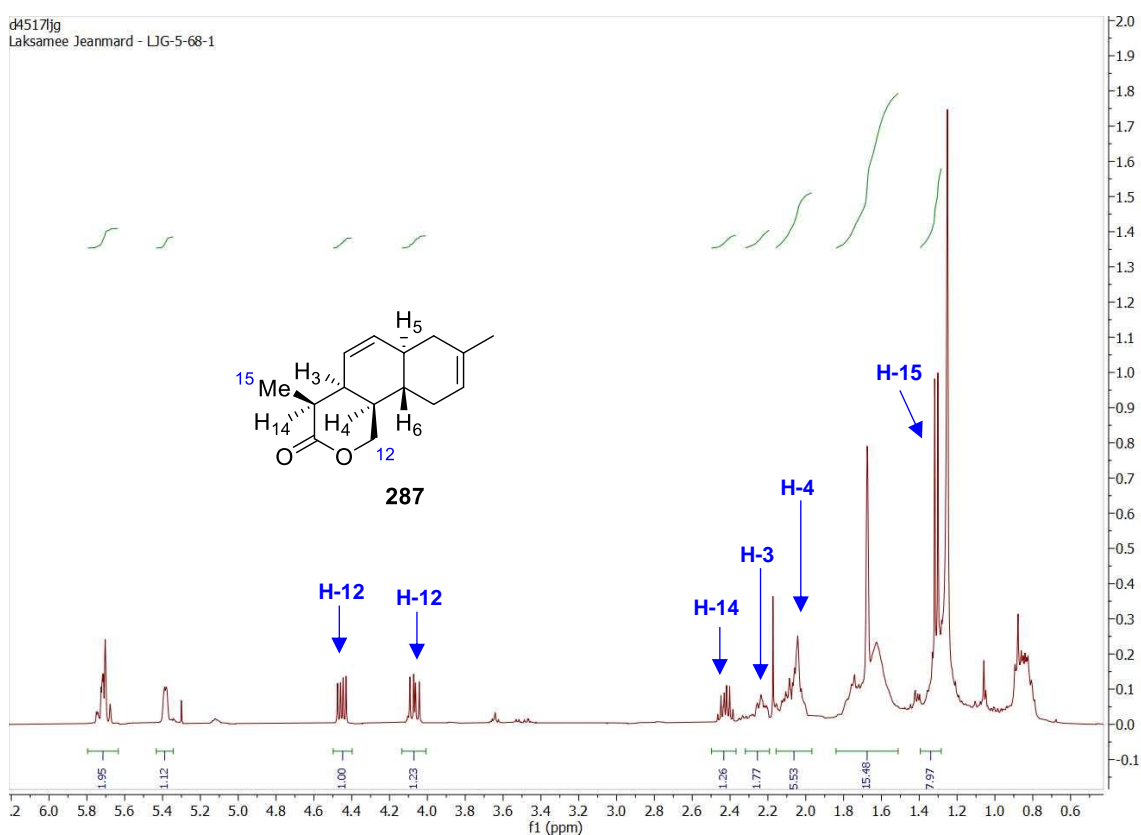


Figure 28: The ^1H NMR spectrum of tricyclic lactone **287**

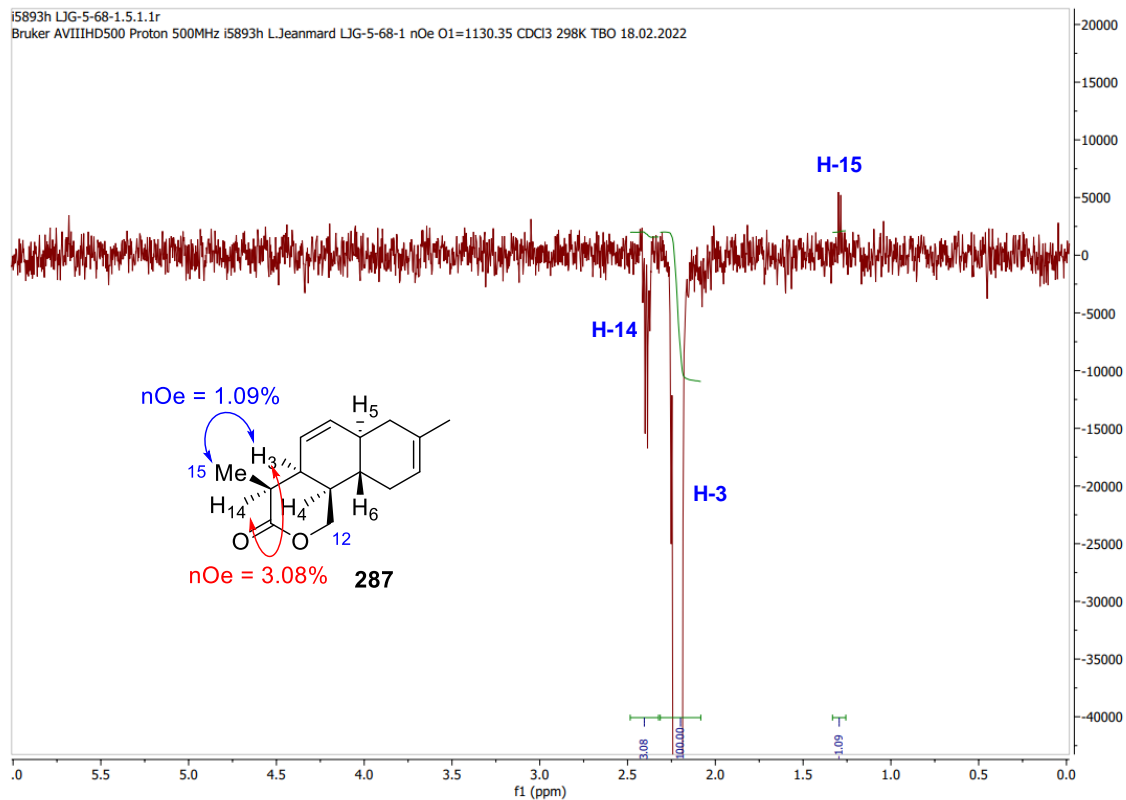


Figure 29: The nOe analysis of H-3 in tricyclic lactone 287

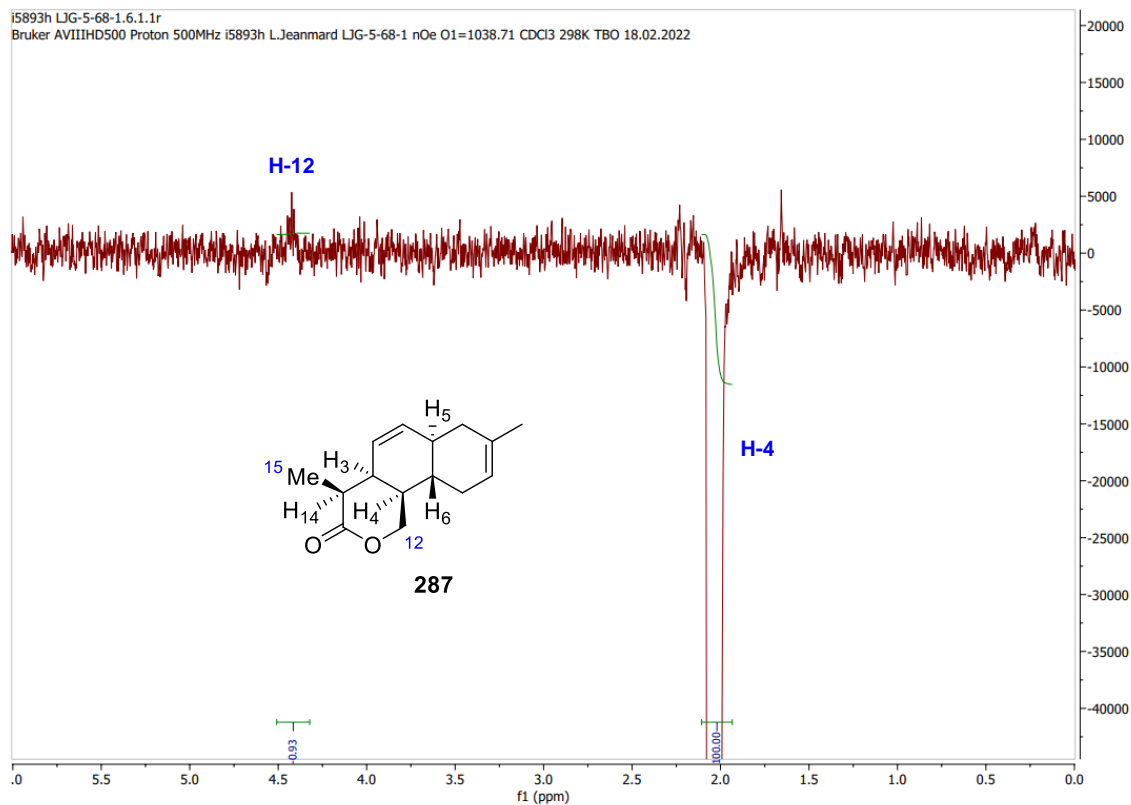


Figure 30: The nOe analysis of H-4 in tricyclic lactone 287

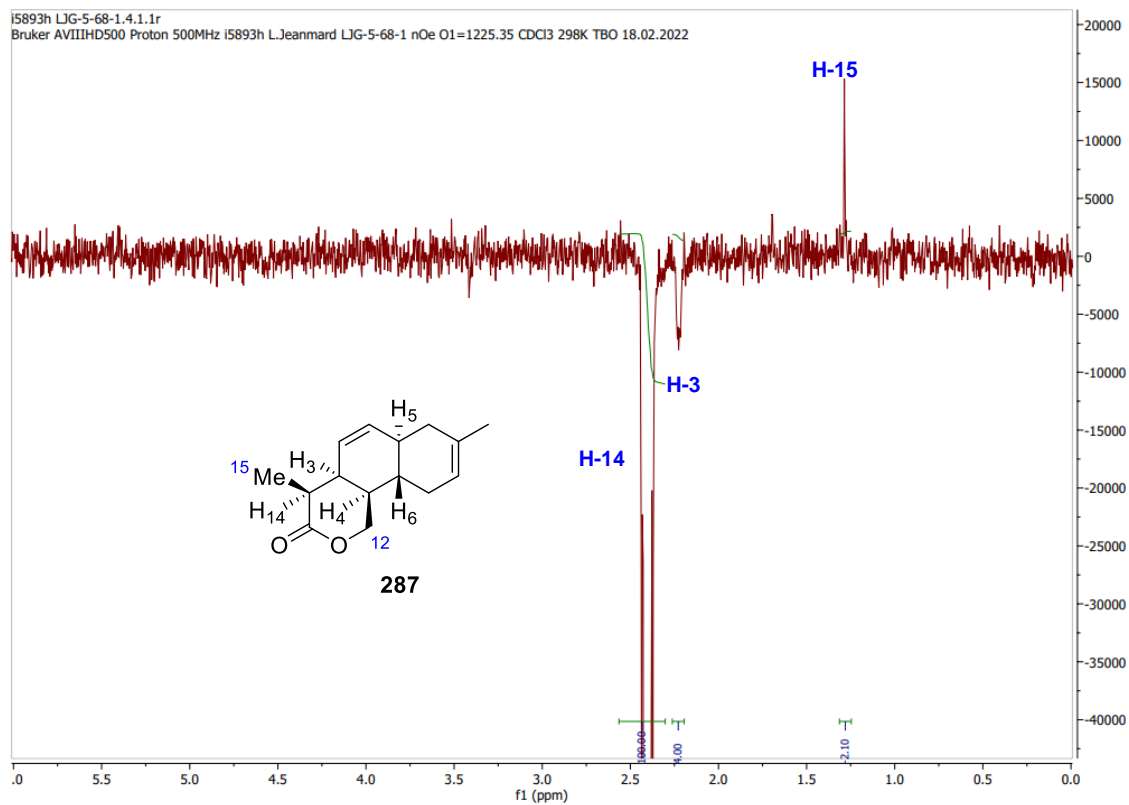


Figure 31: The nOe analysis of H-14 in tricyclic lactone **287**

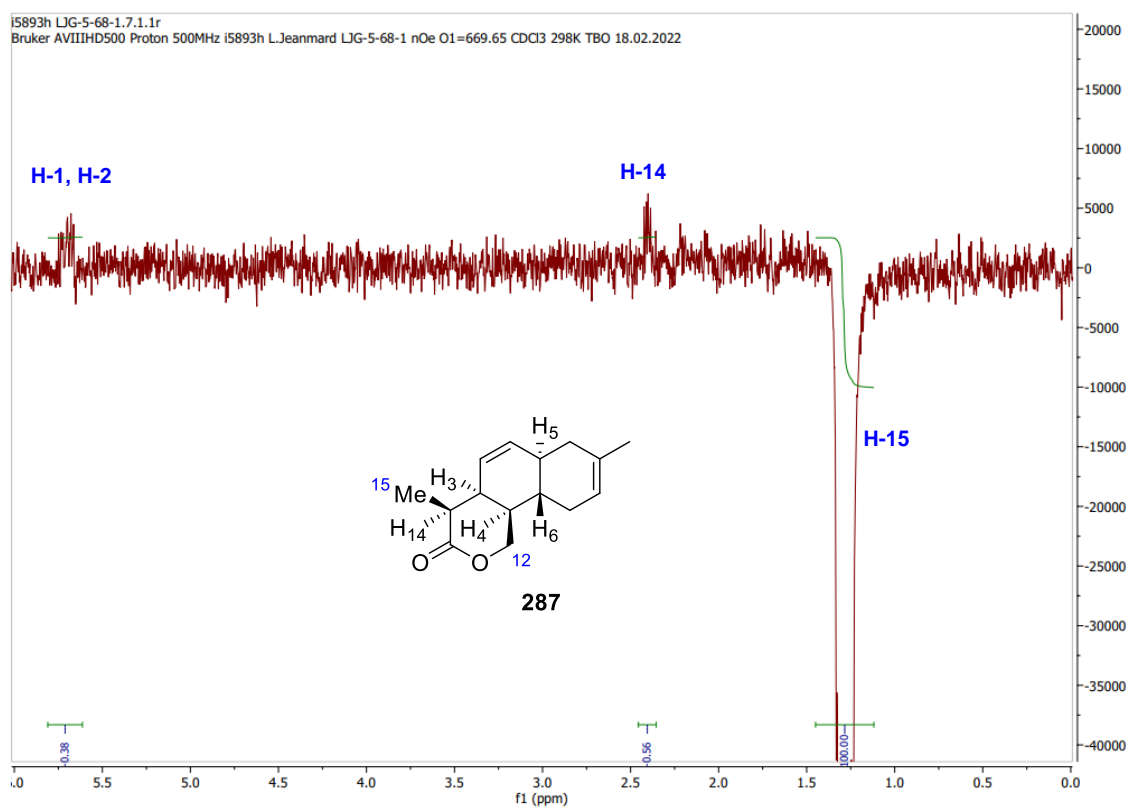


Figure 32: The nOe analysis of H-15 in tricyclic lactone **287**

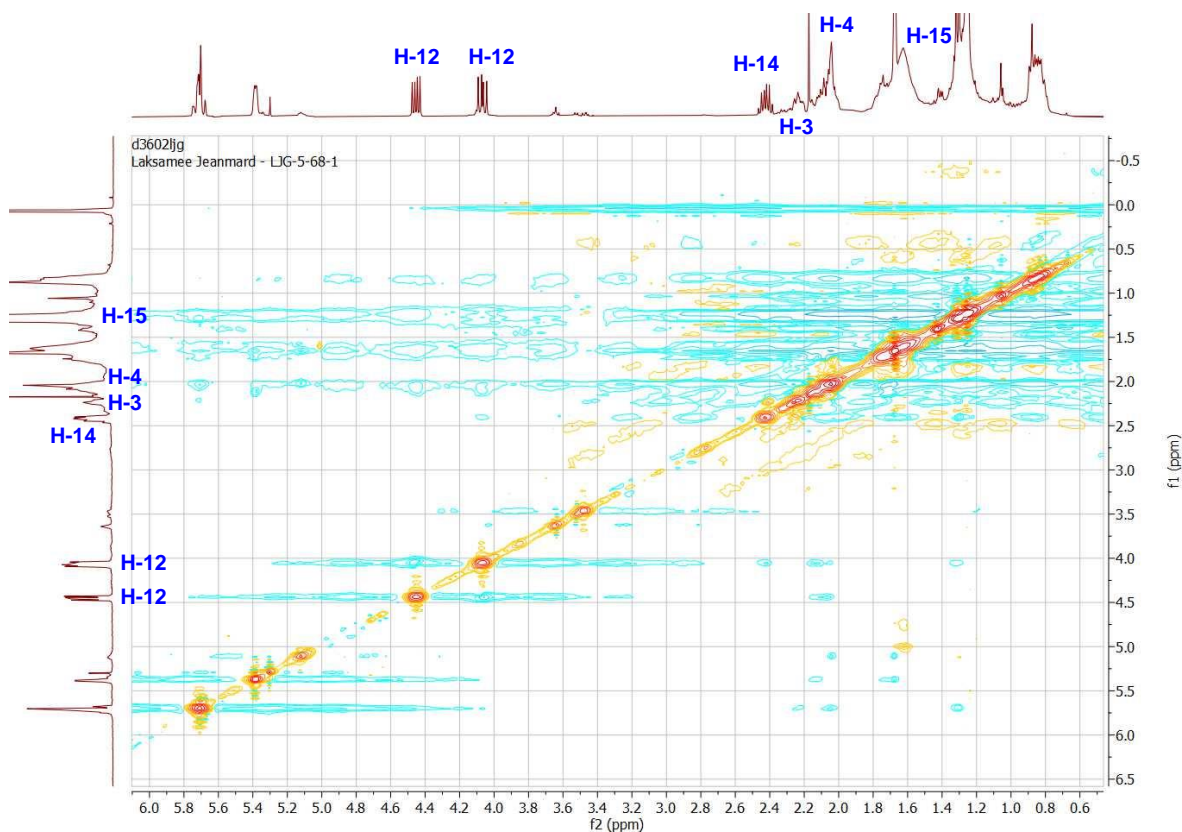


Figure 33: The 2D NOESY analysis of tricyclic lactone **287**

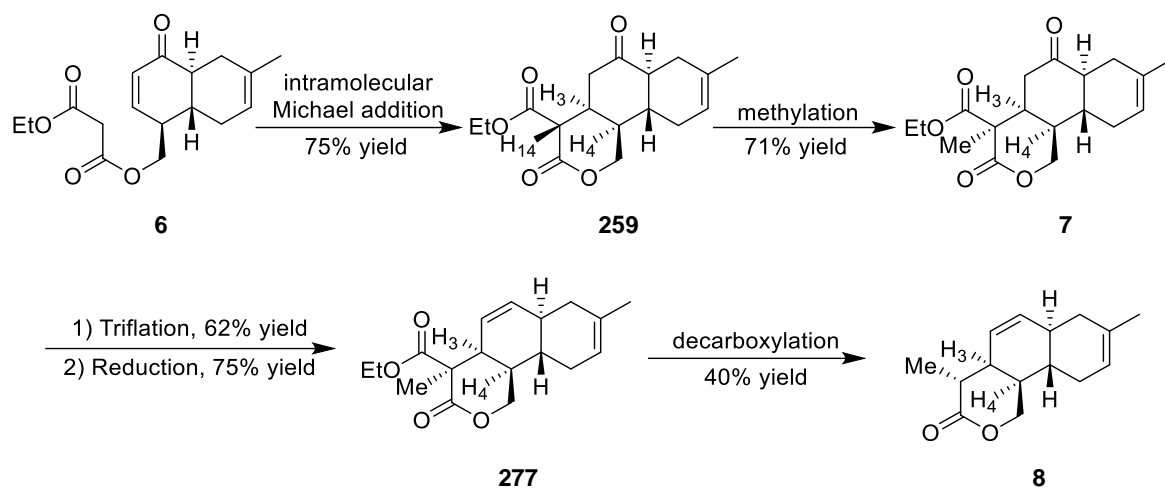
According to the nOe and NOESY data, through space correlations were observed between H-3 and H-4, and between H-3 and protons from the 15-methyl group substituent in the major product **8** indicating that the tricyclic lactone **8** was the requisite anthracimycin core. Similar correlations were not seen in the minor product **287**.

With the desired lactone **8** in hand, the next step would be synthesising the anthracimycin core. However, several steps also suffered from a lack of consistency upon scale-up, and the instability of the tricyclic lactone series was problematic. These considerations led us to devise an improved route to the anthracimycin core **8**. The following section will describe new attempted approaches to achieve the target molecule.

2.8 Alternative approaches to access the anthracimycin core

2.8.1 Palladium catalysed cyclisation

Since we encountered difficulties accessing the core structure of the natural product from enone malonate **6** through five troublesome steps (**Scheme 90**), we decided to pursue an alternative route to promptly access the target in high quantity.

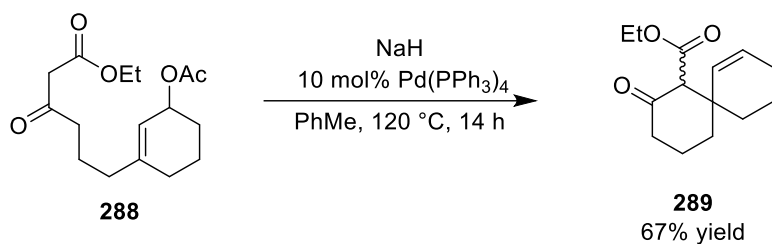


Scheme 90: The formation of the anthracimycin core **8**

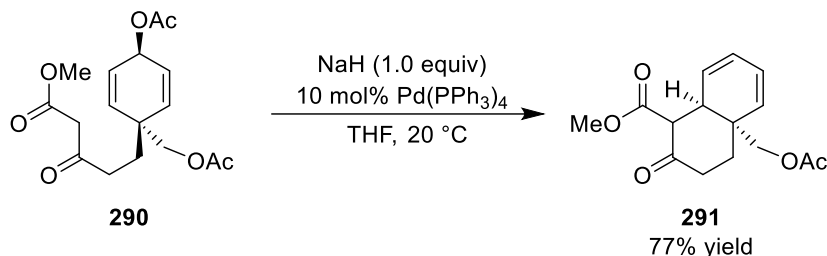
An alternative pathway would be to construct the tricyclic ring and form the alkene moiety in a single step. Our attention turned to the Tsuji-Trost reaction, which is the Pd-catalysed inter- or intramolecular allylation of nucleophiles. The cyclisation generally takes place via the addition of a nucleophile onto a π -allylpalladium intermediate. Important examples of intramolecular Pd-catalysed allylation are outlined in **Scheme 91**.

Godleski and Valpey employed the Pd-catalysed cyclisation of acetate **288** in the presence of NaH and Pd(PPh₃)₄ to furnish the spirocyclic compound **289** in 67% yield (**Scheme 91A**).¹⁰⁷ The second example of the formation of *cis*-decalin derivative **291** was reported by Shibasaki and co-workers in 2012.¹⁰⁸ Treatment of π -allyl precursor **290** with NaH and Pd(PPh₃)₄ in THF generated the desired bicyclic ring **291** in good yield (**Scheme 91B**). Another example came from Pandey's synthesis on the biphasic 6-*endo-trig* Tsuji-Trost cyclisation of **292**.¹⁰⁹ The use of Pd(PPh₃)₄ catalyst, K₂CO₃, and benzyltriethylammonium chloride generated the cyclised product **293** smoothly in quantitative yield (**Scheme 91C**).

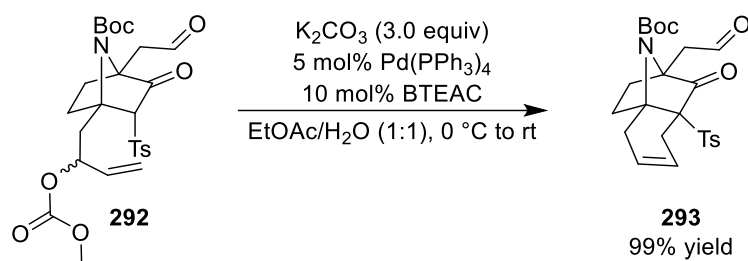
A) Godleski's synthesis



B) Shibasaki's synthesis

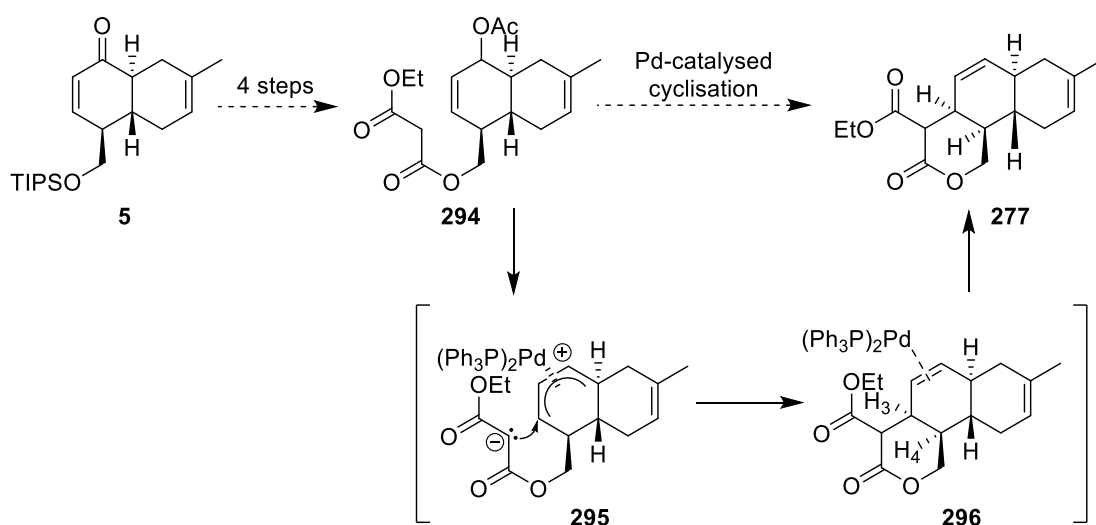


C) Pandey's synthesis



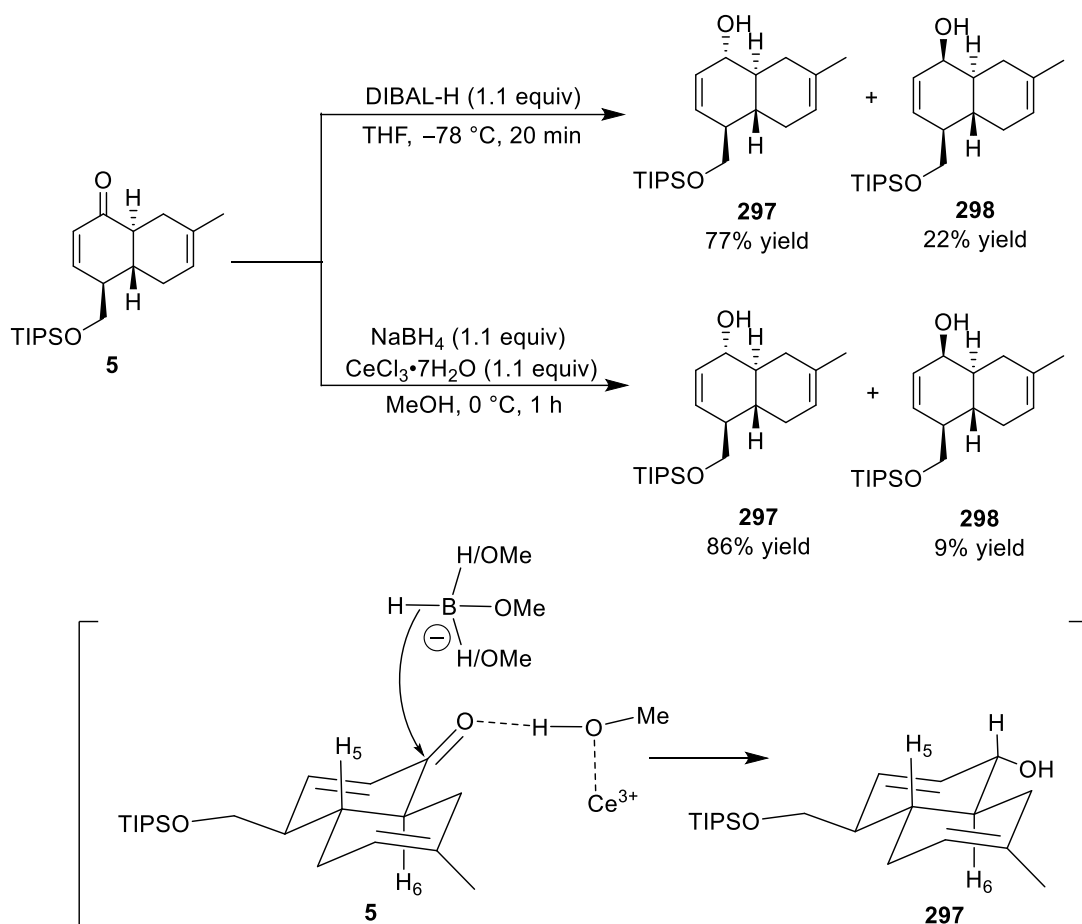
Scheme 91: Examples of Pd-catalysed cyclisation^{107–108}

Based on the relevant precedent above, we envisaged utilising the Pd-catalysed cyclisation to accomplish a lactone functionality and install an alkene moiety for **277**. Consequently, we proposed a new synthetic route requiring malonate **294** as a π -allyl precursor as shown in **Scheme 92**.



Scheme 92: The proposed synthetic route for the Pd-catalysed cyclisation of **294**

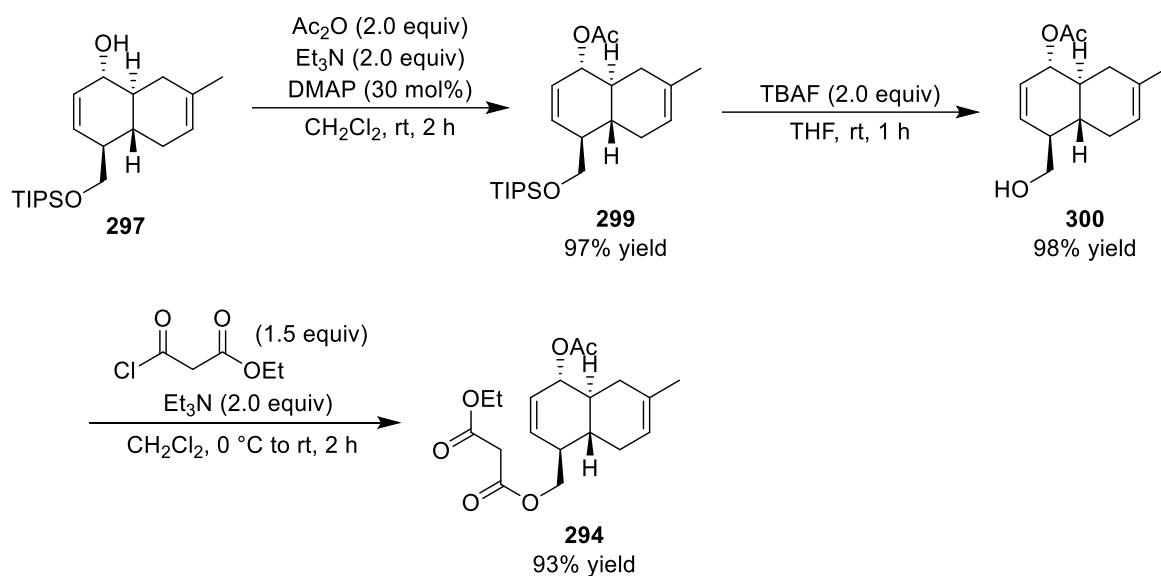
The formation of malonate **294** would be achieved in four steps from enone *trans*-decalin **5** as shown in **Scheme 92**. The DIBAL-H reduction of enone **5** at $-78\text{ }^{\circ}\text{C}$ afforded allylic alcohols **297** and **298** in 77% and 22% yields, respectively.⁶⁶ Since we had two diastereomers **297** and **298** in hand, we decided that the major allylic alcohol **297** should be pursued in the key Pd-catalysed cyclisation. To gain more allylic alcohol **297**, the selectivity of the reduction reaction was enhanced. Luche reduction was then investigated by employing enone **5** with NaBH_4 and $\text{CeCl}_3\cdot 7\text{H}_2\text{O}$ in MeOH at $0\text{ }^{\circ}\text{C}$ to furnish the desired allylic alcohol **297** in 86% yield together with its diastereomer **298** in 9% yield.¹¹⁰ The stereochemistry of the major product **297** can be explained via axial delivery of hydride onto the ketone functionality (**Scheme 93**).¹¹¹



Scheme 93: The formation of allylic alcohols **297** and **298**

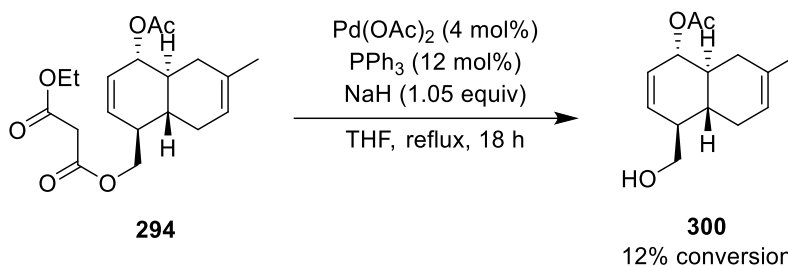
In three steps, the allylic alcohol **297** was then converted to the π -allyl precursor **294**. First, acetylation of allylic alcohol **297** in the presence of acetic anhydride, Et_3N and catalytic DMAP delivered the requisite acetate **299** in excellent yield (97% yield).¹¹² Next, the silyl group of **299** was smoothly removed by TBAF to give alcohol **300** in 98% yield. Finally, the

π -allyl precursor **294** was obtained in 93% yield from the alcohol **300** employing ethyl malonyl chloride and Et₃N as shown in **Scheme 94**.



Scheme 94: The formation of π -allyl precursor **294**

With the π -allyl precursor **294** in hand, the formation of tricyclic lactone **277** via Pd-catalysed cyclisation of **294** was then investigated. To screen conditions, the key reaction would be performed on a small scale, and a stock solution of sodium hydride would be required. A palladium catalyst was prepared *in situ* by a stock solution of Pd(OAc)₂ and PPh₃. Malonate **294** was treated with a stock solution of sodium hydride (1.05 equivalents) to generate a portion of anion, which was added into a stock solution of Pd(OAc)₂ and PPh₃. Unfortunately, none of the desired lactone **277** was observed after 18 hours in refluxing toluene, while the undesired alcohol **300** was obtained in 12% conversion as illustrated in **Scheme 95**.



Scheme 95: The attempted Pd-catalysed cyclisation of malonate **294**

The formation of alcohol **300** may be explained by the high temperature or the presence of water in the reaction which led to the hydrolysis. As a small portion of sodium hydride (1.05 equivalents) was required for a small-scale reaction, we thought that an insufficient amount of sodium hydride might not lead to generation of the carbanion for cyclisation. Therefore, producing a portion of anion on a small-scale reaction in the presence of bases was intensively screened.

Our efforts to achieve tricyclic lactone **277** through the Pd-catalysed cyclisation of malonate **294** were investigated further under various bases as shown in **Table 12**. Following Pandey's protocol, use of K_2CO_3 (2.5 equivalents)¹⁰⁹ under the same conditions provided alcohol **300** in 7% conversion. However, the desired tricyclic lactone **277** could not be detected after 16 hours (entry 2). The tertiary amine base conditions were then studied. None of the desired lactone **277** was observed by treatment of malonate **294** with DBU (1.5 equivalents), while the alcohol **300** was obtained in 40% conversion (entry 3). Another tertiary amine base was investigated under similar conditions. The unreacted malonate **294** was recovered quantitatively under the conditions of Et_3N (1.5 equivalents) after reflux for 16 hours (entry 4). Unfortunately, diol **301** was obtained as a single product in >99% conversion under the conditions of NaOEt (1.1 equivalents) as shown in entry 5.

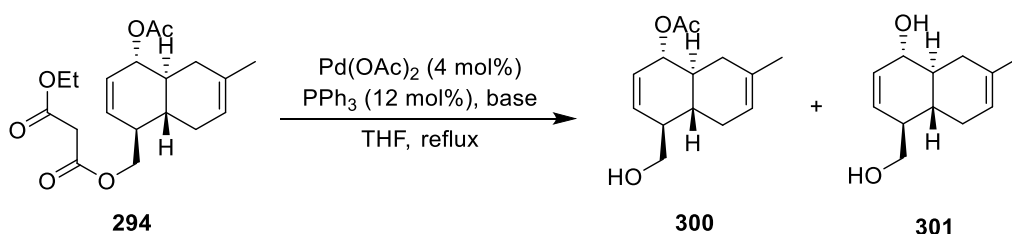


Table 12: Screening conditions for the Pd-catalysed cyclisation of acetate **294**

Entry	Base	Time (hours)	Result (conversion) ^a
1	NaH (1.05 equiv)	18	300 in 12%
2	K_2CO_3 (2.5 equiv)	16	300 in 7%
3	DBU (1.5 equiv)	16	300 in 40%
4	Et_3N (1.5 equiv)	16	n.r.
5	NaOEt (1.1 equiv)	20	301 in >99%

^a % conversion was determined by integration of 1H NMR

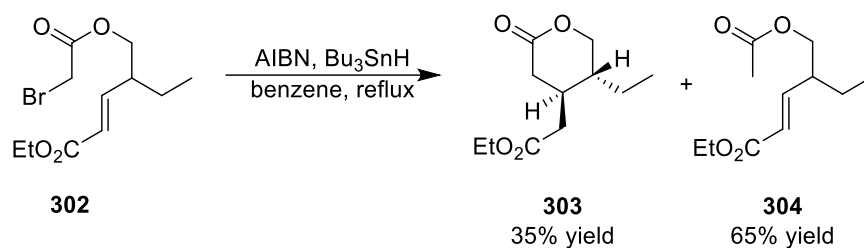
Overall, the attempted formation of tricyclic lactone **277** through the Pd-catalysed cyclisation of malonate **294** under various bases did not proceed well. However, alcohol **300** was obtained by hydrolysis of the malonyl group in the presence of sodium hydride, potassium carbonate, or sodium ethoxide. In addition, employing sodium ethoxide unexpectedly removed both acetyl and malonyl groups. Owing to the failure of all cases, our attention turned to the literature for deeply understanding the mechanism and stereochemistry. In consideration of Shibasaki's synthesis (see **Scheme 91**), the acetate leaving group was located on the top face of the precursor **290**. The addition of palladium to **290** was proposed from the opposite face of the leaving group to form the π -allyl precursor. Finally, the lactone ring was cyclised from the same face of the carbanion, which was opposite to the Pd-complex affording the retention of stereochemistry compared to the stereochemistry of the acetate group. Due to the postulated mechanism, we revised our method to choose alcohol **298** as a π -allyl precursor instead of alcohol **297** to afford the cyclised product, which was suggested for future work.

2.8.2 Radical cyclisation

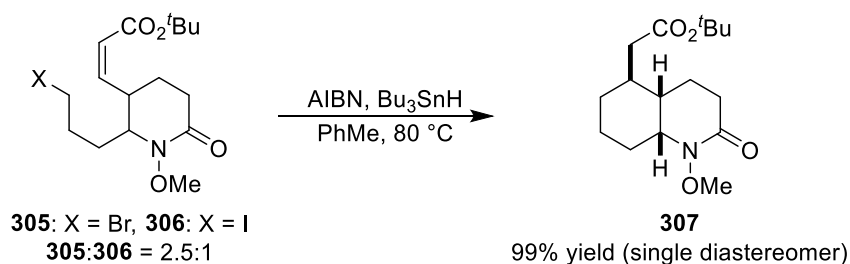
One method for ring formation by carbon-carbon bond formation is free radical-mediated cyclisation. Due to its versatility, this method is extensively used for five-membered ring construction in the synthesis of various natural products. However, a few formations of the six-membered ring system have been reported.¹¹³ Two examples of radical cyclisation to construct a six-membered ring are illustrated in **Scheme 96**.

The lactone formation was reported by Ihara and co-workers using bromoacetate **302** as a key precursor.¹¹³ Radical cyclisation of **302** was conducted by heating Bu_3SnH in the presence of azoisobutyronitrile (AIBN) in refluxing benzene to furnish lactone **303** as a single diastereomer in 35% yield. However, the reduction product **304** was also found as a major product with 65% yield (**Scheme 96A**). Another example of accomplishing a six-membered ring system was presented in Sato and Chida's synthesis.¹¹⁴ The highly stereoselective radical cyclisation of a mixture of bromo *Z*-enoate **305** and iodo *Z*-enoate **306** was satisfyingly achieved under the conditions of Bu_3SnH and AIBN, in toluene at 80 °C to afford the bicyclic *N*-methoxylactam **307** in 99% yield as a single diastereomer as illustrated in **Scheme 96B**.

A) Ihara's synthesis

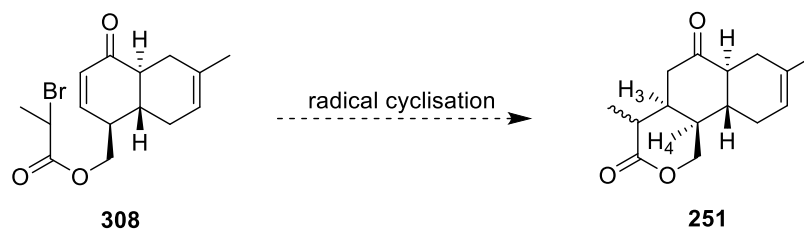


B) Chida's synthesis



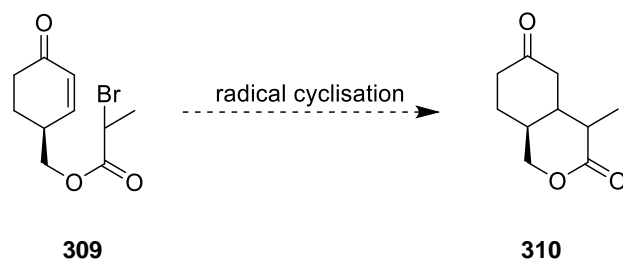
Scheme 96: Examples of the radical cyclisation to construct a six-membered ring^{113–114}

Inspired by the examples above, the radical cyclisation strategy was chosen to avoid the multistep synthesis of the anthracimycin core and thus save time. Hence, bromo propionate **308** would be a reasonable precursor to form the tricyclic lactone **251** (**Scheme 97**).



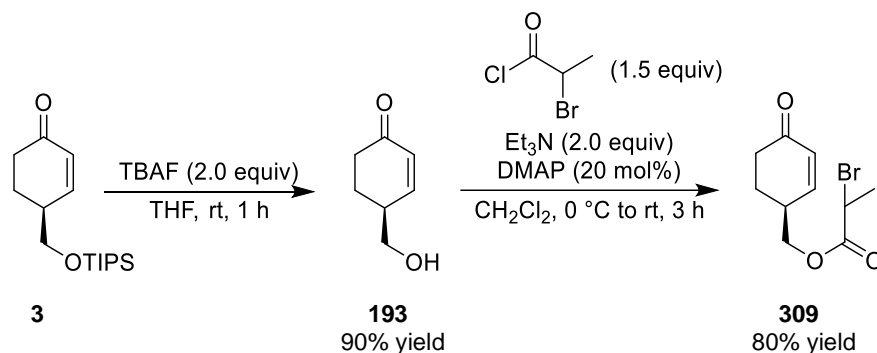
Scheme 97: The proposed synthesis of tricyclic lactone **251** via a radical cyclisation

The stereochemical outcome of such radical cyclisations can be effectively rationalised according to the substrate-like transition state. Since the stereochemistry of tricyclic lactone is necessary for total synthesis, using an enantioenriched precursor would be convenient for us to determine the stereochemistry configuration of the lactone ring. To save our precious enone **308**, enantioenriched bromo propionate **309** would be a model study to use simply to see whether we could form the lactone ring via a radical cyclisation reaction with the desired stereochemistry necessary for the natural product (**Scheme 98**).



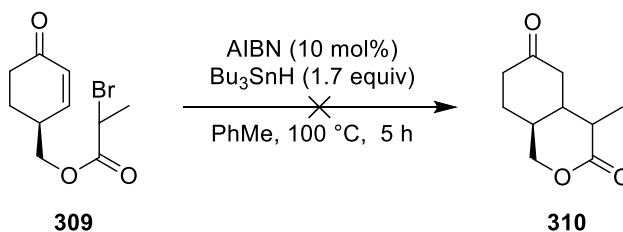
Scheme 98: The proposed model study to investigate the radical cyclisation

We began the preparation of bromo propionate **309** from enantioenriched enone **3**. Desilylation of alcohol **3** with TBAF effectively produced alcohol **193** in 90% yield. The resultant primary alcohol **193** was coupled with 2-bromopropionyl chloride (1.5 equivalents) in the presence of triethylamine and DMAP to afford the desired bromo propionate **309** in 80% yield as demonstrated in **Scheme 99**.¹¹⁵



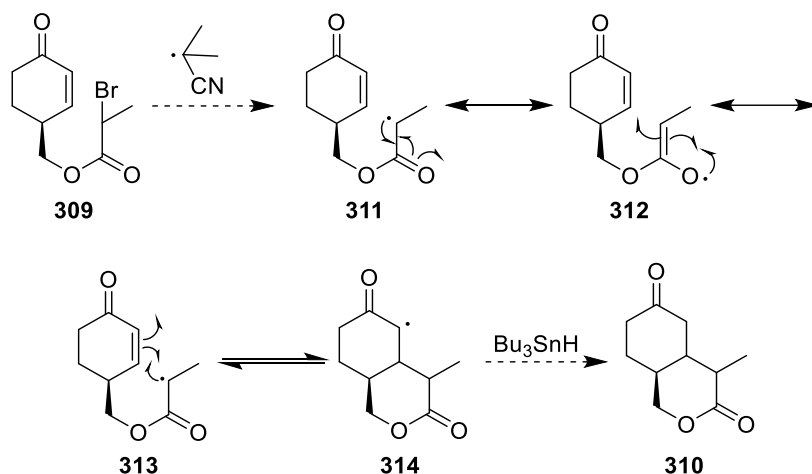
Scheme 99: The synthesis of bromine propionate **309**

To investigate the radical cyclisation, bromo precursor **309** was heated in toluene at 100 °C under a slow addition of Bu₃SnH (1.7 equivalents) and AIBN (10 mol%) solution. The conversion to bicyclic lactone **310** could not be observed while monitoring the reaction frequently for a period of 5 hours. Unfortunately, none of the cyclised product **310** could be obtained after extended efforts in repeating the reaction (**Scheme 100**).

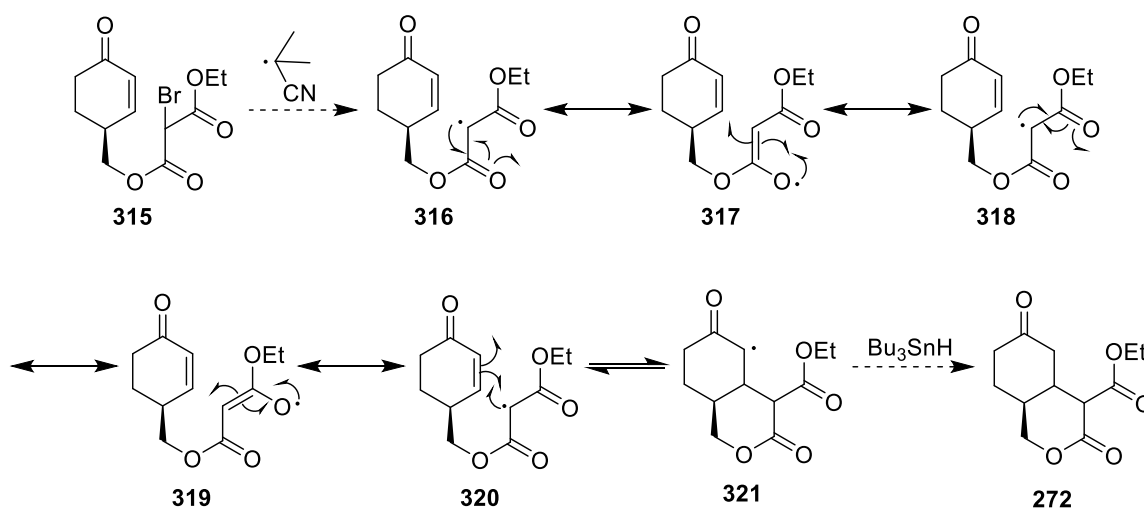


Scheme 100: The attempted synthesis of bicyclic lactone **310** via a radical cyclisation

As the radical cyclisation of bromo propionate **310** proved unsuccessful, we anticipated enhancing the stability of the initiated secondary radical by switching starting material to bromo malonate **315**. The malonyl moiety can stabilise the initially formed radical before trapping the cyclised radical. The stabilisation of the formed radical by the propionyl group compared to the malonyl group are outlined in **Scheme 101–102**.



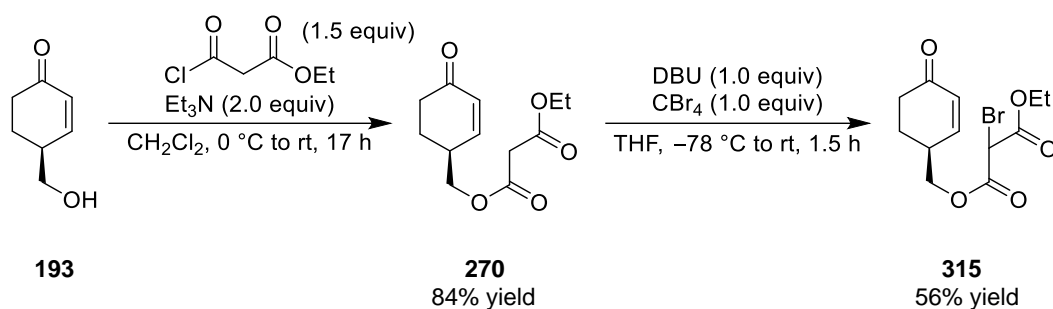
Scheme 101: Stabilisation of initially formed radical by the propionyl group of **309**



Scheme 102: Stabilisation of initially formed radical by the malonyl group of **315**

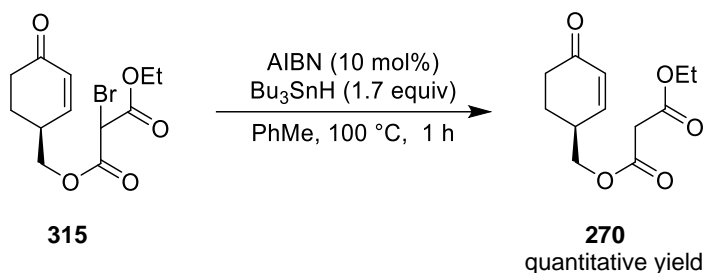
In order to explore our hypothesis, the alternative radical cyclisation precursor **315** would be prepared from enantioenriched alcohol **193**. A coupling of alcohol **193** with ethyl malonyl chloride delivered the desired malonate **270** in good yield. Bromination of **270** was

carried out under the conditions of DBU and CBr_4 to give bromo malonate **315** in 56% yield (**Scheme 103**).¹¹⁶



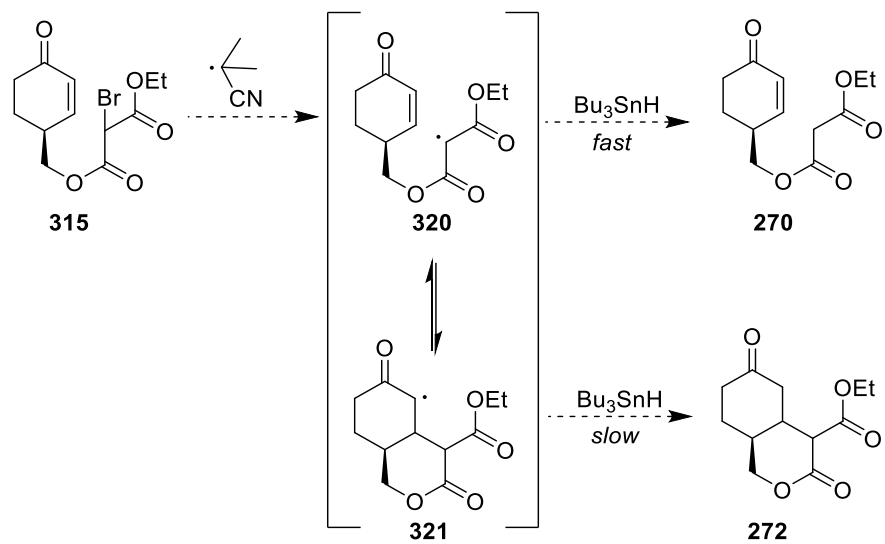
Scheme 103: The synthesis of bromo malonate **315**

With the bromo malonate **315** in hand, similar conditions to the propionate **309** were applied. The radical cyclisation of malonate **315** was performed in toluene at the temperature of 100 °C under a slow addition of a pre-mixed solution of Bu_3SnH (1.7 equivalents) and AIBN (10 mol%) via a syringe pump. Unfortunately, malonate **270**, the simple reduction product, was observed and isolated in quantitative yield (**Scheme 104**).



Scheme 104: The attempted radical cyclisation of bromo malonate **315**

In an attempted formation of bicyclic lactone **272** via a radical cyclisation, it appears that the rate of termination process trapping the generated radical with a hydride from Bu_3SnH was faster than the cyclisation proposed in **Scheme 105**. It would be the reason to explain the formation of the reduction product **270** instead of the desired cyclised product **272**. To overcome this, we slowed the addition of a pre-mixed solution of Bu_3SnH and AIBN and diluted the concentration of the reaction mixture. However, none of the desired lactone **272** was observed after our extended efforts. Therefore, due to a lack of time, optimisation of the cyclisation conditions was no longer pursued.

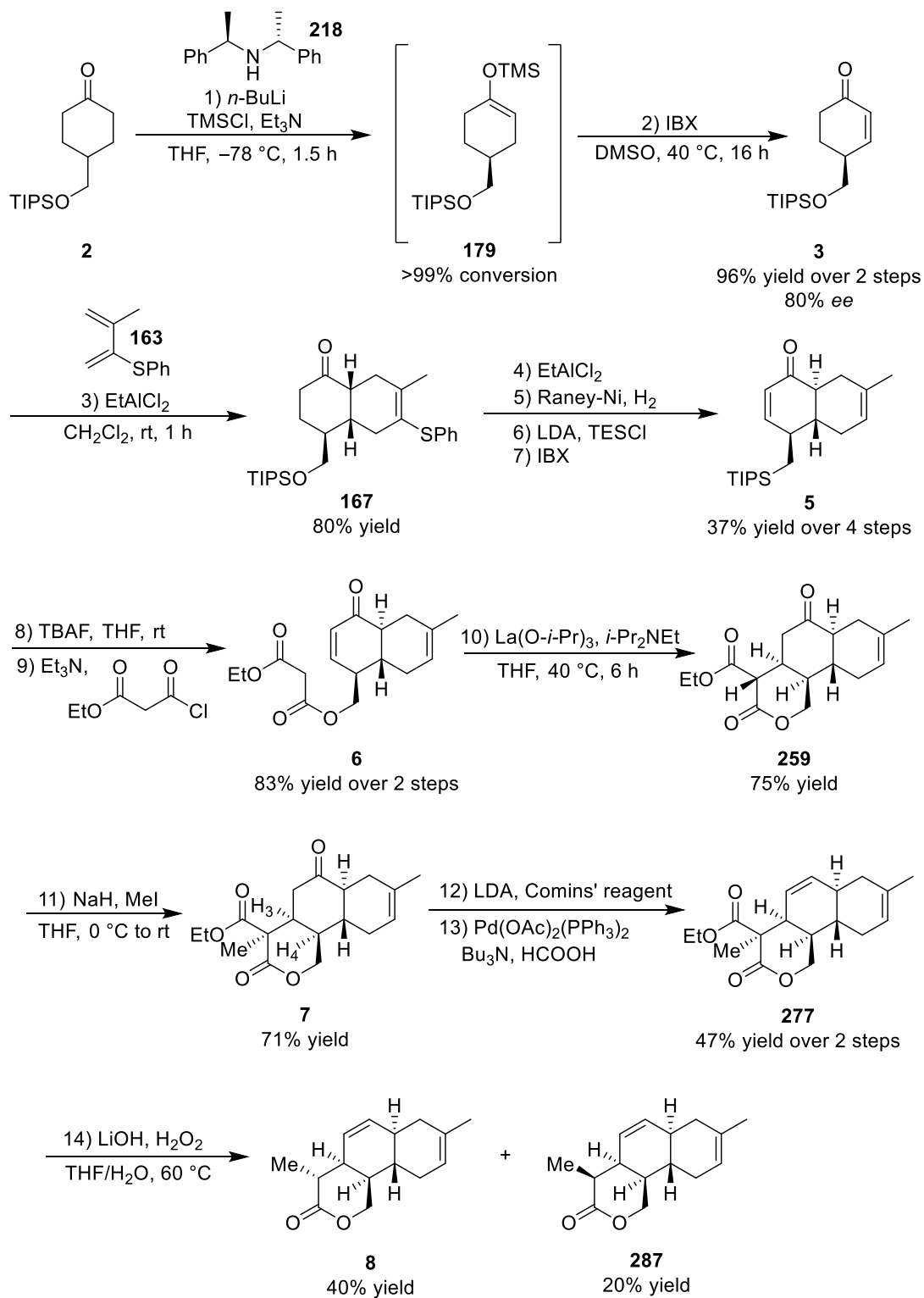


Scheme 105: The proposed mechanism to form the reduction product **270**

3. Conclusion

The asymmetric synthesis of anthracimycin core **8** was achieved in 14 steps from the known cyclohexanone **2** (Scheme 106). A sequence of enantioselective enolisation using the chiral lithium amide base (Simpkins's base)/IBX oxidation efficiently allowed the formation of enantiomerically enriched cyclohexenone **3** with 80% enantiomeric excess, which was an essential building block for the stereo- and regioselective Diels–Alder cycloaddition to afford the decalin scaffold. The challenging task was the introduction of a side chain to the enone *trans*-decalin **5**. To access the anthracimycin core, several approaches were screened. First, the Hosomi–Sakurai addition of enone *trans*-decalin with allyltrimethylsilane furnished the desired product in poor yield, while the chlorination product was mainly obtained. In terms of the Mukaiyama–Michael addition strategy, the steric hindrance of *cis*-decalin was investigated to see the conformation effect. However, the epimer of anthracimycin core and the aldol adduct were obtained under various Lewis acid conditions. On the other hand, the intramolecular Michael addition as the key strategy of our synthesis worked well for the stereocontrolled side chain installation and established the requisite stereochemistry for the natural product.

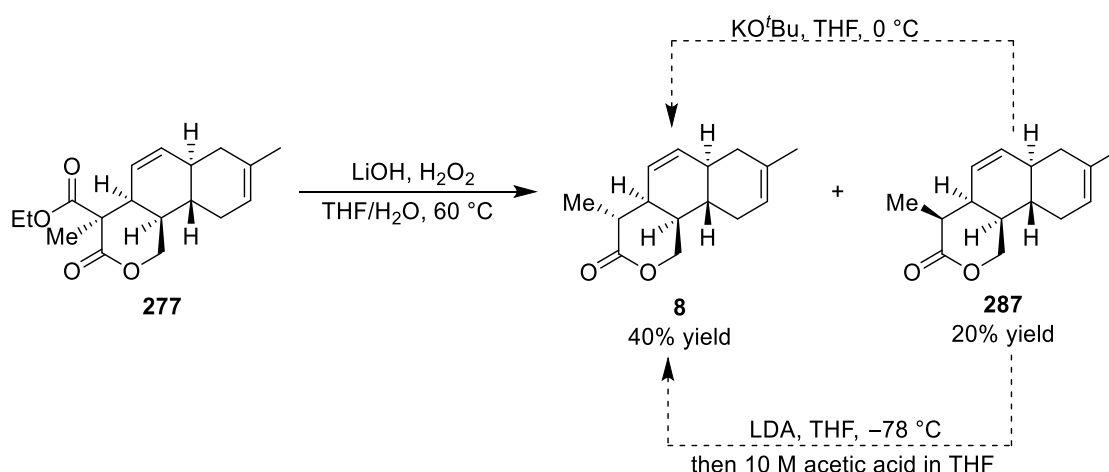
Interestingly, exploiting a metal complexation enhanced the acidity of malonate precursor **6** to the point where a tertiary amine base can be used. The combination of lanthanide salt La(O-*i*-Pr)₃ and Hunig's base gave the best results for synthesising tricyclic lactone **259**. The transformation of tricyclic lactone **259** to the anthracimycin core **8** was accomplished in four steps: methylation, vinyl triflation/reduction and decarboxylation. However, several steps also suffered from a lack of consistency upon scale-up, and the instability of the tricyclic lactone series was problematic. These considerations led us to explore alternative routes. However, both palladium-catalysed intramolecular addition and radical-promoted cyclisation failed to provide the desired cyclised product.



Scheme 106: The formation of the anthracimycin core **8**

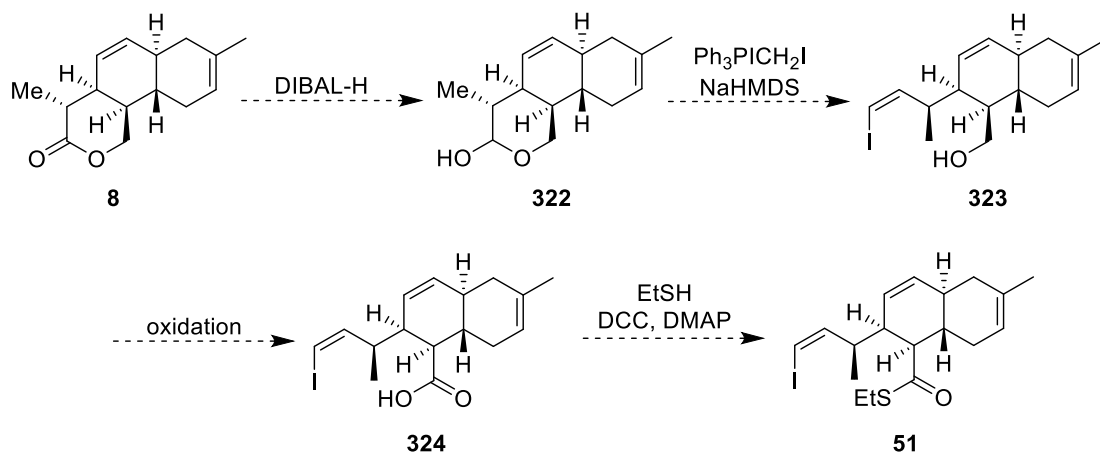
4. Future Work

Since the anthracimycin core **8** would be used to achieve the total synthesis, this would be worth converting the minor diastereomer **287** to the requisite lactone **8** in order to gain more precious material for the next steps. However, it is unclear whether the anthracimycin core **8** will be the kinetic or thermodynamic product. Therefore, employing two possible kinetic and thermodynamic conditions for epimerisation of **287** to **8** would be investigated (**Scheme 107**).



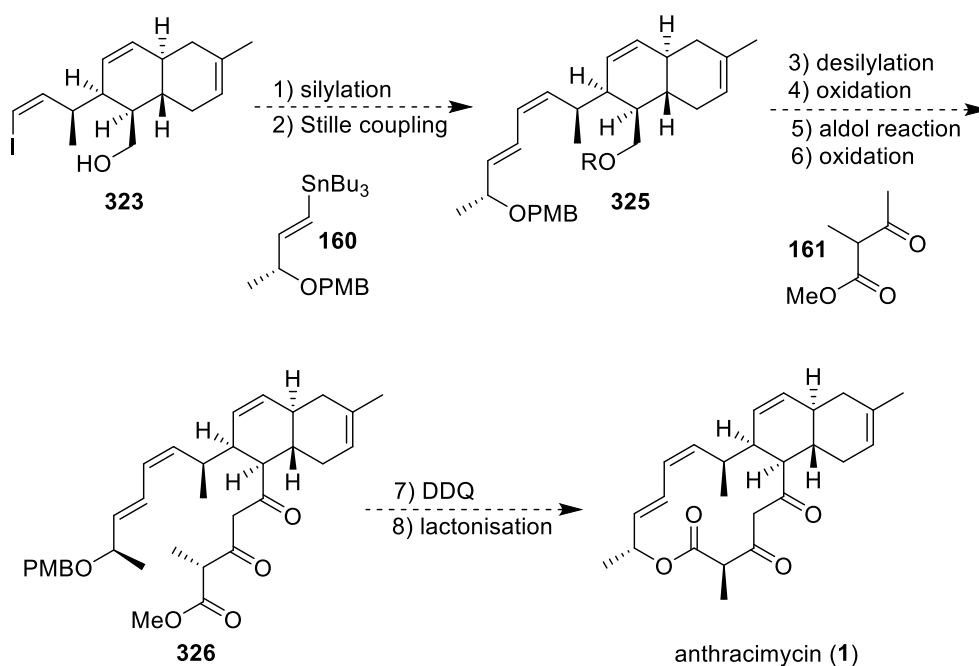
Scheme 107: The proposed kinetic and thermodynamic epimerisation conditions for **287**

Once sufficient tricyclic lactone **8** is in hand, we envision intercepting the precedentated Brimble's intermediate **51**²⁶ in four steps. Due to lack of time, this would be a promising plan to publish the formal synthesis of anthracimycin core with different key strategies. In the proposed synthetic direction, we anticipate reducing lactone **8** to lactol **322**, which would then be coupled with iodophosphonium salt²⁶ through a Wittig olefination providing the (*Z*)-vinyl iodide moiety.^{117,118} During the alkene formation, the lactol ring would be opened to deliver alcohol **323**. Then, the resultant primary alcohol **323** could be oxidised to carboxylic acid **324**. Finally, Brimble's thioester **51** could be derived from **324** and thiol via thioester formation (**Scheme 108**).



Scheme 108: The proposed synthetic route to intercept Brimble's intermediate **51**

However, the completion of anthracimycin (**1**) is still our main purpose. It is possible that we could intercept Brimble's thioester **51**, so alcohol **323** would be in hand. To address the target molecule **1**, alcohol **323** would be protected with the silyl group and subjected to Stille coupling to generate the conjugated diene **325**. To introduce the diketo group, desilylation would be employed to give the alcohol intermediate. Subsequently, oxidation of the resultant alcohol would provide the aldehyde motif, followed by the aldol condensation with **161** affording the core structure **326**. For the end-game, the PMB group would be removed by DDQ. Finally, macrocyclisation would allow us to achieve **1** as shown in **Scheme 109**.



Scheme 109: The proposed synthetic route to achieve anthracimycin (**1**)

5. Experimental

5.1 General information

Unless otherwise stated, all reactions were performed in oven- or flamed-dried glassware. Tetrahydrofuran, dichloromethane, toluene, diethyl ether and dimethylformamide were all purified using Innovative Technology Solvent Purification System. Diisopropylamine, diisopropyl ethylamine, trimethylsilyl chloride and triethylsilyl chloride were distilled from calcium hydride. All other solvents and reagents were obtained from commercial sources and used without further purification. Column chromatography was performed on Silica gel 60 (220–240 mesh) supplied by Fluorochem or Merck using forced flow (flash column) with the solvent systems indicated. Thin-layer chromatography (TLC) was performed on Merck Silica gel 60 F₂₅₄. The plates were developed using ultraviolet light, acidic aqueous ceric ammonium molybdate and basic aqueous potassium permanganate. ¹H, ¹³C and 2D NMR spectroscopic data were recorded on a Jeol ECX-400 and a Jeol ECS-400 at ambient temperature. ¹H and ¹³C NMR spectra are reported in parts per million (ppm) on the δ scale and referenced as follows: CDCl₃ 7.26 ppm, C₆D₆ 7.16 ppm for ¹H NMR; CDCl₃ 77.16 ppm, the central line of triplet and C₆D₆ 128.06 ppm, the central line of triplet for ¹³C NMR. The data are presented as follows: chemical shift, multiplicity (s = singlet, d = doublet, t = triplet, q = quartet, quint = quintet, m = multiplet, br = broad), coupling constant (s) in hertz (Hz), and integration. Infrared (IR) spectra were recorded on a PerkinElmer UATR Two FT-IR spectrometer. Mass spectrometry was performed by the University of York mass spectrometry service using electron spray ionisation (ESI) and atmospheric pressure chemical ionisation (APCI) techniques. The optical rotations were carried out using an ADP450 polarimeter. Melting points were measured using a Stuart SMP3 apparatus. Enantiopurity was determined using HPLC on an Agilent series 1100 equipped with a diode array UV detector using a CHIRALPAK® IC column (15 cm). All numbering on the structures below is for the benefit of characterisation and does not necessarily conform to IUPAC rules.

5.2 General procedure for IBX oxidation of TMS-enol ether

To a solution of crude TMS-enol ether (1.0 equiv) in DMSO (0.07 M) was added IBX (5.0 equiv). The reaction mixture was stirred at 40 °C under N₂ atmosphere overnight before being cooled to room temperature. The reaction mixture was quenched with a saturated aqueous solution of NaHCO₃ and diluted with hexane. The organic layer was separated, and the aqueous layer was extracted with hexane (x3). The combined organic layers were washed with brine, dried over anhydrous Na₂SO₄ and concentrated *in vacuo*.

5.3 General procedure for Diels–Alder cycloaddition

To a solution of enone (1.0 equiv) in CH₂Cl₂ (0.4 M) was added a 1.0 M solution of EtAlCl₂ in hexane (0.2 equiv) and the mixture was stirred under N₂ atmosphere at room temperature for 10 minutes. After this time, a solution of sulfur-substituted diene (10.0 equiv) in CH₂Cl₂ (4.0 M) was added to the mixture and the reaction mixture was stirred at room temperature for a further 1 hour. The reaction mixture was then quenched with Rochelle's salt 10% aqueous solution and stirred vigorously overnight. The organic layer was separated, and the aqueous layer was extracted with CH₂Cl₂ (x3). The combined organic layers were washed with brine, dried over anhydrous Na₂SO₄ and concentrated *in vacuo*.

5.4 General procedure for epimerisation

To a solution of *cis*-decalin (1.0 equiv) in CH₂Cl₂ (0.2 M) was added a 1.0 M solution of EtAlCl₂ in hexane (0.25 equiv) and the reaction mixture was stirred under N₂ atmosphere at room temperature for 3 days. The reaction mixture was then quenched with Rochelle's salt 10% aqueous solution and stirred vigorously overnight. The organic layer was separated, and the aqueous layer was extracted with CH₂Cl₂ (x3). The combined organic layers were washed with brine, dried over anhydrous Na₂SO₄ and concentrated *in vacuo*.

5.5 General procedure for selective hydrogenation

To a solution of *trans*-decalin (1.0 equiv) in acetone (0.01 M) was added an excess of unwashed Raney Nickel (50% in H₂O, 30.0 equiv) and the reaction mixture was stirred under H₂ atmosphere at room temperature for 1 hour. After this time, the reaction was filtered

through Celite and washed with CH₂Cl₂. The filtrate was dried over anhydrous Na₂SO₄ and concentrated *in vacuo*.

5.6 General procedure for TES-enol ether formation

To a solution of freshly distilled diisopropylamine (1.2 equiv) in THF (1.0 M) at –78 °C was added *n*-BuLi (1.2 equiv) dropwise. The solution was stirred under N₂ atmosphere at –78 °C for 45 minutes before a solution of ketone (1.0 equiv) in THF (0.26 M) was added. The mixture was stirred at –78 °C for 1 hour and then added freshly distilled triethylsilyl chloride (1.3 equiv). The reaction mixture was stirred at –78 °C for a further 30 minutes before being warmed to room temperature for 30 minutes. The mixture was then quenched with H₂O and diluted with Et₂O. The organic layer was separated, and the aqueous layer was extracted with Et₂O (x3). The organic layers were washed with brine, dried over anhydrous Na₂SO₄ and concentrated *in vacuo*.

5.7 General procedure for IBX oxidation of TES-enol ether

To a solution of TES-enol ether (1.0 equiv) in DMSO (0.1 M) was added IBX (2.5 equiv). The reaction mixture was stirred under N₂ atmosphere at 60 °C for 3 days before being cooled to room temperature. The mixture was quenched with a saturated aqueous solution of NaHCO₃ and diluted with Et₂O. The organic layer was separated, and the aqueous layer was extracted with Et₂O (x3). The combined organic layers were washed with brine, dried over anhydrous Na₂SO₄ and concentrated *in vacuo*.

5.8 General procedure for TIPS deprotection

To a solution of enone (1.0 equiv) in THF (0.1 M) was added a 1.0 M solution of TBAF in THF (2.0 equiv). The reaction mixture was stirred under N₂ atmosphere at room temperature for 2 hours. The mixture was then quenched with H₂O and diluted with EtOAc. The organic layer was separated, and the aqueous layer was extracted with EtOAc (x3). The combined organic layers were washed with brine, dried over anhydrous Na₂SO₄ and concentrated *in vacuo*.

5.9 General procedure for hydrazone formation

To a solution of ketone (1.0 equiv) in dry MeOH (0.02 M) was added 3Å MS, 2,4-dinitrophenyl hydrazine (3.0 equiv), followed by glacial acetic acid (0.04 M). The reaction mixture was stirred under N₂ atmosphere at 50 °C for 3.5 hours before being cooled to room temperature. The mixture was quenched with a saturated aqueous solution of NaHCO₃ and diluted with CH₂Cl₂. The organic layer was separated, and the aqueous layer was extracted with CH₂Cl₂ (x3). The combined organic layers were washed with brine, dried over anhydrous Na₂SO₄ and concentrated *in vacuo*.

5.10 General procedure for propionate formation

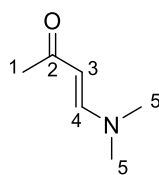
To a solution of alcohol (1.0 equiv) in pyridine (0.14 M) was added DMAP (0.2 equiv), followed by propionyl chloride (10.0 equiv). The reaction mixture was stirred under N₂ atmosphere at room temperature overnight. The mixture was then diluted with EtOAc, and the organic layer was washed with a saturated aqueous solution of CuSO₄ (x3). The organic layer was washed with brine, dried over anhydrous Na₂SO₄ and concentrated *in vacuo*.

5.11 General procedure for malonate formation

To a solution of alcohol (1.0 equiv) and Et₃N (2.0 equiv) in CH₂Cl₂ (0.2 M) at 0 °C was slowly added ethyl malonyl chloride (1.5 equiv). The reaction mixture was stirred under N₂ atmosphere at 0 °C to room temperature for 2 hours. The mixture was then diluted with CH₂Cl₂ and washed with a saturated aqueous solution of NaHCO₃ (x3) and brine. The organic layer was dried over anhydrous Na₂SO₄ and concentrated *in vacuo*.

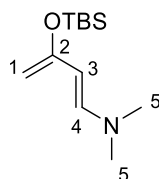
5.12 Methods and characterisation of compounds

4-(Dimethylamino)-3-butene-2-one (190)



To a 2.0 M solution of dimethylamine in THF (14.7 mL, 29.4 mmol, 1.2 equiv) at 0 °C was added a solution of *trans*-4-methoxy-3-butene-2-one (2.5 mL, 24.5 mmol) in THF (5 mL) over a period of 15 minutes. The resulting light orange solution was stirred under N₂ atmosphere at 0 °C and allowed to reach room temperature for 2.5 hours. The reaction mixture was concentrated *in vacuo* and purified by kugelrohr distillation (130–132 °C at 8 mbar) to afford vinylogous amine **190** as a light yellow oil (2.65 g, 95% yield): *R_f* = 0.38 in (20% MeOH/EtOAc); IR (ATR) ν_{\max} 3409, 2921, 1558 (C=O), 1420, 1356, 1260, 1112, 966, 596 cm⁻¹; ¹H NMR (400 MHz, CDCl₃) δ 7.40 (1H, d, *J* = 12.7 Hz, H-4), 4.98 (1H, d, *J* = 12.7 Hz, H-3), 2.98 (3H, brs, H-5) 2.75 (3H, brs, H-5) 2.03 (3H, s, H-1) ppm; ¹³C NMR (100 MHz, CDCl₃) δ 195.3 (C-2), 152.7 (C-4), 96.6 (C-3), 44.7 (C-5), 37.0 (C-5), 28.0 (C-1) ppm; HRMS (ESI) *m/z* calcd for C₆H₁₁NNaO (M+Na⁺) 136.0733, found 136.0728. The characterisation data matched the literature.⁶⁸

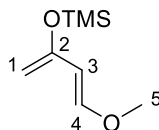
1-(Dimethylamino)-3-(*tert*-butyldimethyl)-1,3-butadiene (191)



To a solution of KHMDS (12 mL of 11% in toluene, 5.32 mmol, 3.0 equiv) in THF (5 mL) at -78 °C was added a solution of 4-dimethylamino-3-butene-2-one (200 mg, 1.77 mmol) in THF (1.7 mL) over a period of 15 minutes. The mixture was warmed to -30 °C and stirred under N₂ atmosphere at the same temperature for 2 hours. Then, the stirred mixture was cooled to -78 °C and treated with a solution of TBSCl (359 mg, 2.30 mmol, 1.3 equiv) dissolved in THF (1.7 mL). The reaction mixture was allowed to reach room temperature for 17 hours. The mixture was then diluted with Et₂O (30 mL), filtered through Celite and

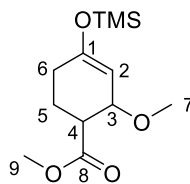
washed with Et₂O (3 x 10 mL). The filtrate was concentrated *in vacuo* to give diene **191** as a yellow oil, which was directly used for the next step without purification (686 mg, >99% conversion): *R_f* = 0.64 in (10% EtOAc/hexane); ¹H NMR (400 MHz, CDCl₃) δ 6.57 (1H, d, *J* = 13.1 Hz, H-4), 4.79 (1H, d, *J* = 13.1 Hz, H-3), 3.92 (1H, s, H-1) 3.83 (1H, s, H-1) 2.70 (6H, s, H-5), 0.97 (9H, s, (OSi(CH₃)₂C(CH₃)₃), 0.19 (6H, s, (OSi(CH₃)₂C(CH₃)₃) ppm; ¹³C NMR (100 MHz, CDCl₃) δ 156.6 (C-2), 141.1 (C-4), 96.1 (C-3), 86.0 (C-1), 40.7 (C-5), 26.0 (OSi(CH₃)₂C(CH₃)₃), 18.5 (OSi(CH₃)₂C(CH₃)₃), -4.4 (OSi(CH₃)₂C(CH₃)₃) ppm; HRMS (ESI) *m/z* calcd for C₁₂H₂₅NNaOSi (M+Na⁺) 250.1603, found 250.1598. The characterisation data matched the literature.⁶⁸

Methoxy-3-trimethylsilyloxy-1,3-butadiene (**194**)



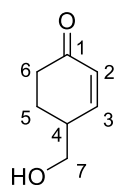
A solution of ZnCl₂ (0.17 g, 1.2 mmol, 3.0 mol%) in Et₃N (12.2 mL, 89.5 mmol, 2.2 equiv) was stirred at room temperature for 1 hour. To this solution was added a solution of *trans*-4-methoxy-3-butene-2-one (4.0 mL, 40.7 mmol) in benzene (20 mL), followed by TMSCl (10.3 mL, 81.4 mmol, 2.0 equiv) over a period of 30 minutes. The reaction mixture was stirred under N₂ atmosphere at 40 °C for 19 hours before being cooled to room temperature and diluted with Et₂O (150 mL). The mixture was filtered through Celite and washed with Et₂O. The filtrate was concentrated *in vacuo* and purified by kugelrohr distillation (40–42 °C at 2 mbar) to give diene **194** as a colourless oil (4.56 g, 65% yield): *R_f* = 0.60 in (10% EtOAc/hexane); ¹H NMR (400 MHz, CDCl₃) δ 6.83 (1H, d, *J* = 12.6 Hz, H-4), 5.35 (1H, d, *J* = 12.6 Hz, H-3), 4.11 (1H, s, H-1) 4.06 (1H, s, H-1) 3.58 (3H, s, H-5), 0.23 (9H, s, OSi(CH₃)₃) ppm. This compound was characterised only by ¹H NMR due to its volatility and instability and the data matched the literature.⁷⁰

Methyl 2-methoxy-4-(trimethylsilyloxy)cyclohex-3-enecarboxylate (**195**)



To a solution of diene **194** (0.43 g, 2.5 mmol) in toluene (1.7 mL) was added methyl acrylate (0.40 mL, 4.4 mmol, 1.7 equiv). The reaction mixture was stirred under N₂ atmosphere at 80 °C for 45 hours. The reaction mixture was then cooled to room temperature and concentrated *in vacuo* to yield a mixture of two diastereomers of cyclohexene **195** as a yellow oil, which was directly used for the next step without purification (569 mg, >99% conversion, 88% crude yield): *R_f* = 0.45 in (30% EtOAc/hexane); ¹H NMR (400 MHz, CDCl₃) δ 5.14 (1H, d, *J* = 5.7 Hz, H-2), 4.99–4.97 (1H, m, H-2), 4.27–4.23 (1H, m, H-3), 4.11 (1H, dd, *J* = 4.8, 4.8 Hz, H-3), 3.71 (3H, s, H-9), 3.70 (3H, s, H-9), 3.32 (3H, s, H-7), 3.29 (3H, s, H-7), 2.62–2.57 (1H, m, H-4), 2.54–2.49 (1H, m, H-4), 2.11–1.85 (8H, m, H-6 + H-5), 0.21 (9H, s, OSi(CH₃)₃) 0.20 (9H, s, OSi(CH₃)₃) ppm. This compound was characterised only by ¹H NMR due to its volatility and instability and the data matched the literature.⁷¹

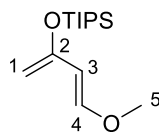
4-(Hydroxymethyl)cyclohex-2-en-1-one (*rac*-**193**)



Method A: To a suspension of LiAlH₄ (54 mg, 1.4 mmol, 1.4 equiv) in Et₂O (5.5 mL) at –78 °C was added a solution of crude cyclohexene **195** (0.26 g, 1.0 mmol) in Et₂O (4.0 mL). The reaction mixture was stirred under N₂ atmosphere at –78 °C for 4 hours and then allowed to reach 0 °C. The reaction mixture was quenched with H₂O (0.05 mL), 15% NaOH (0.05 mL) followed by H₂O (0.15 mL) and allowed to reach room temperature. The mixture was added Na₂SO₄ and stirred at room temperature for 15 minutes before being filtered. The filtrate was concentrated *in vacuo*. The crude residue was purified by silica gel flash column chromatography (50% EtOAc/hexane) to afford racemic alcohol **193** as a yellow oil (56 mg, 44% yield).

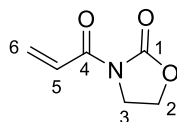
Method B: Racemic alcohol **193** was prepared from racemic silyl ether **3** (0.31 g, 1.1 mmol) using the general procedure for TIPS deprotection (see page 141). The crude residue was purified by silica gel flash column chromatography (40–60% EtOAc/hexane) to give racemic alcohol **193** as a yellow oil (106 mg, 77% yield): $R_f = 0.17$ in (60% EtOAc/hexane); IR (ATR) ν_{\max} 3406 (O-H), 2927, 2871, 1662 (C=O), 1393, 1256, 1083, 1048, 845 cm^{-1} ; $^1\text{H NMR}$ (400 MHz, CDCl_3) δ 6.97 (1H, ddd, $J = 10.2, 2.4, 1.2$ Hz, H-3), 6.06 (1H, dd, $J = 10.2, 2.6$ Hz, H-2), 3.73 (1H, dd, $J = 10.4, 6.4$ Hz, H-7), 3.67 (1H, dd, $J = 10.4, 6.6$ Hz, H-7), 2.64 (1H, dddddd, $J = 9.8, 6.6, 6.4, 4.8, 2.6, 2.4$ Hz, H-4), 2.55 (1H, ddd, $J = 16.8, 4.8, 4.8$ Hz, H-6), 2.40 (1H, ddd, $J = 16.8, 12.6, 4.8$ Hz, H-6), 2.13 (1H, dddddd, $J = 13.4, 4.8, 4.8, 4.8, 1.2$ Hz, H-5), 1.81 (1H, dddd, $J = 13.4, 12.6, 9.8, 4.8$ Hz, H-5) ppm; $^{13}\text{C NMR}$ (100 MHz, CDCl_3) δ 199.9 (C-1), 151.5 (C-3), 130.5 (C-2), 65.3 (C-7), 39.1 (C-4), 36.8 (C-6), 25.5 (C-5) ppm; HRMS (ESI) m/z calcd for $\text{C}_7\text{H}_{10}\text{NaO}_2$ ($\text{M}+\text{Na}^+$) 149.0573, found 149.0572.

Methoxy-3-triisopropylsiloxy-1,3-butadiene (**202**)



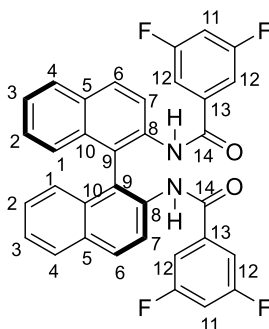
To a solution of *trans*-4-methoxy-3-butene-2-one (1.0 mL, 9.8 mmol) and Et_3N (3.7 mL, 26 mmol, 2.7 equiv) in Et_2O (16 mL) at 0 °C was added TIPSOTf (2.9 mL, 11 mmol, 1.1 equiv) dropwise. The reaction mixture was stirred under N_2 atmosphere and allowed to reach room temperature for 18 hours. The mixture was quenched with a saturated aqueous solution of NaHCO_3 (20 mL). The organic layer was separated, and the aqueous layer was extracted with Et_2O (3 x 20 mL). The combined organic layers were washed with brine, dried over anhydrous Na_2SO_4 and concentrated *in vacuo* to give the title diene **202** as a light yellow oil (2.86 g, quantitative crude yield) which was used directly in the next reaction without further purification: $R_f = 0.68$ in (10% EtOAc/hexane); IR (ATR) ν_{\max} 2945, 2868, 1652, 1464, 1319, 1210, 1024, 883, 681 cm^{-1} ; $^1\text{H NMR}$ (400 MHz, CDCl_3) δ 6.96 (1H, d, $J = 12.4$ Hz, H-4), 5.34 (1H, d, $J = 12.4$ Hz, H-3), 4.05 (2H, s, H-1), 3.59 (3H, s, H-5), 1.23 (3H, hept, $J = 7.1$ Hz, ($\text{OSi}(\underline{\text{C}}\text{H}(\text{CH}_3)_2)_3$), 1.11 (18H, d, $J = 7.1$ Hz, ($\text{OSi}(\text{CH}(\underline{\text{C}}\text{H}_3)_2)_3$)) ppm; $^{13}\text{C NMR}$ (100 MHz, CDCl_3) δ 154.5 (C-2), 150.3 (C-4), 103.4 (C-3), 90.2 (C-1), 56.5 (C-5), 18.2 ($\text{OSi}(\text{CH}(\underline{\text{C}}\text{H}_3)_2)_3$), 13.0 ($\text{OSi}(\underline{\text{C}}\text{H}(\text{CH}_3)_2)_3$) ppm; HRMS (ESI) m/z calcd for $\text{C}_{14}\text{H}_{29}\text{O}_2\text{Si}$ ($\text{M}+\text{H}^+$) 257.1931, found 257.1935. The characterisation data matched the literature.⁷⁵

3-Acryloyloxazolidin-2-one (201)



To a solution of 2-oxazolidinone (255 mg, 2.93 mmol), DMAP (47 mg, 0.39, 0.13 equiv) and acrylic acid (0.26 mL, 3.8 mmol, 1.3 equiv) in CH₂Cl₂ (4 mL) at 0 °C was added DCC (791 mg, 3.8 mmol, 1.3 equiv) in one portion. After 10 minutes, the reaction mixture was stirred under N₂ atmosphere and allowed to reach room temperature for 18 hours. The mixture was diluted with CH₂Cl₂ (4 mL), filtered through Celite and washed with CH₂Cl₂ (3 x 10 mL). The combined organic layers were washed with a saturated aqueous solution of NaHCO₃ (20 mL) and brine (20 mL), dried over anhydrous Na₂SO₄ and concentrated *in vacuo*. The crude residue was purified by silica gel flash column chromatography (20% EtOAc/hexane) to afford amide **201** as a white solid (130 mg, 32% yield): **Melting point** = 80–82 °C; **R_f** = 0.10 in (20% EtOAc/hexane); **IR** (ATR) ν_{max} 2930, 1781 (C=O), 1677 (C=O), 1613, 1391, 1363, 1227, 1122, 1022, 752, 694 cm⁻¹; **¹H NMR** (400 MHz, CDCl₃) δ 7.50 (1H, dd, *J* = 16.5, 9.6 Hz, H-5), 6.55 (1H, d, *J* = 16.5 Hz, H-6), 5.91 (1H, d, *J* = 9.6 Hz, H-6) 4.44 (2H, t, *J* = 8.0 Hz, H-2) 4.09 (2H, t, *J* = 8.0 Hz, H-3) ppm; **¹³C NMR** (100 MHz, CDCl₃) δ 166.2 (C-4), 153.5 (C-1), 132.0 (C-5), 127.1 (C-6), 62.3 (C-2), 42.7 (C-3) ppm; **HRMS** (ESI) *m/z* calcd for C₆H₇NNaO₃ (M+Na⁺) 164.0318, found 164.0313. The characterisation data matched the literature.⁷⁷

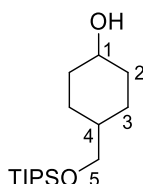
(*S*)-*N,N'*-([1,1'-Binaphthalene]-2,2'-diyl)bis(3,5-difluorobenzamide) (203)



To a solution of (*S*)-1,1'-binaphthyl-2,2'-diamine (99 mg, 0.35 mmol) in CH₂Cl₂ (3.5 mL) at 0 °C was added an aqueous solution of 10% NaOH (2.2 mL), followed by 3,5-difluorobenzoyl chloride (0.13 mL, 1.04 mmol). The reaction mixture was stirred at 0 °C for 40 minutes before being allowed to reach room temperature. The organic layer was separated, and

the aqueous layer was extracted with CH₂Cl₂ (3 x 10 mL). The combined organic layers were washed with brine, dried over anhydrous Na₂SO₄ and concentrated *in vacuo*. The crude residue was purified by silica gel flash column chromatography (20% EtOAc/hexane) to afford BINAMIDE **203** as a white solid (191 mg, 97% yield); **Melting point** = 114–116 °C; **R_f** = 0.23 in (20% EtOAc/hexane); **IR** (ATR) ν_{\max} 1654, 1593 (C=O), 1500, 1321, 1123, 989, 728 cm⁻¹; **¹H NMR** (400 MHz, CDCl₃) δ 8.48 (2H, d, *J* = 8.9 Hz, H-1), 8.14 (2H, d, *J* = 8.9 Hz, H-4), 8.03 (2H, d, *J* = 8.2 Hz, H-6) 7.67 (2H, brs, N-H) 7.54 (2H, ddd, *J* = 8.0, 7.3, 1.2 Hz, H-2), 7.40 (2H, ddd, *J* = 8.0, 7.3, 1.2 Hz, H-3), 7.29 (2H, d, *J* = 8.2 Hz, H-7), 6.84–6.79 (2H, m, H-11), 6.70–6.68 (4H, m, H-12) ppm; **HRMS** (ESI) *m/z* calcd for C₃₄H₂₀F₄N₂NaO₂ (M+Na⁺) 587.1353, found 587.1347. The characterisation data matched the literature.⁷⁴

4-(((Triisopropylsilyl)oxy)methyl)cyclohexan-1-ol (**165**)

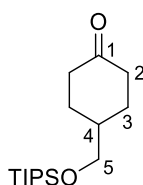


To a suspension of LiAlH₄ (3.60 g, 94.8 mmol, 2.0 equiv) in THF (150 mL) at 0 °C was slowly added ethyl 4-oxocyclohexanecarboxylate (7.5 mL, 47.4 mmol). The reaction mixture was stirred under N₂ atmosphere at 0 °C and allowed to reach room temperature for 18 hours. The reaction mixture was then cooled back to 0 °C and quenched with H₂O (3.6 mL), 15% NaOH (3.6 mL), followed by H₂O (10.8 mL). The mixture was stirred for a further 15 minutes and allowed to reach room temperature. Anhydrous MgSO₄ was added, and the mixture was filtered through Celite, which was washed with Et₂O. The combined organic layers were concentrated *in vacuo* to give diol as a white sticky residue (6.17 g) which was directly used for the next step without further purification.

To a solution of the above crude diol (6.17 g, 47.4 mmol) in CH₂Cl₂ (190 mL) was added imidazole (4.84 g, 71.1 mmol, 1.5 equiv), DMAP (590 mg, 4.74 mmol, 0.1 equiv), followed by triisopropylsilyl chloride (11.2 mL, 52.1 mmol, 1.1 equiv). The reaction mixture was stirred under N₂ atmosphere at room temperature for 16 hours. After this time, an aqueous solution of 2 M HCl (75 mL) was added, and the organic layer was separated. The aqueous layer was extracted with CH₂Cl₂ (3 x 50 mL). The combined organic layers were washed with

H₂O (50 mL) and brine (50 mL), dried over anhydrous Na₂SO₄ and concentrated *in vacuo*. The crude product was purified by silica gel flash column chromatography (10–30% EtOAc/hexane) to yield a 1:2 mixture of alcohol **165** as a colourless oil (11.8 g, 87% over two steps). **Alcohol minor isomer 165**: *R_f* = 0.36 in (20% EtOAc/hexane); **IR** (ATR) ν_{\max} 3350 (O-H), 2925, 2865, 1463, 1197, 1064, 882, 783, 680 cm⁻¹; **¹H NMR** (400 MHz, CDCl₃) δ 4.01–3.98 (1H, m, H-1), 3.50 (2H, dd, *J* = 18.2, 6.1 Hz, H-5), 1.75–1.69 (2H, m, H-2 + H-3), 1.60–1.51 (5H, m, H-2 + H-3 + H-4) 1.45–1.37 (2H, m, H-2 + H-3), 1.11–0.97 (21H, m, OSi(CH(CH₃)₂)₃) ppm; **¹³C NMR** (100 MHz, CDCl₃) δ 68.1 (C-1), 67.2 (C-5), 39.5 (C-4), 32.2 (C-2), 23.6 (C-3), 18.2 (OSi(CH(CH₃)₂)₃), 12.1 (OSi(CH(CH₃)₂)₃) ppm; **HRMS** (ESI) *m/z* calcd for C₁₆H₃₄NaO₂Si (M+Na⁺) 309.2220, found 309.2211. **Alcohol major isomer 165**: *R_f* = 0.25 in (20% EtOAc/hexane); **IR** (ATR) ν_{\max} 3339 (O-H), 2928, 2865, 1463, 1115, 1067, 882, 802, 681 cm⁻¹; **¹H NMR** (400 MHz, CDCl₃) δ 3.55 (1H, dd, *J* = 10.8, 10.8, 4.2, 4.2 Hz, H-1), 3.46 (2H, dd, *J* = 18.9, 6.2 Hz, H-5), 2.02–1.96 (2H, m, H-2), 1.85–1.79 (2H, m, H-2) 1.51–1.37 (2H, m, H-3 + H-4), 1.30–1.19 (3H, m, H-3), 1.12–0.95 (21H, m, OSi(CH(CH₃)₂)₃) ppm; **¹³C NMR** (100 MHz, CDCl₃) δ 71.4 (C-1), 68.5 (C-5), 39.9 (C-4), 35.3 (C-2), 27.9 (C-3), 18.2 (OSi(CH(CH₃)₂)₃), 12.1 (OSi(CH(CH₃)₂)₃) ppm; **HRMS** (ESI) *m/z* calcd for C₁₆H₃₄NaO₂Si (M+Na⁺) 309.2220, found 309.2214.

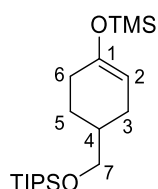
4-(((Triisopropylsilyloxy)methyl)cyclohexan-1-one (**2**)



To a solution of oxalyl chloride (2.73 mL, 32.2 mmol, 1.20 equiv) in CH₂Cl₂ (250 mL) at –78 °C was added DMSO (2.38 mL, 33.6 mmol, 1.25 equiv) dropwise. The mixture was stirred under N₂ atmosphere at –78 °C for 1 hour before being added a solution of alcohol **165** (7.69 g, 26.8 mmol) in CH₂Cl₂ (30 mL). The reaction mixture was stirred at –78 °C for 1 hour before being added Et₃N (18.7 mL, 134 mmol, 5.0 equiv). The mixture was allowed to reach room temperature for 1.5 hours. After this time, the mixture was quenched with H₂O (16 mL) and 2 M HCl (78 mL). The organic layer was separated, and the aqueous layer was extracted with CH₂Cl₂ (3 x 60 mL). The combined organic layers were washed with 2M HCl (50 mL) and brine (50 mL), dried over anhydrous Na₂SO₄ and concentrated *in vacuo*. The

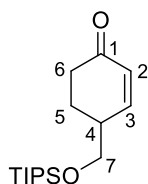
crude residue was purified by silica gel flash column chromatography (5–10% EtOAc/hexane) to afford cyclohexanone **2** as a colourless oil (7.49 g, 98% yield): $R_f = 0.27$ in (10% EtOAc/hexane); IR (ATR) ν_{\max} 2943, 2866, 1717 (C=O), 1463, 1121, 1104, 1067, 882, 682 cm^{-1} ; $^1\text{H NMR}$ (400 MHz, CDCl_3) δ 3.60 (2H, d, $J = 6.2$ Hz, H-5), 2.41 (2H, ddd, $J = 14.3, 4.8, 3.1$ Hz, H-2), 2.34 (2H, ddd, $J = 14.3, 12.6, 6.2$ Hz, H-2), 2.11 (2H, dddd, $J = 13.2, 6.2, 6.2, 3.1$ Hz, H-3), 1.95 (1H, ttttd, $J = 12.6, 6.2, 6.2, 3.6$ Hz, H-4), 1.46 (2H, dddd, $J = 13.2, 12.6, 12.6, 4.8$ Hz, H-3), 1.14–1.03 (21H, m, $\text{OSi}(\text{CH}(\text{CH}_3)_2)_3$) ppm; $^{13}\text{C NMR}$ (100 MHz, CDCl_3) δ 212.6 (C-1), 67.4 (C-5), 40.7 (C-2), 39.2 (C-4), 29.4 (C-3), 18.2 ($\text{OSi}(\text{CH}(\text{CH}_3)_2)_3$), 12.1 ($\text{OSi}(\text{CH}(\text{CH}_3)_2)_3$) ppm; HRMS (ESI) m/z calcd for $\text{C}_{16}\text{H}_{32}\text{NaO}_2\text{Si}$ ($\text{M}+\text{Na}^+$) 307.2064, found 307.2063.

Triisopropyl((4-((trimethylsilyl)oxy)cyclohex-3-en-1-yl)methoxy)silane (*rac*-179)



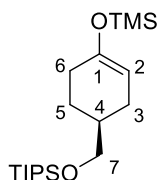
To a solution of freshly distilled diisopropylamine (0.36 mL, 2.5 mmol, 1.2 equiv) in THF (3 mL) at -78 °C, was added *n*-BuLi (1.4 mL of a 1.89 M solution in hexane, 2.5 mmol, 1.2 equiv) dropwise. After stirring for 45 minutes, to this solution was added a solution of cyclohexanone **2** (0.60 g, 2.1 mmol) in THF (9 mL) and stirred for a further 1 hour. Freshly distilled trimethylsilyl chloride (0.35 mL, 2.7 mmol, 1.3 equiv) was added at -78 °C. The reaction mixture was stirred at -78 °C for 15 minutes and allowed to reach room temperature. The reaction mixture was quenched with a saturated aqueous solution of NaHCO_3 (10 mL) and diluted with Et_2O (10 mL). The organic layer was separated, and the aqueous layer was extracted with Et_2O (3 x 20 mL). The combined organic layers were washed with brine, dried over anhydrous Na_2SO_4 and concentrated *in vacuo* to give racemic TMS-enol ether **179** as a light yellow oil, which was directly used for the next step without purification (749 mg, >99% conversion).

4-(((Triisopropylsilyl)oxy)methyl)cyclohex-2-en-1-one (*rac*-**3**)



Racemic enone **3** was prepared from crude racemic TMS-enol ether **179** (0.75 g, 2.1 mmol) using the general procedure for IBX oxidation of TMS-enol ether (see page 140). The crude residue was purified by silica gel flash column chromatography (5–10% EtOAc/hexane) to yield racemic cyclohexenone **3** as a light yellow oil (515 mg, 87% yield over two steps): R_f = 0.22 in (10% EtOAc/hexane); IR (ATR) ν_{\max} 2943, 2892, 2866, 1683 (C=O), 1463, 1113, 1069, 882, 788, 682 cm^{-1} ; $^1\text{H NMR}$ (400 MHz, CDCl_3) δ 6.99 (1H, ddd, J = 10.2, 2.8, 1.4 Hz, H-3), 6.05 (1H, dd, J = 10.2, 2.4 Hz, H-2), 3.75 (1H, dd, J = 9.6, 6.4 Hz, H-7), 3.68 (1H, dd, J = 9.6, 6.9 Hz, H-7), 2.62 (1H, dddddd, J = 9.9, 6.9, 6.4, 4.6, 2.8, 2.4 Hz, H-4), 2.54 (1H, ddd, J = 16.8, 4.6, 4.6 Hz, H-6), 2.38 (1H, ddd, J = 16.8, 12.6, 5.0 Hz, H-6), 2.10 (1H, dddddd, J = 13.1, 5.0, 4.6, 4.6, 1.4 Hz, H-5), 1.79 (1H, dddd, J = 13.1, 12.6, 9.9, 4.6 Hz, H-5), 1.11–1.01 (21H, m, $\text{OSi}(\text{CH}(\text{CH}_3)_2)_3$) ppm; $^{13}\text{C NMR}$ (100 MHz, CDCl_3) δ 200.1 (C-1), 152.3 (C-3), 130.1 (C-2), 66.0 (C-7), 39.6 (C-4), 36.9 (C-6), 25.6 (C-5), 18.1 ($\text{OSi}(\text{CH}(\text{CH}_3)_2)_3$), 12.0 ($\text{OSi}(\text{CH}(\text{CH}_3)_2)_3$) ppm; HRMS (ESI) m/z calcd for $\text{C}_{16}\text{H}_{30}\text{NaO}_2\text{Si}$ ($\text{M}+\text{Na}^+$) 305.1907, found 305.1904. The enantiomeric excess was determined by HPLC analysis using CHIRALCEL[®] IC column eluting with 1% *i*-PrOH/hexane (flow rate = 1.0 mL/min, temp = 40 °C, λ = 216 nm): retention time = 14.8, 15.6 min.

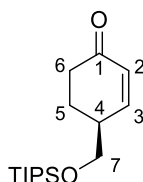
(*S*)-Triisopropyl((4-(((trimethylsilyl)oxy)cyclohex-3-en-1-yl)methoxy)silane (**179**)



To a solution of (+)-bis[*(R)*-1-phenylethyl]amine (3.2 mL, 14.0 mmol, 1.3 equiv) in THF (43 mL) at -78 °C, was slowly added *n*-BuLi (6.85 mL of a 1.89 M solution in hexane, 12.9 mmol, 1.2 equiv). The pink solution was stirred under N_2 atmosphere at -78 °C for 30 minutes. Freshly distilled trimethylsilyl chloride (6.85 mL, 53.9 mmol, 5.0 equiv) was added dropwise at -78 °C where upon it turned colourless. After an additional 10 minutes, a solution of

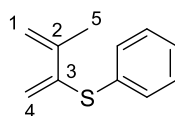
cyclohexanone **2** (3.06 g, 10.8 mmol) in THF (5 mL) was slowly added. The mixture was stirred for a further 1.5 hours before being treated with freshly distilled trimethylamine (13.7 mL, 108 mmol, 10.0 equiv) at $-78\text{ }^{\circ}\text{C}$, followed by a saturated aqueous solution of NaHCO_3 (14 mL) below $-20\text{ }^{\circ}\text{C}$. The mixture was allowed to reach room temperature. The organic layer was separated, and the aqueous layer was extracted with hexane (3 x 40 mL). The combined organic layers were washed with 3 N citric acid and 1 N citric acid (until all the amine byproduct was removed as determined by TLC and ninhydrin stain), and a saturated aqueous solution of NaHCO_3 and brine. The organic layer was dried over anhydrous Na_2SO_4 and concentrated *in vacuo* to give the crude product **179** as a pale oil, which was directly used for the next step without purification (3.85 g, >99% conversion).

(S)-4-(((Triisopropylsilyl)oxy)methyl)cyclohex-2-en-1-one (3)



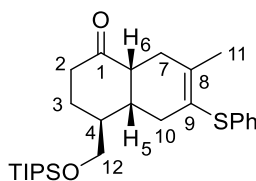
(S)-Enone **3** was prepared from crude (S)-silyl enol ether **179** (3.85 g, 10.8 mmol) using the general procedure for IBX oxidation of TMS-enol ether (see page 140). The crude residue was purified by silica gel flash column chromatography (2% EtOAc/hexane) to afford (S)-cyclohexenone **3** as a pale oil (2.93 g, 96% yield over two steps, 80% *ee*): $R_f = 0.19$ in (10% EtOAc/hexane); $[\alpha]_D^{20} = -78.9$ (*c* 1.00, CHCl_3); IR (ATR) ν_{max} 2942, 2891, 2865, 1682 (C=O), 1462, 1111, 1068, 881, 786, 681 cm^{-1} ; $^1\text{H NMR}$ (400 MHz, CDCl_3) δ 7.00 (1H, ddd, $J = 10.2, 2.6, 1.4$ Hz, H-3), 6.05 (1H, dd, $J = 10.2, 2.4$ Hz, H-2), 3.75 (1H, dd, $J = 9.6, 6.4$ Hz, H-7), 3.67 (1H, dd, $J = 9.6, 6.9$ Hz, H-7), 2.62 (1H, ddddd, $J = 9.9, 6.9, 6.4, 4.6, 2.6, 2.4$ Hz, H-4), 2.54 (1H, ddd, $J = 16.8, 4.6, 4.6$ Hz, H-6), 2.39 (1H, ddd, $J = 16.8, 12.8, 5.0$ Hz, H-6), 2.09 (1H, ddddd, $J = 13.2, 5.0, 4.6, 4.6, 1.4$ Hz, H-5), 1.79 (1H, dddd, $J = 13.2, 12.8, 9.9, 4.6$ Hz, H-5), 1.11–1.01 (21H, m, $\text{OSi}(\text{CH}(\text{CH}_3)_2)_3$) ppm; $^{13}\text{C NMR}$ (100 MHz, CDCl_3) δ 200.1 (C-1), 152.3 (C-3), 130.1 (C-2), 66.0 (C-7), 39.6 (C-4), 36.9 (C-6), 25.6 (C-5), 18.1 ($\text{OSi}(\text{CH}(\text{CH}_3)_2)_3$), 12.0 ($\text{OSi}(\text{CH}(\text{CH}_3)_2)_3$) ppm; HRMS (ESI) m/z calcd for $\text{C}_{16}\text{H}_{30}\text{NaO}_2\text{Si}$ ($\text{M}+\text{Na}^+$) 305.1907, found 305.1903. The enantiomeric excess was determined by HPLC analysis using CHIRALCEL[®] IC column eluting with 1% *i*-PrOH/hexane (flow rate = 1.0 mL/min, temp = $40\text{ }^{\circ}\text{C}$, $\lambda = 216\text{ nm}$): retention time = 15.0 min (major isomer), 16.0 min (minor isomer).

3-Methyl-2-phenylthio-1,3-butadiene (163)



In a pressure vessel were placed Pd(OAc)₂ (69 mg, 0.31 mmol, 0.02 equiv), THF (7.6 mL), 2-methyl-1-buten-3-yne (1.5 mL, 15.7 mmol) and finally thiophenol (1.6 mL, 15.7 mmol, 1.0 equiv). The reaction mixture was stirred at 50 °C for 16 hours. After this period, the mixture was filtered through Celite and washed with EtOAc (50 mL). The filtrate was concentrated *in vacuo*. The crude product was purified by silica gel flash column chromatography (100% hexane) to yield diene **163** as a light yellow oil (2.35 g, 85% yield): *R_f* = 0.26 (100% hexane); **IR** (ATR) ν_{\max} 3074, 3060, 2977, 1573, 1478, 1439, 1440, 1375, 1119, 1025 cm⁻¹; **¹H NMR** (400 MHz, CDCl₃) δ 7.31–7.16 (5H, m, Ar-H), 5.55 (1H, s, H-1), 5.52 (1H, s, H-4), 5.22 (1H, d, *J* = 1.2 Hz, H-1), 5.06 (1H, d, *J* = 1.2 Hz, H-4), 1.96 (3H, s, H-5) ppm; **¹³C NMR** (100 MHz, CDCl₃) δ 144.2 (C-3), 140.9 (C-2), 134.8 (C-Ar), 131.4 (2CH-Ar), 129.2 (2CH-Ar), 127.1 (CH-Ar), 117.5 (C-1), 116.9 (C-4), 21.4 (C-5) ppm; **HRMS** (APCI) *m/z* calcd for C₁₁H₁₃S (M+H⁺) 177.0732, found 177.0735. The characterisation data matched the literature.⁸³

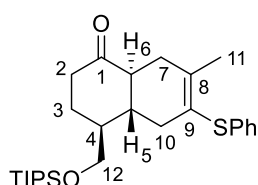
(4*S*,4*aR*,8*aR*)-7-Methyl-6-(phenylthio)-4-(((triisopropylsilyl)oxy)methyl)-3,4,4*a*,5,8,8*a*-hexahydronaphthalen-1(2*H*)-one (167)



Cis-decalin **167** was prepared from (*S*)-enone **3** (0.38 g, 1.4 mmol) and diene **163** (2.05 g, 11.6 mmol, 10.0 equiv) using the general procedure for Diels–Alder cycloaddition (see page 140). The crude residue was purified by silica gel flash column chromatography (5% Et₂O/hexane) to yield the desired *cis*-decalin **167** as a yellow oil (488 mg, 80% yield): *R_f* = 0.07 (5% Et₂O/hexane); $[\alpha]_{\text{D}}^{20}$ = +18.6 (*c* 0.976, CHCl₃); **IR** (ATR) ν_{\max} 2941, 2865, 1715 (C=O ketone), 1476, 1462, 1108, 1069, 882, 739, 689 cm⁻¹; **¹H NMR** (400 MHz, CDCl₃) δ 7.26–7.22 (2H, m, Ar-H), 7.16–7.10 (3H, m, Ar-H), 3.81 (1H, dd, *J* = 9.9, 6.0 Hz, H-12), 3.77 (1H, dd, *J* = 9.9, 6.2 Hz, H-12), 2.89 (1H, ddd, *J* = 5.0, 5.0, 4.0 Hz, H-6), 2.69 (1H, dd, *J* = 18.0, 4.0 Hz, H-7), 2.46 (1H, dddd, *J* = 9.3, 9.3, 5.0, 5.0 Hz, H-5), 2.41–2.30 (2H, m, H-2), 2.20–2.11 (3H, m,

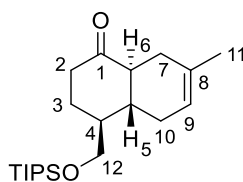
H-10 + H-7), 1.99 (3H, s, H-11), 1.97–1.89 (2H, m, H-3), 1.81–1.73 (1H, m, H-4), 1.10–0.99 (21H, m, OSi(CH(CH₃)₂)₃) ppm; ¹³C NMR (100 MHz, CDCl₃) δ 212.6 (C-1), 140.2 (C-9), 136.6 (C-Ar), 129.0 (2CH-Ar), 128.0 (2CH-Ar), 125.4 (CH-Ar), 121.2 (C-8), 65.3 (C-12), 45.5 (C-6), 39.0 (C-4), 37.6 (C-5), 37.5 (C-2), 35.2 (C-10), 31.3 (C-7), 25.6 (C-3), 21.4 (C-11), 18.2 (OSi(CH(CH₃)₂)₃), 12.0 (OSi(CH(CH₃)₂)₃) ppm; HRMS (ESI) *m/z* calcd for C₂₇H₄₂NaO₂SSi (M+Na⁺) 481.2567, found 481.2573.

(4*S*,4*aR*,8*aS*)-7-Methyl-6-(phenylthio)-4-(((triisopropylsilyl)oxy)methyl)-3,4,4*a*,5,8,8*a*-hexahydronaphthalen-1(2*H*)-one (4)



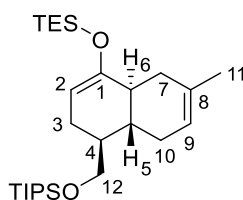
Trans-decalin **4** was prepared from *cis*-decalin **167** (1.55 g, 3.38 mmol) using the general procedure for epimerisation (see page 140). The crude residue was purified by silica gel flash column chromatography (5% Et₂O/hexane) to yield the desired *trans*-decalin **4** as a yellow oil (1.25 g, 81% yield): *R_f* = 0.07 (5% Et₂O/hexane); [α]_D²⁰ = +65.6 (*c* 0.231, CHCl₃); IR (ATR) ν_{max} 2941, 2865, 1713 (C=O ketone), 1476, 1120, 1070, 883, 740, 687 cm⁻¹; ¹H NMR (400 MHz, CDCl₃) δ 7.26–7.21 (2H, m, Ar-H), 7.18–7.10 (3H, m, Ar-H), 3.64 (1H, dd, *J* = 9.9, 3.1 Hz, H-12), 3.58 (1H, dd, *J* = 9.9, 5.0 Hz, H-12), 2.55–2.40 (4H, m, H-2 + H-10 + H-7), 2.39–2.32 (2H, m, H-6 + H-7), 2.17–2.08 (2H, m, H-3 + H-10), 1.99 (3H, s, H-11), 1.85–1.70 (2H, m, H-3 + H-5), 1.68–1.60 (1H, m, H-4), 1.00–0.90 (21H, m, OSi(CH(CH₃)₂)₃) ppm; ¹³C NMR (100 MHz, CDCl₃) δ 211.8 (C-1), 140.7 (C-9), 136.2 (C-Ar), 129.0 (2CH-Ar), 128.3 (2CH-Ar), 125.6 (CH-Ar), 121.6 (C-8), 64.2 (C-12), 49.1 (C-6), 44.8 (C-4), 41.7 (C-5), 41.3 (C-2), 38.1 (C-10), 32.4 (C-7), 30.0 (C-3), 21.6 (C-11), 18.1 (OSi(CH(CH₃)₂)₃), 12.0 (OSi(CH(CH₃)₂)₃) ppm; HRMS (ESI) *m/z* calcd for C₂₇H₄₂NaO₂SSi requires (M+Na⁺) 481.2567, found 481.2567.

(4*S*,4*aR*,8*aS*)-7-Methyl-4-(((triisopropylsilyl)oxy)methyl)-3,4,4*a*,5,8,8*a*-hexahydronaphthalen-1(2*H*)-one (168)



Trans-decalin **168** was prepared from *trans*-decalin **4** (0.34 g, 0.74 mmol) using the general procedure for selective hydrogenation (see page 140). The crude residue was purified by silica gel flash column chromatography (2% EtOAc/hexane) to deliver the desired *trans*-decalin **168** as a light yellow oil (224 mg, 86% yield): $R_f = 0.10$ (2% EtOAc/hexane); $[\alpha]_D^{20} = +46.1$ (c 1.21, CHCl₃); IR (ATR) ν_{\max} 2941, 2865, 1713 (C=O ketone), 1462, 1118, 1098, 882, 787, 682 cm⁻¹; ¹H NMR (400 MHz, CDCl₃) δ 5.34–5.28 (1H, m, H-9), 3.82 (1H, dd, $J = 9.8, 2.4$ Hz, H-12), 3.64 (1H, dd, $J = 9.8, 5.3$ Hz, H-12), 2.50–2.37 (2H, m, H-2), 2.36–2.11 (5H, m, H-6 + H-7 + H-3 + H-5 + H-10), 2.07–2.02 (1H, m, H-7), 1.92–1.81 (1H, m, H-10), 1.67 (3H, s, H-11), 1.65–1.55 (2H, m, H-4 + H-3), 1.08–1.02 (21H, m, OSi(CH(CH₃)₂)₃) ppm; ¹³C NMR (100 MHz, CDCl₃) δ 212.6 (C-1), 133.1 (C-8), 119.2 (C-9), 64.7 (C-12), 49.4 (C-6), 45.1 (C-4), 41.4 (C-2), 40.2 (C-5), 31.7 (C-10), 30.2 (C-7), 29.7 (C-3), 23.6 (C-11), 18.2 (OSi(CH(CH₃)₂)₃), 12.1 (OSi(CH(CH₃)₂)₃) ppm; HRMS (ESI) m/z calcd for C₂₁H₃₈NaO₂Si (M+Na⁺) 373.2533, found 373.2534.

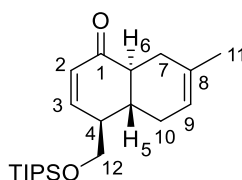
Triethyl(((4*S*,4*aR*,8*aS*)-7-methyl-4-(((triisopropylsilyl)oxy)methyl)-3,4,4*a*,5,8,8*a*-hexahydronaphthalen-1-yl)oxy)silane (200)



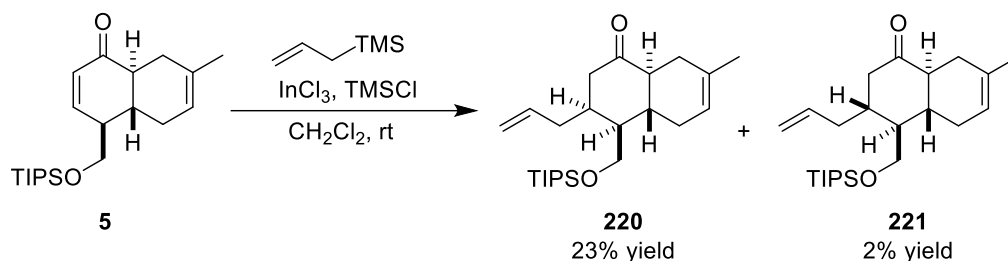
Silyl enol ether **200** was prepared from *trans*-decalin **168** (2.61 g, 7.54 mmol) using the general procedure for TES-enol ether formation (see page 141). The crude residue was purified by silica gel flash column chromatography (2% Et₂O/hexane) to yield the desired TES-enol ether **200** as a yellow oil (3.16 g, 91% yield): $R_f = 0.34$ (2% Et₂O/hexane); $[\alpha]_D^{20} = +73.7$ (c 0.379, CHCl₃); IR (ATR) ν_{\max} 2951, 2867, 1666, 1462, 1200, 1113, 1013, 882, 729

cm⁻¹; **¹H NMR** (400 MHz, CDCl₃) δ 5.39–5.33 (1H, m, H-9), 4.83 (1H, ddd, *J* = 5.7, 1.7, 1.7 Hz, H-2), 3.76 (1H, dd, *J* = 9.6, 3.4 Hz, H-12), 3.58 (1H, dd, *J* = 9.6, 6.2 Hz, H-12), 2.28 (1H, dd, *J* = 15.2, 4.0 Hz, H-7), 2.23–1.96 (4H, m, H-10 + H-3 + H-6), 1.80–1.69 (2H, m, H-3 + H-7), 1.67 (3H, s, H-11), 1.52–1.39 (2H, m, H-4 + H-5), 1.07–1.03 (21H, m, OSi(CH(CH₃)₂)₃), 0.98 (9H, t, *J* = 7.8 Hz, (OSi(CH₂CH₃)₃)), 0.68 (6H, q, *J* = 7.8 Hz, (OSi(CH₂CH₃)₃)) ppm; **¹³C NMR** (100 MHz, CDCl₃) δ 152.1 (C-1), 134.2 (C-8), 120.5 (C-9), 102.3 (C-2), 65.3 (C-12), 41.5 (C-6), 41.3 (C-4), 38. (C-5), 34.3 (C-10), 30.4 (C-7), 27.9 (C-3), 23.8 (C-11), 18.2 (OSi(CH(CH₃)₂)₃), 12.1 (OSi(CH(CH₃)₂)₃), 7.0 (OSi(CH₂CH₃)₃), 5.2 (OSi(CH₂CH₃)₃) ppm; **HRMS** (APCI) *m/z* calcd for C₂₇H₅₃O₂Si (M+H⁺) 465.3579, found 465.3586.

(4*S*,4*aR*,8*aS*)-7-Methyl-4-(((triisopropylsilyl)oxy)methyl)-4*a*,5,8,8*a*-tetrahydronaphthalen-1(4*H*)-one (5)

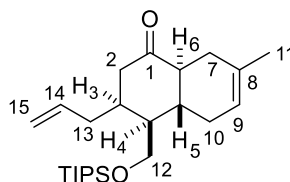


Enone *trans*-decalin **5** was prepared from TES-enol ether **200** (72 mg, 0.15 mmol) using the general procedure for IBX oxidation of TES-enol ether (see page 141). The crude residue was purified by silica gel flash column chromatography (2% Et₂O/hexane) to produce the enone *trans*-decalin **5** as a light yellow oil (32 mg, 59% yield): *R_f* = 0.14 (5% Et₂O/ hexane); [α]_D²⁰ = +125.2 (c 0.328, CHCl₃); **IR** (ATR) *v*_{max} 2942, 2866, 1674 (C=O ketone), 1463, 1393, 1114, 882, 783, 683 cm⁻¹; **¹H NMR** (400 MHz, CDCl₃) δ 7.07 (1H, dd, *J* = 10.2, 1.9 Hz, H-3), 6.07 (1H, dd, *J* = 10.2, 2.8 Hz, H-2), 5.37–5.29 (1H, m, H-9), 3.97 (1H, dd, *J* = 9.7, 4.2 Hz, H-12), 3.65 (1H, dd, *J* = 9.7, 7.2 Hz, H-12), 2.45–2.26 (4H, m, H-7 + H-4 + H-6), 2.10–1.81 (3H, m, H-5 + H-10), 1.69 (3H, s, H-11), 1.10–1.02 (21H, m, OSi(CH(CH₃)₂)₃) ppm; **¹³C NMR** (100 MHz, CDCl₃) δ 201.3 (C-1), 152.2 (C-3), 133.3 (C-8), 129.2 (C-2), 118.9 (C-9), 63.8 (C-12), 46.1 (C-6), 45.9 (C-4), 36.3 (C-5), 31.2 (C-7), 30.3 (C-10), 23.6 (C-11), 18.1 (OSi(CH(CH₃)₂)₃), 12.0 (OSi(CH(CH₃)₂)₃) ppm; **HRMS** (ESI) *m/z* calcd for C₂₁H₃₆NaO₂Si (M+Na⁺) 371.2377, found 371.2370.



To a solution of enone **5** (33 mg, 0.096 mmol) and InCl_3 (4.6 mg, 0.019 mmol, 0.2 equiv) in CH_2Cl_2 (0.3 mL) at room temperature, were added freshly distilled trimethylsilyl chloride (0.013 mL, 0.096 mmol, 1.0 equiv), followed by allyltrimethylsilane (0.017 mL, 0.106 mmol, 1.1 equiv). The reaction mixture was stirred under N_2 atmosphere at room temperature for 30 minutes before being quenched with a saturated aqueous solution of NaHCO_3 (3 mL) and diluted with CH_2Cl_2 (3 mL). The organic layer was separated, and the aqueous layer was extracted with CH_2Cl_2 (3×3 mL). The combined organic layers were washed with brine, dried over anhydrous Na_2SO_4 and concentrated *in vacuo*. The crude product was purified by silica gel flash column chromatography (5% Et_2O /hexane) to yield decalin **220** (9 mg, 23% yield) and decalin **221** (1 mg, 2% yield).

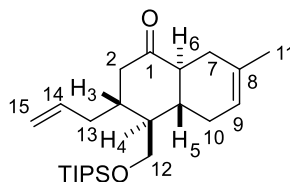
(3*S,4*S**,4*aR**,8*aS**)-3-Allyl-7-methyl-4-(((triisopropylsilyl)oxy)methyl)-3,4,4*a*,5,8,8*a*-hexahydronaphthalen-1(2*H*)-one (**220**)**



Decalin 220 (a light yellow oil): $R_f = 0.51$ (10% EtOAc /hexane); $^1\text{H NMR}$ (400 MHz, CDCl_3) δ 5.71 (1H, dddd, $J = 16.7, 10.3, 8.4, 5.8$ Hz, H-14), 5.38–5.26 (1H, m, H-9), 5.04 (1H, d, $J = 10.3$ Hz, H-15), 5.03 (1H, d, $J = 16.7$ Hz, H-15), 3.91 (1H, dd, $J = 9.9, 5.2$ Hz, H-12), 3.62 (1H, dd, $J = 9.9, 9.9$ Hz, H-12), 2.59–2.49 (2H, m, H-3 + H-2), 2.42 (1H, dd, $J = 14.1, 6.0$ Hz, H-2), 2.31–2.21 (2H, m, H-6 + H-13), 2.20–2.09 (2H, m, H-10 + H-7), 2.09–1.98 (2H, m, H-4 + H-7), 1.93–1.81 (1H, m, H-10), 1.67 (3H, s, H-11), 1.65–1.55 (2H, m, H-13 + H-5), 1.13–1.05 (21H, m, $\text{OSi}(\text{CH}(\text{CH}_3)_2)_3$) ppm; $^{13}\text{C NMR}$ (100 MHz, CDCl_3) δ 212.1 (C-1), 136.7 (C-14), 133.3 (C-8), 119.2 (C-9), 117.1 (C-15), 62.7 (C-12), 49.9 (C-6), 47.5 (C-4), 44.8 (C-2), 37.1 (C-3), 37.0 (C-5), 31.9 (C-13), 31.7 (C-10), 29.6 (C-7), 23.6 (C-11), 18.2 ($\text{OSi}(\text{CH}(\text{CH}_3)_2)_3$), 12.1

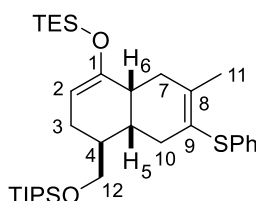
(OSi(CH₃)₂)₃) ppm. HRMS (ESI) *m/z* calcd for C₂₄H₃₈NaO₄ (M+Na⁺) 413.2662, found 413.2678.

(3*R,4*S**,4*aR**,8*aS**)-3-Allyl-7-methyl-4-(((triisopropylsilyl)oxy)methyl)-3,4,4*a*,5,8,8*a*-hexahydronaphthalen-1(2*H*)-one (221)**



Decalin 221 (a light yellow oil): *R_f* = 0.58 (10% EtOAc/hexane); ¹H NMR (400 MHz, CDCl₃) δ 5.75 (1H, dddd, *J* = 15.8, 11.4, 7.2, 7.2 Hz, H-14), 5.34–5.28 (1H, m, H-9), 4.99 (1H, d, *J* = 11.4 Hz, H-15), 4.98 (1H, d, *J* = 15.8 Hz, H-15), 3.84 (1H, dd, *J* = 9.8, 5.2 Hz, H-12), 3.58 (1H, dd, *J* = 9.8, 9.8 Hz, H-12), 2.66–2.57 (1H, m, H-3), 2.52 (1H, dd, *J* = 13.6, 3.4 Hz, H-2), 2.44 (1H, dd, *J* = 13.8, 5.4 Hz, H-2), 2.27–2.12 (3H, m, H-13 + H-6 + H-10), 2.11–2.05 (2H, m, H-7), 2.00–1.93 (1H, m, H-4), 1.93–1.80 (1H, m, H-10), 1.75–1.70 (1H, m, H-13), 1.67 (3H, s, H-11), 1.65–1.58 (1H, m, H-5), 1.10–1.04 (21H, m, OSi(CH₃)₂)₃) ppm. The characterisation data matched the previous work in the Clarke group.⁶⁶

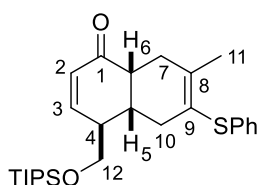
Triethyl(((4*S,4*aR**,8*aR**)-7-methyl-6-(phenylthio)-4-(((triisopropylsilyl)oxy)methyl)-3,4,4*a*,5,8,8*a*-hexahydronaphthalen-1-yl)oxy)silane (231)**



Silyl enol ether **231** was prepared from *cis*-decalin **167** (0.36 g, 0.79 mmol) using the general procedure for TES-enol ether formation (see page 141). The crude residue was purified by silica gel flash column chromatography (1% Et₂O/hexane) to yield the desired TES-enol ether **231** as a light yellow oil (339 mg, 78% yield): *R_f* = 0.65 (1% Et₂O/hexane); IR (ATR) ν_{max} 2939, 2909, 2868, 1667, 1176, 1109, 1006, 882, 737, 690 cm⁻¹; ¹H NMR (400 MHz, CDCl₃) δ 7.30–7.21 (4H, m, Ar-H), 7.19–7.13 (1H, m, Ar-H), 4.74 (1H, dd, *J* = 3.6, 3.6 Hz, H-2), 3.62

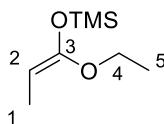
(1H, dd, $J = 9.8, 4.4$ Hz, H-12), 3.57 (1H, dd, $J = 9.8, 5.9$ Hz, H-12), 2.47 (1H, m, H-10), 2.41–2.25 (4H, m, H-6 + H-10 + H-7), 2.20–2.07 (3H, m, H-3 + H-5), 2.00 (3H, s, H-11), 1.81–1.70 (1H, m, H-4), 1.06–0.98 (30H, m, OSi(CH(CH₃)₂)₃, OSi(CH₂CH₃)₃), 0.72 (6H, q, $J = 7.9$ Hz, OSi(CH₂CH₃)₃) ppm; ¹³C NMR (100 MHz, CDCl₃) δ 152.9 (C-1), 139.6 (C-9), 136.7 (C-8), 128.9 (2CH-Ar), 128.7 (2CH-Ar), 125.6 (CH-Ar), 122.0 (C-Ar), 100.8 (C-2), 64.8 (C-12), 36.5 (C-6), 35.2 (C-10), 35.0 (C-4), 34.3 (C-5), 33.3 (C-7), 26.4 (C-3), 21.6 (C-11), 18.2 (OSi(CH(CH₃)₂)₃), 12.0 (OSi(CH(CH₃)₂)₃), 6.9 (OSi(CH₂CH₃)₃), 5.2 (OSi(CH₂CH₃)₃) ppm; HRMS (APCI) m/z calcd for C₃₃H₅₇O₂SSi₂ (M+H⁺) 573.3612, found 573.3600.

(4*S,4*aR**,8*aR**)-7-Methyl-6-(phenylthio)-4-(((triisopropylsilyl)oxy)methyl)-4*a*,5,8,8*a*-tetrahydronaphthalen-1(4*H*)-one (229)**

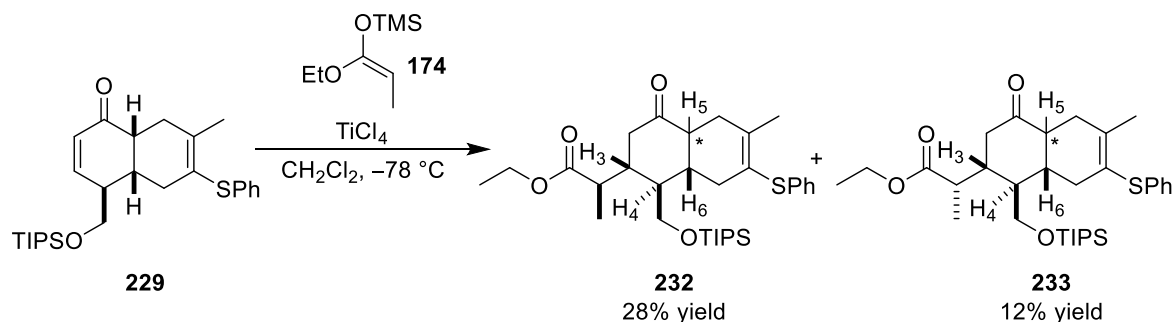


Enone *cis*-decalin **229** was prepared from TES-enol ether **231** (0.39 g, 0.69 mmol) using the general procedure for IBX oxidation of TES-enol ether (see page 141). The crude residue was purified by silica gel flash column chromatography (50% CH₂Cl₂/hexane) to yield enone *cis*-decalin **229** as a light yellow oil (153 mg, 48% yield): $R_f = 0.26$ (50% CH₂Cl₂/hexane); IR (ATR) ν_{\max} 2942, 2865, 1681 (C=O), 1477, 1463, 1110, 882, 739, 690 cm⁻¹; ¹H NMR (400 MHz, CDCl₃) δ 7.24–7.22 (2H, m, Ar-H), 7.16–7.11 (3H, m, Ar-H), 6.79 (1H, dd, $J = 10.2, 3.6$ Hz, H-3), 5.99 (1H, dd, $J = 10.2, 1.8$ Hz, H-2), 3.83 (1H, dd, $J = 9.8, 5.9$ Hz, H-12), 3.72 (1H, dd, $J = 9.8, 5.6$ Hz, H-12), 2.90 (1H, ddd, $J = 5.9, 5.9, 4.6$ Hz, H-6), 2.74 (1H, dd, $J = 18.0, 4.6$ Hz, H-7), 2.58 (1H, dddd, $J = 7.2, 7.2, 5.9, 4.9$ Hz, H-5), 2.46 (1H, dddd, $J = 7.2, 5.9, 5.6, 3.6, 1.8$ Hz, H-4), 2.33–2.16 (3H, m, H-7 + H-10), 2.00 (3H, s, H-11), 1.09–0.95 (21H, m, OSi(CH(CH₃)₂)₃) ppm; ¹³C NMR (100 MHz, CDCl₃) δ 200.7 (C-1), 149.8 (C-3), 140.7 (C-9), 136.3 (C-Ar), 129.0 (2CH-Ar), 128.7 (C-2), 128.5 (2CH-Ar), 125.7 (CH-Ar), 121.7 (C-8), 63.9 (C-12), 43.2 (C-6), 42.2 (C-4), 35.0 (C-5), 33.8 (C-10), 31.3 (C-7), 21.5 (C-11), 18.1 (OSi(CH(CH₃)₂)₃), 12.0 (OSi(CH(CH₃)₂)₃) ppm; HRMS (APCI) m/z calcd for C₂₇H₄₁O₂SSi (M+H⁺) 457.2591, found 457.2603.

(E)-((1-Ethoxyprop-1-en-1-yl)oxy)trimethylsilane (174)



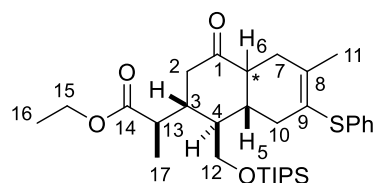
To a solution of freshly distilled diisopropylamine (1.47 mL, 10.4 mmol, 1.2 equiv) in THF (10.4 mL) at $-78\text{ }^{\circ}\text{C}$, was slowly added *n*-BuLi (5.10 mL of a solution 2.07 M in hexane, 10.4 mmol, 1.2 equiv), and the mixture was stirred at $-78\text{ }^{\circ}\text{C}$ for 45 minutes. The mixture was added a solution of ethyl propionate (1.0 mL, 8.7 mmol) in THF (11.3 mL). The reaction mixture was stirred at $-78\text{ }^{\circ}\text{C}$ for 1 hour before being added freshly distilled trimethylsilyl chloride (1.32 mL, 10.4 mmol, 1.2 equiv). The reaction mixture was stirred under N_2 atmosphere at $-78\text{ }^{\circ}\text{C}$ for a further 30 minutes and allowed to reach room temperature for 2 hours. The solvent was removed *in vacuo*. The crude product was purified by kugelrohr distillation (room temperature at 0.5 mbar) to yield the desired TMS-silyl ketene acetal **174** as a light yellow oil (830 mg, 55% yield): $^1\text{H NMR}$ (400 MHz, C_6D_6) δ 3.90 (1H, q, $J = 6.8\text{ Hz}$, H-2), 3.79 (2H, q, $J = 7.2\text{ Hz}$, H-4), 1.74 (3H, d, $J = 6.8\text{ Hz}$, H-1), 1.10 (3H, t, $J = 7.2\text{ Hz}$, H-5), 0.15 (9H, s, $\text{OSi}(\text{CH}_3)_3$) ppm. This compound was characterised only by $^1\text{H NMR}$ due to its volatility and instability and the data matched the literature.⁹⁴



To a solution of enone *cis*-decalin **229** (0.12 g, 0.27 mmol) in CH_2Cl_2 (2.7 mL) at $-78\text{ }^{\circ}\text{C}$, was added TiCl_4 (0.04 mL, 0.35 mmol, 1.3 equiv). The mixture was stirred at $-78\text{ }^{\circ}\text{C}$ for 5 minutes before being added TMS-silyl ketene acetal **174** (0.08 mL, 0.54 mmol, 2.0 equiv). The reaction mixture was stirred under N_2 atmosphere at $-78\text{ }^{\circ}\text{C}$ for 30 minutes. After this time, the mixture was quenched with a saturated aqueous solution of NaHCO_3 (5 mL) at $-78\text{ }^{\circ}\text{C}$ and warmed to room temperature for 30 minutes. The organic layer was separated, and the aqueous layer was extracted with CH_2Cl_2 (3 x 5 mL). The combined organic layers were washed with a saturated aqueous solution of NaHCO_3 (10 mL) and brine (10 mL), dried over

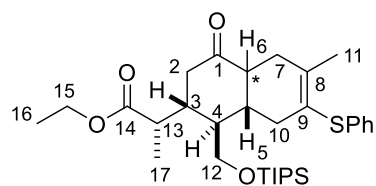
anhydrous Na₂SO₄ and concentrated *in vacuo*. The crude product was purified by silica gel flash column chromatography (5–10% Et₂O/hexane) to yield ester **232** (42 mg, 28% yield) and ester **233** (19 mg, 12% yield).

Ethyl (*R*)-2-((1*R,2*R**,4*aR**,8*aR**)-6-methyl-4-oxo-7-(phenylthio)-1-(((triisopropylsilyl)oxy)methyl)-1,2,3,4,4*a*,5,8,8*a*-octahydronaphthalen-2-yl)propanoate (**232**)**



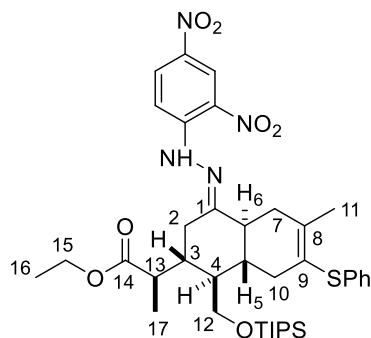
Ester 232 (a yellow oil): *R_f* = 0.15 (10% Et₂O/hexane); IR (ATR) ν_{max} 2932, 2866, 1730 (C=O ester), 1715 (C=O ketone), 1464, 1381, 1179, 1150, 1110, 882, 740, 687 cm⁻¹; ¹H NMR (400 MHz, C₆D₆) δ 7.26 (2H, d, *J* = 7.5 Hz, Ar-H), 7.07 (2H, t, *J* = 7.5 Hz, Ar-H), 6.94 (1H, t, *J* = 7.5 Hz, Ar-H), 4.01 (1H, dd, *J* = 10.9, 2.2 Hz, H-12), 3.98–3.86 (2H, m, H-15), 3.67 (1H, d, *J* = 10.9 Hz, H-12), 3.03 (1H, qd, *J* = 7.2, 3.6 Hz, H-13), 2.77 (1H, dd, *J* = 13.6, 4.0 Hz, H-2), 2.75–2.68 (1H, m, H-10), 2.57 (1H, dd, *J* = 13.6, 13.6 Hz, H-2), 2.49 (1H, dd, *J* = 18.6, 11.2 Hz, H-7), 2.26 (1H, dd, *J* = 18.6, 4.8 Hz, H-7), 2.14 (1H, dddd, *J* = 13.6, 10.4, 4.0, 3.6 Hz, H-3), 2.08–1.95 (2H, m, H-5 + H-10), 1.92 (3H, s, H-11), 1.79 (1H, ddd, *J* = 11.2, 11.2, 4.8 Hz, H-6), 1.51 (1H, dd, *J* = 10.4, 10.4 Hz, H-4), 1.07 (3H, d, *J* = 7.2 Hz, H-17), 0.97–0.87 (24H, m, H-16 + OSi(CH(CH₃)₂)₃) ppm; ¹³C NMR (100 MHz, C₆D₆) δ 208.5 (C-1), 174.2 (C-14), 142.0 (C-9), 137.2 (C-Ar), 129.3 (2CH-Ar), 128.4 (2CH-Ar), 125.6 (CH-Ar), 121.7 (C-8), 60.0 (C-15), 59.5 (C-12), 49.0 (C-6), 47.4 (C-4), 42.1 (C-3), 41.3 (C-2), 40.2 (C-5), 39.4 (C-13), 39.1 (C-10), 33.0 (C-7), 21.6 (C-11), 18.2 (OSi(CH(CH₃)₂)₃), 15.7 (C-17), 14.3 (C-16), 12.2 (OSi(CH(CH₃)₂)₃) ppm; HRMS (APCI) *m/z* calcd for C₃₂H₅₁O₄SSi (M+H⁺) 559.3272, found 559.3277.

Ethyl (S)-2-((1R*,2R*,4aR*,8aR*)-6-methyl-4-oxo-7-(phenylthio)-1-(((triisopropylsilyl)oxy)methyl)-1,2,3,4,4a,5,8,8a-octahydronaphthalen-2-yl)propanoate (233)



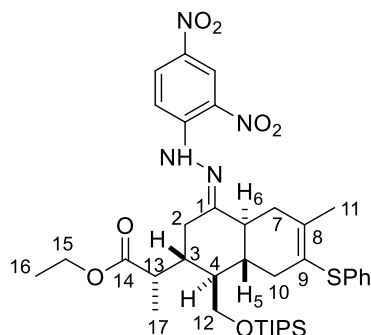
Ester 233 (a yellow oil): $R_f = 0.09$ (10% Et₂O/hexane); **IR** (ATR) ν_{\max} 2921, 2866, 1731 (C=O ester), 1716 (C=O ketone), 1463, 1370, 1187, 1144, 1106, 882, 740, 689 cm⁻¹; **¹H NMR** (400 MHz, C₆D₆) δ 7.27 (2H, dd, $J = 7.6, 1.2$ Hz, Ar-H), 7.08 (2H, t, $J = 7.6$ Hz, Ar-H), 6.95 (1H, td, $J = 7.6, 1.2$ Hz, Ar-H), 3.93 (1H, dq, $J = 7.4, 3.7$ Hz, H-15), 3.91–3.77 (2H, m, H-15), 3.53 (1H, dd, $J = 10.9, 2.0$ Hz, H-12), 3.49 (1H, dd, $J = 10.9, 2.0$ Hz, H-12), 2.97 (1H, qd, $J = 7.2, 3.6$ Hz, H-13), 2.72 (1H, dddd, $J = 13.2, 10.8, 3.7, 3.6$ Hz, H-3), 2.69–2.63 (1H, m, H-4), 2.49–2.43 (1H, m, H-10), 2.42 (1H, dd, $J = 13.3, 3.7$ Hz, H-2), 2.28 (1H, dd, $J = 18.6, 4.9$ Hz, H-7), 2.09 (1H, dd, $J = 13.3, 13.3$ Hz, H-2), 2.04–1.87 (2H, m, H-7 + H-10), 1.92 (3H, s, H-11), 1.73 (1H, ddd, $J = 11.4, 11.4, 4.9$ Hz, H-6), 1.01 (3H, d, $J = 7.2$ Hz, H-17), 1.00–0.98 (22H, m, H-5 + OSi(CH(CH₃)₂)₃), 0.93 (3H, t, $J = 7.2$ Hz, H-16) ppm; **¹³C NMR** (100 MHz, C₆D₆) δ 208.3 (C-1), 174.5 (C-14), 141.7 (C-9), 137.1 (C-Ar), 129.3 (2CH-Ar), 128.5 (2CH-Ar), 125.8 (CH-Ar), 121.8 (C-8), 60.5 (C-15), 59.8 (C-12), 49.0 (C-6), 46.1 (C-5), 41.6 (C-2), 40.2 (C-3), 39.9 (C-13), 39.7 (C-4), 39.0 (C-10), 33.0 (C-7), 21.6 (C-12), 18.3 (OSi(CH(CH₃)₂)₃), 14.2 (C-16), 12.3 (OSi(CH(CH₃)₂)₃), 9.4 (C-17) ppm; **HRMS** (APCI) m/z calcd for C₃₂H₅₁O₄SSi (M+H⁺) 559.3272, found 559.3265.

Ethyl (*R*)-2-((1*R,2*R**,4*aS**,8*aS**,*E*)-4-(2-(2,4-dinitrophenyl)hydrazono)-6-methyl-7-(phenylthio)-1-(((triisopropylsilyl)oxy)methyl)-1,2,3,4,4*a*,5,8,8*a*-octahydronaphthalen-2-yl)propanoate (**234**)**



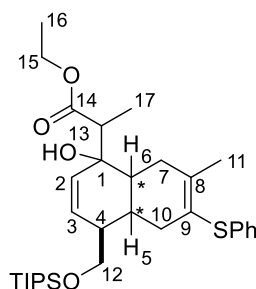
Hydrazone **234** was prepared from ketone **232** (11 mg, 0.02 mmol) using the general procedure for hydrazone formation (see page 142). The crude residue was purified by silica gel flash column chromatography (10% EtOAc/hexane) to afford hydrazone **232** as a yellow oil (13 mg, 90% yield): $R_f = 0.26$ (10% EtOAc/hexane); IR (ATR) ν_{\max} 3322 (NH), 2924, 2865, 1728 (C=O), 1617 (C=N), 1592, 1334, 1110, 833, 743, 689 cm^{-1} ; $^1\text{H NMR}$ (400 MHz, CDCl_3) δ 11.37 (1H, brs, N-H), 9.15 (1H, d, $J = 2.6$ Hz, Ar-H), 8.35 (1H, dd, $J = 9.6, 2.6$ Hz, Ar-H), 7.99 (1H, d, $J = 9.6$ Hz, Ar-H), 7.25–7.11 (5H, m, Ar-H), 4.18–4.04 (2H, m, H-15), 3.96 (1H, dd, $J = 11.0, 2.4$ Hz, H-12), 3.73 (1H, dd, $J = 11.0, 1.2$ Hz, H-12), 3.06 (1H, dd, $J = 13.4, 3.3$ Hz, H-2), 3.00 (1H, qd, $J = 7.2, 3.6$ Hz, H-13), 2.73–2.53 (3H, m, H-7 + H-10), 2.41 (1H, ddd, $J = 11.6, 11.6, 4.8$ Hz, H-6), 2.17 (1H, dd, $J = 13.4, 13.4$ Hz, H-2), 2.09 (3H, s, H-11), 2.08–2.01 (1H, m, H-10), 1.91 (1H, dddd, $J = 13.4, 10.2, 3.6, 3.4$ Hz, H-3), 1.89–1.81 (1H, m, H-5), 1.46–1.39 (1H, m, H-4), 1.31 (3H, d, $J = 7.2$ Hz, H-17), 1.24 (3H, t, $J = 7.2$ Hz, H-16), 0.98–0.87 (21H, m, $\text{OSi}(\text{CH}(\text{CH}_3)_2)_3$) ppm; $^{13}\text{C NMR}$ (100 MHz, CDCl_3) δ 174.6 (C-14), 160.9 (C-1), 145.7 (C-Ar), 141.1 (C-9), 137.8 (C-Ar), 136.2 (C-Ar), 130.2 (CH-Ar), 129.2 (C-Ar), 129.1 (2CH-Ar), 128.3 (2CH-Ar), 125.7 (CH-Ar), 123.8 (CH-Ar), 121.8 (C-8), 116.5 (CH-Ar), 60.5 (C-15), 59.1 (C-12), 47.6 (C-4), 44.3 (C-6), 41.5 (C-3), 40.7 (C-5), 39.1 (C-13), 38.7 (C-10), 34.4 (C-7), 26.8 (C-2), 21.9 (C-11), 18.1 ($\text{OSi}(\text{CH}(\text{CH}_3)_2)_3$), 16.0 (C-17), 14.4 (C-16), 12.0 ($\text{OSi}(\text{CH}(\text{CH}_3)_2)_3$) ppm; HRMS (APCI) m/z calcd for $\text{C}_{38}\text{H}_{55}\text{N}_4\text{O}_7\text{SSi}$ ($\text{M}+\text{H}^+$) 739.3555, found 739.3581.

Ethyl (S)-2-((1R*,2R*,4aS*,8aS*,E)-4-(2-(2,4-dinitrophenyl)hydrazono)-6-methyl-7-(phenylthio)-1-(((triisopropylsilyl)oxy)methyl)-1,2,3,4,4a,5,8,8a-octahydronaphthalen-2-yl)propanoate (235)



Hydrazone **235** was prepared from ketone **233** (17 mg, 0.03 mmol) using the general procedure for hydrazone formation (see page 142). The crude residue was purified by silica gel flash column chromatography (10% EtOAc/hexane) to give hydrazone **235** as a yellow oil (12 mg, 60% yield): $R_f = 0.23$ (10% EtOAc/hexane); IR (ATR) ν_{\max} 3320 (N-H), 2922, 2853, 1730 (C=O), 1618 (C=N), 1459, 1334, 1139, 833, 743, 689 cm^{-1} ; $^1\text{H NMR}$ (400 MHz, CDCl_3) δ 11.23 (1H, brs, N-H), 9.14 (1H, d, $J = 2.4$ Hz, Ar-H), 8.34 (1H, dd, $J = 9.6, 2.4$ Hz, Ar-H), 7.99 (1H, d, $J = 9.6$ Hz, Ar-H), 7.25–7.13 (5H, m, Ar-H), 4.29–4.14 (2H, m, H-15), 3.77–3.64 (2H, m, H-12), 2.98 (1H, qd, $J = 7.2, 3.2$ Hz, H-13), 2.77 (1H, dd, $J = 13.8, 3.0$ Hz, H-2), 2.72–2.62 (2H, m, H-7), 2.58 (1H, dd, $J = 18.4, 4.3$ Hz, H-10), 2.47–2.34 (2H, m, H-10 + H-3), 2.17–2.14 (1H, m, H-5), 2.10 (3H, s, H-11), 1.97 (1H, dd, $J = 13.8, 13.8$ Hz, H-2), 1.92–1.86 (1H, m, H-6), 1.38–1.25 (1H, m, H-4), 1.20 (3H, t, $J = 7.2$ Hz, H-16), 1.12 (3H, d, $J = 7.2$ Hz, H-17), 0.97–0.88 (21H, m, $\text{OSi}(\text{CH}(\text{CH}_3)_2)_3$) ppm; $^{13}\text{C NMR}$ (100 MHz, CDCl_3) δ 175.2 (C-14), 160.3 (C-1), 145.7 (C-Ar), 140.8 (C-9), 137.8 (C-Ar), 136.1 (C-Ar), 130.1 (CH-Ar), 129.3 (C-Ar), 129.1 (2CH-Ar), 128.5 (2CH-Ar), 125.8 (CH-Ar), 123.8 (CH-Ar), 121.8 (C-8), 116.5 (CH-Ar), 61.1 (C-15), 59.5 (C-12), 46.6 (C-4), 44.4 (C-3), 40.7 (C-6), 39.5 (C-13), 38.9 (C-5), 38.7 (C-10), 34.4 (C-7), 27.6 (C-2), 21.3 (C-11), 18.1 ($\text{OSi}(\text{CH}(\text{CH}_3)_2)_3$), 14.3 (C-16), 12.0 ($\text{OSi}(\text{CH}(\text{CH}_3)_2)_3$), 9.6 (C-17) ppm; HRMS (APCI) m/z calcd for $\text{C}_{38}\text{H}_{55}\text{N}_4\text{O}_7\text{SSi}$ ($\text{M}+\text{H}^+$) 739.3555, found 739.3533.

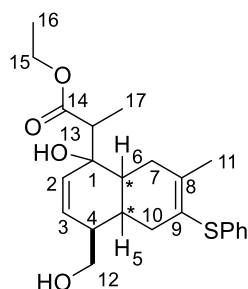
Ethyl 2-((4*S,4*aR**,8*aR**)-1-hydroxy-7-methyl-6-(phenylthio)-4-(((triisopropylsilyl)oxy)methyl)-1,4,4*a*,5,8,8*a*-hexahydronaphthalen-1-yl)propanoate (**238**)**



To a solution of enone *cis*-decalin **229** (32 mg, 0.07 mmol) in CH₂Cl₂ (0.8 mL) at –78 °C was added Yb(OTf)₃ (57 mg, 0.07 mmol, 1.0 equiv). The mixture was stirred at –78 °C for 10 minutes before TMS-silyl ketene acetal **174** (0.02 mL, 0.14 mmol, 2.0 equiv) was added. The reaction mixture was stirred under N₂ atmosphere at –78 °C for 1.5 hours before being quenched with a saturated aqueous solution of NaHCO₃ (1.2 mL). The mixture was allowed to reach room temperature and diluted with CH₂Cl₂ (2 mL). The organic layer was separated, and the aqueous layer was extracted with CH₂Cl₂ (3 x 2 mL). The combined organic layers were washed with brine, dried over anhydrous Na₂SO₄ and concentrated *in vacuo*. The crude product was then dissolved in THF (0.5 mL) and treated with 2 M HCl (0.5 mL). The reaction mixture was stirred at room temperature for 30 minutes. The mixture was then quenched with H₂O (5 mL) and diluted with EtOAc (5 mL). The organic layer was separated, and the aqueous layer was extracted with EtOAc (3 x 5 mL). The combined organic layers were washed with brine, dried over anhydrous Na₂SO₄ and concentrated *in vacuo*. The crude product was purified by silica gel flash column chromatography (5–10% Et₂O/hexane) to yield alcohol **238** as a light yellow oil (7 mg, 17% yield): *R_f* = 0.25 (10% Et₂O/hexane); **IR** (ATR) ν_{\max} 3505 (O-H), 2926, 2866, 1711 (C=O), 1462, 1376, 1188, 1112, 883, 742, 690 cm⁻¹; **¹H NMR** (400 MHz, C₆D₆) δ 7.28 (2H, dd, *J* = 7.8, 1.2 Hz, Ar-H), 7.05 (2H, t, *J* = 7.8 Hz, Ar-H), 6.95 (1H, tt, *J* = 7.8, 1.2 Hz, Ar-H), 5.81 (1H, ddd, *J* = 10.2, 2.0, 2.0 Hz, H-2), 5.71 (1H, dd, *J* = 10.2, 2.2 Hz, H-3), 4.19–4.13 (1H, brs, O-H), 3.95–3.81 (2H, m, H-15), 3.54 (1H, dd, *J* = 9.6, 3.2 Hz, H-12), 3.40 (1H, dd, *J* = 9.6, 5.0 Hz, H-12), 2.83 (1H, q, *J* = 7.2 Hz, H-13), 2.65 (1H, dd, *J* = 18.4, 5.0 Hz, H-7), 2.50–2.38 (3H, m, H-7 + H-10), 2.34–2.27 (1H, m, H-6), 2.18–2.11 (1H, m, H-4), 2.10–2.03 (1H, m, H-5), 2.00 (3H, s, H-11), 1.22 (3H, d, *J* = 7.2 Hz, H-17), 1.05–1.01 (21H, m, OSi(CH(CH₃)₂)₃), 0.92 (3H, t, *J* = 7.2 Hz, H-16) ppm; **¹³C NMR** (100 MHz, C₆D₆) δ 177.8 (C-14), 142.3 (C-9), 137.3 (C-Ar), 132.8 (C-2), 130.9 (C-3), 129.4 (2CH-Ar), 129.2 (2CH-Ar), 125.8 (CH-Ar), 121.1 (C-8), 73.7 (C-1), 64.8 (C-12), 60.6 (C-

15), 47.0 (C-13), 38.6 (C-4), 37.7 (C-6), 35.2 (C-10), 31.2 (C-7), 30.6 (C-5), 21.9 (C-11), 18.3 (OSi(CH₂CH₃)₂)₃, 14.1 (C-16), 12.2 (OSi(CH₂CH₃)₂)₃, 12.1 (C-17) ppm; HRMS (APCI) *m/z* calcd for C₃₈H₄₂O₃SSi (M-H₂O+H⁺) 540.3093, found 540.3181.

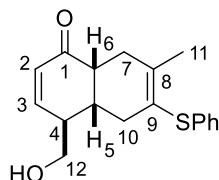
Ethyl 2-((4*S,4*aR**,8*aR**)-1-hydroxy-4-(hydroxymethyl)-7-methyl-6-(phenylthio)-1,4,4*a*,5,8,8*a*-hexahydronaphthalen-1-yl)propanoate (**236**)**



To a solution of enone *cis*-decalin **229** (22 mg, 0.048 mmol) in CH₂Cl₂ (1.0 mL) at -78 °C was added TBSOTf (17 μL, 0.072 mmol, 1.5 equiv). The mixture was stirred at same temperature for 2 minutes before being added a solution of TMS-silylketene acetal **174** (15 mg, 0.072 mmol, 1.5 equiv) in CH₂Cl₂ (0.2 mL). The reaction mixture was stirred under N₂ atmosphere at -78 °C for 2 hours before being quenched with 2 M HCl (1.0 mL) and warmed to room temperature. The organic layer was separated, and the aqueous layer was extracted with CH₂Cl₂ (3 x 3 mL). The combined organic layers were washed with brine, dried over anhydrous Na₂SO₄ and concentrated *in vacuo*. The crude product was purified by silica gel flash column chromatography (10–40% EtOAc/hexane) to afford diol **236** as a light yellow oil (5 mg, 27% yield): *R_f* = 0.31 (40% EtOAc/hexane); IR (ATR) ν_{\max} 3463 (O-H), 2923, 1709 (C=O), 1477, 1374, 1336, 1189, 1023, 742, 693 cm⁻¹; ¹H NMR (400 MHz, C₆D₆) δ 7.25 (2H, dd, *J* = 7.4, 1.2 Hz, Ar-H), 7.04 (2H, t, *J* = 7.4 Hz, Ar-H), 6.94 (1H, tt, *J* = 7.4, 1.2 Hz, Ar-H), 5.76 (1H, ddd, *J* = 10.4, 2.0, 2.0 Hz, H-2), 5.53 (1H, dd, *J* = 10.4, 2.4 Hz, H-3), 3.93–3.79 (2H, m, H-15), 3.18 (1H, dd, *J* = 10.6, 3.5 Hz, H-12), 3.01 (1H, dd, *J* = 10.6, 5.6 Hz, H-12), 2.69 (1H, q, *J* = 7.2 Hz, H-13), 2.57 (1H, dd, *J* = 18.4, 5.2 Hz, H-7), 2.47–2.24 (3H, m, H-7 + H-10), 2.24–2.16 (1H, m, H-6), 2.03–1.97 (1H, m, H-4), 1.97 (3H, s, H-11), 1.80–1.72 (1H, m, H-5), 1.15 (3H, d, *J* = 7.2 Hz, H-17), 0.87 (3H, t, *J* = 7.2 Hz, H-16) ppm; ¹³C NMR (100 MHz, C₆D₆) δ 177.6 (C-14), 142.3 (C-9), 137.4 (C-Ar), 133.4 (C-2), 129.8 (C-3), 129.1 (2CH-Ar), 128.4 (2CH-Ar), 125.8 (CH-Ar), 121.0 (C-9), 73.6 (C-1), 63.8 (C-12), 60.7 (C-15), 47.0 (C-13), 38.4 (C-4), 37.7

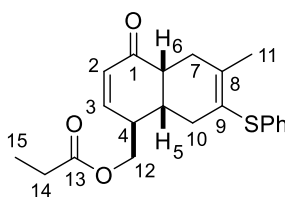
(C-6), 35.1 (C-10), 31.2 (C-7), 30.9 (C-5), 21.8 (C-11), 14.0 (C-16), 12.1 (C-17) ppm; **HRMS** (APCI) m/z calcd for $C_{23}H_{29}O_3S$ ($M-H_2O+H^+$) 385.1832, found 385.1821.

(4*S,4*aR**,8*aR**)-4-(Hydroxymethyl)-7-methyl-6-(phenylthio)-4*a*,5,8,8*a*-tetrahydronaphthalen-1(4*H*)-one (253)**



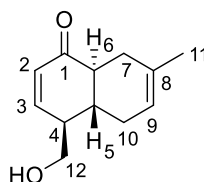
Alcohol **253** was prepared from enone **229** (35 mg, 0.076 mmol) using the general procedure for TIPS deprotection (see page 141). The crude residue was purified by silica gel flash column chromatography (40% EtOAc/hexane) to deliver alcohol **253** as a light brown oil (22 mg, 93% yield): $R_f = 0.10$ (40% EtOAc/hexane); **IR** (ATR) ν_{max} 3418 (O-H), 2915, 1672 (C=O ketone), 1477, 1439, 1391, 1205, 1026, 742, 692 cm^{-1} ; **1H NMR** (400 MHz, $CDCl_3$) δ 7.29–7.22 (2H, m, Ar-H), 7.18–7.11 (3H, m, Ar-H), 6.80 (1H, dd, $J = 10.2, 3.8$ Hz, H-3), 6.02 (1H, dd, $J = 10.2, 1.8$ Hz, H-2), 3.79 (1H, dd, $J = 10.7, 6.0$ Hz, H-12), 3.69 (1H, dd, $J = 10.7, 5.8$ Hz, H-12), 2.90 (1H, ddd, $J = 6.1, 5.4, 4.4$ Hz, H-6), 2.72 (1H, dd, $J = 18.0, 5.4$ Hz, H-7), 2.54 (1H, dddd, $J = 6.1, 6.1, 5.5, 5.5$ Hz, H-5), 2.45 (1H, ddddd, $J = 6.0, 5.8, 5.5, 3.8, 1.8$ Hz, H-4), 2.31–2.19 (3H, m, H-7 + H-10), 2.00 (3H, s, H-11) ppm; **^{13}C NMR** (100 MHz, $CDCl_3$) δ 200.4 (C-1), 148.9 (C-3), 140.7 (C-9), 136.2 (C-Ar), 129.2 (C-2), 129.1 (2CH-Ar), 128.6 (2CH-Ar), 125.8 (CH-Ar), 121.6 (C-8), 63.2 (C-12), 43.2 (C-6), 41.7 (C-4), 35.1 (C-5), 33.7 (C-10), 31.3 (C-7), 21.5 (C-11) ppm; **HRMS** (APCI) m/z calcd for $C_{18}H_{21}O_2S$ ($M+H^+$) 301.1262, found 301.1266.

((1*S,4*aR**,8*aR**)-6-Methyl-4-oxo-7-(phenylthio)-1,4,4*a*,5,8,8*a*-hexahydronaphthalen-1-yl)methyl propionate (254)**



Propionate **254** was prepared from alcohol **253** (21 mg, 0.07 mmol) using the general procedure for propionate formation (see page 142). The crude residue was purified by silica gel flash column chromatography (10–20% EtOAc/hexane) to give propionate **254** as a light yellow oil (20 mg, 78% yield): R_f = 0.29 (20% EtOAc/hexane); IR (ATR) ν_{\max} 2921, 2851, 1739 (C=O ester), 1682 (C=O ketone), 1477, 1179, 1084, 742 cm^{-1} ; $^1\text{H NMR}$ (400 MHz, CDCl_3) δ 7.29–7.21 (2H, m, Ar-H), 7.18–7.11 (3H, m, Ar-H), 6.70 (1H, dd, J = 10.2, 3.8 Hz, H-3), 6.02 (1H, dd, J = 10.2, 1.8 Hz, H-2), 4.26 (1H, dd, J = 11.2, 6.2 Hz, H-12), 4.07 (1H, dd, J = 11.2, 5.9 Hz, H-12), 2.88 (1H, ddd, J = 6.1, 5.2, 4.1 Hz, H-6), 2.73 (1H, dd, J = 18.2, 5.2 Hz, H-7), 2.60 (1H, ddd, J = 6.2, 5.9, 5.6, 3.8, 1.8 Hz, H-4), 2.47 (1H, dddd, 6.1, 6.1, 5.6, 5.6 Hz, H-5), 2.33 (2H, q, J = 7.6 Hz, H-14), 2.30–2.20 (3H, m, H-7 + H-10), 2.00 (3H, s, H-11), 1.14 (3H, t, J = 7.6 Hz, H-15) ppm; $^{13}\text{C NMR}$ (100 MHz, CDCl_3) δ 199.9 (C-1), 174.4 (C-13), 147.5 (C-3), 140.6 (C-9), 136.0 (C-Ar), 129.3 (C-2), 129.1 (2CH-Ar), 128.5 (2CH-Ar), 125.9 (CH-Ar), 121.5 (C-8), 64.0 (C-12), 43.0 (C-6), 38.6 (C-4), 35.5 (C-5), 33.6 (C-10), 31.2 (C-7), 27.6 (C-14), 21.5 (C-11), 9.2 (C-15) ppm; HRMS (APCI) m/z calcd for $\text{C}_{21}\text{H}_{25}\text{O}_3\text{S}$ ($\text{M}+\text{H}^+$) 357.1519, found 357.1513.

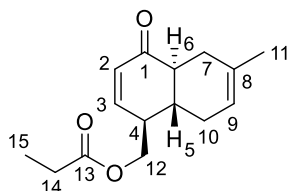
(4*S*,4*aR*,8*aS*)-4-(Hydroxymethyl)-7-methyl-4*a*,5,8,8*a*-tetrahydronaphthalen-1(4*H*)-one (256)



Alcohol **256** was prepared from enone *trans*-decalin **5** (0.29 g, 0.83 mmol) using the general procedure for TIPS deprotection (see page 141). The crude residue was purified by silica gel flash column chromatography (30–40% EtOAc/hexane) to afford alcohol **256** as a light orange oil (157 mg, 98% yield): R_f = 0.21 (40% EtOAc/hexane); $[\alpha]_D^{20}$ = +155.8 (c 0.451,

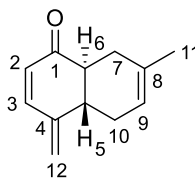
CHCl₃); IR (ATR) ν_{\max} 3413 (O-H), 2915, 2883, 1661 (C=O ketone), 1437, 1394, 1190, 1044, 780 cm⁻¹; ¹H NMR (400 MHz, CDCl₃) δ 7.01 (1H, dd, J = 10.2, 2.0 Hz, H-3), 6.10 (1H, ddd, J = 10.2, 1.8, 1.8 Hz, H-2), 5.40–5.28 (1H, m, H-9), 3.93 (1H, dd, J = 10.6, 4.1 Hz, H-12), 3.68 (1H, dd, J = 10.6, 6.4 Hz, H-12), 2.49–2.26 (4H, m, H-6 + H-4 + H-10), 2.09–1.88 (3H, m, H-5 + H-7), 1.69 (3H, s, H-11) ppm; ¹³C NMR (100 MHz, CDCl₃) δ 201.2 (C-1), 151.5 (C-3), 133.3 (C-8), 130.0 (C-2), 118.8 (C-9), 63.0 (C-12), 45.9 (C-6), 45.5 (C-4), 36.0 (C-5), 31.1 (C-7), 30.3 (C-10), 23.5 (C-11) ppm; HRMS (ESI) m/z calcd for C₁₂H₁₆NaO₂ (M+Na⁺) 215.1043, found 215.1045.

((1S,4aS,8aR)-6-Methyl-4-oxo-1,4,4a,5,8,8a-hexahydronaphthalen-1-yl)methyl propionate (252)



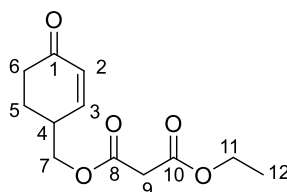
Propionate **252** was prepared from alcohol **256** (0.15 g, 0.79 mmol) using the general procedure for propionate formation (see page 142). The crude residue was purified by silica gel flash column chromatography (20% EtOAc/hexane) to give propionate **252** as a light yellow oil (194 mg, 98% yield): R_f = 0.28 (20% EtOAc/hexane); $[\alpha]_D^{20}$ = +130.3 (c 0.381, CHCl₃); IR (ATR) ν_{\max} 2909, 1738 (C=O ester), 1672 (C=O ketone), 1438, 1383, 1177, 1083, 780 cm⁻¹; ¹H NMR (400 MHz, CDCl₃) δ 6.86 (1H, dd, J = 10.2, 2.0 Hz, H-3), 6.09 (1H, dd, J = 10.2, 2.9 Hz, H-2), 5.42–5.28 (1H, m, H-9), 4.38 (1H, dd, J = 11.2, 3.8 Hz, H-12), 4.09 (1H, dd, J = 11.2, 6.3 Hz, H-12), 2.52 (1H, dddddd, J = 6.3, 5.9, 3.8, 2.9, 2.0 Hz, H-4), 2.44–2.31 (3H, m, H-6 + H-10), 2.35 (2H, q, J = 7.6 Hz, H-14), 2.09–1.94 (2H, m, H-7), 1.94–1.86 (1H, m, H-5), 1.70 (3H, s, H-11), 1.14 (3H, t, J = 7.6 Hz, H-15) ppm; ¹³C NMR (100 MHz, CDCl₃) δ 200.7 (C-1), 174.6 (C-13), 150.1 (C-3), 133.3 (C-8), 130.0 (C-2), 118.7 (C-9), 64.1 (C-12), 46.0 (C-6), 42.8 (C-4), 36.7 (C-5), 30.9 (C-7), 30.1 (C-10), 27.6 (C-14), 23.5 (C-11), 9.2 (C-15) ppm; HRMS (ESI) m/z calcd for C₁₅H₂₀NaO₃ (M+Na⁺) 271.1302, found 271.1302.

(4a*S*,8a*S*)-7-Methyl-4-methylene-4a,5,8,8a-tetrahydronaphthalen-1(4*H*)-one (257)



To a suspension of KH (9 mg, 0.23 mmol, 1.2 equiv) in DMF (1.7 mL) at $-30\text{ }^{\circ}\text{C}$, was slowly added a solution of propionate **252** (47 mg, 0.19 mmol) in DMF (6.0 mL) over 10 minutes. The reaction mixture was stirred under N_2 atmosphere at same temperature for 3.5 hours. The mixture was then quenched with H_2O (5 mL) and diluted with isopropyl ether (5 mL). The organic layer was separated, and the aqueous layer was extracted with isopropyl ether (3×5 mL). The combined organic layers were washed with brine, dried over anhydrous Na_2SO_4 and concentrated *in vacuo*. The crude product was purified by silica gel flash column chromatography (20% Et_2O /hexane) to afford conjugated enone **257** as a light yellow oil (4 mg, 14% yield): $R_f = 0.31$ (20% Et_2O /hexane); IR (ATR) ν_{max} 2958, 2920, 2854, 1670 (C=O ketone), 1584, 1434, 1288, 1118, 914 cm^{-1} ; $^1\text{H NMR}$ (400 MHz, CDCl_3) δ 7.09 (1H, d, $J = 10.0$ Hz, H-3), 5.98 (1H, d, $J = 10.0$ Hz, H-2), 5.45–5.40 (1H, m, H-9), 5.38 (1H, d, $J = 2.7$ Hz, H-12), 5.33 (1H, d, $J = 2.7$ Hz, H-12), 2.69–2.59 (1H, m, H-5), 2.51–2.38 (3H, m, H-6 + H-10), 2.27–2.08 (2H, m, H-7), 1.71 (3H, s, H-11) ppm; $^{13}\text{C NMR}$ (100 MHz, CDCl_3) δ 200.9 (C-1), 147.7 (C-3), 144.7 (C-4), 133.2 (C-8), 127.5 (C-2), 118.9 (C-9), 118.8 (C-12), 46.1 (C-6), 37.9 (C-5), 30.7 (C-10), 29.5 (C-7), 23.5 (C-11) ppm; HRMS (ESI) m/z calcd for $\text{C}_{12}\text{H}_{14}\text{NaO}$ ($\text{M}+\text{Na}^+$) 197.0942, found 197.0930.

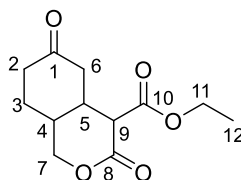
Ethyl ((4-oxocyclohex-2-en-1-yl)methyl) malonate (*rac*-270)



Racemic malonate **270** was prepared from *rac*-alcohol **193** (96 mg, 0.76 mmol) using the general procedure for malonate formation (see page 142). The crude residue was purified by silica gel flash column chromatography (20–30% EtOAc /hexane) to give racemic malonate **270** as a yellow oil (158 mg, 86% yield): $R_f = 0.18$ (30% EtOAc /hexane); IR (ATR)

ν_{\max} 2956, 1730 (C=O ester), 1677 (C=O ketone), 1331, 1269, 1144, 1030 cm^{-1} ; $^1\text{H NMR}$ (400 MHz, CDCl_3) δ 6.83 (1H, ddd, $J = 10.2, 2.3, 1.2$ Hz, H-3), 6.04 (1H, dd, $J = 10.2, 2.5$ Hz, H-2), 4.22 (1H, dd, $J = 11.0, 6.5$ Hz, H-7), 4.17 (2H, q, $J = 7.2$ Hz, H-11), 4.13 (1H, dd, $J = 11.0, 6.5$ Hz, H-7), 3.38 (2H, s, H-9), 2.81 (1H, dddddd, $J = 9.9, 6.5, 6.5, 5.0, 2.5, 2.3$ Hz, H-4), 2.52 (1H, ddd, $J = 16.9, 4.8, 4.8$ Hz, H-6), 2.37 (1H, ddd, $J = 16.9, 12.5, 5.0$ Hz, H-6), 2.12 (1H, dddddd, $J = 13.2, 5.0, 5.0, 4.8, 1.2$ Hz, H-5), 1.80 (1H, dddd, $J = 13.2, 12.5, 9.9, 4.8$ Hz, H-5), 1.25 (3H, t, $J = 7.2$ Hz, H-12) ppm; $^{13}\text{C NMR}$ (100 MHz, CDCl_3) δ 198.8 (C-1), 166.5 (C-8), 166.4 (C-10), 149.5 (C-3), 130.8 (C-2), 66.9 (C-11), 61.8 (C-7), 41.5 (C-9), 36.5 (C-6), 35.8 (C-4), 25.6 (C-5), 14.1 (C-12) ppm; **HRMS** (ESI) m/z calcd for $\text{C}_{12}\text{H}_{16}\text{NaO}_5$ ($\text{M}+\text{Na}^+$) 263.0890, found 263.0891.

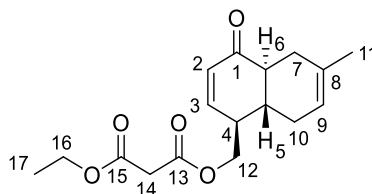
Ethyl 3,6-dioxooctahydro-1*H*-isochromene-4-carboxylate (*rac*-**272**)



To a solution of racemic malonate **270** (52 mg, 0.22 mmol) and $\text{La}(\text{O}-i\text{-Pr})_3$ (75 mg, 0.23 mmol, 1.0 equiv) in THF (1.2 mL), was stirred under N_2 atmosphere at room temperature for 20 minutes before being added freshly distilled diisopropyl ethylamine (0.080 mL, 0.45 mmol, 2.0 equiv). The reaction mixture was stirred at 40 °C for 6 hours and cooled to room temperature. The mixture was quenched with a saturated aqueous solution of NH_4Cl (5 mL) and diluted with EtOAc (5 mL). The organic layer was separated, and the aqueous layer was extracted with EtOAc (3 x 10 mL). The combined organic layers were washed with brine, dried over anhydrous Na_2SO_4 and concentrated *in vacuo*. The crude product was purified by silica gel flash column chromatography (50% EtOAc/hexane) to yield lactone **272** as a light yellow oil (41 mg, 78% yield): $R_f = 0.35$ (80% EtOAc/hexane); **IR** (ATR) ν_{\max} 2924, 1716 (C=O ester), 1303, 1251, 1214, 1154, 1041 cm^{-1} ; $^1\text{H NMR}$ (400 MHz, CDCl_3) δ 4.43 (1H, dd, $J = 11.8, 4.6$ Hz, H-7), 4.26 (2H, q, $J = 7.2$ Hz, H-11), 4.22 (1H, dd, $J = 11.8, 7.4$ Hz, H-7), 3.31 (1H, d, $J = 10.1$ Hz, H-9), 3.04–2.93 (1H, m, H-5), 2.54–2.45 (3H, m, H-2 + H-6 + H-4), 2.36 (1H, ddd, $J = 17.1, 11.9, 5.1$ Hz, H-2), 2.32–2.24 (1H, m, H-6), 2.01 (1H, dddd, $J = 14.0, 5.1, 5.1, 5.1$ Hz, H-3), 1.81 (1H, dddd, $J = 14.0, 11.9, 11.9, 4.7$ Hz, H-3), 1.30 (3H, t, $J = 7.2$ Hz, H-12) ppm; $^{13}\text{C NMR}$ (100 MHz, CDCl_3) δ 208.5 (C-1), 167.9 (C-8), 167.1 (C-10), 70.6 (C-7),

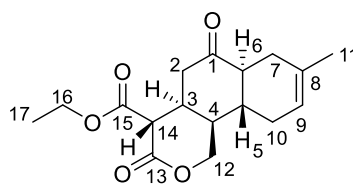
62.4 (C-11), 51.0 (C-9), 42.5 (C-6), 38.3 (C-2), 33.4 (C-5), 31.4 (C-4), 23.2 (C-3), 14.2 (C-12) ppm; **HRMS** (ESI) m/z calcd for $C_{12}H_{16}NaO_5$ ($M+Na^+$) 263.0890, found 263.0891.

Ethyl (((1*S*,4*aS*,8*aR*)-6-methyl-4-oxo-1,4,4*a*,5,8,8*a*-hexahydronaphthalen-1-yl)methyl)malonate (6**)**



Malonate **6** was prepared from alcohol **256** (0.18 g, 0.93 mmol) using the general procedure for malonate formation (see page 142). The crude residue was purified by silica gel flash column chromatography (20–40% EtOAc/hexane) to give malonate **6** as a light yellow oil (243 mg, 85% yield): R_f = 0.49 (40% EtOAc/ hexane); $[\alpha]_D^{20}$ = +127.7 (c 0.315, $CHCl_3$); **IR** (ATR) ν_{max} 2920, 1734 (C=O ester), 1673 (C=O ketone), 1330, 1268, 1149, 1033 cm^{-1} ; **1H NMR** (400 MHz, $CDCl_3$) δ 6.85 (1H, dd, J = 10.2, 2.1 Hz, H-3), 6.09 (1H, dd, J = 10.2, 2.8 Hz, H-2), 5.40–5.30 (1H, m, H-9), 4.44 (1H, dd, J = 11.2, 3.8 Hz, H-12), 4.20 (1H, dd, J = 11.2, 6.6 Hz, H-12), 4.18 (2H, q, J = 7.2 Hz, H-16), 3.39 (2H, s, H-14), 2.59–2.50 (1H, m, H-4), 2.46–2.32 (3H, m, H-6 + H-10), 2.10–1.85 (3H, m, H-7 + H-5), 1.69 (3H, s, H-11), 1.26 (3H, t, J = 7.2 Hz, H-17) ppm; **^{13}C NMR** (100 MHz, $CDCl_3$) δ 200.4 (C-1), 166.7 (C-13), 166.4 (C-15), 149.6 (C-3), 130.3 (C-8), 130.2 (C-2), 118.6 (C-9), 65.2 (C-12), 61.8 (C-16), 46.0 (C-6), 42.6 (C-4), 41.6 (C-14), 36.6 (C-5), 30.9 (C-7), 30.1 (C-10), 23.5 (C-11), 14.2 (C-17) ppm; **HRMS** (ESI) m/z calcd for $C_{17}H_{22}NaO_5$ ($M+Na^+$) 329.1359, found 329.1360.

Ethyl (4*S*,4*aS*,6*aS*,10*aR*,10*bR*)-8-methyl-3,6-dioxo-3,4,4*a*,5,6,6*a*,7,10,10*a*,10*b*-decahydro-1*H*-benzo[*h*]isochromene-4-carboxylate (259**)**



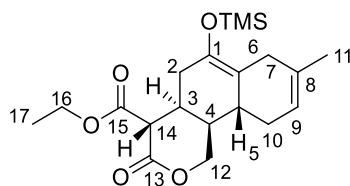
Method A: To a suspension of NaH (3 mg, 0.067 mmol, 1.1 equiv, 60% w/w in mineral oil) in DMF (1.0 mL) at 0 °C, was added a solution of malonate **6** (19 mg, 0.061 mmol) in DMF (2.5 mL). The reaction mixture was stirred at 0 °C for 1 hour and allowed to reach room temperature for 4 hours. The mixture was then quenched with H₂O (3 mL) and diluted with isopropyl ether (5 mL). The organic layer was separated, and the aqueous layer was extracted with isopropyl ether (3 × 3 mL). The combined organic layers were washed with brine, dried over anhydrous Na₂SO₄ and concentrated *in vacuo*. The crude product was purified by silica gel flash column chromatography (20–40% EtOAc/hexane) to furnish tricyclic lactone **259** (6 mg, 30% yield, 38% based on recovered malonate **6**).

Method B: To a mixture of malonate **6** (46 mg, 0.15 mmol) and La(O-*i*-Pr)₃ (53 mg, 0.16 mmol, 1.0 equiv) in THF (1.2 mL), was stirred under N₂ atmosphere at room temperature for 10 minutes. Freshly distilled *i*-Pr₂NEt (0.052 mL, 0.31 mmol, 2.0 equiv) was then added. The reaction mixture was stirred at 40 °C for a further 7 hours. The mixture was then cooled to room temperature, quenched with saturated aqueous solution of NaHCO₃ (3 mL) and diluted with EtOAc (3 mL). The organic layer was separated, and the aqueous layer was extracted with EtOAc (5 × 3 mL). The combined organic layers were washed with brine, dried over anhydrous Na₂SO₄ and concentrated *in vacuo*. The crude product was purified by silica gel flash column chromatography (Et₂O:CH₂Cl₂:hexane = 15:40:45) to afford tricyclic lactone **259** (35 mg, 75% yield).

Tricyclic lactone 259 (a white solid): *R*_f = 0.23 (40% EtOAc/hexane); [α]_D²⁰ = +91.8 (c 0.257, CHCl₃); IR (ATR) ν_{max} 2961, 2916, 1729 (C=O ester), 1437, 1235, 1154, 1035 cm⁻¹. ¹H NMR (400 MHz, CDCl₃) δ 5.39–5.31 (1H, m, H-9), 4.46 (2H, d, *J* = 3.5 Hz, H-12), 4.27 (2H, qd, *J* = 7.2, 1.6 Hz, H-16), 3.27 (1H, d, *J* = 11.4 Hz, H-14), 3.10 (1H, dddd, *J* = 11.4, 5.5, 5.5, 5.0 Hz, H-3), 2.66 (1H, dd, *J* = 14.6, 5.5 Hz, H-2), 2.44–2.31 (3H, m, H-6 + H-10 + H-2), 2.20–2.10 (3H, m, H-4 + H-7), 1.98–1.85 (1H, m, H-10), 1.79 (1H, dddd, *J* = 11.2, 11.2, 11.2, 4.8 Hz, H-5), 1.68 (3H, s, H-11), 1.31 (3H, t, *J* = 7.2 Hz, H-17) ppm; ¹³C NMR (100 MHz, CDCl₃) δ 209.1

(C-1), 168.3 (C-15), 166.3 (C-13), 133.4 (C-8), 118.3 (C-9), 69.1 (C-12), 62.5 (C-16), 50.7 (C-14), 48.8 (C-6), 43.7 (C-2), 38.9 (C-4), 36.5 (C-3), 34.4 (C-5), 31.5 (C-10), 29.7 (C-7), 23.4 (C-11), 14.2 (C-17) ppm; **HRMS** (ESI) m/z calcd for $C_{17}H_{22}NaO_5$ ($M+Na^+$) 329.1359, found 329.1363.

Ethyl (4a*S*,10a*R*,10b*S*)-8-methyl-3-oxo-6-((trimethylsilyl)oxy)-3,4,4a,5,7,10,10a,10b-octahydro-1*H*-benzo[*h*]isochromene-4-carboxylate (273)

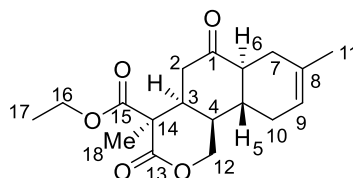


To a solution of malonate **6** (47 mg, 0.15 mmol) and $MgCl_2$ (30 mg, 0.31 mmol, 2.0 equiv) in DCE (1.6 mL), was added Et_3N (0.13 mL, 0.92 mmol, 6.0 equiv). The reaction mixture was stirred at room temperature for 30 minutes before being added $TMSCl$ (0.1 mL, 0.77 mmol, 5.0 equiv). The reaction mixture was stirred at the same temperature for 2 hours. Another portion of $MgCl_2$ (32 mg, 0.33 mmol, 2.0 equiv), Et_3N (0.13 mL, 0.92 mmol, 6.0 equiv) and $TMSCl$ (0.1 mL, 0.77 mmol, 5.0 equiv) were added. The reaction mixture was then heated to 40 °C. After 16 hours, the reaction mixture was cooled to room temperature and quenched with saturated aqueous solution of $NaHCO_3$ (3 mL) and diluted with CH_2Cl_2 (3 mL). The organic layer was separated, and the aqueous layer was extracted with CH_2Cl_2 (3 × 3 mL). The combined organic layers were washed with brine (10 mL), dried over Na_2SO_4 and concentrated *in vacuo*. which was directly used for the next step without purification to give a mixture of silyl enol ether **273** and lactone **259** with a 3.5:1 ratio.

Silyl enol ether **273** (a light yellow oil): R_f = 0.45 (40% EtOAc/hexane); **IR** (ATR) ν_{max} 2958, 2918, 1729 (C=O ester), 1252, 1152, 1060, 875, 844 cm^{-1} ; **1H NMR** (400 MHz, $CDCl_3$) δ 5.41–5.34 (1H, m, H-9), 4.42 (1H, dd, J = 11.6, 4.6 Hz, H-12), 4.38 (1H, dd, J = 11.6, 5.8 Hz, H-12), 4.25 (2H, q, J = 7.0 Hz, H-16), 3.48 (H, d, J = 7.8 Hz, H-14), 3.02–2.91 (1H, m, H-10), 2.74–2.66 (1H, m, H-3), 2.47–2.34 (2H, m, H-10 + H-7), 2.33–2.24 (1H, m, H-2), 2.21–2.12 (1H, m, H-5), 2.00–1.89 (2H, m, H-7 + H-4), 1.87–1.76 (1H, m, H-2), 1.67 (3H, s, H-11), 1.30 (3H, t, J = 7.0 Hz, H-17), 0.18 (9H, s, $OSi(CH_3)_3$) ppm; **^{13}C NMR** (100 MHz, $CDCl_3$) δ 169.1 (C-15), 166.6 (C-13), 138.8 (C-1), 133.5 (C-8), 119.4 (C-9), 113.6 (C-6), 70.9 (C-12), 62.2 (C-16), 51.2

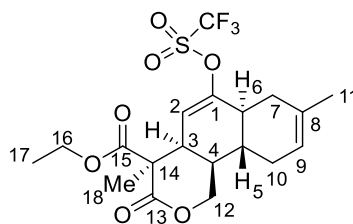
(C-14), 35.0 (C-4), 33.0 (C-3), 32.7 (C-2), 32.5 (C-7), 31.8 (C-5), 31.2 (C-10), 23.3 (C-11), 14.2 (C-17), 0.84 (OSi(CH₃)₃) ppm; **HRMS** (ESI) *m/z* calcd for C₂₀H₃₀NaO₅Si (M+Na⁺) 401.1755, found 401.1768.

Ethyl (4*R*,4*aS*,6*aS*,10*aR*,10*bR*)-4,8-dimethyl-3,6-dioxo-3,4,4*a*,5,6,6*a*,7,10,10*a*,10*b*-decahydro-1*H*-benzo[*h*]isochromene-4-carboxylate (7)



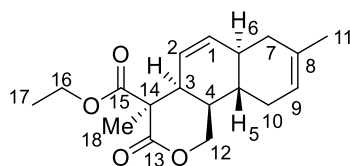
To a solution of tricyclic lactone **259** (14 mg, 0.045 mmol) in THF (1.5 mL) at 0 °C, was added NaH (4 mg, 0.07 mmol, 1.5 equiv, 60% in mineral oil) in one portion. The reaction mixture was stirred at same temperature for 5 minutes, and then added methyl iodide (0.01 mL, 0.09 mmol, 2.0 equiv). The reaction mixture was warmed to room temperature and stirred for 6 hours before being quenched with saturated aqueous solution of NH₄Cl (3 mL) and diluted with EtOAc (3 mL). The organic layer was separated, and the aqueous layer was extracted with EtOAc (3 × 5 mL). The combined organic layers were washed with brine, dried over anhydrous Na₂SO₄ and concentrated *in vacuo*. The crude product was purified by silica gel flash column chromatography (20–40% EtOAc/hexane) to deliver tricyclic lactone **7** as a yellow oil (10 mg, 71% yield): *R_f* = 0.23 (40% EtOAc/hexane); [α]_D²⁰ = +94.9 (c 0.889, CHCl₃); **IR** (ATR) ν_{max} 2915, 1730 (C=O ester), 1711 (C=O ester), 1675 (C=O ketone), 1448, 1369, 1224, 1113, 1023 cm⁻¹; **¹H NMR** (400 MHz, CDCl₃) δ 5.41–5.29 (1H, m, H-9), 4.40 (1H, dd, *J* = 12.0, 4.2 Hz, H-12), 4.31–4.25 (1H, m, H-12), 4.24 (1H, dq, *J* = 10.8, 7.2 Hz, H-16), 4.08 (1H, dq, *J* = 10.8, 7.2 Hz, H-16), 3.09 (1H, dd, *J* = 15.0, 7.4 Hz, H-2), 2.55–2.40 (2H, m, H-2 + H-3), 2.32–2.17 (2H, m, H-7 + H-10), 2.17–2.06 (3H, m, H-6 + H-5 + H-4), 2.06–1.95 (1H, m, H-7), 1.86–1.74 (1H, m, H-10), 1.68 (3H, s, H-11), 1.55 (3H, s, H-18), 1.26 (3H, t, *J* = 7.2 Hz, H-17) ppm; **¹³C NMR** (100 MHz, CDCl₃) δ 210.9 (C-1), 171.3 (C-13), 170.7 (C-15), 133.6 (C-8), 118.9 (C-9), 68.4 (C-12), 62.2 (C-16), 52.2 (C-14), 48.6 (C-6), 40.5 (C-5), 38.8 (C-2), 38.2 (C-3), 34.0 (C-4), 31.0 (C-7), 30.8 (C-10), 23.5 (C-18), 23.4 (C-11), 13.9 (C-17) ppm; **HRMS** (ESI) *m/z* calcd for C₁₈H₂₄NaO₅ (M+Na⁺) 343.1516, found 343.1510.

Ethyl (4*R*,4*aR*,6*aS*,10*aR*,10*bR*)-4,8-dimethyl-3-oxo-6-(((trifluoromethyl)sulfonyl)oxy)-3,4,4*a*,6*a*,7,10,10*a*,10*b*-octahydro-1*H*-benzo[*h*]isochromene-4-carboxylate (282**)**

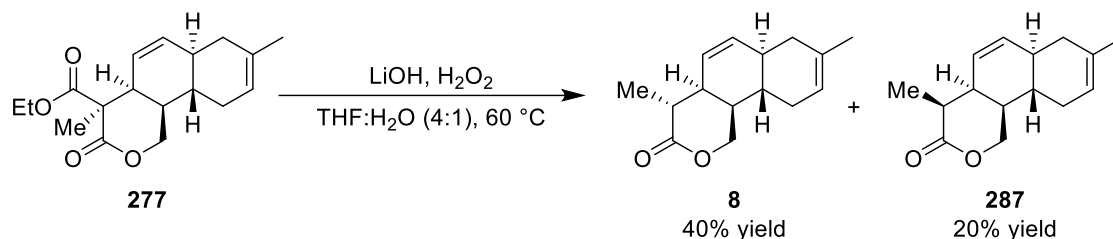


To a solution of freshly distilled diisopropylamine (0.2 mL, 1.43 mmol, 1.5 equiv) in THF (1.5 mL), was cooled to $-78\text{ }^{\circ}\text{C}$ and added *n*-BuLi (0.6 mL of a 2.5 M solution in hexane, 1.5 mmol, 1.5 equiv) dropwise. The stock solution of LDA was stirred at $-78\text{ }^{\circ}\text{C}$ for 45 minutes before adding dropwise into a solution of ketone **7** (32 mg, 0.099 mmol) in THF (0.29 mL). The mixture was stirred at $-78\text{ }^{\circ}\text{C}$ for 2 hours before adding a solution of *N*-(5-chloro-2-pyridyl)triflimide (61 mg, 0.15 mmol, 1.5 equiv) in THF (0.1 mL). The reaction mixture was stirred at $-78\text{ }^{\circ}\text{C}$ for 20 minutes and allowed to warm up to room temperature. The reaction mixture was quenched with H_2O (3 mL) and diluted with Et_2O (3 mL). The organic layer was separated, and the aqueous layer was extracted with Et_2O (3 x 5 mL). The combined organic layers were washed with brine, dried over anhydrous Na_2SO_4 and concentrated *in vacuo*. The crude product was purified by silica gel flash column chromatography (10–30% EtOAc /hexane) to afford vinyl triflate **282** as a light yellow oil (28 mg, 62% yield): $R_f = 0.29$ (30% EtOAc /hexane); $[\alpha]_D^{20} = +42.6$ (c 0.996, CHCl_3); **IR** (ATR) ν_{max} 2924, 2854, 1737 (C=O ester), 1418, 1214, 1143, 920 cm^{-1} ; **$^1\text{H NMR}$** (400 MHz, CDCl_3) δ 5.89–5.81 (1H, dd, $J = 4.3, 2.2$ Hz, H-2), 5.42–5.32 (1H, m, H-9), 4.50 (1H, dd, $J = 12.3, 7.1$ Hz, H-12), 4.20 (2H, qd, $J = 7.0, 1.2$ Hz, H-16), 4.09 (1H, dd, $J = 12.3, 9.2$ Hz, H-12), 2.76–2.68 (1H, m, H-3), 2.49–2.37 (1H, m, H-6), 2.32–2.23 (2H, m, H-10), 2.23–2.15 (1H, m, H-4), 2.15–2.05 (1H, m, H-7), 2.02–1.87 (1H, m, H-7), 1.81–1.73 (1H, m, H-5), 1.71 (3H, s, H-11), 1.64 (3H, s, H-18), 1.33–1.15 (3H, m, H-17) ppm; **$^{13}\text{C NMR}$** (100 MHz, CDCl_3) δ 171.1 (C-13), 170.4 (C-15), 152.2 (C-1), 133.0 (C-8), 119.6 (C-9), 115.8 (C-2), 68.0 (C-12), 62.4 (C-16), 53.0 (C-14), 40.7 (C-3), 38.4 (C-6), 35.9 (C-5), 35.4 (C-4), 32.5 (C-10), 30.4 (C-7), 23.5 (C-11), 22.3 (C-18), 14.1 (C-17) ppm; **HRMS** (ESI) m/z calcd for $\text{C}_{19}\text{H}_{23}\text{F}_3\text{NaO}_7\text{S}$ ($\text{M}+\text{Na}^+$) 475.1009, found 475.1010.

Ethyl (4*R*,4*aS*,6*aR*,10*aS*,10*bR*)-4,8-dimethyl-3-oxo-3,4,4*a*,6*a*,7,10,10*a*,10*b*-octahydro-1*H*-benzo[*h*]isochromene-4-carboxylate (277)

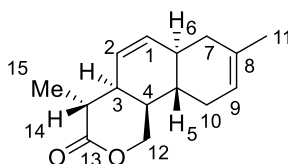


To a solution of vinyl triflate **282** (24 mg, 0.052 mmol) in DMF (3.2 mL) were added tributylamine (0.045 mL, 0.18 mmol, 3.5 equiv), Pd(OAc)₂(PPh₃)₂ (4 mg, 0.049 mmol, 0.095 equiv), followed by formic acid (0.006 mL, 0.13 mmol, 2.5 equiv). The reaction mixture was stirred at 50 °C for 2.5 hours. After this time, the reaction mixture was cooled to room temperature, quenched with H₂O (5 mL) and diluted with isopropyl ether (5 mL). The organic layer was separated, and the aqueous layer was extracted with isopropyl ether (3 × 5 mL). The combined organic layers were washed with brine, dried over anhydrous Na₂SO₄ and concentrated *in vacuo*. The crude product was purified by silica gel flash column chromatography (10–15% EtOAc/hexane) to give tricyclic lactone **277** as a yellow oil (12 mg, 75% yield): *R_f* = 0.23 (20% EtOAc/hexane); [α]_D²⁰ = +50.3 (c 0.885, CHCl₃); IR (ATR) ν_{max} 2913, 1737 (C=O ester), 1447, 1378, 1228, 1109, 1025 cm⁻¹; ¹H NMR (400 MHz, CDCl₃) δ 5.84–5.72 (2H, m, H-1 + H-2), 5.39–5.29 (1H, m, H-9), 4.48 (1H, dd, *J* = 12.2, 7.2 Hz, H-12), 4.23–4.06 (3H, m, H-12 + H-16), 2.50–2.41 (1H, m, H-3), 2.19–2.12 (1H, m, H-4), 2.12–1.96 (3H, m, H-6 + H-10), 1.67 (3H, s, H-11), 1.63 (3H, s, H-18), 1.43–1.36 (1H, m, H-7), 1.36–1.31 (1H, m, H-5), 1.27–1.24 (1H, m, H-7), 1.24 (3H, t, *J* = 7.2 Hz, H-17) ppm; ¹³C NMR (100 MHz, CDCl₃) δ 172.5 (C-15), 171.0 (C-13), 134.2 (C-8), 133.6 (C-2), 123.1 (C-1), 119.9 (C-9), 68.7 (C-12), 61.9 (C-16), 53.4 (C-14), 41.2 (C-3), 36.8 (C-10), 36.7 (C-4), 36.1 (C-6), 34.6 (C-5), 30.1 (C-7), 23.5 (C-11), 22.4 (C-18), 14.1 (C-17) ppm; HRMS (ESI) *m/z* calcd for C₁₈H₂₄NaO₄ (M+Na⁺) 327.1567, found 327.1571.



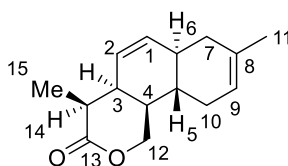
To a solution of ester **277** (15 mg, 0.048 mmol) in 0.5 mL of THF:H₂O (4:1), were added H₂O₂ (0.022 mL, 0.19 mmol, 4.0 equiv), followed by LiOH (2 mg, 0.09 mmol, 2.0 equiv). The reaction mixture was stirred at 60 °C for 5 hours before being added another portion of LiOH (2 mg, 0.09 mmol, 2.0 equiv). The reaction mixture was stirred for a further 1.5 hours and allowed to reach room temperature. The mixture was diluted with Et₂O (5 mL) and washed with aqueous solution of 5% metasodium bisulfite (5 mL) and brine (5 mL). The organic layer was dried over anhydrous Na₂SO₄ and concentrated *in vacuo*. The crude product was purified by silica gel flash column chromatography (10–20% EtOAc/hexane) to deliver tricyclic lactone **8** (5 mg, 40% yield) and tricyclic lactone **287** (2 mg, 20% yield).

(4*R*,4*aS*,6*aR*,10*aS*,10*bR*)-4,8-Dimethyl-1,4,4*a*,6*a*,7,10,10*a*,10*b*-octahydro-3*H*-benzo[*h*]isochromen-3-one (8**)**

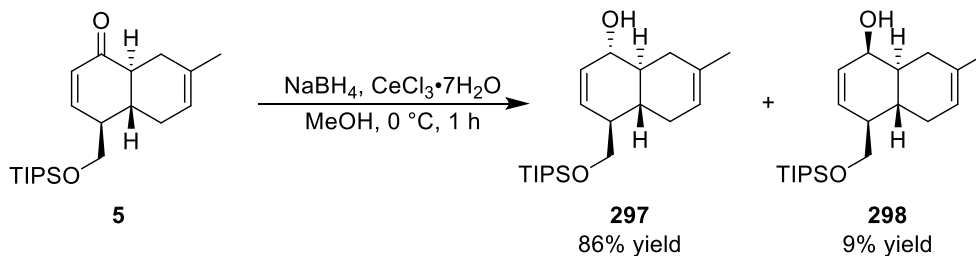


Lactone 8 (a light yellow oil): $R_f = 0.40$ (30% EtOAc/hexane); $[\alpha]_D^{20} = +81.2$ (c 0.222, CHCl₃); **IR** (ATR) ν_{max} 2960, 2920, 1744 (C=O ester), 1440, 1261, 1176, 1103, 790 cm⁻¹; **¹H NMR** (400 MHz, CDCl₃) δ 5.72 (1H, ddd, $J = 10.0, 2.1, 2.1$ Hz, H-1), 5.57 (1H, ddd, $J = 10.0, 3.1, 3.1$ Hz, H-2), 5.41–5.34 (1H, m, H-9), 4.39 (1H, dd, $J = 11.6, 3.4$ Hz, H-12), 4.33 (1H, dd, $J = 11.6, 3.0$ Hz, H-12), 2.95 (1H, dddd, $J = 10.1, 8.9, 3.1, 2.1$ Hz, H-3), 2.84 (1H, dq, $J = 10.1, 7.0$ Hz, H-14), 2.35–2.27 (2H, m, H-7), 2.09–1.91 (5H, m, H-4 + H-5 + H-6 + H-10), 1.65 (3H, s, H-11), 1.23 (3H, d, $J = 7.0$ Hz, H-15) ppm; **¹³C NMR** (100 MHz, CDCl₃) δ 176.1 (C-13), 134.8 (C-1), 133.9 (C-8), 124.1 (C-2), 120.1 (C-9), 67.3 (C-12), 38.7 (C-4), 37.3 (C-14), 37.1 (C-10), 35.5 (C-3), 33.3 (C-5), 30.5 (C-6), 30.2 (C-7), 23.5 (C-11), 12.6 (C-15) ppm; **HRMS** (ESI) m/z calcd for C₁₅H₂₀NaO₂ (M+Na⁺) 255.1356, found 255.1362.

(4*S*,4*aS*,6*aR*,10*aS*,10*bR*)-4,8-Dimethyl-1,4,4*a*,6*a*,7,10,10*a*,10*b*-octahydro-3*H*-benzo[*h*]isochromen-3-one (**287**)

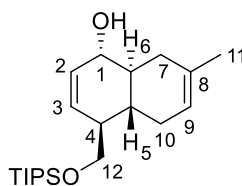


Lactone 287 (a light yellow oil): $R_f = 0.48$ (30% EtOAc/hexane); $[\alpha]_D^{20} = +37.7$ (c 0.079, CHCl_3); IR (ATR) ν_{max} 2923, 2849, 1751 (C=O ester), 1454, 1278, 1181, 1107, 787 cm^{-1} ; $^1\text{H NMR}$ (400 MHz, CDCl_3) δ 5.76–5.66 (2H, m, H-1 + H-2), 5.41–5.36 (1H, m, H-9), 4.45 (1H, dd, $J = 11.8, 6.4$ Hz, H-12), 4.07 (1H, dd, $J = 11.8, 8.0$ Hz, H-12), 2.42 (1H, dq, $J = 11.6, 6.8$ Hz, H-14), 2.27–2.19 (1H, m, H-3), 2.15–1.98 (4H, m, H-4, H-5, H-6, H-10), 1.81–1.48 (3H, m, H-7 + H-10), 1.67 (3H, s, H-11), 1.31 (3H, d, $J = 6.8$ Hz, H-15) ppm; $^{13}\text{C NMR}$ (100 MHz, CDCl_3) δ 176.3 (C-13), 134.2 (C-8), 133.5 (C-1), 125.8 (C-2), 120.1 (C-9), 69.0 (C-12), 38.7 (C-14), 38.2 (C-3), 37.0, 36.9, 36.3, 35.1, 29.9, 23.5 (C-11), 14.0 (C-15) ppm; HRMS (ESI) m/z calcd for $\text{C}_{15}\text{H}_{20}\text{NaO}_2$ ($\text{M}+\text{Na}^+$) 255.1356, found 255.1360.



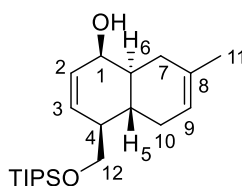
To a solution of enone *trans*-decalin **5** (52 mg, 0.15 mmol) and $\text{CeCl}_3 \cdot 7\text{H}_2\text{O}$ (62 mg, 0.16 mmol, 1.1 equiv) in MeOH (0.8 mL) at 0 °C, was added NaBH_4 (6.5 mg, 0.16 mmol, 1.1 equiv) in one portion. The reaction mixture was stirred at 0 °C for 1 hour before being quenched with saturated aqueous solution of NH_4Cl (5 mL). The mixture was then diluted with CH_2Cl_2 (5 mL). The organic layer was separated, and the aqueous layer was extracted with CH_2Cl_2 (3 x 5 mL). The combined organic layers were washed with brine, dried over anhydrous Na_2SO_4 and concentrated *in vacuo*. The crude product was purified by silica gel flash column chromatography (10–20% Et_2O /hexane) to give alcohol **297** (45 mg, 86% yield) and alcohol **298** (5 mg, 9% yield).

(1S,4S,4aR,8aS)-7-Methyl-4-(((triisopropylsilyl)oxy)methyl)-1,4,4a,5,8,8a-hexahydronaphthalen-1-ol (297)



Alcohol 297 (a light yellow oil): $R_f = 0.18$ (20% Et₂O/hexane); $[\alpha]_D^{20} = +129.9$ (c 1.02, CHCl₃); **IR** (ATR) ν_{\max} 3327 (O-H), 2946, 2865, 1463, 1389, 1115, 1092, 882, 783, 682 cm⁻¹; **¹H NMR** (400 MHz, CDCl₃) δ 5.83 (1H, ddd, $J = 10.2, 2.2, 2.2$ Hz, H-2), 5.71 (1H, ddd, $J = 10.2, 2.2, 2.2$ Hz, H-3), 5.38–5.30 (1H, m, H-9), 3.91–3.83 (1H, m, H-1), 3.80 (1H, dd, $J = 9.4, 4.4$ Hz, H-12), 3.51 (1H, dd, $J = 9.4, 7.2$ Hz, H-12), 2.44 (1H, dd, $J = 15.8, 5.0$ Hz, H-7), 2.40–2.30 (1H, m, H-10), 2.02 (1H, ddddd, $J = 7.2, 4.6, 4.4, 2.2, 2.2$ Hz, H-4), 1.84–1.72 (2H, m, H-7 + H-10), 1.67 (3H, s, H-11), 1.60–1.43 (2H, m, H-6 + H-5), 1.09–1.00 (21H, m, OSi(CH(CH₃)₂)₃) ppm; **¹³C NMR** (100 MHz, CDCl₃) δ 132.8 (C-8), 130.9 (C-2), 130.7 (C-3), 119.9 (C-9), 74.1 (C-1), 65.7 (C-12), 46.1 (C-4), 42.5 (C-6), 35.0 (C-7), 33.4 (C-5), 31.5 (C-10), 23.5 (C-11), 18.2 (OSi(CH(CH₃)₂)₃), 12.1 (OSi(CH(CH₃)₂)₃) ppm; **HRMS** (ESI) m/z calcd for C₂₁H₃₈NaO₂Si (M+Na⁺) 373.2533, found 373.2533.

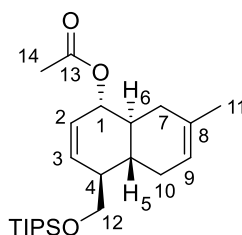
(1R,4S,4aR,8aS)-7-Methyl-4-(((triisopropylsilyl)oxy)methyl)-1,4,4a,5,8,8a-hexahydronaphthalen-1-ol (298)



Alcohol 298 (a light yellow oil): $R_f = 0.31$ (20% Et₂O/hexane); $[\alpha]_D^{20} = +13.8$ (c 0.354, CHCl₃); **IR** (ATR) ν_{\max} 3414 (O-H), 2926, 2865, 1464, 1378, 1114, 1096, 1062, 884, 768, 686 cm⁻¹; **¹H NMR** (400 MHz, CDCl₃) δ 6.12 (1H, ddd, $J = 9.9, 5.5, 2.2$ Hz, H-2), 5.90 (1H, dd, $J = 9.9, 2.6$ Hz, H-3), 5.41–5.27 (1H, m, H-9), 3.90–3.82 (1H, m, H-1), 3.81 (1H, dd, $J = 9.4, 3.6$ Hz, H-12), 3.61 (1H, dd, $J = 9.4, 6.0$ Hz, H-12), 2.45–2.30 (2H, m, H-10 + H-7), 1.99–1.92 (1H, m, H-4), 1.90–1.75 (2H, m, H-10 + H-7), 1.68 (3H, s, H-11), 1.65–1.56 (2H, m, H-6 + H-5), 1.10–0.98 (21H, m, OSi(CH(CH₃)₂)₃) ppm; **¹³C NMR** (100 MHz, CDCl₃) δ 134.0 (C-8), 133.6 (C-3), 129.7

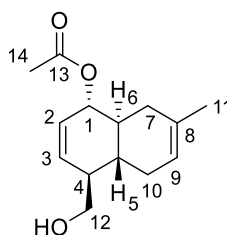
(C-2), 119.1 (C-9), 65.9 (C-1), 65.1 (C-12), 46.4 (C-4), 38.7 (C-6), 32.2 (C-10), 32.0 (C-7), 28.2 (C-5), 23.7 (C-11), 18.2 (OSi(CH(CH₃)₂)₃), 12.1 (OSi(CH(CH₃)₂)₃) ppm; **HRMS** (ESI) *m/z* calcd for C₂₁H₃₈NaO₂Si (M+Na⁺) 373.2533, found 373.2538.

(1S,4S,4aR,8aS)-7-Methyl-4-(((triisopropylsilyl)oxy)methyl)-1,4,4a,5,8,8a-hexahydronaphthalen-1-yl acetate (299)



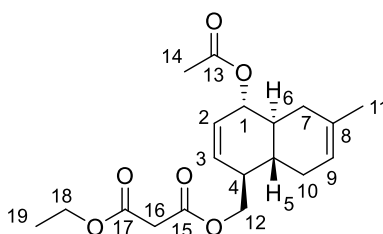
To a solution of alcohol **297** (45 mg, 0.13 mmol) in CH₂Cl₂ (1.0 mL) was added DMAP (5 mg, 0.04 mmol, 0.3 equiv), Et₃N (0.040 mL, 0.26 mmol, 2.0 equiv), followed by acetic anhydride (0.025 mL, 0.26 mmol, 2.0 equiv). The reaction mixture was stirred under N₂ atmosphere at room temperature for 1 hour. After this time, the mixture was quenched with a saturated aqueous solution of NaHCO₃ (5 mL) and diluted with CH₂Cl₂ (5 mL). The organic layer was separated, and the aqueous layer was extracted with CH₂Cl₂ (3 x 5 mL). The combined organic layers were washed with brine, dried over anhydrous Na₂SO₄ and concentrated *in vacuo*. The crude product was purified by silica gel flash column chromatography (2% Et₂O/hexane) to afford acetate **299** as a light yellow oil (49 mg, 97% yield): *R_f* = 0.46 (10% Et₂O/hexane); [α]_D²⁰ = +127.4 (c 1.73, CHCl₃); **IR** (ATR) ν_{max} 2943, 2866, 1736 (C=O ester), 1463, 1369, 1239, 1113, 882 cm⁻¹; **¹H NMR** (400 MHz, CDCl₃) δ 5.90 (1H, ddd, *J* = 10.2, 2.0, 2.0 Hz, H-2), 5.61 (1H, ddd, *J* = 10.2, 2.0, 2.0 Hz, H-3), 5.39–5.30 (1H, m, H-9), 5.18–5.06 (1H, m, H-1), 3.80 (1H, dd, *J* = 9.4, 4.4 Hz, H-12), 3.52 (1H, dd, *J* = 9.4, 7.4 Hz, H-12), 2.38 (1H, ddd, *J* = 16.9, 5.0, 5.0 Hz, H-10), 2.15 (1H, dd, *J* = 14.2, 3.4 Hz, H-7), 2.09 (3H, s, H-16), 2.07–2.00 (1H, m, H-4), 1.87–1.68 (3H, m, H-10 + H-7), 1.64 (3H, s, H-11), 1.58–1.46 (1H, m, H-5), 1.14–0.94 (21H, m, OSi(CH(CH₃)₂)₃) ppm; **¹³C NMR** (100 MHz, CDCl₃) δ 171.4 (C-15), 132.5 (C-8), 132.4 (C-2), 126.8 (C-3), 119.9 (C-9), 76.2 (C-1), 65.6 (C-12), 45.9 (C-4), 38.8 (C-6), 34.7 (C-7), 33.5 (C-5), 31.4 (C-10), 23.5 (C-11), 21.5 (C-16), 18.2 (OSi(CH(CH₃)₂)₃), 21.1 (OSi(CH(CH₃)₂)₃) ppm; **HRMS** (ESI) *m/z* calcd for C₂₃H₄₀NaO₃Si (M+Na⁺) 415.2639, found 415.2645.

**(1*S*,4*S*,4*aR*,8*aS*)-4-(Hydroxymethyl)-7-methyl-1,4,4*a*,5,8,8*a*-hexahydronaphthalen-1-yl
acetate (**300**)**



Alcohol **300** was prepared from silyl ether **299** (49 mg, 0.13 mmol) using the general procedure for TIPS deprotection (see page 141). The crude residue was purified by silica gel flash column chromatography (30% EtOAc/hexane) to deliver alcohol **300** as a white powder (29 mg, 98% yield): **Melting Point** = 85–89 °C; R_f = 0.19 (30% EtOAc/hexane); $[\alpha]_D^{20}$ = +181.3 (*c* 1.16, CHCl₃); **IR** (ATR) ν_{\max} 3412 (O-H), 2912, 1728 (C=O ester), 1372, 1240, 1024, 773 cm⁻¹; **¹H NMR** (400 MHz, CDCl₃) δ 5.79 (1H, ddd, *J* = 10.2, 1.8, 1.8 Hz, H-2), 5.70 (1H, ddd, *J* = 10.2, 2.0, 2.0 Hz, H-3), 5.41–5.24 (1H, m, H-9), 5.19–5.09 (1H, m, H-1), 3.74 (1H, dd, *J* = 10.6, 3.6 Hz, H-12), 3.56 (1H, dd, *J* = 10.6, 5.6 Hz, H-12), 2.46–2.32 (1H, m, H-10), 2.16 (1H, dd, *J* = 15.0, 3.2 Hz, H-7), 2.09 (3H, s, H-14), 2.06–2.00 (1H, m, H-4), 1.93–1.70 (4H, m, H-10 + H-7 + H-6 + H-5), 1.63 (3H, s, H-11) ppm; **¹³C NMR** (100 MHz, CDCl₃) δ 171.4 (C-13), 132.6 (C-11), 131.1 (C-2), 128.9 (C-3), 119.7 (C-9), 75.9 (C-1), 64.3 (C-12), 45.5 (C-4), 38.7 (C-6), 34.6 (C-7), 32.9 (C-5), 31.2 (C-10), 23.4 (C-11), 21.4 (C-14) ppm; **HRMS** (ESI) *m/z* calcd for C₁₄H₂₀NaO₃ (M+Na⁺) 259.1305, found 259.1314.

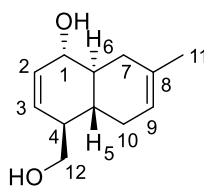
**((1*S*,4*S*,4*aS*,8*aR*)-4-Acetoxy-6-methyl-1,4,4*a*,5,8,8*a*-hexahydronaphthalen-1-yl)methyl
ethyl malonate (**294**)**



Malonate **294** was prepared from alcohol **300** (26 mg, 0.11 mmol) using the general procedure for malonate formation (see page 142). The crude residue was purified by silica gel flash column chromatography (10–20% Et₂O/hexane) to yield malonate **294** as a light

yellow oil (37 mg, 93% yield): $R_f = 0.11$ (20% Et₂O/hexane); $[\alpha]_D^{20} = +127.5$ (c 1.34, CHCl₃); **IR** (ATR) ν_{\max} 2915, 1730 (C=O ester), 1370, 1235, 1147, 1024, 772 cm⁻¹; **¹H NMR** (400 MHz, CDCl₃) δ 5.71 (1H, ddd, $J = 10.2, 2.0, 2.0$ Hz, H-2), 5.65 (1H, ddd, $J = 10.2, 2.0, 2.0$ Hz, H-3), 5.37–5.30 (1H, m, H-9), 5.18–5.10 (1H, m, H-1), 4.27 (1H, dd, $J = 10.9, 4.1$ Hz, H-12), 4.19 (2H, q, $J = 7.2$ Hz, H-18), 4.04 (1H, dd, $J = 10.9, 6.5$ Hz, H-12), 3.37 (2H, s, H-16), 2.39 (1H, ddd, $J = 16.9, 5.0, 5.0$ Hz, H-10), 2.27–2.19 (1H, m, H-4), 2.19–2.13 (1H, m, H-7), 2.09 (3H, s, H-14), 1.90–1.70 (3H, m, H-10 + H-7 + H-6), 1.64 (3H, s, H-11), 1.61–1.51 (1H, m, H-5), 1.27 (3H, t, $J = 7.2$ Hz, H-19) ppm; **¹³C NMR** (100 MHz, CDCl₃) δ 171.3 (C-13), 166.8 (C-15), 166.5 (C-17), 132.6 (C-8), 130.3 (C-2), 128.4 (C-3), 119.5 (C-9), 75.7 (C-1), 66.7 (C-12), 61.8 (C-18), 42.4 (C-4), 41.7 (C-16), 38.6 (C-6), 34.5 (C-7), 33.7 (C-5), 30.9 (C-10), 23.4 (C-11), 21.4 (C-14), 14.2 (C-19) ppm; **HRMS** (ESI) m/z calcd for C₁₉H₂₆NaO₆ (M+Na⁺) 373.1622, found 373.1624.

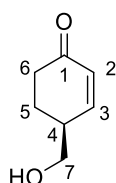
(1S,4S,4aR,8aS)-4-(Hydroxymethyl)-7-methyl-1,4,4a,5,8,8a-hexahydronaphthalen-1-ol (301)



To a solution of malonate **294** (18 mg, 0.05 mmol) in THF (0.5 mL) at 0 °C, was added a fresh stock solution of NaOEt (0.055 mL, 0.058 mmol, 1.2 equiv) dropwise. The mixture was stirred at 0 °C for 30 minutes before being slowly transferred into a stock solution of Pd(OAc)₂ (0.5 mg, 0.021 mmol, 4 mol %) and PPh₃ (1.7 mg, 0.063 mmol, 12 mol%) in THF (0.5 mL) over 5 minutes at room temperature. The reaction mixture was stirred under the reflux for 20 hours. After this time, the mixture was cooled to room temperature and quenched with saturated aqueous solution of NH₄Cl (2 mL). The mixture was then diluted with Et₂O (2 mL). The organic layer was separated, and the aqueous layer was extracted with Et₂O (3 x 3 mL). The combined organic layers were washed with brine, dried over anhydrous Na₂SO₄ and concentrated *in vacuo*. The crude product was purified by silica gel flash column chromatography (30–50% EtOAc/hexane) to give diol **301** as a light yellow oil (9 mg, 86% yield): $R_f = 0.16$ (50% EtOAc/hexane); $[\alpha]_D^{20} = +70.8$ (c 0.445, CHCl₃); **IR** (ATR) ν_{\max} 3326 (O-H), 2921, 2886, 1435, 1046, 771 cm⁻¹; **¹H NMR** (400 MHz, CDCl₃) δ 5.83 (1H,

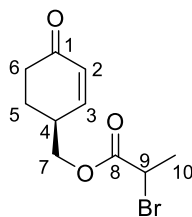
ddd, $J = 10.2, 2.3, 2.3$ Hz, H-2), 5.71 (1H, ddd, $J = 10.2, 2.3, 2.3$ Hz, H-3), 5.40–5.32 (1H, m, H-9), 3.97–3.86 (1H, m, H-1), 3.75 (1H, dd, $J = 10.6, 3.6$ Hz, H-12), 3.58 (1H, dd, $J = 10.6, 5.5$ Hz, H-12), 2.50–2.41 (1H, m, H-7), 2.41–2.32 (1H, m, H-10), 2.10–1.97 (1H, m, H-4), 1.67 (3H, s, H-11), 1.63–1.52 (2H, m, H-5 + H-6) ppm; $^{13}\text{C NMR}$ (100 MHz, CDCl_3) δ 133.0 (C-2), 132.9 (C-8), 129.7 (C-3), 119.8 (C-9), 73.8 (C-1), 64.4 (C-12), 45.8 (C-4), 42.4 (C-6), 35.0 (C-7), 32.7 (C-5), 31.2 (C-10), 23.5 (C-11) ppm; **HRMS** (ESI) m/z calcd for $\text{C}_{12}\text{H}_{18}\text{NaO}_2$ ($\text{M}+\text{Na}^+$) 217.1199, found 217.1199.

(S)-4-(Hydroxymethyl)cyclohex-2-en-1-one (193)



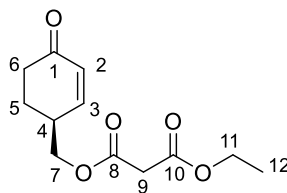
(S)-Alcohol **193** was prepared from (S)-enone **3** (0.31 g, 1.1 mmol) using the general procedure for TIPS deprotection (see page 141). The crude residue was purified by silica gel flash column chromatography (50–80% EtOAc/hexane) to give (S)-alcohol **193** as a yellow oil 124 mg, 90% yield): $R_f = 0.24$ (80% EtOAc/hexane); $[\alpha]_D^{20} = -46.1$ (c 1.69, CHCl_3); **IR** (ATR) ν_{max} 3390 (O-H), 2927, 2873, 1657 (C=O ketone), 1393, 1079, 1049, 845 cm^{-1} ; $^1\text{H NMR}$ (400 MHz, CDCl_3) δ 6.97 (1H, ddd, $J = 10.2, 2.1, 1.2$ Hz, H-3), 6.04 (1H, dd, $J = 10.2, 2.4$ Hz, H-2), 3.70 (1H, dd, $J = 10.4, 6.4$ Hz, H-7), 3.64 (1H, dd, $J = 10.4, 6.6$ Hz, H-7), 2.62 (1H, dddddd, $J = 9.8, 6.6, 6.4, 5.0, 2.4, 2.1$ Hz, H-4), 2.52 (1H, ddd, $J = 16.8, 4.6, 4.6$ Hz, H-6), 2.38 (1H, ddd, $J = 16.8, 12.6, 5.0$ Hz, H-6), 2.11 (1H, dddddd, $J = 13.3, 5.0, 5.0, 4.6, 1.2$ Hz, H-5), 1.79 (1H, dddd, $J = 13.3, 12.6, 9.8, 4.6$ Hz, H-5) ppm; $^{13}\text{C NMR}$ (100 MHz, CDCl_3) δ 200.2 (C-1), 152.0 (C-5), 130.3 (C-6), 65.2 (C-7), 39.1 (C-4), 36.7 (C-2), 25.5 (C-3) ppm; **HRMS** (ESI) m/z calcd for $\text{C}_7\text{H}_{10}\text{NaO}_2$ ($\text{M}+\text{Na}^+$) 149.0573, found 149.0573.

((S)-4-Oxocyclohex-2-en-1-yl)methyl 2-bromopropanoate (309)



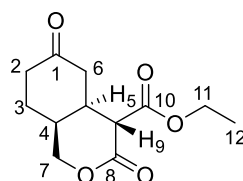
To a solution of (*S*)-alcohol **193** (22 mg, 1.7 mmol) in CH₂Cl₂ (1 mL) at 0 °C was added DMAP (5 mg, 0.04 mmol, 20 mol%), Et₃N (0.05 mL, 0.35 mmol, 2.0 equiv) and 2-bromopropionyl chloride (0.03 mL, 0.26 mmol, 1.5 equiv), respectively. The reaction mixture was stirred under N₂ from 0 °C and then allowed to reach room temperature for 3 hours. The reaction mixture was quenched with saturated aqueous solution of NaHCO₃ (3 mL) and diluted with CH₂Cl₂ (3 mL), The organic layer was separated, and the aqueous layer was extracted with CH₂Cl₂ (3 × 3 mL). The combined organic layers were washed with brine, dried over anhydrous Na₂SO₄ and concentrated *in vacuo*. The crude product was purified by silica gel flash column chromatography (20–40% EtOAc/hexane) to afford bromopropionate **309** as a light yellow oil (37 mg, 80% yield): *R_f* = 0.28 in (40% EtOAc/hexane); IR (ATR) ν_{\max} 2955, 2930, 1737 (C=O ester), 1677 (C=O ketone), 1337, 1219, 1156, 1061, 838 cm⁻¹; ¹H NMR (400 MHz, CDCl₃) δ 6.85 (1H, dd, *J* = 10.2, 2.2 Hz, H-3), 6.07 (1H, dd, *J* = 10.2, 2.5 Hz, H-2), 4.38 (1H, q, *J* = 6.9 Hz, H-9), 4.30 (1/2H, dd, *J* = 11.0, 6.5 Hz, H-7), 4.21 (1H, d, *J* = 6.5 Hz, H-7), 4.11 (1/2H, dd, *J* = 11.0, 6.5 Hz, H-7), 2.92–2.76 (1H, m, H-4), 2.55 (1H, ddd, *J* = 16.9, 4.8, 4.8 Hz, H-6), 2.40 (1H, ddd, *J* = 16.9, 12.5, 5.0 Hz, H-6), 2.21–2.11 (1H, m, H-5), 1.90–1.84 (1H, m, H-5), 1.82 (1H, d, *J* = 6.9 Hz, H-10) ppm; ¹³C NMR (100 MHz, CDCl₃) δ 198.8 (C-1), 170.2 (C-8), 149.3 (C-3), 131.0 (C-2), 67.4 (C-7), 39.7 (C-9), 36.5 (C-6), 35.9 (C-4), 25.7 (C-5), 21.6 (C-10) ppm; HRMS (ESI) *m/z* calcd for C₁₀H₁₁⁷⁹BrNaO₃ (M+Na⁺) 282.9940, found 282.9934.

(S)-Ethyl ((4-oxocyclohex-2-en-1-yl)methyl) malonate (**270**)



(S)-Malonate **270** was prepared from (S)-alcohol **193** (31 mg, 0.25 mmol) using the general procedure for malonate formation (see page 142). The crude residue was purified by silica gel flash column chromatography (30% EtOAc/hexane) to give (S)-malonate **270** as a yellow oil (50 mg, 84% yield): $R_f = 0.18$ (30% EtOAc/hexane); $[\alpha]_D^{20} = -44.4$ (c 0.559, CHCl₃); IR (ATR) ν_{\max} 2955, 1732 (C=O ester), 1680 (C=O ketone), 1331, 1269, 1150, 1032 cm⁻¹; ¹H NMR (400 MHz, CDCl₃) δ 6.85 (1H, ddd, $J = 10.2, 2.1, 1.4$ Hz, H-3), 6.08 (1H, dd, $J = 10.2, 2.6$ Hz, H-2), 4.24 (1H, dd, $J = 11.0, 6.5$ Hz, H-7), 4.20 (2H, q, $J = 7.2$ Hz, H-11), 4.16 (1H, dd, $J = 11.0, 6.7$ Hz, H-7), 3.41 (2H, s, H-9), 2.83 (1H, dddddd, $J = 10.0, 6.7, 6.5, 5.0, 2.6, 2.1$ Hz, H-4), 2.55 (1H, ddd, $J = 16.9, 4.7, 4.7$ Hz, H-6), 2.40 (1H, ddd, $J = 16.9, 12.7, 5.0$ Hz, H-6), 2.15 (1H, dddddd, $J = 13.2, 5.0, 5.0, 4.7, 1.4$ Hz, H-5), 1.83 (1H, dddd, $J = 13.2, 12.7, 10.0, 4.7$ Hz, H-5), 1.28 (3H, t, $J = 7.2$ Hz, H-12) ppm; ¹³C NMR (100 MHz, CDCl₃) δ 199.0 (C-1), 166.6 (C-8), 166.5 (C-10), 149.6 (C-3), 130.9 (C-2), 67.0 (C-11), 61.9 (C-7), 41.6 (C-9), 36.6 (C-6), 35.9 (C-4), 25.7 (C-5), 14.2 (C-12) ppm; HRMS (ESI) m/z calcd for C₁₂H₁₆NaO₅ (M+Na⁺) 263.0890, found 263.0887.

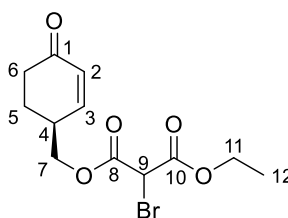
Ethyl (4S)-1,8-dioxooctahydro-1H-isochromene-9-carboxylate (**272**)



To a solution of malonate **270** (47 mg, 0.19 mmol) and La(O-*i*-Pr)₃ (64 mg, 0.19 mmol, 1.0 equiv) in THF (1.1 mL), was stirred under N₂ atmosphere at room temperature for 20 minutes before being added freshly distilled diisopropyl ethylamine (0.070 mL, 0.39 mmol, 2.0 equiv). The reaction mixture was stirred at 40 °C for 3.5 hours and cooled to room temperature. The mixture was quenched with saturated aqueous solution of NH₄Cl (5 mL) and diluted with EtOAc (5 mL). The organic layer was separated, and the aqueous layer was

extracted with EtOAc (3 x 10 mL). The combined organic layers were washed with brine, dried over anhydrous Na₂SO₄ and concentrated *in vacuo*. The crude product was purified by silica gel flash column chromatography (50% EtOAc/hexane) to yield lactone **272** as a yellow solid (32 mg, 67% yield); **Melting Point** = 89–92 °C; **R_f** = 0.35 (80% EtOAc/hexane); **[α]_D²⁰** = –53.4 (c 0.915, CHCl₃); **IR** (ATR) ν_{max} 2923, 1718 (C=O ester), 1303, 1254, 1154, 1040 cm⁻¹; **¹H NMR** (400 MHz, CDCl₃) δ 4.43 (1H, dd, *J* = 11.6, 4.6 Hz, H-7), 4.26 (2H, qd, *J* = 7.2, 1.4 Hz, H-11), 4.22 (1H, dd, *J* = 11.6, 7.4 Hz, H-7), 3.31 (1H, d, *J* = 10.1 Hz, H-9), 3.03–2.93 (1H, m, H-5), 2.55–2.45 (3H, m, H-2 + H-6 + H-4), 2.37 (1H, ddd, *J* = 17.5, 12.2, 5.4 Hz, H-2), 2.33–2.25 (1H, m, H-6), 2.02 (1H, dddd, *J* = 14.1, 5.4, 5.4, 5.4 Hz, H-3), 1.81 (1H, dddd, *J* = 14.1, 12.2, 12.2, 4.7 Hz, H-3), 1.30 (3H, t, *J* = 7.2 Hz, H-12) ppm; **¹³C NMR** (100 MHz, CDCl₃) δ 208.5 (C-1), 167.9 (C-8), 167.1 (C-10), 70.6 (C-7), 62.4 (C-11), 51.0 (C-9), 42.5 (C-6), 38.3 (C-2), 33.4 (C-5), 31.4 (C-4), 23.2 (C-3), 14.2 (C-12) ppm; **HRMS** (ESI) *m/z* calcd for C₁₂H₁₆NaO₅ (M+Na⁺) 263.0890, found 263.0890.

1-Ethyl 3-(((S)-4-oxocyclohex-2-en-1-yl)methyl) 2-bromomalonate (**315**)



To a solution of (*S*)-malonate **270** (25 mg, 1.07 mmol) in THF (1.4 mL) was added DBU (0.017 mL, 1.07 mmol, 1.0 equiv). The mixture was stirred under N₂ at 0 °C for 1 hour before being cooled to –78 °C and added CBr₄ (37 mg, 1.07 mmol, 1.0 equiv). The reaction mixture was stirred at –78 °C for 40 minutes and then allowed to reach room temperature. The reaction mixture was quenched with saturated aqueous solution of NH₄Cl (3 mL) and diluted with Et₂O (3 mL). The organic layer was separated, and the aqueous layer was extracted with Et₂O (3 x 3 mL). The combined organic layers were washed with brine, dried over anhydrous Na₂SO₄ and concentrated *in vacuo*. The crude product was purified by silica gel flash column chromatography (20–40% EtOAc/hexane) to furnish bromomalonate **315** as a light yellow oil (13 mg, 38% yield): **R_f** = 0.23 in (40% EtOAc/hexane); **IR** (ATR) ν_{max} 2960, 2925, 1742 (C=O ester), 1679 (C=O ketone), 1392, 1245, 1146, 1025 cm⁻¹; **¹H NMR** (400 MHz, CDCl₃) δ 6.83 (1H, ddd, *J* = 10.2, 1.9, 1.9 Hz, H-3), 6.09 (1H, ddd, *J* = 10.2, 3.1, 3.1 Hz, H-2), 4.86 (1H, s, H-9), 4.42–4.19 (4H, m, H-7 + H-11), 2.95–2.81 (1H, m, H-4), 2.57 (1H, dddd, *J* = 16.9, 4.5,

4.5, 4.5 Hz, H-6), 2.48–2.35 (1H, m, H-6), 2.23–2.11 (1H, m, H-5), 1.92–1.77 (1H, m, H-5), 1.34 (3H, t, $J = 7.2$ Hz, H-12), 1.31 (3H, t, $J = 7.2$ Hz, H-12) ppm; ^{13}C NMR (100 MHz, CDCl_3) δ 198.7 (C-1), 198.6 (C-1), 164.7 (C-8), 164.5 (C-8), 163.3 (C-10), 163.2 (C-10), 148.8 (C-3), 148.5 (C-3), 131.3 (C-2), 131.2 (C-2), 69.8 (C-7), 68.4 (C-7), 65.1 (C-11), 63.6 (C-11), 42.0 (C-9), 36.5 (C-6), 35.9 (C-6), 30.4 (C-4), 25.6 (C-5), 14.0 (C-12), 13.9 (C-12) ppm; HRMS (ESI) m/z calcd for $\text{C}_{12}\text{H}_{15}^{79}\text{BrNaO}_5$ ($\text{M}+\text{Na}^+$) 340.9995, found 340.9997.

6. Abbreviations

[α]	specific rotation
α	alpha
Å	angstrom
Ac	acetyl
ACP	acyl carrier protein
AIBN	azobisisobutyronitrile
APCI	atmospheric pressure chemical ionisation
aq	aqueous
ATR	attenuated total reflection
β	beta
BHT	butylated hydroxy toluene (2,6-di- <i>tert</i> -butyl-4-methylphenol)
BINOL	1,1'-bi-2-naphthol
Bn	benzyl
br	broad
brsm	based on recovered starting material
BTEAC	benzyltriethylammonium chloride
<i>n</i> -BuLi	butyl lithium
°C	degrees Celsius
<i>C</i>	concentration
cat.	catalyst
CH ₂ Cl ₂	dichloromethane
CHCl ₃	chloroform
cm ⁻¹	wavenumber(s)
conv	conversion
CSA	camphorsulfonic acid
δ	chemical shift in parts per million
d	doublet
dd	doublet of doublet
ddt	doublet of triplet
DBU	1,8-diazabicyclo[5.4.0]undec-7-ene
DCB	1,2-dichlorobenzene

DCE	1,2-dichloroethane
DCM	dichloromethane
DDQ	2,3-dichloro-5,6-dicyano- <i>p</i> -benzoquinone
DIBAL-H	diisobutylaluminum hydride
DIPA	diisopropylamine
DIPEA	<i>N,N</i> -diisopropylethylamine
DMAP	<i>N,N</i> -dimethylaminopyridin-4-amine
DMF	dimethylformamide
DMP	Dess–Martin periodinane
DMPU	1,3-dimethyl-3,4,5,6-tetrahydro-2(1 <i>H</i>)-pyrimidinone
DMSO	dimethylsulfoxide
DNA	deoxyribonucleic acid
dpm	dipivaloylmethanato
dppf	1,1'-bis(diphenylphosphino)ferrocene
dr	diastereomeric ratio
<i>ee</i>	enantiomeric excess
EC ₅₀	half maximal effective concentration
equiv	equivalent
ESI	electro spray ionisation
Et	ethyl
Et ₂ O	diethyl ether
EtOAc	ethylacetate
Et ₃ N	triethylamine
g	gram(s)
h	hour(s)
hept	heptet
HPLC	high-performance liquid chromatography
HRMS	high-resolution mass spectrometry
Hz	hertz
IBX	2-iodoxy benzoic acid
IC ₅₀	half maximal inhibitory concentration
IMDA	intramolecular Diels–Alder
<i>i</i> -Pr	isopropyl

IPA	isopropyl alcohol
IR	infrared spectroscopy
<i>J</i>	coupling constant (Hz)
KHMDS	potassium hexamethyldisilazide
LDA	lithium diisopropylamide
m	multiplet
m.p.	melting point
M	molar
Me	methyl
MeOH	methanol
mg	milligram
MIC	minimum inhibitory concentration
min	minutes
mL	milliliter
mol	mole
mol%	mole percent
MOM	methoxymethyl
MRSA	methicillin resistant <i>Staphylococcus aureus</i>
MS	mass spectrometry
M.S.	molecular sieves
<i>m/z</i>	mass-to-charge ratio
NaHMDS	sodium bis(trimethylsilyl)amide
nm	nanometer(s)
nM	nano molar
NMR	nuclear magnetic resonance spectroscopy
nOe	nuclear overhauser effect
NOESY	nuclear overhauser effect spectroscopy
PdCl ₂	palladium chloride
Pd(OAc) ₂	palladium acetate
Ph	phenyl
PKS	polyketide synthase
PMB	<i>p</i> -methoxybenzyl
ppm	part(s) per million

PTSA	<i>p</i> -toluenesulfonic acid
Py	pyridine
q	quartet
qn	quintet
<i>rac</i> -	racemic
<i>R_f</i>	retention factor (in chromatography)
RNA	ribonucleic acid
rt	room temperature
s	singlet
sext	sextet
t	triplet
<i>t</i> -Bu	tert-butyl
TBAF	tetra- <i>n</i> -butylammonium fluoride
TBD	1,5,7-triazabicyclo[4.4.0]dec-5-ene
TBS	<i>t</i> -butyldimethylsilyl
TES	triethylsilyl
temp	temperature
Tf	trifluoromethanesulfonate
TFA	trifluoroacetic acid
THF	tetrahydrofuran
TIPS	triisopropylsilyl
TLC	thin layer chromatography
TMS	trimethylsilyl
TMSE	trimethylsilyl ester
Ts	<i>p</i> -toluenesulfonyl
TS	transition state
μ	micro
ν	vibration frequency (cm ⁻¹)
VRSA	vancomycin resistant <i>Staphylococcus aureus</i>

7. References

- 1 P. M. Dewick, *Medicinal natural products: a biosynthetic approach*, Wiley, Chichester, West Sussex, England; New York, NY, USA, 2nd ed., 2002.
- 2 D. A. Dias, S. Urban and U. Roessner, *Metabolites*, 2012, **2**, 303–336.
- 3 R. A. Maplestone, M. J. Stone and D. H. Williams, *Gene*, 1992, **115**, 151–157.
- 4 E. W. Abel, Ed., in *Tutorial Chemistry Texts*, Royal Society of Chemistry, Cambridge, 2007, pp. 105–130.
- 5 D. J. Newman and G. M. Cragg, *J. Nat. Prod.*, 2012, **75**, 311–335.
- 6 J. G. Mahdi, A. J. Mahdi, A. J. Mahdi and I. D. Bowen, *Cell Prolif*, 2006, **39**, 147–155.
- 7 T. F. Molinski, Ed., *Org. Lett.*, 2014, **16**, 3849–3855.
- 8 W. R. Roush, *J. Am. Chem. Soc.*, 2008, **130**, 6654–6656.
- 9 K. J. Hale, *Org. Lett.*, 2013, **15**, 3181–3198.
- 10 C. T. Walsh and T. A. Wencewicz, *J Antibiot*, 2014, **67**, 7–22.
- 11 A. M. Bal, M. Z. David, J. Garau, T. Gottlieb, T. Mazzei, F. Scaglione, P. Tattevin and I. M. Gould, *Journal of Global Antimicrobial Resistance*, 2017, **10**, 295–303.
- 12 M. U. Okwu, M. Olley, A. O. Akpoka, O. E. Izevbuwa, 1 Department of Biological Sciences, College of Natural and Applied Sciences, Igbinedion University Okada, Edo State, Nigeria, and 2 Department of Pathology, Igbinedion University Teaching Hospital, Okada, Edo State, Nigeria, *AIMS Microbiology*, 2019, **5**, 117–137.
- 13 J. S. Wolfson and D. C. Hooper, *ANTIMICROB. AGENTS CHEMOTHER.*, 1985, **28**, 6.
- 14 G. P. Dinos, *British Journal of Pharmacology*, 2017, **174**, 2967–2983.
- 15 D. J. Hardy, D. M. Hensey, J. M. Beyer, C. Vojtko, E. J. McDonald and P. B. Fernandes, *ANTIMICROB. AGENTS CHEMOTHER.*, 1988, **32**, 10.
- 16 M. Z. David, S. Medvedev, S. F. Hohmann, B. Ewigman and R. S. Daum, *Infect. Control Hosp. Epidemiol.*, 2012, **33**, 782–789.
- 17 E. Y. Klein, L. Sun, D. L. Smith and R. Laxminarayan, *American Journal of Epidemiology*, 2013, **177**, 666–674.
- 18 E. Martens and A. L. Demain, *J Antibiot*, 2017, **70**, 520–526.
- 19 A.-C. Uhlemann, M. Otto, F. D. Lowy and F. R. DeLeo, *Infection, Genetics and Evolution*, 2014, **21**, 563–574.
- 20 K. Jungmann, R. Jansen, K. Gerth, V. Huch, D. Krug, W. Fenical and R. Müller, *ACS Chem. Biol.*, 2015, **10**, 2480–2490.

- 21 J. W. Blunt, A. R. Carroll, B. R. Copp, R. A. Davis, R. A. Keyzers and M. R. Prinsep, *Nat. Prod. Rep.*, 2018, **35**, 8–53.
- 22 K. H. Jang, S.-J. Nam, J. B. Locke, C. A. Kauffman, D. S. Beatty, L. A. Paul and W. Fenical, *Angewandte Chemie International Edition*, 2013, **52**, 7822–7824.
- 23 M. E. Hensler, K. H. Jang, W. Thienphrapa, L. Vuong, D. N. Tran, E. Soubih, L. Lin, N. M. Haste, M. L. Cunningham, B. P. Kwan, K. J. Shaw, W. Fenical and V. Nizet, *J. Antibiot.*, 2014, **67**, 549–553.
- 24 S. Alt and B. Wilkinson, *ACS Chem. Biol.*, 2015, **10**, 2468–2479.
- 25 F. L. Sirota, F. Goh, K.-N. Low, L.-K. Yang, S. C. Crasta, B. Eisenhaber, F. Eisenhaber, Y. Kanagasundaram and S. B. Ng, *J. Genomics*, 2018, **6**, 63–73.
- 26 E. K. Davison, J. L. Freeman, W. Zhang, W. M. Wuest, D. P. Furkert and M. A. Brimble, *Org. Lett.*, 2020, **22**, 5550–5554.
- 27 J. L. Freeman, M. A. Brimble and D. P. Furkert, *Org. Chem. Front.*, 2019, **6**, 2954–2963.
- 28 G. Li, S. Kusari and M. Spiteller, *Nat. Prod. Rep.*, 2014, **31**, 1175–1201.
- 29 K. Gerth, H. Steinmetz, G. Höfle and R. Jansen, *Angew. Chem. Int. Ed.*, 2008, **47**, 600–602.
- 30 J. Held, T. Gebru, M. Kalesse, R. Jansen, K. Gerth, R. Müller and B. Mordmüller, *Antimicrob Agents Chemother*, 2014, **58**, 6378–6384.
- 31 C. W. J. Chang, A. Patra, D. M. Roll, P. J. Scheuer, G. K. Matsumoto and J. Clardy, *J. Am. Chem. Soc.*, 1984, **106**, 4644–4646.
- 32 H. Miyaoka, M. Shimomura, H. Kimura, Y. Yamada, H.-S. Kim and W. Yusuke, *Tetrahedron*, 1998, **54**, 13467–13474.
- 33 G. M. König, A. D. Wright and C. K. Angerhofer, *J. Org. Chem.*, 1996, **61**, 3259–3267.
- 34 J. R. Carney and P. J. Scheuer, *Tetrahedron Letters*, 1993, **34**, 3727–3730.
- 35 T. Amagata, J. Xiao, Y.-P. Chen, N. Holsopple, A. G. Oliver, T. Gokey, A. B. Guliaev and K. Minoura, *J. Nat. Prod.*, 2012, **75**, 2193–2199.
- 36 L. Yang, T. Wurm, B. Sharma Poudel and M. J. Krische, *Angew. Chem. Int. Ed.*, 2020, **59**, 23169–23173.
- 37 J. C. W. Lim, T. K. Chan, D. S. Ng, S. R. Sagineedu, J. Stanslas and W. F. Wong, *Clinical and Experimental Pharmacology and Physiology*, 2012, **39**, 300–310.
- 38 Y.-L. Yang, C.-P. Lu, M.-Y. Chen, K.-Y. Chen, Y.-C. Wu and S.-H. Wu, *Chem. Eur. J.*, 2007, **13**, 6985–6991.

- 39 O. L. Rakotonandrasana, F. H. Raharinjato, M. Rajaonarivelo, V. Dumontet, M.-T. Martin, J. Bignon and P. Rasoanaivo, *J. Nat. Prod.*, 2010, **73**, 1730–1733.
- 40 Y. Igarashi, Y. Kim, Y. In, T. Ishida, Y. Kan, T. Fujita, T. Iwashita, H. Tabata, H. Onaka and T. Furumai, *Org. Lett.*, 2010, **12**, 3402–3405.
- 41 K. Ma, D. Liao, S. Yang, X. Li and X. Lei, *Org. Chem. Front.*, 2016, **3**, 251–258.
- 42 T. Yoshimitsu, S. Nojima, M. Hashimoto and T. Tanaka, *Org. Lett.*, 2011, **13**, 3698–3701.
- 43 K. C. Nicolaou, G. S. Tria, D. J. Edmonds and M. Kar, *J. Am. Chem. Soc.*, 2009, **131**, 15909–15917.
- 44 H. Nawa, *Proceedings of the Japan Academy*, 1951, **27**, 436–440.
- 45 M. E. Jung and D. Yoo, *Org. Lett.*, 2011, **13**, 2698–2701.
- 46 W. Hou, B. Liu and H. Xu, *European Journal of Medicinal Chemistry*, 2019, **176**, 378–392.
- 47 J. Jauch, *Angew. Chem. Int. Ed.*, 2008, **47**, 34–37.
- 48 S. V. Ley, A. Abad-Somovilla, J. C. Anderson, C. Ayats, R. Banteli, E. Beckmann, A. Boyer, M. G. Brasca, A. Brice, H. B. Broughton, B. J. Burke, E. Cleator, D. Craig, A. A. Denholm, R. M. Denton, T. Durand-Reville, L. B. Gobbi, M. Göbel, B. L. Gray, R. B. Grossmann, C. E. Gutteridge, N. Hahn, S. L. Harding, D. C. Jennens, L. Jennens, P. J. Lovell, H. J. Lovell, M. L. de la Puente, H. C. Kolb, W.-J. Koo, S. L. Maslen, C. F. McCusker, A. Mattes, A. R. Pape, A. Pinto, D. Santafianos, J. S. Scott, S. C. Smith, A. Q. Somers, C. D. Spilling, F. Stelzer, P. L. Toogood, R. M. Turner, G. E. Veitch, A. Wood and C. Zumburn, *Chem. Eur. J.*, 2008, **14**, 10683–10704.
- 49 P. M. Mirzayans, R. H. Powner, C. M. Williams and P. V. Bernhardt, *Eur. J. Org. Chem.*, 2012, **2012**, 1633–1638.
- 50 A. Salatino, M. L. F. Salatino and G. Negri, *J. Braz. Chem. Soc.*, 2007, **18**, 11–33.
- 51 M. Bian, Z. Wang, X. Xiong, Y. Sun, C. Matera, K. C. Nicolaou and A. Li, *J. Am. Chem. Soc.*, 2012, **134**, 8078–8081.
- 52 X. Si, Z. Zhang, C. Zheng, Z. Li and Q. Cai, *Angew. Chem. Int. Ed.*, 2020, **59**, 18412–18417.
- 53 N. Rahn and M. Kalesse, *Angew. Chem. Int. Ed.*, 2008, **47**, 597–599.
- 54 H. Miyaoka, Y. Abe, N. Sekiya, H. Mitome and E. Kawashima, *Chem. Commun.*, 2012, **48**, 901–903.
- 55 S. V. Pronin and R. A. Shenvi, *J. Am. Chem. Soc.*, 2012, **134**, 19604–19606.

- 56 T. Fukuzaki, S. Kobayashi, T. Hibi, Y. Ikuma, J. Ishihara, N. Kanoh and A. Murai, *Org. Lett.*, 2002, **4**, 2877–2880.
- 57 L. Zhu, C. Zhou, W. Yang, S. He, G.-J. Cheng, X. Zhang and C.-S. Lee, *J. Org. Chem.*, 2013, **78**, 7912–7929.
- 58 K. C. Nicolaou, L. Shi, M. Lu, M. R. Pattanayak, A. A. Shah, H. A. Ioannidou and M. Lamani, *Angew. Chem. Int. Ed.*, 2014, **53**, 10970–10974.
- 59 B. Bradshaw, G. Etxebarria-Jardí and J. Bonjoch, *J. Am. Chem. Soc.*, 2010, **132**, 5966–5967.
- 60 B. Bradshaw, G. Etxebarria-Jardi, J. Bonjoch, S. F. Vióquez, G. Guillena and C. Nájera, *Adv. Synth. Catal.*, 2009, **351**, 2482–2490.
- 61 S. Hess and M. E. Maier, *ChemistrySelect*, 2020, **5**, 7315–7319.
- 62 R. H. Munday, R. M. Denton and J. C. Anderson, *J. Org. Chem.*, 2008, **73**, 8033–8038.
- 63 S. Goncalves, S. Santoro, M. Nicolas, A. Wagner, P. Maillos, F. Himo and R. Baati, *J. Org. Chem.*, 2011, **76**, 3274–3285.
- 64 S. Breitler and E. M. Carreira, *Angew. Chem. Int. Ed.*, 2013, **52**, 11168–11171.
- 65 N. Rahn and M. Kalesse, *Angew. Chem. Int. Ed.*, 2008, **47**, 597–599.
- 66 G. Lodovici, University of York, 2019.
- 67 M. Tokunaga, S. Harada, T. Iwasawa, Y. Obora and Y. Tsuji, *Tetrahedron Letters*, 2007, **48**, 6860–6862.
- 68 S. A. Kozmin and V. H. Rawal, *J. Org. Chem.*, 1997, **62**, 5252–5253.
- 69 S. Danishefsky and T. Kitahara, *J. Am. Chem. Soc.*, 1974, **96**, 7807–7808.
- 70 Y. Cui, H. Jiang, Z. Li, N. Wu, Z. Yang and J. Quan, *Org. Lett.*, 2009, **11**, 4628–4631.
- 71 J. M. Kelly and F. J. Leeper, *Tetrahedron Letters*, 2012, **53**, 819–821.
- 72 S. Hess and M. E. Maier, *ChemistrySelect*, 2020, **5**, 7315–7319.
- 73 K. C. Nicolaou, D. L. F. Gray, T. Montagnon and S. T. Harrison, *Angewandte Chemie International Edition*, 2002, **41**, 996–1000.
- 74 Y. Sudo, D. Shirasaki, S. Harada and A. Nishida, *J. Am. Chem. Soc.*, 2008, **130**, 12588–12589.
- 75 J. Brousseau, A. Xolin and L. Barriault, *Org. Lett.*, 2019, **21**, 1347–1349.
- 76 J. M. Fraile, N. García, C. I. Herrerías, M. Martín and J. A. Mayoral, *ACS Catal.*, 2012, **2**, 56–64.
- 77 C. K. Andrade, R. O. Rocha, O. E. Vercillo, W. A. Silva and R. A. Matos, *Synlett*, 2003, 2351–2352.

- 78 P. O'Brien, *J. Chem. Soc., Perkin Trans.*, 1998, **1**, 1439–1457.
- 79 N. S. Simpkins, *J. Chem. Soc., Chem. Commun.*, 1986, 88–90.
- 80 C. M. Cain, R. P. C. Cousins, G. Coumbarides and N. S. Simpkins, *Tetrahedron*, 1990, **46**, 523–544.
- 81 E. J. Corey and A. W. Gross, *Tetrahedron Letters*, 1984, **25**, 495–498.
- 82 A. B. Smith, E. G. Nolen, R. Shirai, F. R. Blase, M. Ohta, N. Chida, R. A. Hartz, D. M. Fitch, W. M. Clark and P. A. Sprengeler, *J. Org. Chem.*, 1995, **60**, 7837–7848.
- 83 J.-E. Baeckvall and A. Ericsson, *J. Org. Chem.*, 1994, **59**, 5850–5851.
- 84 F. Peng, R. E. Grote, R. M. Wilson and S. J. Danishefsky, *Proc Natl Acad Sci U S A*, 2013, **110**, 10904–10909.
- 85 J. H. Lee and S. Mho, *J. Org. Chem.*, 2015, **80**, 3309–3314.
- 86 A. Hosomi and Hideki, Sakurai, *Tetrahedron Lett.*, 1976, **17**, 1295–1298.
- 87 J. D. Sellars, P. G. Steel and M. J. Turner, *Chem. Commun.*, 2006, 2385–2387.
- 88 N. Kulmert, J. Peverley and J. Robertson, *Tetrahedron Lett.*, 1998, **39**, 3215–3216.
- 89 P. H. Lee, K. Lee, S. Sung and S. Chang, *J. Org. Chem.*, 2001, **66**, 8646–8649.
- 90 P. H. Lee, D. Seomoon, S. Kim, K. Nagaiah, S. V. Damle and K. Lee, *Synthesis*, 2003, 2189–2193.
- 91 K. Hattori and H. Yamamoto, *J. Org. Chem.*, 1993, **58**, 5301–5303.
- 92 F.-M. Liao, X.-T. Gao, X.-S. Hu, S.-L. Xie and J. Zhou, *Science Bulletin*, 2017, **62**, 1504–1509.
- 93 R. Mahrwald, *Chem. Rev.*, 1999, **99**, 1095–1120.
- 94 R. E. Ireland, P. Wipf and J. D. Armstrong, *J. Org. Chem.*, 1991, **56**, 650–657.
- 95 J. Otera, Y. Fujita, N. Sakuta, M. Fujita and S. Fukuzumi, *J. Org. Chem.*, 1996, **61**, 2951–2962.
- 96 E. Kerste, M. P. Beller and U. Koert, *Eur. J. Org. Chem.*, 2020, **2020**, 3699–3711.
- 97 M. L. de la Puente, S. V. Ley, M. S. J. Simmonds and W. M. Blaney, *J. Chem. Soc., Perkin Trans. 1*, 1996, 1523–1529.
- 98 H. Iio, M. Isobe, T. Kawai and T. Goto, *Tetrahedron*, 1979, **35**, 941–948.
- 99 N. Mander and S. P. Sethi, *Tetrahedron Lett.*, 1984, **25**, 5953–5956.
- 100 M. W. Rathke and P. J. Cowan, *J. Org. Chem.*, 1985, **50**, 2622–2624.
- 101 C. Kitsiou, J. J. Hindes, P. l'Anson, P. Jackson, T. C. Wilson, E. K. Daly, H. R. Felstead, P. Hearnshaw and W. P. Unsworth, *Angew. Chem. Int. Ed.*, 2015, **54**, 15794–15798.

- 102 M. A. Brimble, O. C. Finch, A. M. Heapy, J. D. Fraser, D. P. Furkert and P. D. O'Connor, *Tetrahedron*, 2011, **67**, 995–1001.
- 103 D. H. Dethe and B. D. Dherange, *J. Org. Chem.*, 2015, **80**, 4526–4531.
- 104 K. Majima, S. Tosaki, T. Ohshima and M. Shibasaki, *Tetrahedron Lett.*, 2005, **46**, 5377–5381.
- 105 D. L. Comins and A. Dehghani, *Tetrahedron Letters*, 1992, **33**, 6299–6302.
- 106 J. Matsuo, K. Takeuchi and H. Ishibashi, *Org. Lett.*, 2008, **10**, 4049–4052.
- 107 S. A. Godleski and R. S. Valpey, *J. Org. Chem.*, 1982, **47**, 381–383.
- 108 T. Takemoto, Y. Nishikimi, M. Sodeoka and M. Shibasaki, *Tetrahedron Letters*, 1992, **33**, 3527–3530.
- 109 G. Pandey and V. Janakiram, *Chem. Eur. J.*, 2015, **21**, 13120–13126.
- 110 S. Vijgen, K. Nauwelaerts, J. Wang, A. Van Aerschot, I. Lagoja and P. Herdewijn, *J. Org. Chem.*, 2005, **70**, 4591–4597.
- 111 P. Maity, M. Gujjar, R. Vellingiri, T. Lakshminarasimhan, A. J. DelMonte, I. S. Young, M. D. Eastgate and R. Vaidyanathan, *Org. Process Res. Dev.*, 2019, **23**, 2754–2757.
- 112 X.-L. Xu and Z. Li, *Angew. Chem. Int. Ed.*, 2017, **56**, 8196–8200.
- 113 M. Ihara, N. Taniguchi, K. Fukumoto and T. Kametani, *J. Chem. Soc., Chem. Commun.*, 1987, 1438–1439.
- 114 K. Shirokane, Y. Tanaka, M. Yoritate, N. Takayama, T. Sato and N. Chida, *BCSJ*, 2015, **88**, 522–537.
- 115 R. Nouguier, S. Gastaldi, D. Stien, M. Bertrand, F. Villar, O. Andrey and P. Renaud, *Tetrahedron: Asymmetry*, 2003, **14**, 3005–3018.
- 116 K. Gai, X. Fang, X. Li, J. Xu, X. Wu, A. Lin and H. Yao, *Chem. Commun.*, 2015, **51**, 15831–15834.
- 117 P. Klimko, M. Hellberg, M. McLaughlin, N. Sharif, B. Severns, G. Williams, K. Haggard and J. Liao, *Bioorganic & Medicinal Chemistry*, 2004, **12**, 3451–3469.
- 118 K. Ishigami, K. Kadowaki, S. Yamada, S. Aiba, T. Kawasaki, R. Katsuta, A. Yajima, T. Nukada, H. Takikawa and H. Watanabe, *Tetrahedron*, 2020, **76**, 130834.